JEMS

JOURNAL OF ETA MARITIME SCIENCE

Volume: 12 Issue: 1

March 2024

E-ISSN: 2148-9386

www.jemsjournal.org

JEMS
JOURNAL OF ETA MARITIME SCIENCE
2024 / Volume • 12 - Issue • 1

Editorial Board

JEMS
JOURNAL OF ETA MARITIME SCIENCE
2024 / Volume • 12 - Issue • 1

Editorial Board

Journal Info

Please refer to the journal's webpage (www.jemsjournal.org) for " About Us", "Aim and Scope", "Guide for Authors" and "Ethical Policy".

JEMS is currently indexed in Web of Science Emerging Sources Citation Index (ESCI), Tubitak Ulakbim Science Database, Transport Research International Documentation (TRID), Directory of Open Access Journals (DOAJ), EBSCO, J-Gate, Scopus and CNKI.

Owner UCTEA The Chamber of Marine Engineers

Address: Sahrayıcedit Mah. Halk Sk. Golden Plaza No: 29 C Blok K:3 D:6 Kadıköy/İstanbul - Türkiye
Web: gemimo.org **E-mail:** bilgi@gemimo.org **Phone:** +90 216 747 15 51
Fax: +90 216 747 34 35

Publisher Galenos Publishing House
Address: Molla Gürani Mah. Kaçamak Sk. No: 21/1 34093 İstanbul, Türkiye
Phone: +90 (530) 177 30 97 **E-mail:** info@galenos.com.tr **Web:** www.galenos.com.tr

E-ISSN: 2148-9386

Online Publication Date:
March 2024

Journal website:
www.jemsjournal.org

Submit Article:
jag.journalagent.com/jems

Cover Photo:

2024/ Volume 12 / Issue 1
Serdar BOZ, Master Mariner, BEng, MSc, Marine Transportation Engineer
M/T BEKS DAISY, 2023.

JEMS
JOURNAL OF ETA MARITIME SCIENCE
2024 / Volume • 12 - Issue • 1

Contents

DOI: 10.4274/jems.2024.21548

Journal of ETA Maritime Science 2024;12(1):1-1

Selçuk Nas

Dokuz Eylül University Maritime Faculty, Department of Maritime Education and Training, İzmir, Türkiye

Dear Readers,

It gives me great pleasure to present JEMS 12 (1) to our esteemed readers. Every day, more people are becoming interested in JEMS, and the editorial board and reviewers are becoming pickier. This issue includes some interesting and worthwhile studies. Without a doubt, the maritime area will benefit from these studies. I would like to thank the following people: the publishers, who produced high-quality publications by carefully adhering to our publication policies; our reviewers; the editorial board; the section editors; and the authors, who submitted their insightful studies for publication in this issue.

Best Regards,

Prof. Dr. Selçuk NAS

Editor in Chief

Address for Correspondence: Selçuk Nas, Dokuz Eylül University Maritime Faculty, Department of Maritime Education and Training, İzmir, Türkiye
E-mail: snas@deu.edu.tr
ORCID ID: orcid.org/0000-0001-5053-4594

Journal of ETA Maritime Science 2024;12(1):2-13

Optimization of Countermeasures to Stable and Protect Navigation Channels in Dinh An Estuary and Coastal of Tra Vinh Province, Vietnam

Viet Thanh Nguyen, Anh Dan Nguyen, Vinh An Le

Faculty of Civil Engineering, University of Transport and Communications, Hanoi, Vietnam

Abstract

The new navigation channel for large vessels entering the Hau River through the Kenh Tat and Quan Chanh Bo channels was announced in January 2016. The navigation channel route through Dinh An estuary in Soc Trang province to Can Tho port was not deeply concerned by the agency because of the sedimentation phenomenon, which was very serious and complicated. Only small vessels of 1,000-2,000 DWT can pass through the Dinh An estuary navigation channel, whereas large vessels pass through the Kenh Tat and Quan Chanh Bo channels. However, the new navigation channel entering the Hau River is also seriously sedimented, especially in the Cua Dai An area, where the tributary route starts from the Hau River through the Quan Chanh Bo channel and the estuary area in the Duyen Hai harbor basin. These are two important bottlenecks that drastically reduce the throughput capacity of this new navigation channel. This paper proposed five options for the spatial arrangement of works to stabilize and protect the channel through the Dinh An estuary. A MIKE 21 couple mode was used to simulate hydrodynamic and sediment transport in the study area, and the impact of these options on the characteristics, including water level, flow velocity, and bottom topographic change, was analyzed and evaluated. Based on these results, an optimal solution was suggested.

Keywords: Dinh An estuary, Hydrodynamic, Sediment transport, Tra Vinh province

1. Introduction

1.1. Literature Overview

Many seaports are located in estuaries, and the navigation channel entrance faces many challenges in maintaining the design water depth. Regulation work in estuaries and coastal areas has gained many experiences, such as the navigation channel in Mississippi, Changjiang, Qiantang, and Pearl River estuaries [1]. Estuary and coastal areas were more intensively exploited during this century because economic and demographic demands induced an increasing need for new land, better marine facilities for trade and other communications, and better protection against the sea.

The effects of training wall construction in the estuary of the River Lune, United Kingdom The effects of training wall construction in the estuary of the River Lune, United Kingdom, were investigated by the flow model of the morphological algorithm. The results showed that due to the training walls, the initial changes were artificially imposed on the Lune estuary before allowing the hybrid method to further simulate the evolution of the estuary, and these changes affected 5% of the volume of the estuary [2].

Based on the hypothesis that the deposition in Mersey was controlled by hydrodynamic flow and related sediment transport outside the estuary induced by training wall construction, the Mersey Estuary has now evolved toward a stable state. The results of the hydrodynamic model simulated in 1906, 1936, and 1977 estimated the potential sediment transport changes outside the Estuary. They indicated a significant increase in potential sediment supply to the mouth of the EEstuary during peak accretion [3].

Tönis et al. [4] investigated the development of the sand volume in the Haringvliet estuary, Netherlands, after

Address for Correspondence: Viet Thanh Nguyen, Faculty of Civil Engineering, University of Transport and Communications, Hanoi, Vietnam
E-mail: vietthanh@utc.edu.vn
ORCID ID: orcid.org/0000-0003-3964-2871

Received: 13.08.2023
Last Revision Received: 11.11.2023
Accepted: 04.12.2023

To cite this article: V. T. Nguyen, A. D. Nguyen, and V. A. Le. "Optimization of Countermeasures to Stable and Protect Navigation Channels in Dinh An Estuary and Coastal of Tra Vinh Province, Vietnam." *Journal of ETA Maritime Science*, vol. 12(1), pp. 2-13, 2024.

closure using bathymetric measurements from 1970, 1972, 1979, 1980, 1986, and 1990 until 1999. The results showed that the changes in sand volume above the Dutch Ordnance Level (NAP) of 10 m relative to 1970 had been determined. The area of these volumes was carefully chosen to diminish the effects of all other human interventions.

Zhao et al. [5] applied Delft 3D to study the combined effect of river discharge regulation and estuarine morphology on the salinity dynamics of the Yangtze estuary of the Changjiang River. The results indicate spatial changes in salinity due to the morphological evolution of the estuary.

In Vietnam, numerous researchers have studied estuarine regulation and achieved significant achievements in improving maritime and inland waterway transport. An evaluation of the back siltation volume of each excavation and dredging period from 2010 to 2014 in the Bach Dang navigation channel to Hai Phong port was conducted by Nguyen et al. [6]. The results indicated that numerous factors, such as sediment and hydrodynamic conditions, are the major reason for increasing back siltation in the Bach Dang navigation channel. Based on the research and solutions for preventing sedimentation in the Thuan An estuary and for protection from erosion of the coastline from the Thuan An to Hoa Duan coasts, a series of countermeasures were proposed, and an analysis of advantages and disadvantages was conducted to select the solution for the protection of coastal erosion and estuary stability [7]. Nguyen et al. [6] proposed two regulation schemes for improving water depth and reducing sedimentation in Phan Thiet fishing port, Binh Thuan province, Vietnam, and showed that capital dredging of the harbor basin and navigation channel is required according to scheme No. 1 and then careful monitoring of the effects of the scheme by follow-up surveys at least twice a year, and review of the plan taking into account the priority, timing, and extent of the facilities [8]. Nguyen et al. [9] investigated factors controlling the variation of sediment transport in the Nhat Le Estuary, Quang Binh province, Vietnam. The results showed that nearshore waves controlled sediment transport and estuarine morphology. Other research on the hydrodynamic and sediment transport of the Mekong River Delta has been conducted to provide solutions for coastal protection, erosion prevention, and estuary regulation [10-19].

1.2. Case Study

Navigation channels for large vessels entering the Hau River to load or unload cargo in Can Tho Ports play an important role in the development of the Mekong Delta economy. This study studied the Dinh An estuary's navigation channel, as shown in Figure 1. This dynamic and unstable channel has a high back siltation intensity [20-24]. The mechanism of back siltation discussed by Nguyen et al. [25] indicated that five factors control the back siltation process in the Dinh An navigation channel, including the increasing elevation gap between the channel and the nearby seabed, the disadvantages of the hydrodynamic regime, many sources of sediment, salt edge, and mixing and wave-induced sediment transport in the navigation channel.

Figure 1. *Study area of Dinh An estuary and the coast of Tra Vinh province*

Many scientists and consulting companies in Vietnam and other countries have conducted basic studies and proposed navigation channel routes to improve the water depth and stability of the navigation channel. In 1998, the Heacon consulting company from Belgium conducted a project titled "Feasibility Study for the Improvement of the Entrance Channel to the Bassac River" and proposed five options for the regulation of the navigation channel in Dinh An estuary. The navigation channel has a width of 100 m and depth of -4.7 m, allowing vessels 5,000 DWT to enter during the high tide period with 6 h of waiting time. The vessel's 20,000 DWT half load can be entered with a waiting time of approximately 4.5 h. If a vessel with 20,000 DWT half load entered continuously, the proposed channel width was 110 m. The basic dredged volume was approximately 2.8-3.0 million cubic meters of silt and exceptionally fine sand. The annual maintenance dredged volume was approximately 4.0 million cubic meters. Under extreme conditions, this volume reached approximately 5.0-5.5 million cubic meters [26].

The project "Feasibility study for improvement of the Bassac River" was conducted by SNC-Lavalin International Incorporation, Canada, in association with Royal Haskoning, Delft Hydraulics, the Netherlands, and Southern Transport Engineering Design Incorporation (TEDI-South), Vietnam in 2002 [23]. Based on the investigated data and assessment methods, they proposed four schemes of navigation channels, including a movable navigation channel, a fixed navigation channel (dredging or not dredging), a fixed

navigation channel that supplemented the discharge from the Tran De distributary, and a new channel from the Quan Chanh Bo channel and a new section of the bypass, as shown in Figure 1.

Dang and Nguyen studied the influence of the enlargement of the Quan Chanh Bo channel on hydrodynamic and sediment transport in the Dinh An estuary, Vietnam. The results indicated that the Quan Chanh Bo and Kenh Tat channels significantly changed the hydrodynamic, wave, and sediment transport modes of the Dinh An estuary and the surrounding coastal area. Particularly, when the current velocity in this area increased, the deposition in Dinh An decreased, while the deposition tended to increase in the Quan Chanh Bo channel. In addition, erosion was observed in the Kenh Tat channel [27].

Based on the new navigation channel from the Hau River to the Quan Chanh Bo channel and then to the Kenh Tat channel (Figure 1), the PortCoast Consultants studied hydrodynamics, wave transformation, and sediment transportation in a large-scale model and selected a new navigation channel combined with the Duyen Hai port. Two jetties protected the sea segment of the new navigation channel, and the entire navigation channel for large vessels entering the Hau River through the Kenh Tat and Quan Chanh Bo channels was put into use in January 2016. The new navigation channel was effective in the first few years. However, after approximately two years of use, sedimentation began to develop strongly, especially in the Dai An estuary, the Quan Chanh Bo channel entrance, and the Duyen Hai port basin [28]. Because of the appearance of the fluid mud layer in the navigation channel, sedimentation became more serious [29].

Nguyen and Zheng studied four regulation options to reduce deposition in the navigation channel of Dinh An estuary without the new channel (Figure 1). They proposed conducting capital dredging (Option 1) and conducting surveys at least twice a year. If the situation is negative, Option 2 should be selected for regulation in the navigation channel [30].

This article proposed five options (Option 2 to Option 6) for the spatial arrangement of works to stabilize and protect the channel through the Dinh An estuary. Hydrodynamic and sedimentary regimes in the study area were simulated using numerical simulation with a coupled model. Based on the results, this paper analyzed and evaluated the effect of proposal options on natural conditions (Option 1), such as water level, flow velocity, and bottom topographic change, and proposed the optimal solution.

2. Data Characteristics

The tidal regime in the Tra Vinh Sea is meso-tidal with tidal ranges from 2.5 to 4.1 m [25,31]. Wind data from 1988 to 2020 at Con Dao Island, far from the Tra Vinh coast, at approximately 150 km indicated that the dominant wind direction is W and SW in the summer and NE in the winter. The maximum wind speed is about 12 m/s in W and SW, and about 16 m/s in the NE [20]. Offshore wave at 9.17^0N, 107.08^0E, the wave height ranges from 0.88 to 3.58 m and the wave period changes from 4.3 to 9.6 s in the dry season. Wave height of 1.29 m and period of 5.8 s in the flood season.

The median particle size ranged between 2.5 and 3.9 μm. The percentage of clay fraction (particle size <2 mm) is approximately 15-20% of the suspended sediment [18,32]. sediment transport from the Bassac River had a high transport rate of approximately 22 million tons per year in 1992; however, it reduced to 47.4 million tons in 2020 [33].

3. Numerical Simulation and Verification

In this study, the MIKE 21 program was used in the simulation. The coupled model was constructed using Mike 21 HD, SW, and MT modules and verified by the observation data presented in [23]. The model with the computational domain covered the upstream (Tra Vinh and Dai Ngai stations) and adjacent areas around the Dinh An Estuary, with the plan dimensions being around 120x120 km. The south boundary, north boundary, and offshore boundary were approximately 50, 60 , and 70 km from the Dinh An Estuary, respectively. An overview of the model used in the analysis is shown in Figure 2.

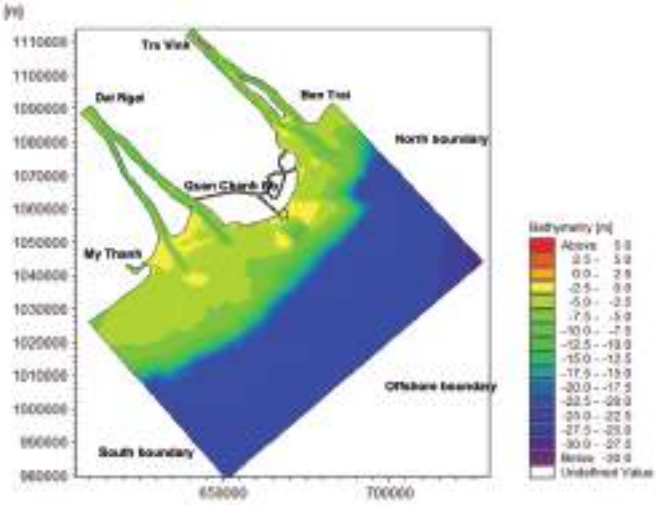

Figure 2. *Domain of the numerical model*

Hydrodynamics model setup with Tra Vinh, My Thanh, and Dai Ngai boundaries in the upstream and three boundaries in the sea. The discharges measured in November 2017 were used for three upstream boundaries. The water levels at My Thanh and Ben Trai were used for the South and North boundaries, respectively. Offshore boundary used

water level estimated from the Tide Prediction of height of Mike 21 Tool box, and the data was calibrated by the water level at My Thanh and Ben Trai stations.

The spectral wave model setup based on the model suggestion, the offshore wave boundary applied measurement data at W7 (9°30'0.00" N, 106°30'0.00" E) in November 2017 with maximum wave height and period of 2.54 m and 12.99 s. The mean wave direction was 58.85^0. South and North are parallel boundaries. The three upstream boundaries are closed boundaries.

Mud transport model setup based on suspended sediment concentration (SSC) measured in three upstream boundaries. The North and South boundaries applied the section boundaries type with SSC ranges from 0 (in offshore) to 0.15 kg/m^3 nearshore. The offshore boundary SSC is zero.

The coupled model was continuously verified using observation data in November 2017 [34]. The coupled model performance was assessed using the mean absolute error and root mean square error between the observed and simulated data [35,36]. The observed data were collected at point W7 (9°30'0.00" N, 106°30'0.00" E), far from the shoreline of about 5.5 km, from 12 to 18/9/2017. The results of the verification are shown in Table 1.

Table 1. *RMSE and MAE for model verification*

Parameters	RMSE	Difference (%)	MAE	Difference (%)
Water level at Ben Trai (m)	0.23	7.0	0.21	5.7
Water level at Dai Ngai (m)	0.28	8.5	0.27	7.8
Water level at My Thanh (m)	0.11	4.0	0.10	2.8
Water level at Tra Vinh (m)	0.20	6.8	0.16	5.3
Salinity at Ben Trai (PSU)	1.2	20.3	1.1	19.4
Salinity at Dai Ngai (PSU)	1.1	18.2	0.9	14.2

As mentioned above, this study conducted numerical analysis for six options. Option 1 was simulated with the existing state (without any structures), as shown in Figure 3. From Options 2 to 6, there were five solutions with different layouts of structures. This paper evaluated the advantages and disadvantages of each Option from 2 to 6 and then compared them with Option 1. On the basis of these comparisons, the most reasonable option was proposed.

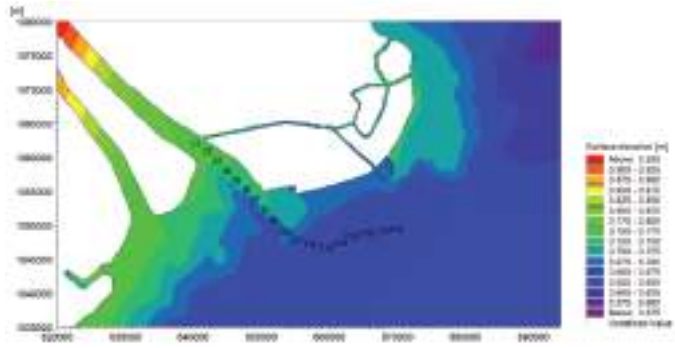

Figure 3. *Layout of Option 1 (Without structures)*

Figure 4 shows the layout of Option 2. This option is proposed to provide a defined channel by two jetties between the river mouth on both sides. There were two jetties running along the navigation channel. The north jetty started at the Ho Tau headland and consisted of two segments. The length of the first segment (N1) was 5.03 km, that of the second segment (N2) was 4.35 km, and that of the third segment (N3) was 10.14 km. The south jetty has three-segment symbols of S1, S2, and S3, with lengths of 16.45, 7.06, and 10.44 km, respectively. It departed from the right bank of the estuary, including. The crest level of all structures determined on the basis of the TCCS 02:2017/CHHVN [37] was +4.0 m (CD system). The heads of the two jetties were extended until a contour line of -9.0 m. The total length of the two jetties was 54.47 km. This option only focused on the stability and protection of the navigation channel in the Dinh An estuary.

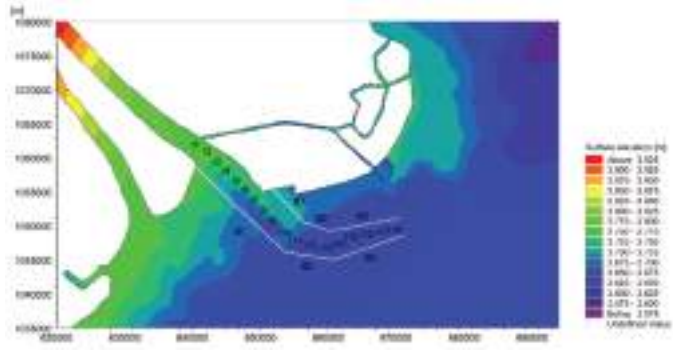

Figure 4. *Layout of Option 2*

Option 3 provided a channel defined by a jetty on the south bank of the navigation channel, which is the same as Option 2, as presented in Figure 5. Three groins, N1, N2, and N3, were located on the north bank of the Dinh An estuary. Groin N1 started at Ho Tau headland and had a length of 4.42 km, groin N2 had a length of 6.15 km, and groin N3 had an length of 8.75 km. The total length of the structures

was 53.27 km, and the crest level of all structures was +4.0 m (CD system). Three groins regulate river and coastal flow to stabilize the navigation channel and limit erosion in the coastal area from north of the Dinh An estuary to the Duyen Hai port.

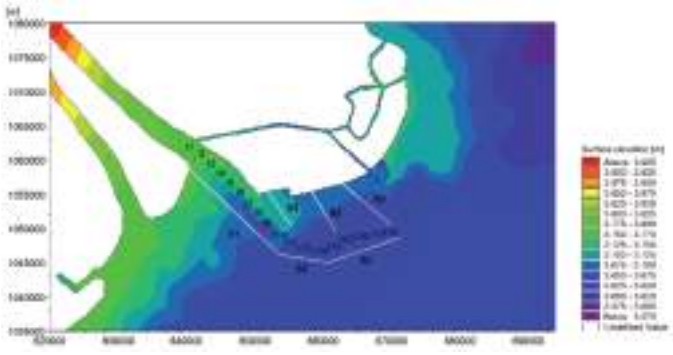

Figure 5. *Layout of Option 3*

The layout of Option 4 is shown in Figure 6. Option 4 had the south jetty the same as Option 2. On the north bank, there were two groins and two detached breakwaters. The groins N1 and N3 were the same as Option 3, and the two detached breakwaters D2 and D3 had lengths of 5.08 km and 4.44 km, respectively. Groin N3 was the same as N3 in Option 3, with an 8.75 km length. The total length of the structures was 56.64 km, and the crest level of all structures was +4.0 m. Two groins (N1 and N3) were combined with two detached breakwaters (D2 and D3) to reduce wave energy and coastal erosion of the Tra Vinh coast.

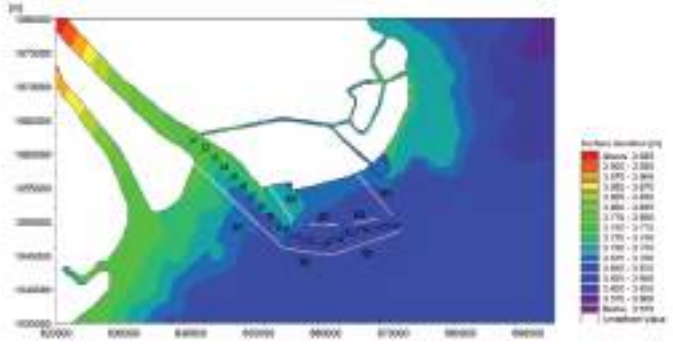

Figure 6. *Layout of Option 4*

The layout of Option 5 was the same as that of Option 4. However, groin N3 north of the estuary was excluded, as shown in Figure 7. The length of the detached breakwater D2 was 6.03 km. The total length of the structures was 49.48 km, and the crest level of all structures was +4.0 m (CD system). This option also mainly focused on the stability of the navigation channel, and it could reduce the southeast wave impacting the coast of Tra Vinh province.

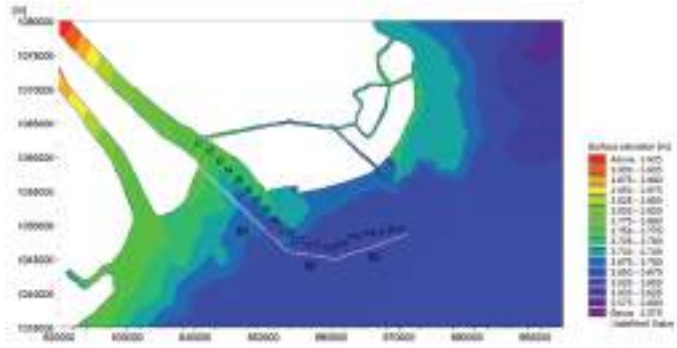

Figure 7. *Layout of Option 5*

Figure 8 illustrates the layout of Option 6. It had a south jetty like Option 2 and a T-shaped groin north of the estuary. The T-shaped groin had two segments: segment N1 had a 7.81 km length and segment N2 had a 7.56 km length. The total length of the structures was 49.32 km, and the crest level of all structures was +4.0 m (CD system). This alternative protected the channel and the coast of Tra Vinh province from waves generated by both northeast and southeast winds.

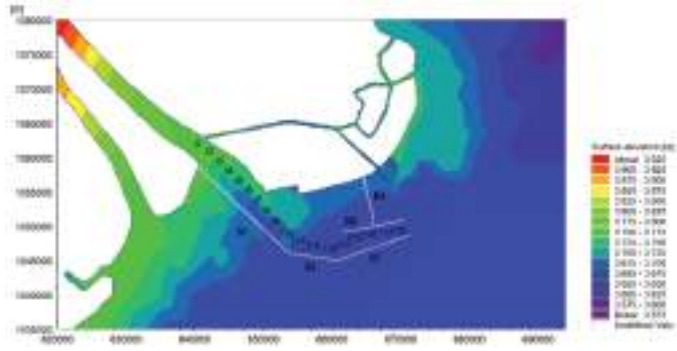

Figure 8. *Layout of Option 6*

The verification results in Table 1 indicate that the coupled model was consistent with the observation data and had the reliability to simulate hydrodynamics, wave propagation, and sediment transport. After model verification, six options were simulated by the coupled model in the dry season (May 2004) and flood season (Sep 2004). The numerical model analyzed the influence of countermeasures on water level, current speed, and bed thickness change. Based on the characteristics of these factors, this study adopted countermeasures for the stability and protection of the navigation channel in Dinh An estuary.

4. Results and Discussion

4.1. Change in Water Level

The water level changed due to regulation structures through 18 points symboled from T1 to T18 along the

navigation channel (The locations of 18 points are shown in Figure 3). The maximum, minimum, and average water levels of Options 1 to 5 changing along the navigation channel were compared with those of Option 1 (without structures).

A comparison of the maximum water level changes along the navigation channel of the five options in the dry season is plotted in Figure 9a. The results indicated that the regulation structures reduced the water level along the navigation channel. Options 3 and 6 were similar and gave the lowest values with a maximum water level lower than Option 1, approximately 0.35-0.67 m. In contrast, Option 5 showed the highest maximum water level among the five options. It was just lower than Option 1, around 0.07 to 0.31 m.

The results of the minimum water level change along the navigation channel shown in Figure 9b demonstrate that the presentation of regulation structures led to an increase in the minimum water level along the navigation channel. The minimum water level of Option 2 from T1 to T14 increased from 0.42 to 0.75 m and then rapidly decreased; in Option 3, it increased from 0.37-0.64 m from T1 to T16 and rapidly decreased and was only higher than Option 1 by approximately 0.12-0.13 m; in Option 4, it gradually increased by approximately 0.16-0.46 m; in Option 5, it increased from 0.16-0.38 m from T1 to T14 and then rapidly decreased; and in Option 6, it increased from 0.45-0.63 m from T1 to T15 and then rapidly decreased. However, it was still higher than Option 1, about 0.08-0.15 m.

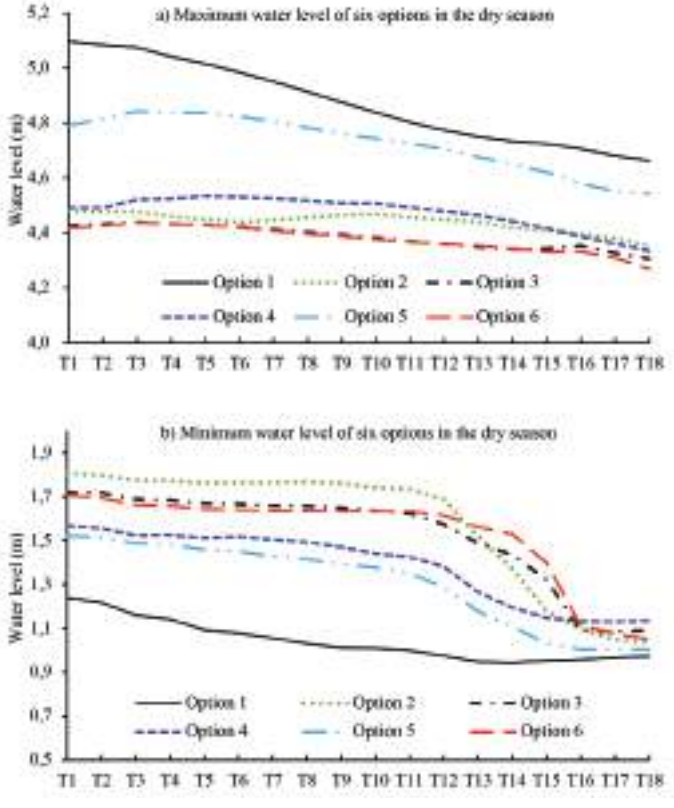

Figure 9. *Comparison of the maximum and minimum water levels of the six options in the dry season*

The average water level change along the navigation channel of the six options in the dry season is plotted in Figure 10. The result indicated that, after arranging the regulation structures, the average water level undergoes two distinct periods with a division around T14 and T15; from T1 to T15, the average water level was higher than Option 1, and from T15 to T18, it was lower than Option 1. This showed that the water level change of Option 4 gradually changed along the navigation channel.

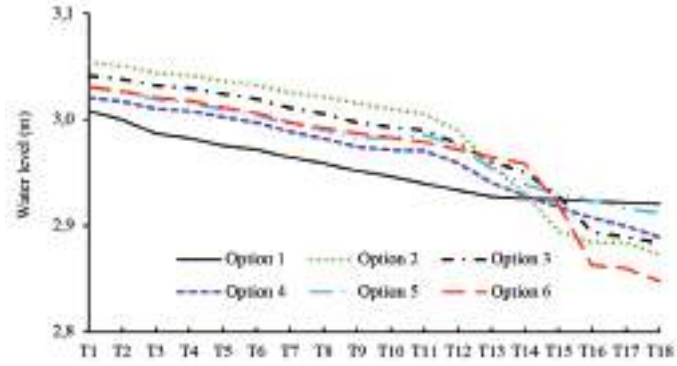

Figure 10. *A comparison of the average water level of the six options in the dry season*

In the dry season, the results indicate that Options 4 and 5 caused gradual changes in water levels. Two options did not cause the water level to change dramatically as the remaining options, especially in the area from T12 to T16. Similarly, the water level changed through 18 points along the navigation channel due to the regulation structures. The results of the maximum, minimum, and average water level changes in the six options are summarized as follows.

The maximum water levels of the five options of regulation work are lower than Option 1. In Option 2, it decreased from 0.25 to 0.16 m from T1 to T14 and then increased slightly from T15 to T18. However, it was still lower than that in Option 1, from 0.16 to 0.19 m; in Option 3, the maximum water level decreased from 0.18 to 0.33 m from T1 to T15, and then it increased about 0.16-0.21 m from T15 to T18. Option 4 gradually decreased by about 0.11-0.22 m along the navigation channel; Option 5 gradually decreased from T1 to T10 and then changed slightly offshore; Option 6 changed the maximum water level like Option 1. However, it was lower than Option 1, about 0.2-0.3 m (Figure 11a).

Figure 11b shows the results of the minimum water level change along the navigation channel. The regulation structures led to an increase in the minimum water level along the navigation channel. The water level changed

slightly in Option 2 from T1 to T10. It was higher than Option 1, about 0.60-0.77 m. However, from T11 to T18, it rapidly decreased and was only higher than Option 1, approximately 0.05 m. In Option 3, it mostly remained stable from t1 to t6 and then gradually decreased from T5 to T12. After that, it decreased from T13 to T16 and remained constant from T17 to the sea. Option 4's minimum water level was higher than that of Option 1. It increased slightly from T1 to T6 and then gradually decreased from T6 to T13. It slowly decreased from T13 to T16 and did not change from T17 to the sea. The water level in Option 5 was the same as that in Option 4. However, the water level change intensity was smaller than that in Option 4. In Option 6, it slightly changed from T1 to T13 and rapidly decreased from T13 to T16. Finally, it stabilized in the offshore area.

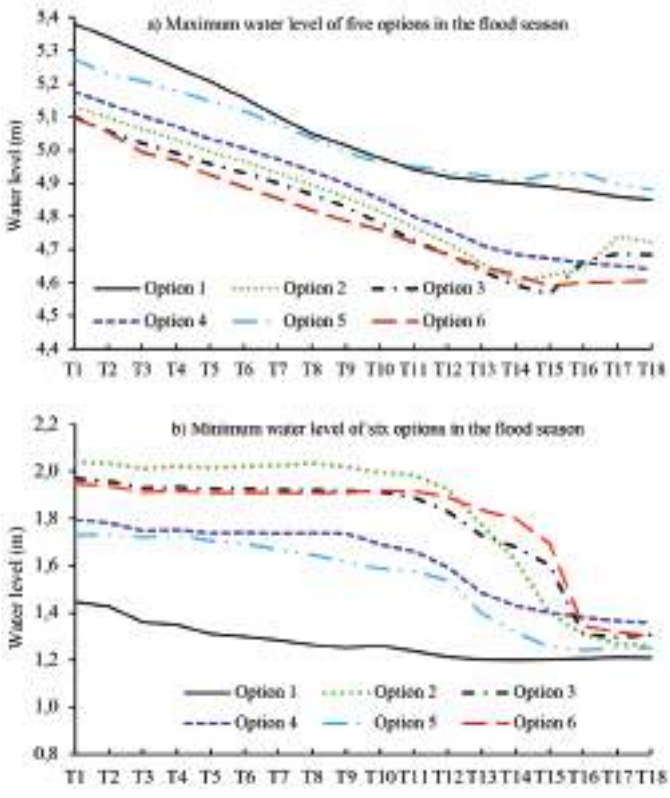

***Figure 11**. A comparison of the minimum water level of six options in the flood season*

The average water level change along the navigation channel of the six options in the flood season is plotted in Figure 12. As shown in the figure, after arranging the regulation structures, the average water level was higher than that of Option 1. The highest value occurred in Option 2. Option 2, 3, and 6 rapidly decreased from T12 to T16. Option 4 and 5 gradually decreased along the navigation channel, and Option 5 was lower than the others. The results also indicated that the two options, 4 and 5, did not cause dramatic water level changes compared with the other options, especially in the area from T12 to T16.

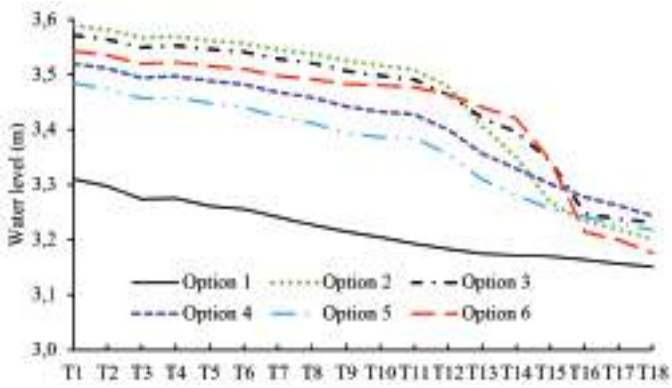

***Figure 12**. A comparison of the average water level of the five options in the flood season*

4.2. Current Speed Change

In this section, the speed of the high flood tide, high ebb tide, low flood tide, and low ebb tide currents in the dry season changed because of the regulation structures considered through 18 points along the navigation channel (The locations of 18 points were shown in Figure 3).

The maximum high flood tide current speed along the navigation channel is plotted in Figure 13a. The result indicated that after arranging the regulation structures, the maximum current speed of Options 2, 3, and 6 underwent two distinct periods with a division at T13. From T1 to T12, the maximum high flood tide current speed of the five options was lower than that of Option 1. However, from T13 to T18, they increased and increased. These options showed a high current speed increase dramatically from T14 to T18. The result of Option 4 showed undergoing two distinct periods with the division point at T12. From T1 to T12, it fluctuated around 1.0; from T14, it increased significantly toward the seaside. For Option 5, the trend from T1 to T12 was mostly similar to Option 4, but from T12, it was the opposite, with the current speed decreasing.

The average high flood tide current speed change along the navigation channel is plotted in Figure 13b. The figure shows that the regulation structures of Options 2 and 6 decreased the current speed from section T1 to T11. However, the current speed rapidly increased again from T11 to T16. Options 4 and 5 showed that the current speed was reduced and lower than that of Option 1 from section T1 to T5, then increased and higher than Option 1. From sections T14 to T18, the current speed of Option 4 increased significantly, while Option 5's speed decreased slowly, similar to the trend of Option 1.

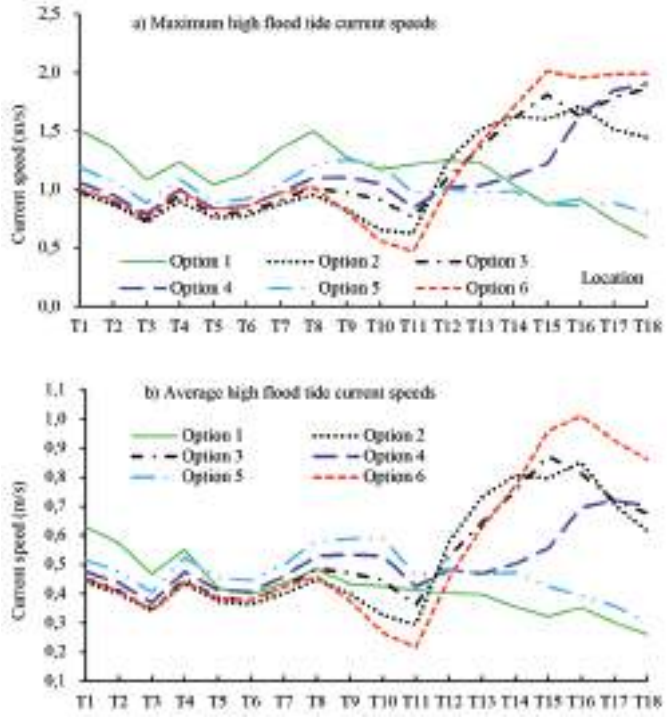

***Figure 13**. High flood tide current speeds during changes in the dry season*

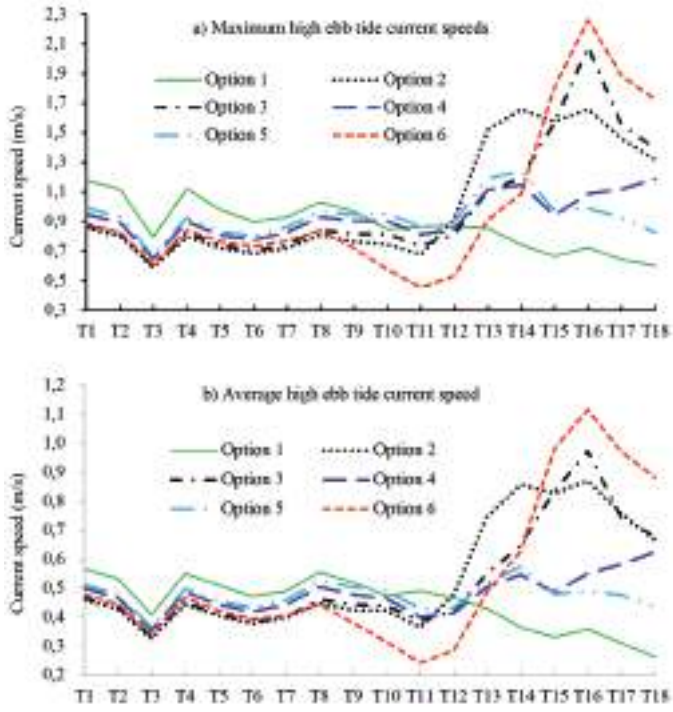

***Figure 14**. High ebb tide current speed changes during the dry season*

Figure 14a presents the results of the maximum high ebb tide current speed change along the navigation channel. After arranging the regulation structures, the maximum current speed of all options underwent two distinct periods with a division at section T13. From section T1 to T12, the maximum high ebb tide current speed was lower than that of Option 1, except for Options 4 and 5 in section T10. From section T13 to T18, they increased and were higher than those of Option 1. Especially in Options 3 and 6, the current speed increased dramatically and peaked at section T16 with a value equal to three times that of Option 1.

Figure 14b plots the average high ebb tide current speed change in the dry season. Similar to the maximum average of high ebb, tide current speeds changed along the navigation channel and underwent two distinct periods with a division at section T13. From sections T1 to T12, the average high ebb tide current speed was lower than that of Option 1. However, from sections T13 to T18, they were larger than those of Option 1. The results also showed that Options 2, 3, and 6 conducted high-current speeds in the offshore navigation channel, especially at section T16.

The results indicated that Options 4 and 5 induced a moderate current speed change. Both options induced an increase in the current speed in the curvature and offshore segments (from section T13 to T18) of the navigation channel.

The maximum high flood tide current speed change along the navigation channel during the flood season is plotted in Figure 15. The result indicated that the regulation works of Options 2, 3, and 6 changed underwent two distinct periods with a division at section Tt13. From sections T1 to T12, the current speed was reduced and lower than that of Option 1. However, from section T13 to T18, it increased and was higher than Option 1 by approximately twice. In Option 6, the current speed increased dramatically and reached its highest point at section T16. In Option 4, the current speed gradually changed from T1 to T15 and rapidly increased in the offshore part of the navigation channel. In Option 5, the current speed was changed and was almost lower than that in Option 1. The result showed that in section T11, the current speed was the lowest.

The average high flood tide current speed change along the navigation channel is plotted in Figure 16a. The results show that the regulation structures of Options 2, 3, and 6 changed and underwent two distinct periods with a division at T11. From T1 to T12, the current speed was lower than that of Option 1. However, from T13 to T18, it was significantly increased and larger than Option 1 by approximately two times. In Option 6, from section T11 to T16, it increased six times. In Option 4, the current speed gradually changed from T1 to T15 and rapidly increased. In Option 5, the current speed changed slightly, and the current range of Option 5 was the smallest.

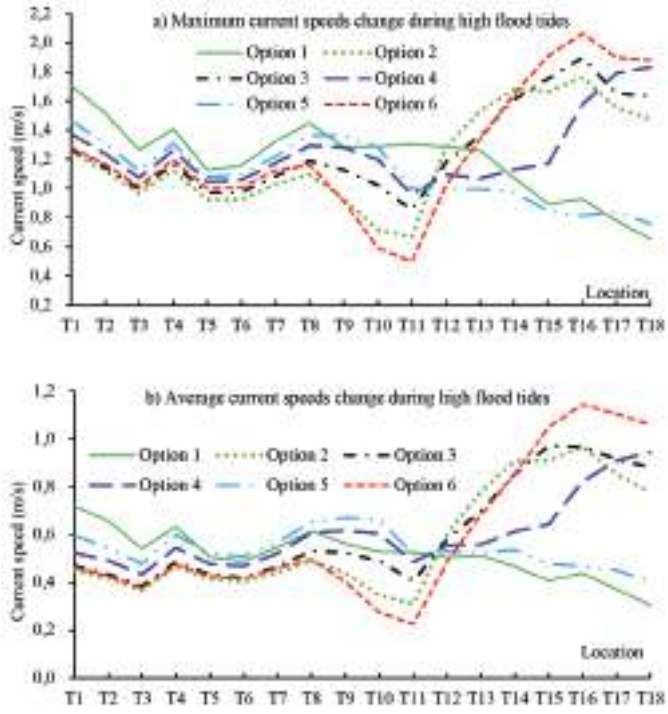

***Figure 15**. Current speeds change during high flood tides during the flood season*

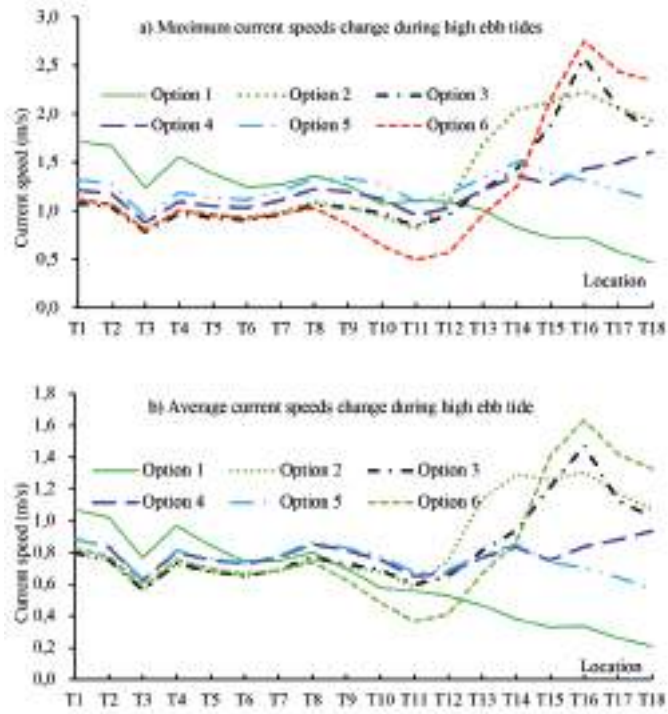

***Figure 16**. Current speeds change during high ebb tides in the flood season*

The maximum high ebb tide current speed results are plotted in Figure 16b, which shows that the current tended to decrease upstream of the navigation channel. Subsequently, it increased from section T13 to T18, especially Options 2, 3, and 6. For the average high ebb tide, the current speed showed the same trend as the maximum current speed, as shown in Figure 16. These results indicated that Options 4 and 5 induced a medium change in the current speed. Both options increased the current speed at the offshore part of the navigation channel.

4.3. Change in the Longitudinal Profile of the Navigation Channel

The bed thickness change of the longitudinal profile of the navigation channel during the flood season is presented in Figure 17. The results showed that Options 1, 2, 5, and 6 induced depositions in the navigation channel. Options 1 and 5 induced deposition in the offshore part, whereas Options 2 and 6 did so around section T11. In contrast, Options 3 and 4 caused erosion of the navigation channel, and the erosion intensity of Option 4 was higher than Option 3.

The change in bed thickness of the longitudinal profile of the navigation channel in the dry season is presented in Figure 18. As seen from the figure, in Option 1, deposition appeared in the estuary and offshore part of the navigation channel. Erosion was observed in the middle of the navigation channel. In Option 2, high deposition occurred

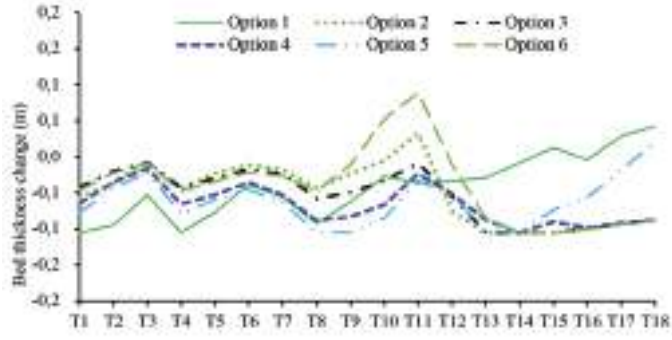

***Figure 17**. Total change in seabed thickness along the navigation channel in the flood season*

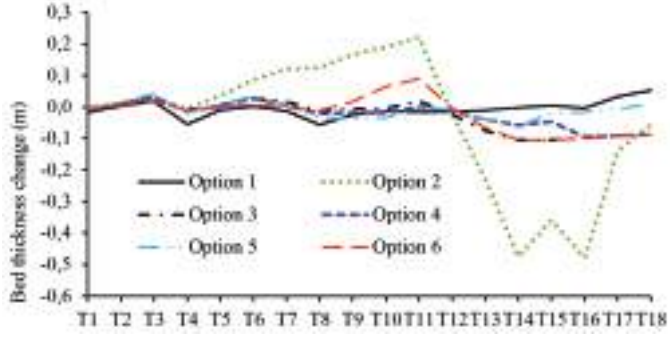

***Figure 18**. Bed thickness changed along the navigation channel during the dry season*

from the estuary to section T11, and the navigation channel was eroded from section T12 to offshore and especially from section T14 to T16. The channel bed eroded significantly by 0.45 m after 18 days. In Option 3, the channel bed deposited slightly from section T1 to T11 and eroded from T11 to T18. The erosion was approximately 0.1 m after 18 days. In Option 4, the deposition was found in sections T2 to T7. The erosion was presented from sections T8 to T18, increasing at the offshore part of the navigation channel. Option 5 increased the deposition at the offshore part of the navigation channel, whereas in Option 6, the channel bed was deposited in the upstream part, especially around sections T10 and T11.

4.4. Evaluate the Advantages and Disadvantages of the Options

Option 1 (Without structures) meets the natural equilibrium and supports environmental values with minimal human impact. Without any technical solutions, it will reduce the impact on the environment. The tidal flats stabilize without continual disturbance, and the ecosystem matures. It becomes more available as a habitat for invertebrates and a feeding area for wading and other birdlife. However, some disadvantages could occur, such as potential perceived negative implications for flood management and a possible negative impact on the ports and back siltation often occurring in the navigation channel.

In Option 2, the structures removed the constant, which was needed to dredge the navigation channel, increase the channel flow velocity, induce sediment in suspension, and prevent deposition. Aesthetics were improved by removing "unsightly" mud flats in the Dinh An estuary, and the people enjoyed the benefits of a large recreational area on the foreshore on both sides of the jetties. In addition, it reduced greenhouse gas emissions from dredging activities. Option 2 dramatically changed the water level and current speed for the disadvantage, especially from sections T11 to T16. The results also indicated high deposition at Dinh An Estuary and the head of the north jetty. The deposition at the head of the north jetty tended to move south during the flood season. The erosion occurred significantly from section T13 to T17, and the erosion depth reached 1.2 m in the dry season. A major discharge of greenhouse gasses was released during construction activities. There was a considerable risk of damage during flooding due to overtopping, saturation, debris, and potential perturbations to the north jetty area related to changed tidal conditions (reduced tidal prism).

The structures of Option 3 removed the constant that needed to dredge the navigation channel, improved opportunities for reclamation activities around the groin system, and recreational and water sports-based tourism. It reduces greenhouse gas emissions from dredging activities. However, the drawback included dramatically changing the water level and current speed, especially from sections T15 to T18. Potential deposition occurred in groin systems. The deposition area in the northeast of groin N3 moved southward, and a huge volume of greenhouse gasses was spread during construction activities. The unconsolidated area for the new channel presented difficulties due to the slippage loss of mudflats, which induced biodiversity and ecological habitat loss. The risk of damage during flooding is lower than that of Option 2.

The good point of Option 4 was the removal of the constant need to dredge the navigation channel. In addition, it increased the current speed in the navigation channel to keep the sediment in suspension and reduce deposition. Thus, it improved the opportunities for reclamation activities in the north bank for recreational and tourism water sports-based activities. It also reduces greenhouse gas emissions from dredging activities. The disadvantages could appear, such as potential deposition between groins and detached breakwaters, and a huge volume of greenhouse gasses can be spread during construction activities. The unconsolidated area for the new channel presented difficulties from slippage-loss of mudflats induced biodiversity and ecological habitat loss, potential perturbations to the groin area related to changes in tidal conditions (reduced tidal prism), and loss of intertidal and associated environmental impacts.

Option 5 had benefits similar to Option 4. The advantages of Option 6 were the same as those of Option 4, and the disadvantages consisted of potential deposition at both sides of the T-shaped groin, and the others were the same as Option 5.

4.5. Selection Criteria

A multi-criteria analysis process includes reviewing the critical aspects of technical, environmental, social, and economic impacts as follows:

a. Technical criteria

- The structures eliminate the constant need to dredge in the navigation channel.
- Increase current speed in navigation to keep sediment in suspension and reduce deposition.
- Ensure safety of vessel operation in the navigation channel.
- Improved opportunities for reclamation activities.

b. Environmental impact criteria

- Aesthetics are improved by removing "unsightly" mud flats in the Dinh An estuary.

- Reduced greenhouse gas emissions from dredging activities.

The public may benefit from the recreational area on the foreshore.

c. Social and Economic Impact Criteria

- Improved opportunities for recreational and tourism activities.
- Local economic growth.
- Flood mitigation.

4.6. Propose Countermeasures for the Navigation Channel in the Dinh An Estuary

The results above and the selection criteria showed that Option 4 almost satisfied the requirements. The main characteristics of Option 4 were as follows:

- The south jetty consists of three segments: S1 has 16.45 km, S2 has 7.06 km, and S3 has 10.44 km.
- Groin N1 started at Ho Tau headland and has a length of 4.42 km, and the N3 groin has an 8.75 km length.
- Detached breakwaters D2 and D3 are 5.08 km and 4.44 km long, respectively.
- The total length of the structures was 53.27 km.
- The crest level of all structures was +4.0 m (CD).

5. Conclusion

Countermeasures significantly influence the hydrodynamics and sediment transport of the Dinh An estuary and coastal Tra Vinh province. The maximum water levels of all proposal options in the dry and flood seasons are lower than natural conditions (Option 1), while the minimum water levels of the five options in both the dry and flood seasons are higher than natural conditions (Option 1). The average ebb tide current speed increases in the offshore segment that provides flow to keep the sediment moving and prevent sedimentation in the navigation channel. Option 4 was proposed to satisfy almost all requirements of the technical, environmental impact, social, and economic impact criteria.

Authorship Contributions

Concept design: V. T. Nguyen, Data Collection or Processing: V. T. Nguyen, Analysis or Interpretation: V. T. Nguyen, A. D. Nguyen, and V. A. Le, Literature Review: V. T. Nguyen, A. D. Nguyen, and V. A. Le, Writing, Reviewing and Editing: V. T. Nguyen, A. D. Nguyen, and V. A. Le.

Funding: This study was financially supported by the Ministry of Education and Training (Vietnam), grant number CT 2022.01.GHA.06.

References

[1] J. Chen, D. Eisma, K. Hotta, and H. J. Walker, *Engineered Coasts* in *Coastal Systems and Continental Margins* B.U. Haq, Editor. 2002, Springer-Science+Business Media, B.V.

[2] J. R. Spearman, M. P. Dearnaley, and J. M. Dennis, "A simulation of estuary response to training wall construction using a regime approach." *Coastal Engineering,* vol. 33, pp. 71-89, May 1998.

[3] C. G. Thomas, J. R. Spearman, and M. J. Turnbull, "Historical morphological change in the Mersey Estuary." *Continental Shelf Research,* vol. 22, pp. 1775-1794, Jul-Aug 2002.

[4] E. Tönis, J. M. T. Stam, and J. van de Graaf, "Morphological changes of the Haringvliet estuary after closure in 1970." *Coastal Engineering,* vol. 44, pp. 191-203, Jan 2002.

[5] L. Zhao, P. Xin, H. Cheng, and A. Chu. "Combined effects of river discharge regulation and estuarine morphological evolution on salinity dynamics in Yangtze Estuary, China." *Estuarine, Coastal and Shelf Science,* vol. 276, pp. 108002, Oct 2022.

[6] V. T. Nguyen, M. D. Do, and M. T. Vu, *Back siltation in Bach Dang navigation channel, Nam Trieu Estuary, Vietnam*, in *River Sedimentation*, S.H. Silke Wieprecht, Karolin Weber, Markus Noack, Kristina Terheiden, Editor. 2016, CRC Press: London, UK.

[7] T. V. An, L. P. Hau, H. H. Khanh, and L. G. Vu, *General research and solution for preventing sedimentation in the Thuan An estuary and for protection from erosion of the coastline from Thuan An to Hoa Duan coasts*. 1999, Vietnam Instute of Water Resources Research: Hanoi, Vietnam (in Vienamese).

[8] N. V. Thanh, *Study of the improvement regulation schemes for Phan Thiet fishing port, Binh Thuan, Vietnam.* 2016 International Conference on Sustainability in Civil Engineering (ICSCE 2016) 26 - 27 November, 2016, Hanoi, Vietnam. (Special issue on sustainability in civil engineerings): *The Transport Journal,* pp. 242-245, 2016.

[9] H. T. Nguyen, C. D. Vu, H. V. Nguyen, and T. D. Nguyen, (2020). *Factors Controlling Variation in Sediment Transport at Nhat Le Estuary*. In: Trung Viet, N., Xiping, D., Thanh Tung, T. (eds) APAC 2019. APAC 2019. Springer, Singapore.

[10] T. Letrung, Q. Li, Y. Li, T. Vukien, and Q. Nguyenthai, "Morphology Evolution of Cuadai Estuary, Mekong River, Southern Vietnam." *Journal of Hydraulic Engineering,* vol. 18: pp. 1122-1132, 2013.

[11] L. T. Thanh, Detection the erosion and deposition processes of Ham Luong Estuary, Mekong River, in *The Spring World Congress on Engineering and Technology (SCET) 2012*. 2012: Xian, China. pp. 6.

[12] V. Q. Thanh, J. Reyns, C. Wackerman, E. Eidam, and D. Roelvink, "Modelling suspended sediment dynamics on the subaqueous delta of the Mekong River." *Continental Shelf Research,* vol. 147, pp. 213-230, Sep 2017.

[13] L. X. Tu, *Research on reasonable solutions and appropriate technologies to prevent erosion and stabilize the coast and the estuaries of the Mekong River, from Tien Giang to Soc Trang*, 2022, Vietnam Academy for Water Resources Research (in Vietnamese).

[14] L. X. Tu, et al. "Sediment transport and morphodynamical modeling on the estuaries and coastal zone of the Vietnamese Mekong Delta." *Continental Shelf Research,* vol. 186, pp. 64-76, Sep 2019.

[15] V. T. Nguyen, M. T. Vu, A. D. Nguyen, V. T. Nguyen, and J. Zheng. *Overview of estuary research and waterway engineering in Vietnam*. in *Proceedings of the 35th 2013 IAHR World Congress (Chengdu 2013*). Chengdu, Sichuan, China: Tsinghua University Press.

[16] V. V. Anikiyev, et al. "Variation in the time-space distribution of suspended matter in the coastal zone of the Mekong River." *Oceanology,* vol. 26, pp. 725-729, 1986.

[17] B. N. Thi, T. Tran, N. K. Phung, and T. Nguyen-Quang, "Numerical investigation on the sediment transport trend of can gio coastal area (Southern Vietnam)." *Journal of Marine Environmental Engineering,* pp. 1-20, Jan 2013.

[18] E. Wolanski, N. N. Huan, L. T. Dao, N. H. Nhan, and N. N. Thuy, "Fine-sediment dynamics in the Mekong River Estuary, Vietnam." *Estuarine, Coastal and Shelf Science,* vol. 43, pp. 565-582, Nov 1996.

[19] V. D. Vinh, S. Ouillon, N. V. Thao, and N. N. Tien. "Numerical simulations of suspended sediment dynamics due to seasonal forcing in the mekong coastal area." *Water,* vol. 8, pp. 255, Jun 2016.

[20] T. V. An, *Study the solutions to stabilized bed of channel in Dinh An estuary service to waterway transport,* in States level project, No. 2003/19, Vietnam Ministry of Science and Technology (in Vietnamese). 2005.

[21] U. N. Manh, *Feasibility study of improvement of Dinh An navigation channel entrance Can Tho port*. 1997, Waterway Construction and Service Company, Vietname Ministry of Transport (In Vietnamese). Hanoi.

[22] V. T. Nguyen, J. H. Zheng, and L. P. Hau. *Morphological evolution of navigation channel in Dinh An estuary, Vietnam* in *7th IAHR Symposium on River, coastal and estuarine morphodynamics*. 2011. Beijing: Tsinghua University Press.

[23] T. N. Viet, *Morphological evolution and back siltation of navigation channel in Dinh An Estuary, Mekong River Delta: understanding, modelling and soluting*. 2012, PhD Thesis, 2012, Hohai University: Nanjing, China.

[24] PORTCOAST, *Feasibility project of the waterway for heavy-tonnage ships to enter the Hau River. Final Report* (in Vietnamese).

[25] V.-T. Nguyen, J.-h. Zheng, and J. S. Zhang, "Mechanism of back siltation in navigation channel in Dinh An Estuary, Vietnam." *Water Science and Engineering,* vol. 6, pp. 178-188, Apr 2013.

[26] Haecon, *Feasibility Study for the Improvement of the Entrance Channel to the Bassac River (Vietnam)* 1998, Mekong River Commission: Can Tho.

[27] D. D. Nguyen, and N. V. Thanh, *Influence of enlargement of Quan Chanh Bo channel on hydrodynamic and sediment transport in Dinh An estuary, Vietnam*. in *Proceedings of the 19th IAHR-APD Congress 2014*. Hanoi, Vietnam: Construction Publishing House.

[28] PECC2, *Report on sedimentation assessment and adjustment of process, annual plan for sediment inspection, dredging and maintenance of Duyen Hai Port*. 2018, Power Engineering Consulting Joint Stock Company 2 (in Vietnamese).

[29] L. V. An, N. V. Thanh, Y. Nakagawa, and N. V. Bo, "Investigation of fluid mud in Duyen Hai port, Tra Vinh province." *Transport and Communications Science Journal,* vol. 71, pp. 553-567, Jun 2020.

[30] Nguyen, V.T. and J.H. Zheng, "Preliminary Study of Regulation Schemes for Navigation Channel in Dinh An Estuary, Vietnam." *Applied Mechanics and Materials,* vol. 212-213, pp. 117-122, Oct 2012.

[31] J. L. Davies, "A morphogenic approach to world shorelines." *Zeitschrift für Geomorphologie, vol*. 8, pp. 127-142, 1964.

[32] S. M. Gagliano, and W. G. McIntire, *Reports on the Mekong River delta,* Coastal Studies Institute Technical Report No. 57, Editor. 1968, Louisiana State University. pp. 143.

[33] N. V. Thanh, *Siltation of the navigation channels in the Mekong River Delta, Vietnam*. in PIANC Asian Seminar 2023-Siltation of Navigation Channels in Asian Region. 2023. Tokyo, Japan: PIANC-Japan.

[34] N. V. Thanh, *Investigation of the impact of the bypass channel and Duyen Hai Thermal Power Center's hydraulic works on the flow field and topographic changes in the coastal area of Tra Vinh province*, University of Transport and Communications (2023).

[35] V. T. Nguyen, M. T. Vu, and C. Zhang, "Numerical investigation of hydrodynamics and cohesive sediment transport in Cua Lo and Cua Hoi Estuaries, Vietnam." *Journal of Marine Science and Engineering,* vol. 9, pp. 1258, Nov 2021.

[36] M.-H. Hsu, A. Y. Kuo, J.-T. Kuo, and W.-C., Liu, "Procedure to calibrate and verify numerical models of estuarine hydrodynamics." *Journal of Hydraulic Engineering,* vol. 125, pp. 162-182, Feb 1999.

[37] Vinamarine, TCCS 02:2017/CHHVN *Breakwater - Design Requirements*. 2017: Hanoi, Vietnam (in Vietnamese).

Journal of ETA Maritime Science 2024;12(1):14-24

Investigation of Scale Effects on Linear Vertical Maneuvering Derivatives of a Submarine

Emre Kahramanoğlu[1], Savaş Sezen[2], Ferdi Çakıcı[3]

[1]İstanbul Technical University Faculty of Maritime, Department of Marine Engineering, İstanbul, Türkiye
[2]Lloyd's Register EMEA, Southampton, United Kingdom
[3]Yıldız Technical University Naval Architecture and Maritime Faculty, Department of Naval Architecture and Marine Engineering, İstanbul, Türkiye

Abstract

This paper aims to show the scale effects of vertical maneuvering derivatives for an underwater vehicle using computational fluid dynamics (CFD). The model scale and full-scale benchmark DARPA suboff hull forms were used in numerical vertical planar motion mechanism simulations to achieve this aim. The heave forces, pitch moments, and Euler coefficients are calculated together with the linear vertical maneuvering derivatives by implementing the Fourier series expansion approach. The results show that the coupled added mass terms are significantly influenced by the scale effects, whereas the impact of scale effects on the decoupled added mass and coupled and decoupled damping terms is negligible. Considering that the effects of the coupled added mass on the vertical maneuvering characteristics are almost negligible, the vertical maneuvering of a submarine is slightly influenced by the scale effects.

Keywords: Submarine, Vertical maneuvering derivatives, Scale effect, CFD

1. Introduction

Having an effective horizontal maneuvering capability is essential for naval submarines because of rapid location and direction change requirements in case of emergencies. However, underwater vehicles can move in 6DOF motions in deep water, and thus, they may need to reach the free surface rapidly to escape hostile attacks, flooding, etc. Therefore, they should have good horizontal and vertical maneuvering capabilities. Two different approaches are generally used to understand the maneuvering behavior of an underwater vehicle or surface vessel. The first is free-running tests, where the vehicle can move freely in an experimental or numerical tank. Although this approach is considered to be the most accurate approach for calculating the maneuvering behavior of a vehicle, it is rather expensive and challenging due to constraints in facilities and numerical solvers. Therefore, as an alternative to this approach, simulation-based methods can be used to determine maneuvering characteristics. In this method, the maneuvering derivatives of a vehicle can be calculated using different mechanisms, such as planar motion mechanism, rotating arm, static drift, circular motion technique. To use the derivatives obtained from numerical or experimental techniques, a mathematical model is required.

1.1. Literature Review

The mathematical model for surface ships was first proposed by Davidson and Schiff [1] and then developed by Abkowitz [2]. Gertler and Hagen [3] also proposed a mathematical model to represent the maneuvering motion of an underwater vehicle for the first time, and this model was further modified by Feldman [4] with crossflow corrections.

The Defense Advanced Research Projects Agency (DARPA) Suboff is one of the most used benchmark underwater vehicle models in the literature. Comprehensive captive model experiments of DARPA were conducted by Roddy [5], and different techniques were used to obtain the maneuvering derivatives in horizontal and vertical planes during the experiments. Following this, Lin et al. [6] and

Address for Correspondence: Emre Kahramanoğlu, İstanbul Technical University Faculty of Maritime, Department of Marine Engineering, İstanbul, Türkiye
E-mail: emrekahramanoglu@gmail.com
ORCID ID: orcid.org/0000-0002-3646-1170

Received: 12.09.2023
Last Revision Received: 14.11.2023
Accepted: 12.12.2023

To cite this article: E. Kahramanoğlu, S. Sezen, and F. Çakıcı. "Investigation of Scale Effects on Linear Vertical Maneuvering Derivatives of a Submarine." *Journal of ETA Maritime Science*, vol. 12(1), pp. 14-24, 2024.

Xiaoyang et al. [7] conducted systematic experiments using the same DARPA Suboff hull form with another scale ratio. The results were compared with the experimental data obtained by Roddy [5]. The experiments performed by Roddy [5] mainly focused on horizontal maneuvering derivatives, whereas the vertical maneuvering derivatives were of great interest for the experiments performed by Lin et al. [6] and Xiaoyang et al. [7]. In another experimental study of DARPA Suboff, the effect of immersion on course-keeping stability was investigated by Efremov and Milanov [8]. They showed that the hydrodynamic derivatives change with immersion and highlighted that the change in derivatives with immersion could cause the loss of course stability of the submarine.

To obtain the horizontal and vertical derivatives, a series of tests were conducted in different facilities for two different model scales of DARPA Suboff, as shown in Table 1.

With the development of numerical techniques, computational fluid dynamics techniques are becoming appealing for calculating the maneuvering characteristics of vessels, similar to other hydrodynamic performance predictions (e.g., Budak and Beji [9], Sezen et al. [10], Sezen et al. [11], Dogrul [12]). In this regard, Table 2a summarizes the studies solely focused on the prediction of horizontal and vertical maneuvering of the DARPA Suboff. Additionally, Table 2b shows the other numerical studies performed using other underwater vehicles. The approaches for predicting the hydrodynamic derivatives are also shown in Table 2a and Table 2b.

Table 1. *Experimental studies of the DARPA Suboff*

	Model scale	Static drift	Pure sway	Pure yaw	Pure heave	Pure pitch
Roddy [5]	1/24	+	+	+	+	+
Lin et al. [6]	1/48	+	+	+	-	-
Efremov and Milanov [8]	1/24	+	-	+	-	-
Xiaoyang et al. [7]	1/48	+	-	-	+	+

Table 2a*. Numerical studies on the maneuvering of DARPA Suboff*

		Static Drift	Rotating Arm	Pure Sway	Pure Yaw	Pure Heave	Pure Pitch	Direct Modelling
Vaz et al. [13]	DARPA	+	-	-	-	-	+	-
Drouet et al. [14]	DARPA	+	-	-	-	-	-	-
Pan et al. [15]	DARPA	+	-	+	+	+	+	-
Zhang et al. [16]	DRDC STR, DARPA, Series 58	-	+	-	-	-	-	-
Can [17]	DARPA, Autosub	+	+	-	-	+	+	-
Duman et al. [18]	DARPA	+	-	-	-	-	-	-
Feng et al. [19]	DARPA	-	-	-	-	-	-	+
Foroushani and Sabzpooshani [20]	DARPA	-	-	+	+	+	+	-
Delen and Kinaci [21]	DARPA	-	-	-	-	-	-	+
Kahramanoglu [22]	DARPA	-	-	+	+	-	-	-
Zhao et al. [23]	DARPA	+	+	-	-	-	-	-
Öztürk et al. [24]	DARPA	+	-	-	-	-	-	-

Table 2b*. Numerical studies on the maneuvering of other underwater vehicles*

	Submarine Model	Static Drift	Rotating Arm	Pure Sway	Pure Yaw	Pure Heave	Pure Pitch	Direct Modelling
Tyagi and Sen [25]	Kempf, Blue Eyes	+	-	-	-	-	-	-
Phillips et al. [26]	Autosub	+	+	-	-	-	-	-
Fureby et al. [27]	DTSO	+	-	-	-	-	-	-
Carrica et al. [28]	Joubert BB2	-	-	-	-	-	-	+
Carrica et al. [29]	Joubert BB2	-	-	-	-	-	-	+
Dubbioso et al. [30]	CNR Insean 2475	-	-	-	-	-	-	+
Nguyen et al. [31]	Self-built	+	+	-	-	-	-	-
Kim et al. [32]	Joubert BB2	-	-	-	-	-	-	+
Zhang et al. [33]	Self-built	-	-	-	-	-	-	+
Doyle et al. [34]	Phoenix	+	-	+	-	-	-	-
Cho et al. [35]	Joubert BB2	+	-	+	+	+	+	-
Han et al. [36]	BB2	-	-	-	-	-	-	+

As summarized above, several studies have investigated horizontal and vertical maneuvering derivatives using numerical and experimental methods on a model scale. As the aim of these investigations is to predict the maneuvering performance of underwater vehicles on a full scale, the coefficients calculated by simulation-based approaches can be greatly influenced by the scale effects. Hence, this might result in a misprediction of the maneuvering performance of underwater vehicles. To the best of the authors' knowledge, there is a research gap in investigating the scale effects on the vertical maneuvering performance of underwater vehicles in the open literature. Therefore, this study aims to explore the scale effects on the vertical maneuvering performance of underwater vehicles. To achieve this aim, two different scales (i.e., model and full-scale) were used in the CFD calculations.

1.2. Aim of the Study

In the leading author's recent study [22], the scale effects on horizontal maneuvering performance were comprehensively investigated using the same benchmark submarine model. This study is a continuation of the recently published study of the leading author [22] by expanding the investigations of scale effects for vertical maneuvering derivatives for the first time in the literature. This paper is organized as follows. Section 2 describes the mathematical model, including the submarine geometry and the physical model. The numerical results are given in Section 3, and the concluding remarks are presented in the last section.

2. Solution Strategy

2.1. Submarine Geometry

The DARPA Suboff model was used in this study. The fully appended submarine form (AFF-8) apart from the wing ring was selected. The 3D geometry of the underwater vehicle is shown in Figure 1. The main properties are given in Table 3 for both scales.

Figure 1. *The submarine geometry used in the present study*

2.2. Equation of Motions

In this study, only pure heaving and pitching motions were considered at a certain surge speed. All simulations were conducted at 3DOF, and the equations of these motions can be derived from Newton's second law, similar to the study of Xiaoyang et al. [7], and written by following the notations explained in SNAME [37]:

$$X = m\left[\dot{u} + wq - x_G q^2 + z_G \dot{q}\right] \quad (1)$$

$$Z = m\left[\dot{w} - uq - z_G q^2 - x_G \dot{q}\right] \quad (2)$$

$$M = I_{YY}\dot{q} + m\left[z_G(\dot{u} + wq) - x_G(\dot{w} - uq)\right] \quad (3)$$

Equations (1-3) represent the surge, heave, and pitch motions, respectively. I_{YY} depicts the moment of inertia for pitch direction while x_G and z_G depict the longitudinal and vertical centers of gravity. u, w and q depict the surge, heave and pitch velocities, respectively, while the dotted terms represent the acceleration. M denotes the pitch moment, while X and Z denote the surge and heave forces, respectively. Although these terms might be due to waves, propeller, hydrostatic, and hydrodynamic loads, this paper focuses only on the term associated with hydrodynamics. Because only the linear terms are taken into consideration, the hydrodynamic loads for heave and pitch motions can be represented as follows, where Z_H and M_H represent the hydrodynamic force in the Z direction and the hydrodynamic moment around the Y axis:

$$Z_H = Z_w w + Z_{\dot{w}} \dot{w} + Z_q q + Z_{\dot{q}} \dot{q} \quad (4)$$

$$M_H = M_w w + M_{\dot{w}} \dot{w} + M_q q + M_{\dot{q}} \dot{q} \quad (5)$$

Table 3. *Main properties of the underwater vehicle*

Main Particular	Unit	λ = 1/24 (Model scale)	λ = 1/1 (Full scale)
Length Overall (L_{OA})	m	4.356	104.54
Length between perpendiculars (L_{PP})	m	4.261	102.26
Maximum Diameter (D_{MAX})	m	0.508	12.192
Displacement (Δ)	tons	0.704	9729.7
Froude Number (Fn)	-	0.515	0.515
Reynolds Number (Rn)	-	$1.4\ 10^7$	$1.7\ 10^9$

Where Z_w and Z_q denote the damping terms in the z-direction due to the heave and pitch velocities, respectively, while the dot products ($Z_{\dot{w}}$ and $Z_{\dot{q}}$) denote the added mass terms due to the heave and pitch acceleration. M_w and M_q represent the damping terms around the y-axis due to heave and pitch velocities, respectively, while the dot products ($M_{\dot{w}}$ and $M_{\dot{q}}$) represent the acceleration terms due to the heave and pitch acceleration around the y-axis.

2.3. Numerical Modeling

2.3.1. Boundary conditions and computational domain

Similar to the recent study of the leading author [22], a computational domain was used to solve the flow around the submarines. The computational domain size was selected according to the ITTC guidelines [38] to avoid potential reflections from the boundaries, as shown in Figure 2. The depth and breadth of the computational domain extends to 4L. Here, the right side of the computational domain was selected as the velocity inlet, while the left side was selected as the pressure outlet. The other boundaries of the computational domain were also defined as the velocity inlet. To satisfy the kinematic boundary conditions, the submarine geometry was defined as a no-slip wall.

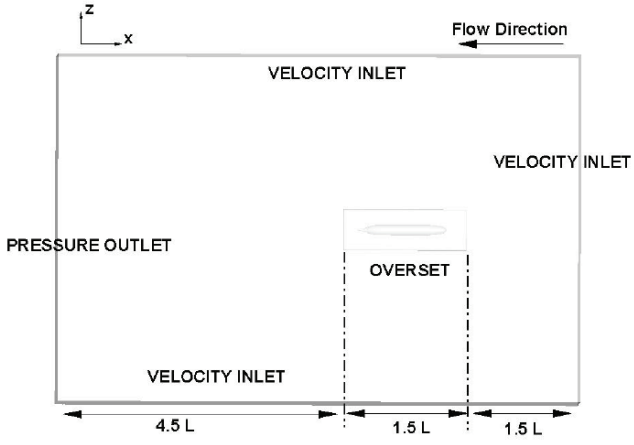

Figure 2. *Sizes of the domain and boundaries*

2.3.2. Meshing strategy and physical modeling

The overset mesh technique was used to accurately model the flow field around the model and full-scale forms. To accurately transfer the information from the overset zone to the static background, the grid structure was enlarged systematically, and the mesh transition was kept as smooth as possible between the background and overset regions. The mesh structure around the submarine hull is shown in Figure 3.

In the CFD simulations, the unsteady RANS method, the k-ω SST turbulence model, and all y+ treatment methods were utilized in a manner similar to the studies in the literature [10,11,22]. To discretize the temporal and convectional terms, a second-order upwind scheme was used. Because the maneuvering motion was modeled in 3DOF, the submarine form was forced only for vertical motion by maintaining a certain surge speed in the CFD simulations.

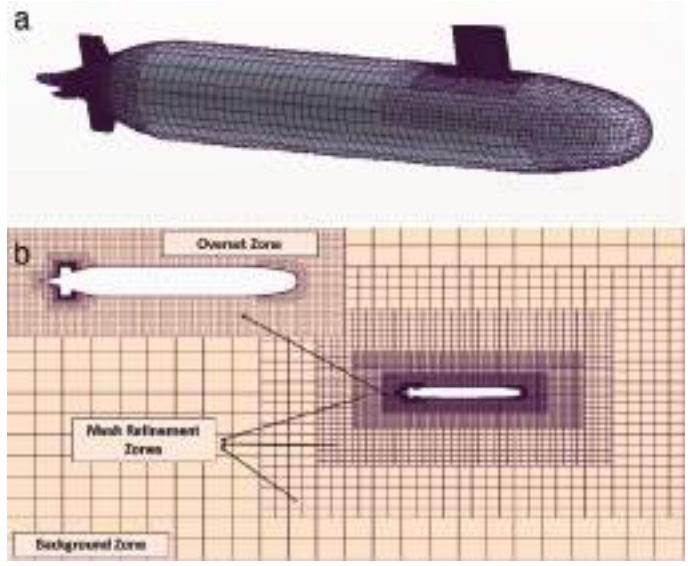

Figure 3. *a) Mesh structure on underwater vehicles. b) Mesh structure of the domain*

3. Results

In this study, pure heave and pure pitch analyses were performed to calculate the vertical maneuvering derivatives for a benchmark submarine, the DARPA Suboff. Thus, the test matrix given in Table 4 was created considering the ITTC recommendations [39] and previous studies in the literature [20,22]. Note that these cases are for the model scale and full scale of DARPA Suboff. In total, there are 16 cases investigated in this study.

The forces, moments, and rotational and translational velocities/accelerations were non-dimensionalized, similar

Table 4a*. Test matrix for pure heaving*

Test No	Heave Amplitude/ L_{pp} [-]	Frequency*L_{pp}/V [-]	w/V [-]
H1	0.0271	1.6630	0.0450
H2	0.0361	1.6630	0.0600
H3	0.0542	1.6630	0.0901
H4	0.0812	1.6630	0.1351

Table 4b*. Test matrix for pure pitching*

Test No	Heave Amplitude/ L_{pp} [-]	Frequency*L_{pp}/V [-]	q*L_{pp}/V [-]
P1	0.0162	2.8142	0.1279
P2	0.0242	2.8142	0.1919
P3	0.0323	2.8142	0.2558
P4	0.0485	2.8142	0.3838

to the findings of the leading author's recent study [22]. The heave force and the pitch moment values were non-dimensionalized by the following equations:

$$Z' = Z/(0.5\rho L^2 V^2) \quad (6)$$

$$M' = M/(0.5\rho L^3 V^2) \quad (7)$$

After calculating the time series of non-dimensional forces and moments, they were defined by applying Fourier series expansion following the methodology given in Equation (8) and Equation (15):

$$Z'(t) = Z'_{cos}\cos(\omega t) + Z'_{sin}\sin(\omega t) \quad (8)$$

$$M'(t) = M'_{cos}\cos(\omega t) + M'_{sin}\sin(\omega t) \quad (9)$$

$$Z'_{cos} = \frac{2}{T}\int 0\ T\ Z'(t)\cos(\omega t)dt \quad (10)$$

$$Z'_{sin} = \frac{2}{T}\int 0\ T\ Z'(t)\sin(\omega t)dt \quad (11)$$

$$M'_{cos} = \frac{2}{T}\int 0\ T\ M'(t)\cos(\omega t)dt \quad (12)$$

$$M'_{cos} = \frac{2}{T}\int 0\ T\ M'(t)\cos(\omega t)dt \quad (13)$$

$$\beta_Z = \arctan\left(\frac{Z_{cos}}{Z_{sin}}\right) \quad (14)$$

$$\beta_M = \arctan\left(\frac{M_{cos}}{M_{sin}}\right) \quad (15)$$

3.1. Uncertainty Analyses

The uncertainty assessment of the present study was conducted by implementing the Grid Convergence Index) method that was proposed by Roache [40] and developed with many studies [41,42]. Similar to previous studies conducted by authors on both surface vessels [43] and underwater vehicles [11,22], the methodology suggested by Celik et al. [44] was used for calculating the temporal and spatial uncertainty.

The H2 test case, shown in Table 4a, was selected to obtain the total uncertainty for the amplitude of the pitch moment obtained from the pure heaving analyses. The convergence of the scalar values and the uncertainty of the numerical solution are given in Figure 4 and Table 5, respectively. It can be understood from Figure 4 that the

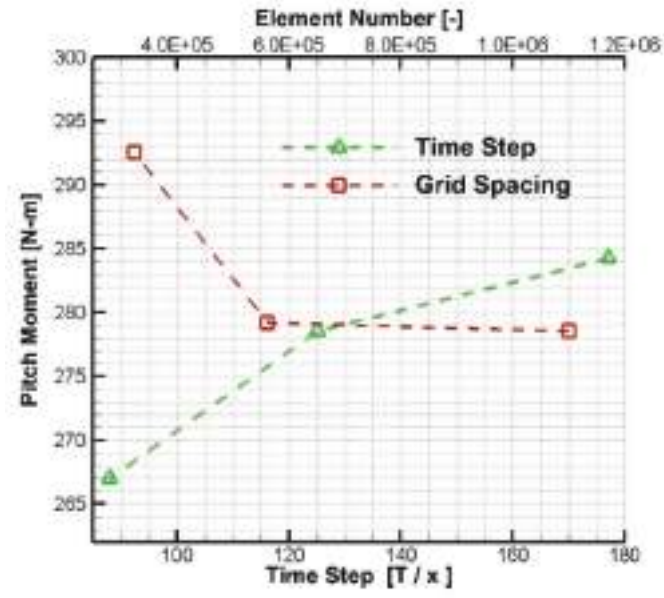

Figure 4. *Convergence of pitch moments*

pitch moment values converge to a scalar value as the number of elements increases or as the time step size decreases. Based on the uncertainty study, a fine grid was selected for CFD simulations. As the difference between the fine and medium time-step sizes is small, the medium time-step size was selected to reduce the computational cost of CFD simulations. In Table 5, T denotes the period of the heave motion, U denotes the uncertainty, R denotes the convergence factor, and r denotes the refinement factor, which was kept constant in all analyses.

3.2. Pure Heaving

Before presenting all numerical data, the obtained results from the numerical method are compared with those presented in the literature. If the moment and forces obtained from different test cases are fitted to a one-degree polynomial, as explained by Yoon et al. [45], the maneuvering derivatives in accordance with the added mass and damping terms can be calculated. A comparison of the maneuvering derivatives is presented in Table 6. According to the results listed in Table 6, there are some differences between the present study and other results

Table 5. *Uncertainty results*

	Element number [-]	Pitch moment [N-m]	Time step size [s]	Pitch moment [N-m]
Fine	1.10×10^6	278.54	T/177	284.26
Medium	5.62×10^5	279.19	T/125	278.54
Coarse	3.24×10^5	292.54	T/88	267.00
R	0.0490		0.4954	
r	1.4142		1.4142	
%U	0.02%		2.47%	
Total uncertainty () = = 2.47 %				

Table 6. *Comparison of derivatives obtained from pure heaving*

	Present study	Roddy (EFD) [5]	Foroushani and Sabzpooshani (CFD) [20]	Zhao et al. (CFD) [23]	Pan et al. (CFD) [15]	Liang et al. (EFD) [7]
Z_w	-0.01736	-0.01391	-0.01468	-0.01331	-0.01570	-0.03560
Z_w	-0.01882	-0.01453	-0.01753	-	-0.01811	-0.01010
M_w	0.01035	0.01032	0.01057	0.01104	0.01009	0.01172
M_w	-0.00622	-0.00056	-0.00080	-	-0.00063	0.00106

presented in the literature. These discrepancies can arise from differences in measurement techniques, the method used to obtain maneuvering derivatives, and variations in experimental condition. Although there are some acceptable differences, the numerical derivatives obtained from the present numerical method generally match well with the results presented in the literature.

Following the validation of the numerical results with experimental and numerical studies in the literature, the scale effects on forces, moments, phases, and derivatives can be investigated in detail. As stated before, pure heaving simulations were conducted using the test cases explained in Table 4, while the Froude number of both scales was kept the same as 0.515. In this simulation, the submarine only heaved; thus, the pitch velocity and pitch acceleration were equal to zero in Equation (4) and Equation (5). Then, the forces and moments, which are functions of only heave velocity and heave acceleration, were decomposed using the Fourier series expansion approach.

In Figure 5, the heave forces in terms of different heave velocities are presented for both scales. According to this figure, the coefficients associated with the cosine term (ZC') for full scale are higher than those of the model scale values. In contrast, the coefficients related to the sinus term (ZS') are lower for all heave velocities in full-scale than the values in the model scale. Only a slight difference in the amplitudes (Z') of both scales is observed over several heave velocities. When the phase of the heave forces is examined, there is a significant difference, especially at lower heave velocities. These differences in phases cause differentiation in the Euler components of the heave force.

In Figure 6, the pitch moments obtained from pure heaving analyses are compared for both scales in terms of different heave velocities. According to Figure 6, the pitch moment amplitudes are similar for both scales, whereas the amplitudes of the full scale are slightly lower than that of the model scale. Although the Euler coefficients related

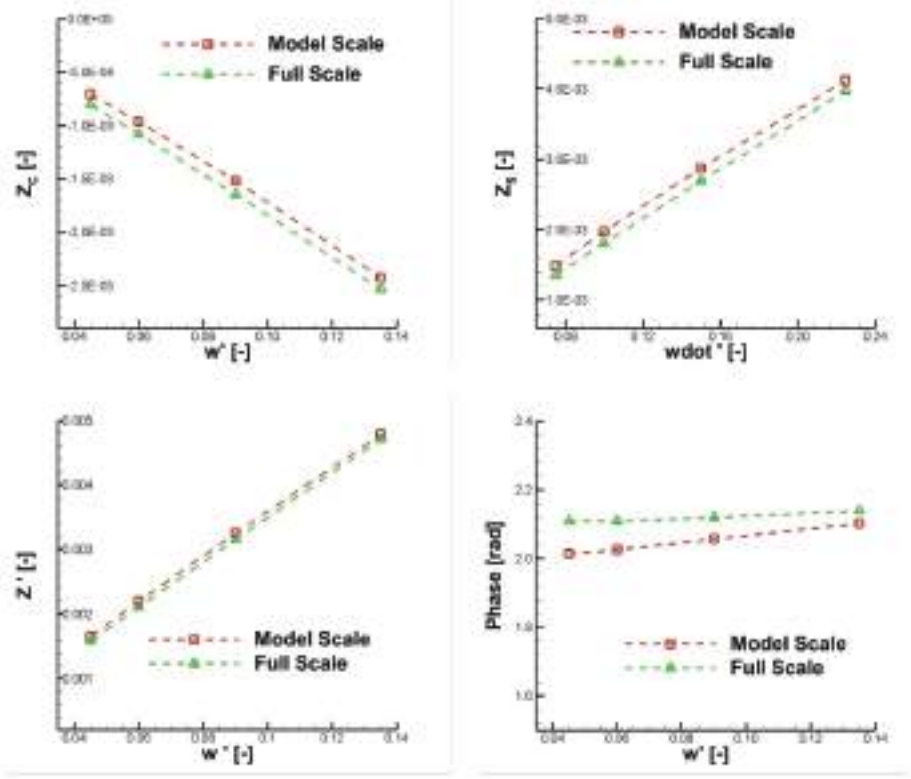

Figure 5. *Heave force, Euler components, and phases in terms of different heave velocities*

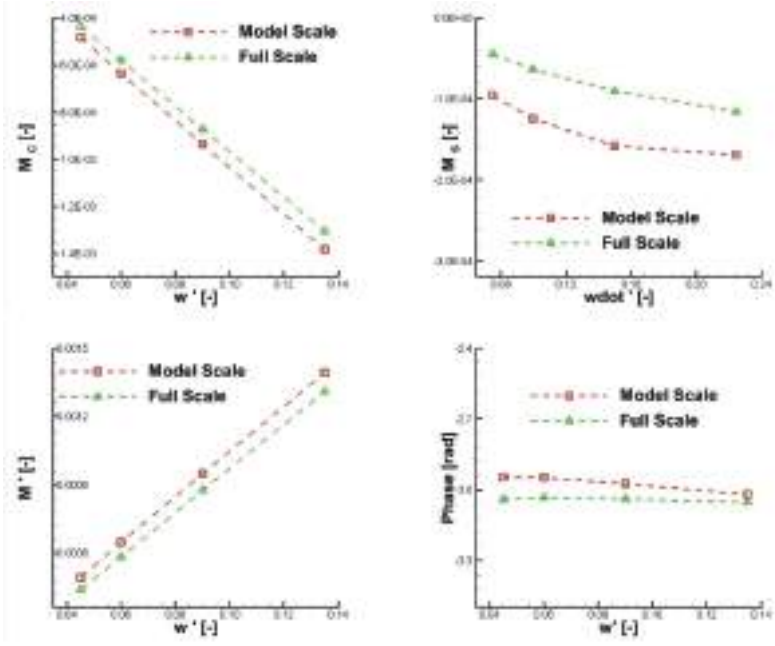

Figure 6. *Pitch moment, Euler components, and phases in terms of different heave velocities*

to the cosine term (M_C') for the model scale are higher, the trend of the general curve of both scales is similar. However, the Euler coefficients related to the sinus term (M_S') for the model scale are higher than those for the full scale. Similar to Figure 5, there is a discrepancy in the phases for both scales.

Table 7 lists the derivatives obtained from the pure heaving simulations for both scales. As underlined before, the methodology presented by Yoon et al. [45] was followed to calculate the maneuvering derivatives. As expected from the data shown in Figure 5, the derivatives for both scales are very similar for Z_w and $Z_{\dot{w}}$. Similarly, M_w values are similar for both models because the slopes of the pitch moment component related to cosine (M_C') are very similar.

Table 7. *Maneuvering derivatives obtained from the pure heaving analyses*

Derivative	Model	Full
Z_w	-0.01736	-0.01853
$Z_{\dot{w}}$	-0.01882	-0.01782
M_w	0.01035	0.00965
$M_{\dot{w}}$	-0.00622	-0.00055

However, contrary to $M_{\dot{w}}$, the value of M_w are greatly influenced by the scale effects. When the data are examined, it is understood that a considerable difference in the coupled added mass occurs because of the phase difference.

3.3. Pure Pitching

The numerical results for the model scale are compared with numerical and/or experimental results presented in the literature in Table 8.

As given in Table 8, the derivatives for the heave force (Z) are generally under predicted, whereas the derivatives related to pitch moment (M) are in good agreement with the derivatives obtained from the literature. The difference in the heave forces was also observed in a previous study [22]. This difference can be associated with the wing ring, which was not modeled in the present study, unlike some other studies. In addition, the numerical parameters selected in this study can also be associated with the difference between the current and other numerical studies.

Similar to the pure heaving analyses, pure pitching analyses were conducted at the same Froude number for both scales according to the test cases listed in Table 4b. Unlike the previous simulation, the heave velocities and

Table 8. *Comparison of derivatives obtained from pure pitching*

	Present study	Roddy (EFD) [5]	Foroushani and Sabzpooshani (CFD) [20]	Zhao et al. (EFD) [46]	Pan et al. (CFD) [15]	Liang et al. (EFD) [7]
Z_q	-0.00484	-0.00755	-0.00682	-0.00796	-0.00778	-0.00164
$Z_{\dot{q}}$	-0.00018	-0.00063	-0.00058	-	-0.00063	-0.00102
M_q	-0.00278	-0.00370	-0.00317	-0.00397	-0.00347	-0.00289
$M_{\dot{q}}$	-0.00094	-0.00086	-0.00102	-	-0.00095	-0.00076

acceleration were set to zero because the underwater vehicle was only forced to perform pitch motion. Therefore, the heave force and pitch moment are considered to be functions of pitch velocity and pitch acceleration in Equation (4) and Equation (5).

The heave forces obtained from the pure pitching analyses in terms of different pitch velocities are shown in Figure 7. The amplitudes (Z') for the model scale are lower than those for the full-scale results, similar to the coefficient related to sinus (Z_S'). Considering the coefficients related to cosine (Z_C'), the sign of the full-scale results changes with different pitch velocities. Although the general trend of the curve is similar for both scales for the amplitudes and the component related to sinus, there is a clear offset between them. Similar to these terms, the phases of different scales show some discrepancies, especially for lower pitch velocities. Thus, the differences in the components are caused by differences in the amplitudes and phases.

In Figure 8, the pitch moments obtained from the different pitch velocities are shown for both scales. According to this figure, the amplitudes of both scales are almost the same for all pitch velocity ranges. The coefficients related to the

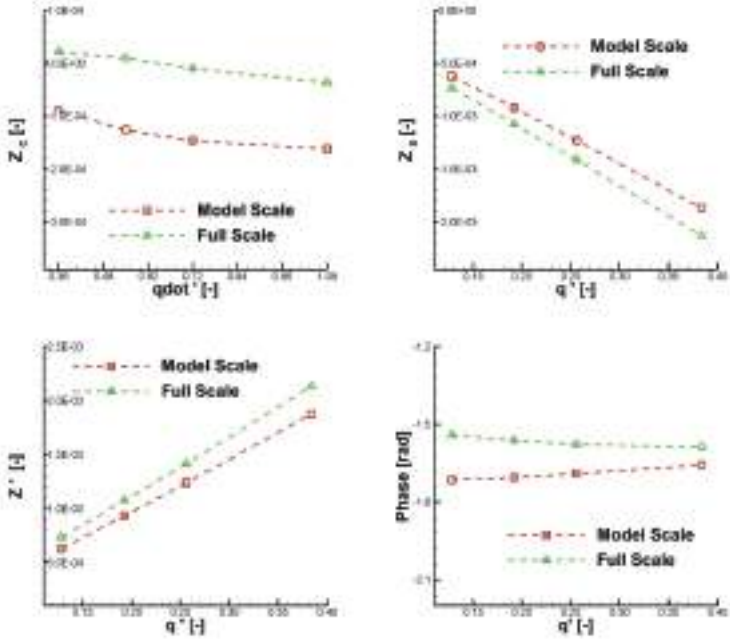

Figure 7. *Heave forces, Euler components, and phases in terms of pitch velocities*

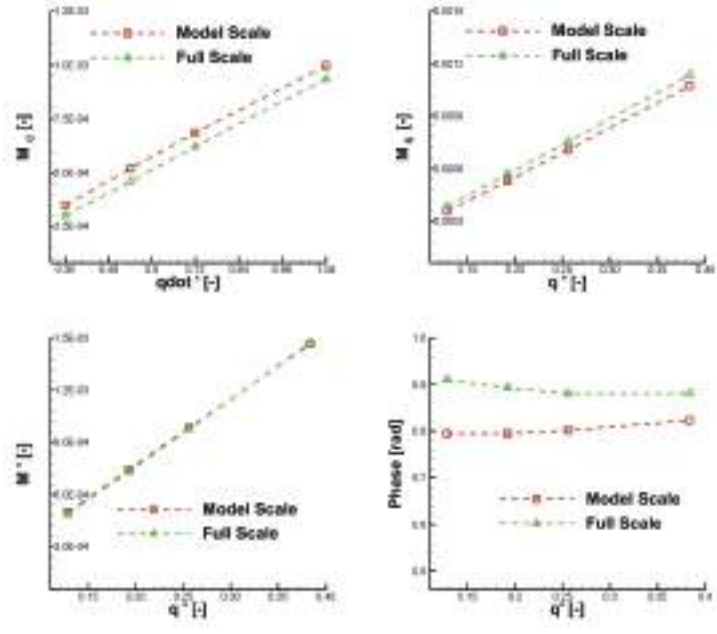

Figure 8. *Heave forces, Euler components, and phases in terms of pitch velocities*

sinus term (M_S') for the model scale are slightly lower than the full-scale results, although the full-scale results for the coefficients related to cosine (M_C') are slightly lower than the model-scale results. The main difference for the Euler components appears to originate from the phase differences for both scales.

The derivatives obtained from the data shown in Figures 7 and 8 are listed in Table 9 for both scales. It should be noted that similar to pure heaving, the derivatives were calculated by fitting a linear curve by following the methodology presented by Yoon et al. [45]. As expected from the data shown in Figure 8, the derivatives related to pitch moments are similar for both scales (M_q and $M_{\dot{q}}$) since these derivatives directly are obtained from the slope of the fitted curves. It can be seen that Z_q values are very close for both models in Table 9, while the value of $Z_{\dot{q}}$ is greatly influenced by the scale effects. The main reason for this is the phase difference observed in the time domain data as well as the difference in the heave force amplitudes obtained from pure pitching analyses (see Figure 7).

Table 9. *Maneuvering derivatives obtained from the pure pitching analyses*

Derivative	Model scale	Full scale
Z_q	-0.00484	-0.00556
$Z_{\dot{q}}$	-0.00018	-0.00002
M_q	-0.00278	-0.00297
$M_{\dot{q}}$	-0.00094	-0.00086

4. Conclusion

In this study, the scale effects on the vertical maneuvering derivatives of a benchmark underwater vehicle were numerically investigated. Pure heaving and pure pitching simulations were conducted for two scales, and the linear vertical maneuvering derivatives were calculated, validated, and compared.

The following outcomes can be summarized as follows:

• The amplitudes of the heave force in pure heaving simulations are slightly affected by the scale effects. The scale effects can be considered negligible for damping (Z_w) and added mass term ($Z_{\dot{w}}$) of the heave force obtained from the pure heaving simulations.

• A pronounced scale effect on pure heaving simulations is found for the cross-coupled added mass term ($M_{\dot{w}}$), whereas the damping term of pitch moment (M_w) are not influenced by the scale effects.

• The scale effects on the pitch moment obtained from the pure pitching simulations are negligible. While there is a phase difference between both scales, this difference doesnot remarkably influence neither damping (M_q) nor added mass term ($M_{\dot{q}}$) of the pitch moment.

• Significant scale effects on the amplitudes were found for the heave force obtained from the pure pitching simulations.

• In addition to the differences in the amplitudes, the phases of the heave force in pure pitching change with scale. Thus, this can cause a remarkable difference in the derivatives, especially for the added mass term ($Z_{\dot{q}}$).

• The damping term of the heave force (Z_q) on pure pitching simulations is considerably affected (i.e., approximately 15%) compared with the cross-coupled damping term (M_w) obtained from pure heaving simulations.

• The main reason for the scale effects appears to be the phase differences between the different scales.

• The scale effect is more pronounced for the cross-coupled added mass terms, similar to the horizontal maneuvering results obtained from the leading author's recent study. Nevertheless, it is expected that the change in the cross-coupled added mass term with the scale ratio should not influence the overall maneuvering performance of the submarine. This is because the contributions of these terms to heave force and pitch moment are rather small.

This study is the second part of ongoing research on predicting the maneuvering performance of the submarine hull form at full scale using direct CFD simulations. Therefore, the authors are currently expanding their research in this field and comparing the results of direct CFD and system-based approaches for full-scale submarine hulls.

Authorship Contributions

Concept design: E. Kahramanoğlu, S. Sezen, and F. Çakıcı, Data Collection or Processing: E. Kahramanoğlu, S. Sezen, and F. Çakıcı, Analysis or Interpretation: E. Kahramanoğlu, S. Sezen, and F. Çakıcı, Literature Review: E. Kahramanoğlu, S. Sezen, and F. Çakıcı, Writing, Reviewing and Editing: E. Kahramanoğlu, S. Sezen, and F. Çakıcı.

Funding: The authors received no financial support for the research, authorship, and/or publication of this article.

References

[1] K. S. M. Davidson, and L. I. Schiff, "Turning and course keeping qualities." *Transactions - The Society of Naval Architects and Marine Engineers,* vol. 54, 1946.

[2] M. A. Abkowitz, *Lectures on Ship Hydrodynamics Steering and Maneuverability.* Technical Report. Hydro and Aerodynamic Laboratory, Lyngby, Denmark. Technical Report Hy-5. 1964.

[3] M. Gertler, and G. Hagen, *Standard Equations of Motion for Submarine Simulation.* Technical Report AD653861, June, 1967.

[4] J. Feldman, DTNSRDC Revised Standard Submarine Equations of Motion. David Taylor Research Center, Ship Performance Department (June), 1979.

[5] R. F. Roddy, Investigation of the Stability and Control Characteristics of Several Configurations of the DARPA Suboff Model (DTRC Model 5470) from Captive Model Experiments. David Taylor Research Center, Departmental Report DTRC/SHD-1298- 08 (September), 1990.

[6] Y. H. Lin, S. H. Tseng, and Y. H. Chen, "The experimental study on maneuvering derivatives of a submerged body SUBOFF by implementing the Planar Motion Mechanism tests." *Ocean Engineering,* vol. 170, pp. 120-135, Dec 2018.

[7] X. Liang, N. Ma, H. Liu, and X. Gu, "Experimental study on the maneuvering derivatives of a half-scale SUBOFF model in the vertical plane." *Ocean Engineering,* vol. 233, pp. 109052, Aug 2021.

[8] D. V. Efremov, and E. M. Milanov, "Hydrodynamics of DARPA SUBOFF submarine at shallowly immersion conditions." *TransNav, the International Journal on Marine Navigation and Safety of Sea Transportation,* vol. 13, pp. 337-342, 2019.

[9] G. Budak, and S. Beji, "Computational resistance analyses of a generic submarine hull form and its geometric variants." *Jounal of Ocean Techonology,* vol. 11, pp. 77-86, Jul 2016

[10] S. Sezen, C. Delen, A. Dogrul, and M. Atlar, "An investigation of scale effects on the self-propulsion characteristics of a submarine." *Applied Ocean Research,* vol. 113, pp. 102728, Aug 2021.

[11] S. Sezen, A. Dogrul, C. Delen, and S. Bal, "Investigation of self-propulsion of DARPA Suboff by RANS method." *Ocean Engineering,* vol. 150, pp. 258-271, 2018.

[12] A. Dogrul, "Numerical prediction of scale effects on the propulsion performance of Joubert BB2 submarine." *Brodogradnja,* vol. 73, pp. 17-42, Apr 2022.

[13] G. Vaz, S. Toxopeus, and S. Holmes, "Calculation of manoeuvring forces on submarines using two viscous-flow solvers," in *Proceedings of the ASME 2010 29th International Conference on Ocean, Offshore and Arctic Engineering, OMAE2010*. June 6-11, Shanghai, China, 2010.

[14] A. Drouet, et al. *Simulation of submarine manoeuvring using Navier-Stokes solver.* International Conference on Computational Methods in Marine Engineering, MARINE 2011 pp. 301-312, 2011.

[15] Y. Pan, H. Zhang, and Q. Zhou, "Numerical prediction of submarine hydrodynamic coefficients using CFD simulation." *Journal of Hydrodynamics,* vol. 24, pp. 840-847, 2012.

[16] J. T. Zhang, J. A. Maxwell, A. G. Gerber, A. G. L. Holloway, and G. D. Watt, "Simulation of the flow over axisymmetric submarine hulls in steady turning." *Ocean Engineering,* vol. 57, pp. 180-196, 2013.

[17] M. Can, *Numerical Simulation of Hydrodynamic Planar Motion Mechanism Test for Underwater Vehicles.* Master of Science Thesis. Middle East Technical University, Ankara, Turkey, 2014.

[18] S. Duman, S. Sezen, and S. Bal, "Propeller effects on maneuvering of a submerged body," in *3rd International Meeting- Progress in Propeller Cavitation and its Consequences: Experimental and Computational Methods for Predictions,* 15-16 November, Istanbul, Turkey. 2018.

[19] D. Feng, X. Chen, H. Liu, Z. Zhang, and X. Wang, "Comparisons of turning abilities of submarine with different rudder configurations," in *Proceedings of the ASME 2018 37th International Conference on Ocean, Offshore and Arctic Engineering,* June 17-22, 2018, Madrid, Spain.

[20] J. A. Foroushani, and M. Sabzpooshani, "Determination of hydrodynamic derivatives of an ocean vehicle using CFD analyses of synthetic standard dynamic tests." *Applied Ocean Research,* vol. 108, pp. 102539, Mar 2021.

[21] C. Delen, and O. K. Kinaci, "Direct CFD simulations of standard maneuvering tests for DARPA Suboff." *Ocean Engineering,* vol. 276, pp. 114202, May 2023.

[22] E. Kahramanoglu, "Numerical investigation of the scale effect on the horizontal maneuvering derivatives of an underwater vehicle." *Ocean Engineering,* vol. 272, pp. 113883, Mar 2023.

[23] B. Zhao, et al. "Hydrodynamic coefficients of the DARPA SUBOFF AFF-8 in rotating arm maneuver - Part II: Test results and discussion." *Ocean Engineering,* vol. 268, pp. 113466, 2023.

[24] H. Öztürk, K. B. Gündüz, and Y. Arıkan Özden, "Numerical investigation of the maneuvering forces of different darpa suboff configurations for static drift condition." *Journal of ETA Maritime Science,* vol. 11, pp. 137-147, 2023.

[25] A. Tyagi, and D. Sen, "Calculation of transverse hydrodynamic coefficients using computational fluid dynamic approach." *Ocean Engineering,* vol. 33, pp. 798-809, Apr 2006.

[26] A. Phillips, M. Furlong, and S. R. Turnock, The use of Computational Fluid Dynamics to Determine the Dynamic Stability of an Autonomous Underwater Vehicle, 10th Numerical Towing Tank Symposium (NuTTS'07), Hamburg, Germany, 2007.

[27] C. Fureby, et al. "Experimental and numerical study of a generic conventional submarine at10° yaw." *Ocean Engineering,* vol. 116, pp. 1-20, 2016.

[28] P. M. Carrica, M. Kerkvliet, F. Quadvlieg, M. Pontarelli, and J. E. Martin, CFD Simulations and Experiments of a Maneuvering Generic Submarine and Prognosis for Simulation of Near Surface Operation, 31st Symposium on Naval Hydrodynamics Monterey, CA, USA, 2016.

[29] P. M. Carrica, Y. Kim, and J. E. Martin, "Vertical zigzag maneuver of a generic submarine." *Ocean Engineering*, vol. 219, pp. 108386, Jan 2021.

[30] G. Dubbioso, R. Broglia, and S. Zaghi, "CFD analysis of turning abilities of a submarine model." *Ocean Engineering,* vol. 129, 459-479, 2017.

[31] T. T. Nguyen, H. K. Yoon, Y. Park, and C. Park, "Estimation of hydrodynamic derivatives of full-scale submarine using RANS solver." *Journal of Ocean Engineering and Technology,* vol. 32, pp. 386-392, 2018.

[32] H. Kim, D. Ranmuthugala, Z. Q. Leong, and C. Chin, "Six-DOF simulations of an underwater vehicle undergoing straight line and steady turning manoeuvres." *Ocean Engineering,* vol. 150, pp. 102-112, 2018.

[33] S. Zhang, H. Li, T. Zhang, Y. Pang, and Q. Chen, "Numerical simulation study on the effects of course keeping on the roll stability of submarine emergency rising." *Applied Sciences,* vol. 9, pp. 3285, 2019.

[34] R. Doyle, T. L. Jeans, A. G. L. Holloway, and D. Fieger, "URANS simulations of an axisymmetric submarine hull undergoing dynamic sway." *Ocean Engineering*, vol. 172, pp. 155-169, Jan 2019.

[35] Y. J. Cho, W. Seok, K. H. Cheon, and S. H. Rhee, "Maneuvering simulation of an X-plane submarine using computational fluid

dynamics," *International Journal of Naval Architecture and Ocean Engineering,* vol. 12, pp. 843-855, 2020.

[36] K. Han, et al. "Six-DOF CFD simulations of underwater vehicle operating underwater turning maneuvers." *Journal of Marine Science and Engineering,* vol. 9, pp. 1451, Dec 2021.

[37] SNAME, Nomenclature for treating the motion of a submerged body through a fluid, The Society of Naval Architects and Marine Engineers, New York, 1950.

[38] ITTC. 2014. Uncertainty analysis in CFD, verification and validation methodology and procedures, ITTC - Recomm. Proced. Guidelines.

[39] ITTC. 1999. Final report and recommendations to the 22nd ITTC.

[40] P. J. Roache, "Verification of codes and calculations." AIAA Journal. vol. 36, pp. 696-702, May 1998.

[41] F. Stern, R. V. Wilson, H. W. Coleman, and E. G. Paterson, "Comprehensive approach to verification and validation of CFD simulations-Part 1: methodology and procedures." *Journal of Fluids Engineering,* vol. 123, pp. 793-802, Dec 2001.

[42] R. V. Wilson, F. Stern, H. W. Coleman, and E. G. Paterson, "Comprehensive approach to verification and validation of CFD simulations-Part 2: application for rans simulation of a cargo/container ship." *Journal of Fluids Engineering,* vol. 123, pp. 803-810, Dec 2001.

[43] F. Cakici, E. Kahramanoglu, S. Duman, and A. D. Alkan, "A new URANS based approach on the prediction of vertical motions of a surface combatant in head waves." *Ocean Engineering,* vol. 162, pp. 21-33, Aug 2018.

[44] I. B. Celik, U. Ghia, P. J. Roache, C. J. Freitas, and P. E. Raad, "Procedure for estimation and reporting of uncertainty due to discretisation in CFD applications." *Journal of Fluids Engineering,* vol. 130, 078001, Jul 2008.

[45] H. Yoon, C. D. Simonsen, L. Benedetti, J. Longo, Y. Toda, and F. Stern, "Benchmark CFD validation data for surface combatant 5415 in PMM maneuvers - Part I: force/moment/motion measurements." *Ocean Engineering,* vol. 109, pp. 705-734, 2015.

[46] B. Zhao, Y. Yun, F. Hu, J. Sun, D. Wu, and B. Huang, "Hydrodynamic coefficients of the DARPA SUBOFF AFF-8 in rotating arm maneuver - Part I: Test technology and validation." *Ocean Engineering,* vol. 266, 113148, 2022.

Journal of ETA Maritime Science 2024;12(1):25-35

Hierarchical Management System for Container Vessels Automated Cargo Handling

Luidmyla Leonidovna Nikolaieva, Taras Yurievitch Omelchenko, Oleksandr Viktorovich Haichenia

Naval Institute, National University, Odesa Maritime Academy, Odesa, Ukraine

Abstract

Hierarchical management system is the next step for the development of container terminals all over the planet. The existing restrictions in transshipment operations are difficult to predict and invariably lead to a decrease in the terminal's throughput. The authors show that in modern control systems for the operation of a port container terminal, most of the automated processes use imperfect work algorithms and require optimal control based on the development of new approaches. The hierarchical multi-level control system proposed in the work, in comparison with traditional control methods, allows to reach the level of minimum energy consumption with the highest possible speed of containers unloading from the ship. For this control system, the authors formulated a model, an algorithm for implementing the work of control controllers and set optimal levels of control over work processes.

Keywords: Hierarchical management system, Port container terminals, Multi-level control system, Operational characteristics

1. Introduction

In recent 20 years could be observed rapid development of container ships with a cargo capacity exceeding 18,000 TEU, and this requires the development of new technologies for their cargo handling. A characteristic example in this case is parking time which grows disproportionately. When the cargo capacity of ships increases from 14,000 to 21,000 TEU, i.e. by 50%, the period of standing time required for complete overloading of the vessel increases by 150% [1].

The concentration of limited transshipment capacities of ports on the processing of "mega-vessels" leads to decrease in their throughput capacity. For this reason, almost all large terminals on the planet are increasingly turning to the modernization and technical support of the vessel's cargo handling processes. A significant part of these processes cannot be predicted and requires the use and sometimes the development of new methods for effective management, as well as requires a decision making in the shortest possible time.

2. Materials and Methods

2.1. Analysis of Trends in Automation of Container Processing Processes

Automated container terminals allow to increase significantly throughput and reduce operating costs. In comparison to general terminals where management is carried out by personnel, this fact is explained by the advantage of using improved automated equipment - automated vehicles, automatic stacker cranes (ASC), etc. Commonly known automatic container terminals in Europe are: Delta ECT (Europe Container Terminals), ECT Euromax, RWG (Rotterdam World Gateway) and HHLA (Hamburger Hafen und Logistik AG). A similar trend is observed in other ports of the world [2]. In China, the first fully automatic terminal of Qingdao QQCTN (Qingdao New Qianwan Container Terminal) entered operation in May 2017.

Cargo handling processes at the terminal can be divided into three types: wharf, warehousing and surface transportation operations. In most cases, containers at terminals with

Address for Correspondence: Luidmyla Leonidovna Nikolaieva, Naval Institute, National University, Odesa Maritime Academy, Odesa, Ukraine
E-mail: ludmila_nikolaeva@yahoo.com
ORCID ID: orcid.org/0000-0002-5887-702X

Received: 27.09.2023
Last Revision Received: 18.12.2023
Accepted: 20.12.2023

To cite this article: L. L. Nikolaieva, T. Y. Omelchenko, and O. V. Haichenia. "Hierarchical Management System for Container Vessels Automated Cargo Handling." *Journal of ETA Maritime Science*, vol. 12(1), pp. 25-35, 2024.

automatization are handled with a use of big quantity of automatic equipment: remotely controlled quay cranes (QC), automated guided vehicles (AGV) and ASC. So, e.g., the Delta ECT terminal in Rotterdam has 36 QCs, 265 AGVs and 137 ASCs. The terminal's annual electricity consumption is about 45,000 MWh. with an annual transshipment volume of 4,300,000 TEU. The terminal produces 71,300 tons of CO2 per year [3].

The development of terminal automation is constant, as almost every year is marked by new developments and new technologies for their use. GPS-based AGV, e.g., provides free behavior and significantly reduces travel time in comparison to standard operational path, or the path guided by different computer operated optical systems. We can state that freedom of AGV behavior enhance the complexity for managing operations inside terminal. From one side, preventing two AGVs from colliding have to be taken into account to provide safety operation. From another side, AGVs interact with different types of equipment (such as QC and ASC) during cargo transportation to or from vessel.

During analysis of terminals functioning, the level of security of their operation is also of particular importance. The operation of almost all non-automated terminals falls under the conclusion that work in the port is extremely dangerous. A typical example for such a conclusion is the work [4], which focuses on the trends of increasing the level of security and studies the possibility of obtaining additional advantages in the field of security by increasing the automation level of container terminals. This article examines the incidence of injuries in ports at the United States West Coast and predicts that frequency of injuries due to the introduction of automation will steadily decrease over time.

2.2. Technical and Operational Characteristics of Equipment

Main part of the automated terminals is focused on the use of automated stacking cranes (Automated Stacking Crane, ASC). The main reason for this fact is a good compatibility of these cranes with various types of automated transport.

For ASC, a stacking height of 6 tiers has become standard. Side-by-side ASCs range in length from 36 to 59 total container spaces (770 to 1,260 feet). Despite the fact that these restrictions are not strict, in a short row of containers, ASCs are not efficiently operated because of the significant price of the facility itself. In a long row the processing time of containers increases significantly. Port terminals in all ports, with the exception of the two in Hamburg, use two identical ASCs on the same set of tracks.

The stacking geometry of modern terminals with ASC is variable. The general majority includes a scheme for placing containers perpendicular to the berth. In recent years, the scheme of parallel arrangement for containers rows along the wharf has started to be used. The width of container rows is almost always equaling the range of eight to ten containers. The exception is the CTA and CTB terminals in Hamburg, which use a scheme of twelve container rows.

3. Management of Terminals

3.1. Problems of Effective Management of Automated Cargo Handling Processes

Three levels of problems are distinguished at container terminals: strategic, tactical and operational, depending on the time limits required to solve certain tasks of this level [5].

Problems solution at the first level concerns the layout of container terminal. At this level should be realized a pick-up of all necessary equipment that will be used for several years. Zhen et al. [6] had compared two different automated port terminals and for these two types he received a quantitative evaluation of their effectiveness; Vis and de Koster [7] had carried out a technical and economic analysis of automated vehicles such as AGV and ALV.

• Tactical problems tend to focus on the level which is answering to equipment capacity and state the amount of facilities needed to complete works expeditiously, ranging from days to months. Alessandri et al. [8] propose a dynamic approach to determine a correct part of available resources of a specific carrier of one modality. He has done it with a use of flow model based on discrete time. The required quantity of AGVs for container terminal which is partially automated was found out with the use of minimum flow algorithm [9].

At the operational level for the time interval from a few minutes to days, the detailed operation of the container handling equipment is decided. This problem solution includes the choice of processing means and the route for containers transportation within the terminal.

In [10], at the operational level, approaches to the solution of container terminal management tasks were classified as: software-based approaches (object-oriented approaches; agent-oriented approaches); analytical approaches (equipment planning; transport assignment; route determination).

Programming-based approaches are used to depict the behavior of container handling facility in an automated container terminal. In the category of programming approaches as the main concepts could be stated object-oriented and agency-oriented languages.

Object-oriented approaches provide a computer model using the concept of "object" characterized by a set of

attributes and methods [11]. Each terminal component (e.g. a single device or vessel) can be considered as an object. Connection of the objects answering to the different equipment is a basis for creation of container terminal [12].

On the basis of object-oriented programming, Duinkerken and Ottjes [13] developed a simulation model. It was done for automated container terminal. Their large-scale terminal was created on the technological traffic management system and for routing this system provides high level safety. The detailed model of the container terminal which was created with the use of object-oriented Plant Simulation model [14] is used to analyze the performance of container terminals. Governing parameter in this model is variating speed of the facilities.

Agent-oriented programming as a main concept uses term "agent" and in the following multiple agents are cooperating between themselves. In this type of programming "agent" answering to computer system which by its own have an ability to act independently on behalf of its user or owner. This system which actually is multi-agent system consists of a number of agents that can communicate with each other by exchanging messages [15].

Henesey [16] proposed a multi-agent approach. Its purpose is to enlarge the efficiency of container terminal by enlarging the capacity of available resources. Disadvantage of this solution is that the main attention is paid to the multi-agent interconnection between the components of the container terminal facilities, but not to the algorithm which regulate control and optimization operational mode of the facility. In other work, Henesey et al. [17] used simulator with "agents" and calculated operational modes when overloading containers with real parameters.

Xiao et al. [18] proposed an apportioned agency system for terminal traffic planning and berth allocation planning. In their system, coordination and cooperation refer to the berth allocation which does not consider a precise coordination between individual parts of facility at the current level of operation.

In addition to software approaches, there are analytical models for mathematical optimization of those operations where equipment planning and transport facilities management are usually considered apart from each other [19]. Facility scheduling is strongly related to the ship's service time and can determine operation and routing of equipment at a given time.

At container terminals, ship service time is the main productivity factor for terminal operators [20]. Because of this reason, the equipment of the automated container port terminal should be used in the optimal way to minimize the time to complete the processing of containers.

Considering the complex structure of automated container terminal operation specific areas (e.g. berths) should be considered to simplify the overall layout of the equipment. For a berth area, the planning task determines the sequence of QC work tasks and the optimal operational time intervals at which they can be completed [21], taking into account the different objectives and constraints of different operations.

In most cases, the problems of assigning a vehicle at a berth are considered under uncertainty conditions to adjust online changes in the terminal environment. The AGV administration problem is mainly treated as an individual research problem and during its solution various simplifying procedures are used. Despite of this, because of the strong interrelationship with the coastline area, loading capacity at the berths must be clearly defined, taking into account a certain algorithm for administrating AGVs.

The routing problem is an important problem. It usually focuses on avoiding collisions and deadlocks between all types of autonomous vehicles. Kim [22] has developed an effective algorithm for predicting and preventing deadlock situations with AGVs. Zeng [23] has described routing algorithm to avoid collisions by giving an ability to vehicles to variate their speed during interaction.

3.2. Types of Container Terminal Operations Management Systems

In our research container terminal was considered as a system which is large-scale and inside of it every different part of facility possesses its own dynamics. Work of various components have to be coordinated among themselves individually.

As a system container terminal consist of large number of subsystems and their control causes many difficulties for management. To solve these problems, there are systems of distributed and hierarchical control. They are applied in various transport areas, such as water and transport networks [5].

During the research, three types of container terminal management were identified: centralized, distributed, hierarchical.

The hierarchical type of control refers to the situation when local controllers are dependent and must respond to the flow of data from all neighboring local controllers. By means of this principle of interaction, a multiscale system of terminal can be divided into a number of levels. For their coordination should be used a hierarchical structure. In this case, during solution large problem is divided to several private sublevel problems. An example of hierarchical management structure is shown in Figure 1.

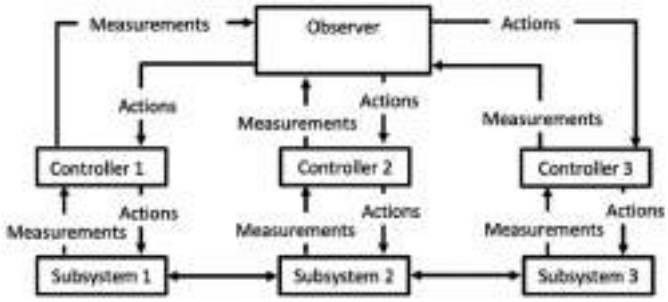

Figure 1. *Hierarchical management system*

From our point of view, all methods of container terminals managing which are based on software technologies should use only a hierarchical management structure. In contrast to analytical methods, they can use the architecture of combined management in a centralized way with the assessment of the hierarchy of the environment in the definition of agents.

It makes sense to use ship service time as a key performance indicator. This criterion has a strong relation with other performance indicators that directly connected with terminal's transport processes. In general, local performance indicators include: time for calculations; time for service; time to complete the work; the volume of electricity consumption; average and relative AGV travel distance; QC operation; operation of AGV and ASC [19].

4. Hierarchical System of Automated Processes Management

4.1. General Model

General scheme (Figure 2) of a container terminal using hierarchical control system for ship cargo processing is a composition of one QC and several AGVs and ASCs. In standard unloading procedure QC takes container out the ship and puts it to an AGV. Then it goes on with container from berth to the area of container stacking. In this area container processing is done by using ASC. In such a cycle, it is very important to take into account the moment when containers are transferred from one equipment to another.

Management of port terminal processes consists of high- and low-level management and could be characterized by dynamical changes in discrete event time interval and continuous time, which reflects the behavior of a big quantity of terminal facility. To control the dynamical changes of the higher level, the problem of planning is solved according to the minimum time of works completion.

At the lower sublevel hierarchical model of the terminal can be described by differential-algebraic equations. Another-higher level, is more complex and description of the system is more notional and should use modeling techniques using

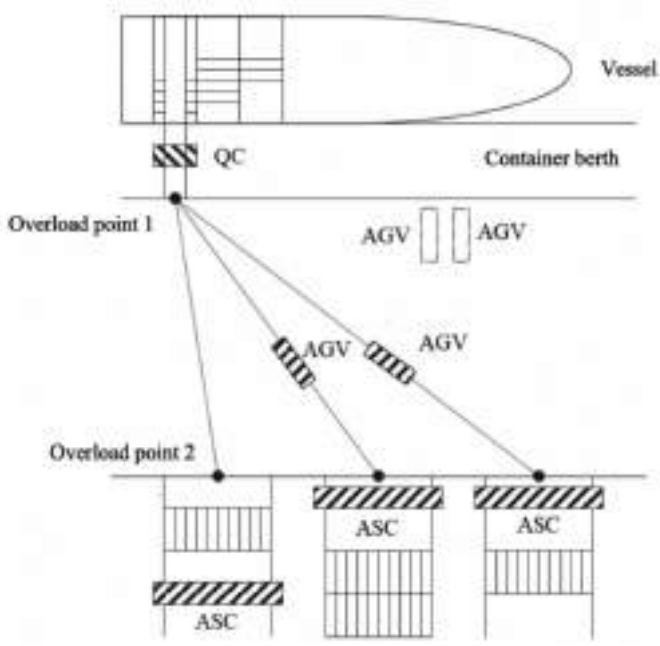

Figure 2. *General scheme of a container ship cargo handling*

discrete events. Management architecture can be built with decomposition of dynamics of all operations in the system. Typically, the controller assigned to the upper level controls the control group of discrete events, and the lower level controller controls the dynamics of the continuous operation of the equipment. The upper layer and the lower layer interact using a special interface which in real time compile continuous signals and signals of discrete events. The signal of discrete state on the higher level causes dynamical changes of continuous procedure in the lower one [24].

Dynamics of container transportation was modeled at two levels: the dynamics of high-level discrete events (Petri networks, the Max-plus equation); continuous-time dynamics of the lower level (differential equations describing the dynamics of container transporting single facility).

At the system highest level, the behavior was reflected by dynamics of a discrete event. It was reflecting during which period of time and in which sequence the number of containers is processed by the available facility units (e.g. QC, AGV, ASC). The operation of facility elements was presented as a flow on three stages in the form of a discrete system where each work went through several stages. At each stage, a set of the same tasks were used. Each of them was performed sequentially and required a certain amount of time. As it is shown in Figure 3 a work was set as the total process where the container was moved from the ship to the place of containers stacking. Single work was

performed using three types of facility: QC, AGV and ASC. Every operation can be divided into three levels: stage 1 - unloading by QC; stage 2 - moving of single AGV; stage 3 - stacking by ASC use.

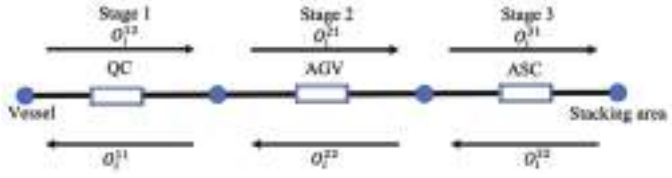

Figure 3. *Discrete system of work performance sequence*

4.2. Sequences of Equipment Working Places During Ship Processing

To describe the operation with three types of facility shown in Figure 3 should be used: P_i^1 - place of container number i on the ship. P_i^2 - transshipment point where container number i is moved from QC to AGV. P_i^3 - transshipment point where container number i is moved from AGV to ASC. P_i^4 - storage location of container number i.

At the first level, two operations O_i^{11} and O_i^{12} are performed. Operation O_i^{11} is defined as QC movement from P_i^2 to P_i^1 for the i-th container. Operation O_i^{12} is defined as QC movement in the reverse direction with the i-th container. In stage 2, two operations O_i^{21} and O_i^{22} are performed also. During these operations AGV moves from P_i^2 to P_i^3 with the i-th container and returns from P_i^3 to P_i^2 after unloading the corresponding i-th container. Operations O_i^{31} and O_i^{32} are performed on stage 3, where ASC transfers the i-th container from P_i^3 to P_i^4 and returns from P_i^4 to P_i^3 after unloading the i-th container respectively.

The hybrid flow problem for the situation presented in Figure 3 consists in finding sequences of equipment working places that optimally provide processing of the vessel.

We represent N as the number of movements for container transportation from vessel to the stack, F as a set of tasks | F | = N. During realization of every operation at each stage, there is a mutual time relation: ending time of the previous stage answers the starting time of the next stage and such time constraints were written in the form:

$$a_i + R\left(1 - \sigma_{ij}^1\right) \geq 0, \forall_i \in F, \tag{1}$$

$$a_i + R\left(1 - \sigma_{ij}^1\right) \geq b_i, \forall_i \in F, \forall_j \in F, i \neq j, \tag{2}$$

$$a_i + t_i^{11} + t_i^{12} \leq b_i, \forall_i \in F, \tag{3}$$

$$b_j + R\left(1 - \sigma_{ij}^2\right) \geq c_i + t_i^{22}, \forall_i \in F, \forall_j \in F, i \neq j, \tag{4}$$

$$b_i + t_i^{21} \leq c_i, \forall_i \in F, \tag{5}$$

$$c_j + R\left(1 - \sigma_{ij}^3\right) \geq c_i + t_i^{31} + t_i^{32}, \forall_i \in F, \forall_j \in F, i \neq j. \tag{6}$$

where $\forall_i \in F_1$ and $\forall_j \in F, i \neq j$; $\sigma_{ij}^1 = 1$ describes that the task j is producing exactly after the task i at the 1 stage; $\sigma_{ij}^1 = 0$; $\sigma_{ij}^2 = 1$ describes that the task j is performed immediately after the task i at stage 2; $\sigma_{ij}^2 = 0$; $\sigma_{ij}^3 = 1$ means that the task j is performed immediately after the task i at stage 3, otherwise $\sigma_{ij}^3 = 0$; a_i - starting time of the task i at stage 1, it answers the moment when QC starts moving to P_i^2; b_i - beginning of the task i at stage 2, it answers the moment when AGV begins moving to P_i^3; c_i - beginning of the task i at stage 3, it answers the moment when ASC starts moving to P_i^4; $t_i^{h_1 h_2}$ - execution time of overloading operations $O_i^{h_1,h_2}$, where $h_1 \in \{1,2,3\}, h_2 \in \{1,2\}$; R - constant number.

Inequality (1) demonstrates the opening task performed by QC. Inequality (2) demonstrates relationship between tasks i and j performed by QC. Inequality (3) represents task i done by AGV when QC finished its operation. Inequality (5) demonstrates that task i is performed by ASC when AGV finished its operation. Inequalities (4) and (6) describe the ratio of task i performed by AGV and task j performed by ASC.

In addition to the time limitations in formulas (1)-(6) discrete control variables σ_{ij}^1 , σ_{ij}^2 and σ_{ij}^3 have constraints too. They ensure that each equipment has one previous operation and one subsequent operation for each stage. However, for the first performed operation j and for the last operation i σ_{ij}^1 , σ_{ij}^2 and σ_{ij}^3 ($i \in$ F, $j \in$ F, $i \neq j$) have to take the value 0. Finally, we define two operations 0 and N +1.

With the use of $\Phi_1 = \Phi \cup \{0\}$ and $\Phi_2 = \Phi \cup \{N+1\}$ we can introduce additional restrictions for the first and last operation. Finally, all restrictions can be written as;

$$\sum_{j \in \Phi_2} \sigma_{ij}^1 = 1, \forall_i \in F, \tag{7}$$

$$\sum_{i \in \Phi_1} \sigma_{ij}^1 = 1, \forall_j \in F, \tag{8}$$

$$\sum_{j \in \Phi} \sigma_{0j}^1 = n_{qc}, \tag{9}$$

$$\sum_{i \in \Phi} \sigma_{i(N+1)}^1 = n_{qc}, \tag{10}$$

$$\sum_{j \in \Phi_2} \sigma_{ij}^2 = 1, \forall_i \in F, \tag{11}$$

$$\sum_{i \in \Phi_1} \sigma_{ij}^2 = 1, \forall_j \in F, \tag{12}$$

$$\sum_{j \in \Phi} \sigma_{0j}^2 = n_{agv}, \tag{13}$$

$$\sum_{i \in \Phi} \sigma_{i(N+1)}^2 = n_{agv}, \tag{14}$$

$$\sum_{j \in \Phi_2} \sigma_{ij}^3 = 1, \forall_i \in F, \tag{15}$$

$$\sum_{i \in \Phi_1} \sigma_{ij}^3 = 1, \forall_j \in F, \tag{16}$$

$$\sum_{j\in\Phi}\sigma^{3}_{0j} = n_{asc}, \quad (17)$$

$$\sum_{i\in\Phi}\sigma^{3}_{i(N+1)} = n_{asc}, \quad (18)$$

Equations 7 and 8 show that for each operation i ∈ F one previous and one subsequent operation would be performed by QC. Equations 9 and 10 reflect the use of n_{qc}. Equations 11 and 12 show that in every operation i ∈ F, there exists only one previous operation and single subsequent operation nominated to a specific AGV. Equations 13 and 14 reflect the use of n_{agv}. Equations 15 and 16 indicate that for every operation i ∈ F one previous and one subsequent operation would be performed by a certain ASC. Equations 17 and 18 reflect the use of n_{asc}.

It is possible to model the hierarchical dynamics of discrete events for three types of equipment during the unloading of a container ship on the basis of (1-18). In this process, the ending time *i* at every point and a chain of operations performed by certain equipment at each stage are variable. They are defined exclusively by the system controller only.

A similar system of equations can be used in modeling of ship loading operations. In this case should be varied the order of QC-AGV-ASC to ASC-AGV-QC and replaced t_i^{22} with t_j^{22} in (4). In this case dynamics of continuous operation of individual parts of equipment can be described as

$$\dot{r}(t) = g(r(t), u(t)), \quad (19)$$

$$\dot{r}_1(t) = r_2(t), \quad (20)$$

$$\dot{r}_2(t) = u(t), \quad (21)$$

where r (t) - a continuous status; u (t) - facility control variable; r_1(t) - position of equipment unit, m; $r_2(t) \in [v_{min}, v_{max}]$ - velocity of equipment unit, m/sec; $u(t) \in [u_{min}, u_{max}]$ - acceleration of equipment unit, m/sec^2.

4.3. Two-Level Structure of the Hierarchical Management System

The structure of the hierarchical container terminal management system can also be described as two-level on a base of proposed method. As one can see in Figure 4, at the top level, the supervisory dispatcher determines the time limits of cargo operations. The stage controller in online mode assigns the value of time interval of every operation to a specific unit of facility. In the proper way to plan operations supervisor have to know the time necessary for each technological operation. Therefore, the upper level requires from hardware dynamics controllers from lower level the value of minimum time needed to perform a certain technological operation. The supervisory dispatcher plans operations and compiles the work schedule on the base of the required time which was received from the controller of the stage.

On a base of the continuous time dynamics and with evaluation of a cost function which was found out over obtained time, the upper level suggests the use of the optimal amount of equipment. When system answering the lower level, it's governed by the dynamics of uninterrupted operation of every individual unit of facility. The controller of lower layer schedules operation of the specified equipment when the value of the time interval for operations from the upper layer is received.

To reduce the consumption volumes of energy, the upper-level controller should provide the maximum level of energy-saving planning. In the case when there is a sufficient time interval, it should maximally increase the duration of all operations [25].

The main aim of the supervisory dispatcher is to achieve the minimum level of energy efficiency. In this case, it is necessary the time schedule for the completion of the n-th number of overload operations reduce to a minimum

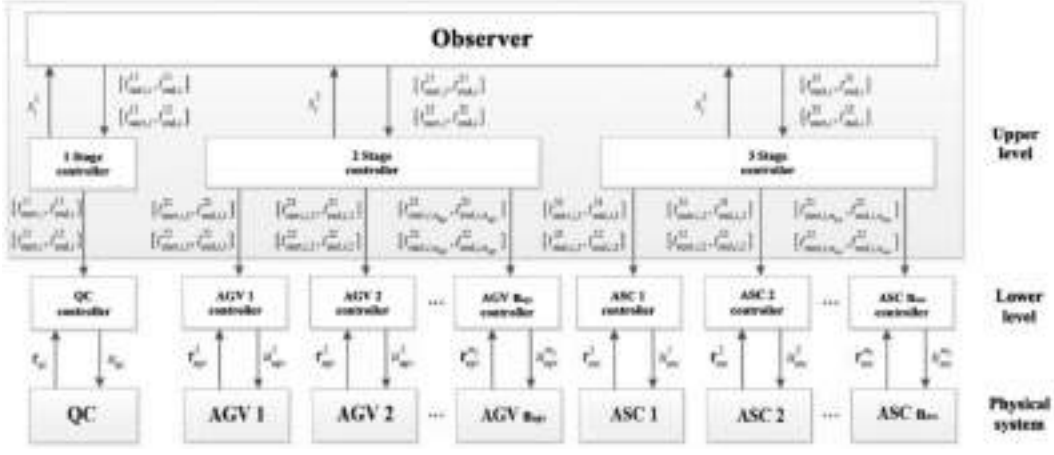

Figure 4. *Common structure of the hierarchical management system*

with considering the maximum time for all operations completion.

If we name for the same equipment all identical operations O_i^{11} and O_i^{12} as $t_i^{11} = t_i^{12}$, and $t_i^{31} = t_i^{32}$ for operations O_i^{31} and O_i^{32} it is possible to express the total time of all operations as $\|t\|_1$ ($\|\cdot\|_1$ – *l*-norm). In this case parameter t was written as

$$t = \left[t_i^{11}, \ldots, t_N^{11}, t_i^{12}, \ldots, t_N^{12}, t_i^{21}, \ldots, t_N^{21}, t_i^{22}, \ldots, t_N^{22}, t_i^{31}, \ldots, t_N^{31}, t_i^{32}, \ldots, t_N^{32}\right]^T$$

Considering the dynamics of discrete events, the optimization problem was formulated in a form;

$$\max_{t,a,b,c,\sigma} \|t\|_1, \quad (22)$$

It should be solved under conditions;

$$\min_{a,b,c,\sigma} \|w\|_\infty, \quad (23)$$

$$s_i^{h_1 h_2} \le t_i^{h_1 h_2}, \forall_i \in \Phi, \quad (24)$$

$$t_i^{11} = t_i^{12}, \forall_i \in \Phi, \quad (25)$$

$$t_i^{31} = t_i^{32}, \forall_i \in \Phi, \quad (26)$$

where $s_i^{h_1 h_2}$ is the lower limit of $t_i^{h_1 h_2}$.

The value of lower limit $s_i^{h_1 h_2}$ could be obtained by the stage controller during the calculation of minimum operating time. Thus, to optimize the system, the equality $s_i^{h_1 h_2} = t_i^{h_1 h_2}$, with $\|w\|_\infty = w_{min}$ should be fulfilled. At the same time, in the first stage, σ_{ij}^1, σ_{ij}^2 and σ_{ij}^3 are used as input data for optimization at the next upper stage.

The highest value of processing time (22) with the minimum overall work schedule can be written using conditions;

$$\|w\|_\infty = w_{min} \quad (27)$$

$$s_i^{h_1 h_2} \le t_i^{h_1 h_2}, \forall_i \in \Phi \quad (28)$$

$$t_i^{11} = t_i^{12}, \forall_i \in \Phi \quad (29)$$

$$t_i^{31} = t_i^{32}, \forall_i \in \Phi \quad (30)$$

To make analysis easier the two-level structure of the hierarchical control system for three types of equipment with these equations can be divided into two stages:

- The first stage, when the lower limit of working time is stated by the controller at the moment when request from the supervisory dispatcher about the time that is necessary for the technological operation is received;

- The second stage, when supervisor set up the time of technological procedures at every stage. The time limits of all operations at every stage are transmitting from the dispatcher to the controller which already assigns the work to a specific piece of facility at every stage.

When using these two stages, the following seven procedures should be performed: the supervisor sends a request for the time which is necessary to realize operation at every stage; the minimum duration for each operation using QC, AGV and ASC is found out by the appropriate stage controller; supervisory dispatcher receives data about duration for each operation from stage controller; supervisory dispatcher calculates work (with condition of minimal energy spending) timetable in three stages; supervisory dispatcher sends to controller the data about time necessary to conduct operations; upper-level controller makes an assignment of every operation to a specific unit of equipment at every stage; QC, AGV, and ASC controller (answering to lower-level) receives data about time duration diapason to calculate trajectories of each equipment to receive minimal energy spending.

The whole procedure of the hierarchical structure for terminal management with all stages shown in Figure 5.

Figure 5. *Procedure of hierarchical management structure*

The analysis of the proposed model makes it possible to conclude that the hierarchical management structure emphasizes the interdependence of the planning task regarding the dynamics of discrete events of all equipment units and the task of optimal control between individual equipment elements with consideration of continuous time dynamics.

5. Results

5.1. Dynamics of Discrete Events in A Hierarchical Control System

To consider the quantity of new containers in the dynamic model of the hierarchical management structure one should use following equations;

$$x(k+1) = Ax(k) + B_1 u(k) + B_2 \delta(k) + B_3 z(k) + B_4 d(k), \quad (31)$$

$$y(k) = Cx(k) + D_1 u(k) + D_2 \delta(k) + D_3 z(k), \quad (32)$$

$$E_2 \delta(k) + E_3 z(k) \le E_1 u(k) + E_4 x(k) + E_5, \quad (33)$$

where $d(k)$ is a term indicating the number of new arriving containers, factors B_4, D_4 show how $d(k)$ makes influence on current state and final output.

These three equations give ability to consider delivery of new containers as an external incoming data in combination with position and velocity of machines. Dynamics of machines which is individual for every unit do not change, but the choice of machines actions remains variable.

To provide evaluation of the model for every stage of time it is necessary to specify value of *d(k)* and for the proposed controller formulate objective function. This function consists of two parts: load capacity and energy efficiency.

We have used completion time and energy consumption as main performance indicators.

Time to complete transportation of all containers, provided that $N_s(k) = N$ and energy consumption of all machines are determined by the equations;

$$k_{finish} = \min k, \tag{34}$$

$$E_{tot} = E_{qc} + E_{agv} + E_{asc}, \tag{35}$$

where E_{tot} is total energy consumption of all technological equipment; E_{qc}, E_{agv} and E_{asc} are QC, AGV, and ASC energy consumption, respectively.

E_{qc} values can be calculated from;

$$E_{qc} = \sum_{k=0}^{N_{sim}-1} E_{qc}(k) \tag{36}$$

$$E_{qc}(k) = \begin{cases} 0.5\, m_{qc}(k) \times \left(v_{qc}^2(k+1) - v_{qc}^2(k)\right) \\ v_{qc}^2(k+1) > v_{qc}^2(k) \end{cases} \tag{37}$$

$$m_{qc} = \begin{cases} m_{qc}^{unload}\, v_{qc}(k+1) < 0 \\ m_{qc}^{load}\, v_{qc}(k+1) > 0 \end{cases} \tag{38}$$

where N_{sim} is a simulation length; m_{qc}^{unload}, m_{agv}^{unload}, m_{asc}^{unload} are weights of QC, AGV and ASC without containers; m_{qc}^{load}, m_{agv}^{load}, m_{asc}^{load} are weights of QC, AGV and ASC with container.

To find the correct N_p it's necessary to check effectiveness of the procedure of all containers processing. This can be done when one changes the value of N_p of the proposed controller. In the case when all containers can be processed completely one should use notation "1". In opposite situation, when all containers cannot be transferred to the stacking area one should use notation "0". During modelling we tested different values of N_p with quantity of containers N equals 10.

Figure 6 shows that a short forecasting horizon has no ability to ensure that all containers will be transferred from the ship to the stack location. Short forecasting horizons have no ability to predict full cooperation between all parts of the system. Due to imperfect prediction units of equipment remain in the same area. That is the main reason why all containers wouldn't be transported to a final stack location with a short forecast horizon.

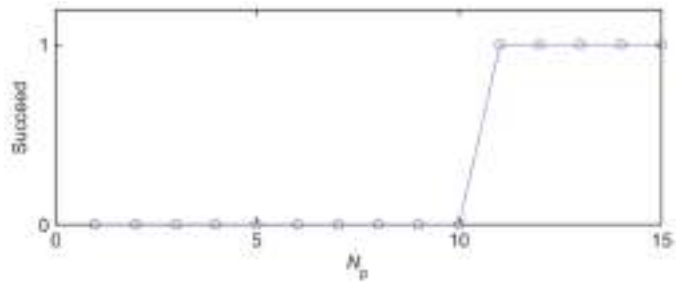

Figure 6. *Effect of simulation in relation to the forecast horizon Np*

5.2. Capacity and Energy Efficiency of Container Terminals Under a Hierarchical Management System

Simulation was done for the general pier scheme shown in Figure 7 in order to determine efficiency indicators.

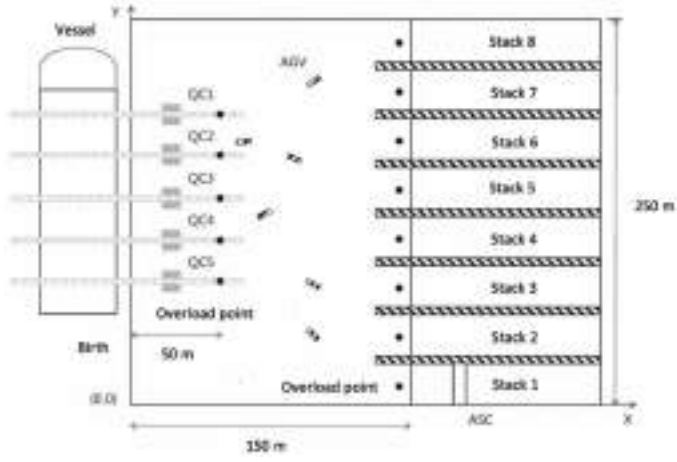

Figure 7. *Scheme of the pier for unloading process*

Figure 8 reflects energy consumption at the minimum completion time for operation and at the optimal energy consumption. In each test, the time of single technological operation of every individual unit of equipment was stated. It was assumed that each piece of equipment worked at maximum speed. The results show that in energy-saving mode, every production equipment does not need to run at maximum speed. Comparison of different power consumption on the graph shows that the maximum energy saving was 37%.

Figures 9 and 10 show traditional and energy-saving graphs when using a hierarchical control system. The number in every block is answering to the serial marking of the unloaded container. In a regular target time of single operation per unit of facility was fixed. Because of necessity

to synchronize different types of technological facility, some devices had a longer waiting time. This can be seen in the graph of AGV and ASC in Figure 9. As one can see in Figure 10 equipment has a more flexible processing time and that is a main reason why time period required to realize an operation by one facility unit can be increased. This fact for energy reduction is beneficial. Reduction of spent energy didn't lead to arising of time necessary to complete operation & As it can be seen in Figures 9 and 10 completion time is fully identical.

6. Discussion

Hierarchical management system for container vessels automated cargo handling, which has been developed during research works has one important advantage. On the lower level the hierarchical model of the system can be described with the use of fairly simple differential-algebraic equations but on a higher level it is based on the use of unique method for modeling discrete processes. High quality management architecture can be created on the base of the process when dynamics of all technological operations in the system of container terminal is divided onto detailed component

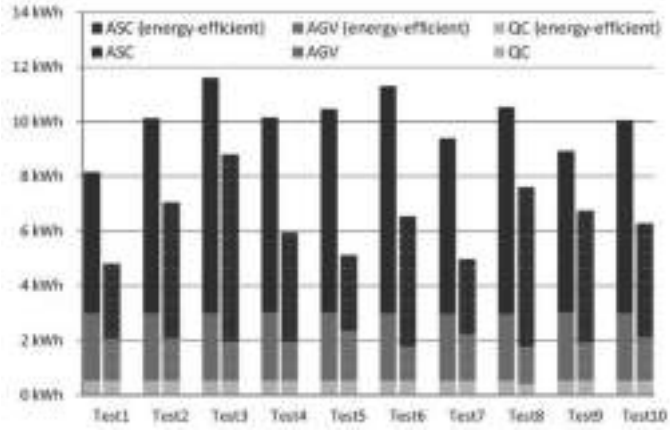

Figure 8. *Energy consumption*

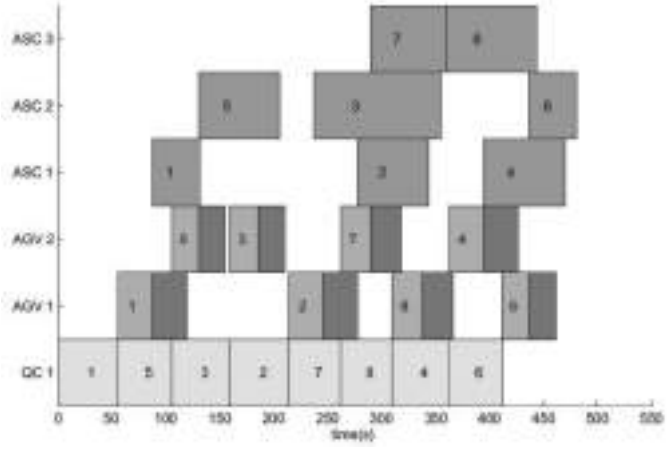

Figure 9. *Schedule of the usual hierarchical management system*

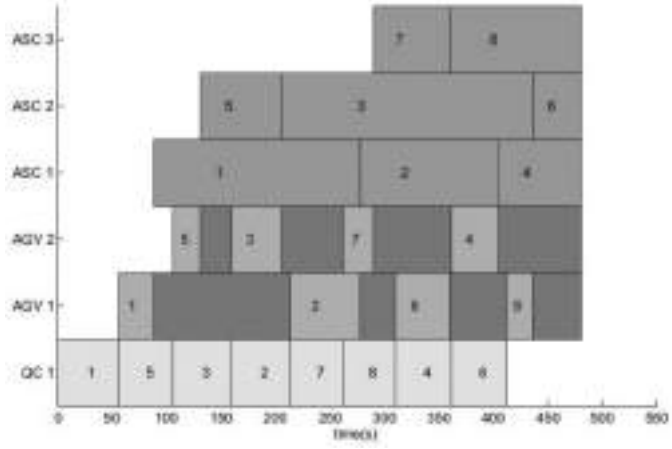

Figure 10. *Energy-saving graph of the hierarchical control system*

hierarchical levels. In the future this type management will be characterized by maximum efficiency, low levels of accumulated energy and improved safety indicators.

At the same time, it can be stated that all current researches should be directed to the development of new concepts and methods that give an ability to optimize the management of automated processes of overloading operations during processing of container vessels. From our point of view, new methods should use algorithms, which during operation of the terminal will be using artificial intelligence.

Main basis for introduction of artificial intelligence inside port terminal management can be algorithms that are stated on the control system which is a hierarchical and described in this article. However, in the future, such algorithms will require a huge amount of accumulated statistical results from the operation of all port terminals in the previous time. It is possible to state, that such statistical data would be containing not only operational technical parameters of local areas of terminal. Such data can, for example, provide precise meteorological indicators that can determine the influence of wind drag force on the speed of unloading containers or the change in energy consumption due to the ambient temperature.

The use of artificial intelligence based on hierarchical control systems will make it possible to change significantly the vessel's stand by hours by increasing the speed of vessel processing and improve the level of safety during the operational hours of container terminals. This optimization is especially important in situations where takes place a constant change in used operating equipment during the processing of a large number of containers.

7. Conclusion

The dynamics of container transportation in port terminal should be thought-out as a hierarchical system which

includes the dynamics of permanent time and individual events. A hierarchical management structure for this system was offered and it contains two interconnected levels. The upper level dedicated during operation for scheduling. At this level time for operation of every unit of facility is stated and minimum time for operation completing is set. The next bottom level consists of a controller which works with every unit of technological facility. At a lower level could be achieved reduction in energy consumption and it could be done by meeting time constraints given by the upper level.

The hierarchical management structure emphasizes the interdependence of the planning task regarding the dynamics of discrete events of all equipment units and the task of optimal control between individual equipment elements taking into account the dynamics of continuous time.

In comparison with traditional container terminal scheduling during simulation was found out that, with the analogical minimum time to complete the process, an optimal approach can save 37% of energy used for its realization.

Authorship Contributions

Concept design: L. L. Nikolaieva, Data Collection or Processing: L. L. Nikolaieva, T. Y. Omelchenko, and O. V. Haichenia, Analysis or Interpretation: L. L. Nikolaieva, and T. Y. Omelchenko, Literature Review: L. L. Nikolaieva, T. Y. Omelchenko, and O. V. Haichenia, Writing, Reviewing and Editing: L. L. Nikolaieva, T. Y. Omelchenko, and O. V. Haichenia.

Funding: The author received no financial support for the research, authorship, and/or publication of this article.

References

[1] Review of Maritime Transport 2022. Reported by the UNCTAD secretariat. Geneva: United Nations; 2022, pp. 174. [Online] Available: https://unctad.org/system/files/official-document/rmt2022_en.pdf

[2] Notteboom T, Pallis A, Rodrigue J-P. Port Economics, Management and Policy, New York: Routledge, 2022, pp. 690. [Online] Available: doi.org/10.4324/9780429318184

[3] Van Jole, J. A. "Control of Automated Container Terminals. A Literature review on automated container handling equipment," Delft: TUDelft; 2014. 72 p. [Online]. Available: http://resolver.tudelft.nl/uuid:bea0917e-6fc7-493a-8bb2-bffd6cb145e4

[4] W. K. Kon, N. S. F. A. Rahman, R.M. Hanafiah, and S. A. Hamid, "The global trends of automated container terminal: a systematic literature review," *Maritime Business Review*, vol. 6, pp. 206-233, 2020. [Online] Available: https://doi.org/10.1108/MABR-03-2020-0016

[5] ITF (2021), Container Port Automation: Impacts and Implications, International Transport Forum Policy Papers, OECD Publishing, Paris. 2021. no. 96, [Online] Available: https://www.itf-oecd.org/sites/default/files/docs/container-port-automation.pdf

[6] L. Zhen, L. H. Lee, E.P. Chew, and D. Chang, "A comparative study on two types of automated container terminal systems." *IEEE Transactions on Automation Science and Engineering*, vol. 9, pp. 56-69, Jan 2012.

[7] I. F. A. Vis, and R. de Koster, "Transshipment of containers at a container terminal: An overview." *European Journal of Operational Research*, vol. 147, pp. 1-16, 2003.

[8] A. Alessandri, C. Cervellera, M. Cuneo, and M. Gaggero, "Modeling and feedback control for resource allocation and performance analysis in container terminals." *IEEE Transactions on Intelligent Transportation Systems*, vol. 9, pp. 601-614, Dec 2008.

[9] Z. Zhuang, Z. Zhang, H. Teng, W. Qin, and H. Fang. "Optimization for integrated scheduling of intelligent handling equipment with bidirectional flows and limited buffers at automated container terminals." *Computers & Operations Research*, vol. 145, pp. 105863, Sep 2022.

[10] A.-K. Schwientek, A.-K. Lange, and J. Carlos, "Literature classification on dispatching of container terminal vehicles," Epubli GmbH, Berlin, vol. 24, pp. 3-36, 2017.

[11] S.-H. Hur, C. Lee, H.-S. Roh, S. Park, and Y. Choi, "Design and simulation of a new intermodal automated container transport system (ACTS) considering different operation scenarios of container terminals." *Journal of Marine Science and Engineering,* vol. 8, pp. 233, Mar 2020.

[12] D. Yi, and L. Tiantian, "Simulation research on u-automated container terminal." *Journal of System Simulation*, vol. 33, pp. 2944-2951, 2021.

[13] M. B. Duinkerken, and J. A. Ottjes, "A simulation model for automated container terminals." *Proceedings of the Business and Industry Simulation Symposium*, vol. 10, pp. 134-139, Oct 2000.

[14] B. Ha, E. Park, and C. Lee, "A simulation model with a low level of detail for container terminals and its applications," *Proceedings of the 2007 Winter Simulation Conference,* pp. 2003-2011, Dec 2007.

[15] G. Tang, L. Guo, Z. Zhao, P. Zhou, D. Zhang, and H. Xu, "A Multi-agent-based simulation model for operations in the automated container terminal with a u-shaped layout." ICCMS 2022: *Proceedings of the 14th International Conference on Computer Modeling and Simulation,* pp. 54-61, Jun 2022.

[16] L. E. Henesey, "Enhancing container terminal performance: a multi agent systems approach," Karlshamn: BTH, Jan 2004.

[17] L. E. Henesey, P. Davidsson, and J. Persson, "Agent based simulation architecture for evaluating operational policies in transshipping containers." *Autonomous Agents and Multi-Agent Systems*, vol. 18, pp. 220-238, Apr 2009.

[18] F. Y. Xiao, P. K. Li, and H. C. Chun, "A distributed agent system for port planning and scheduling." *Advanced Engineering Informatics*, vol. 25, pp. 403-412, Aug 2011.

[19] L. Chen, A. Langevin, and Z. Lu, "Integrated scheduling of crane handling and truck transportation in a maritime container terminal." *European Journal of Operational Research*, vol. 225, pp. 142-152, 2013.

[20] The World Bank, 2023. The Container Port Performance Index 2022: A Comperable Assesment of Performance based on Vessel Time in Port (Fine). World Bank, Washington, DC. pp. 89. [Online]. Available: https://issuu.com/world.bank.publications/docs/k1250

[21] A. Diabat, and E. Theodorou, "An integrated quay crane assignment and scheduling problem." *Computers & Industrial Engineering*, vol. 73, pp. 115-123, Jul 2014.

[22] K. H. Kim, S. M. Jeon, and K. R. Ryu, "Deadlock prevention for automated guided vehicles in automated container terminals." *OR Spectrum*, vol. 28, pp. 659-679, 2006.

[23] J. Zeng, and W. Hsu, "Conflict-free container routing in mesh yard layouts." *Robotics and Autonomous Systems*, vol. 56, pp. 451-460, May 2008.

[24] P. Rendahl, "Continuous vs. discrete time: Some computational insights," *Journal of Economic Dynamics and Control*, vol. 144, 104522, Nov 2022.

[25] L. Chen, T. Dong, J. Peng, and D. Ralescu, "Uncertainty analysis and optimization modeling with application to supply chain management: a systematic review." *Mathematics*, vol. 11, pp. 1-45, May 2023

Journal of ETA Maritime Science 2024;12(1):36-49

Competitiveness Factors of a Shipyard in the Era of New Uses of Oceans

Brais Preto-Fernández[1], Natalia Paleo-Mosquera[1], Almudena Filgueira-Vizoso[2], Ramón Yáñez-Brage[3], Laura Castro-Santos[4]

[1]IES Lamas de Abade, Santiago de Compostela, Department of Education of the Xunta de Galicia, Department of Mathematics, Spain
[2]University of Santiago de Compostela Faculty of Political and Social Sciences, Department of Political Science and Sociology, Santiago de Compostela, Spain
[3]University of A Coruña, Polytechnic School of Engineering of Ferrol, Department of Chemistry, Coruña, Spain
[4]University of A Coruña, Polytechnic School of Engineering of Ferrol, Department of Naval and Industrial Engineering, Coruña, Spain

Abstract

The aim of this paper is to examine the most relevant competitive factors of a shipyard. The method conducted interviews and questionnaires with multiple agents related to the company and analyzed several institutional, business, and academic documents. The case of study considered was the manufacturing center of Navantia, S.A. in the Ferrol estuary (A Coruña, North-West of Spain). The results indicate that the five most important competitive factors are the government and political support, the production organization, the product technology, manpower, and skills and knowledge. Thus, these five competitive factors are critical to analyze the competitiveness of a shipyard with the characteristics of the one studied for new uses of the ocean, such as offshore wind, wave energy, or aquaculture.

Keywords: Competitiveness factor, Shipyard, Shipbuilding, Oceans, Offshore renewable energies

1. Introduction

The European shipbuilding industry decayed in the 1990s mainly because of the great international competition in East Asia [1]. They usually carried out traditional shipbuilding [2]: building and repairing civil and military vessels.

Nowadays, the European shipbuilding industry has a chance of diversifying its order books to introduce new products derived from the offshore wind sector. Shipyards are the facilities where offshore wind platforms [3], both fixed and floating, are built. Therefore, Europe can lead the new era of uses of the sea by providing additional activities to its shipyards. It will generate thousands of jobs in different sectors, such as shipbuilding, industrial engineering, energy sector, and maintenance, which will enrich the areas where they were carried out.

Husumer Schiffswerft, FR. Fassmer and Abeking & Rasmussen are German shipyards that consider the offshore wind sector as a complementary business [1]. Since 2014, the Navantia Fene shipyard has built 29 fixed offshore wind structures called jackets for the Wikinger project and floating offshore wind substructures (5 spar Hywind platforms for the Hywind Scotland Pilot Park of Statoil offshore wind farm in United Kingdom and 5 semisubmersible WindFloat platforms for Portugal) [4].

Therefore, knowing what the most important factors for competitiveness are in marine clusters [5,6], and, mainly, in the shipbuilding industry, is critical in order to introduce the shipbuilding sector in one of the new uses of the ocean [7,8]: generating electricity using offshore energy [9] or aquaculture.

Address for Correspondence: Almudena Filgueira-Vizoso, University of Santiago de Compostela Faculty of Political and Social Sciences, Department of Political Science and Sociology, Santiago de Compostela, Spain
E-mail: almudena.filgueira.vizoso@udc.es
ORCID ID: orcid.org/0000-0002-2212-8094

Received: 15.05.2023
Last Revision Received: 21.12.2023
Accepted: 26.12.2023

To cite this article: B. P. Fernández, N. P. Mosquera, A. F. Vizoso, R. Y. Brage, and L. Castro-Santos. "Competitiveness Factors of a Shipyard in the Era of New Uses of Oceans." *Journal of ETA Maritime Science*, vol. 12(1), pp. 36-49, 2024.

The goal of this paper is to identify the most relevant competitiveness factors of a shipyard [10,11]. Considering far away the conventional competitiveness factors (cost, delivery time and quality). The case study analyses the manufacturing center of Navantia, S.A., the Ferrol estuary (A Coruña, North-West of Spain). The complete list of competitiveness factors is suitable for people who are responsible for a shipyard to help you see where the competitiveness of a shipyard could be improved with a view to new uses of the oceans, such as offshore renewable energies.

2. Materials and Methods

2.1. Definition of Competitiveness

A large quantity of definitions of competitiveness were studied. The term competitiveness is no longer a static and purely economic concept and now includes factors such as culture, environmental sustainability, politics, human resource training, and spatial location. Thus, the definition of competitiveness acquires greater complexity, giving rise to many definitions for the same term. Rojas and Sepúlveda [12] stated that these definitions "*range from very specific and limited proposals, in which one of the central axes was international trade, to broader, complex and general ones that are confused with concepts such as development and economic growth, incorporating from purely economic aspects to those of a technical, socio-political and cultural nature*".

In addition, Bejarano et al. [13] indicated that "*It is possible to find definitions at several levels: those based on the firm, those based on the sector, and those that refer to the national economy as a whole. In the definitions that refer to the firm's competitiveness, the ability to design, produce, and sell goods in the global market (and to defend the domestic market) is usually emphasized, having as a parameter the efficiency standards in force in the world market. Those definitions that refer to the sector or the economy as a whole do not differ essentially from those just mentioned, except that the condition is added that competitiveness must lead to an improvement in the standard of living*".

Based on the table of Castellanos et al. [14], which orders the definitions by authors, levels, and according to the approach given to competitiveness, and adding the different definitions found in other reference texts, the definitions given by different authors are presented below, giving the term competitiveness, separating them according to the approaches and according to whether they correspond to the macroeconomic, industrial, or microeconomic level (see Table 1).

A) Macroeconomic Level

1. An approach that relates competitiveness to the results of foreign trade

- "*Capacity of a country (or group of countries) to face (to meet) competition at the world level. It includes both the ability of a country to export and sell in foreign markets and its ability to defend its own domestic market with respect to an excessive import penetration*" [15].
- "*A country's ability to create, produce, distribute, and/or serve products in international markets obtaining increasing profits on their resources*" [16].
- "*Sustainable ability to earn profits and maintain market share*" [17].
- "*Ability of a country, a sector or a particular company, to participate in extreme markets*" [18].
- "*Increase or at least a maintenance in participation no volume traded internationally or for certain areas or segments of the world market in which the product is competing*" [19].
- "*The capacity of said economy to supply and supply its internal market and to export goods and services abroad*" [20].
- "*A competitive economy is one that exports goods and services profitably at world market prices*" [21].
- "*Trade competitiveness is the ability of a country to effectively compete with foreign supply of goods and services in markets domestic and foreign*" [22].

2. An approach that relates competitiveness to the contribution of foreign trade to growth and general well-being

- "*The ability to produce, distribute, and provide the service of goods in the international economy in competition with goods and services produced in other countries and to do so in a way that raises the standard of living*" [16].
- "*The degree to which a nation can, under free and fair market conditions, produce goods and services that meet the requirements of international markets and, simultaneously, maintain or expand your real income citizenship*" [23].
- "*The degree to which a country, in an open market world, produces goods and services that meet market demands and simultaneously expands its GDP and GDP per capita by at least as quickly as their trading partners*" [24].
- "*A country's ability to achieve fundamental policy objectives economic growth, such as growth in income and employment, without incurring difficulties in the balance of payments*" [25].
- "*The ability to provide an acceptable rate of growth and a sustained standard of living for its citizens, while efficiently*

providing employment without reducing the potential life growth of future generations" [26].

3. Approach that relates competitiveness to the results of foreign trade

- "*The production of goods and services of higher quality and lower price than domestic and international competitors, which translates into increasing benefits to a nation's inhabitants by maintaining and increasing real incomes.*" Porter, (1990) [27], cited by Castellanos et al. [14].
- "*National competitiveness is the extent to which a nation, under free and fair market conditions, can produce goods and services that can successfully pass the test of international markets, maintaining and even increasing at the same time the real income of his citizenship*" [28].
- "*Competitiveness reflects the extent to which a nation, in a system of free trade and fair market conditions, can produce goods and services that pass the test of international markets, while maintaining and increasing income real of his people along deadline*" [29].
- "*A national economy is competitive when it is able, through its exports, to pay for the imports necessary for its growth, growth that must be accompanied by a standard of living*" [30].
- "*The sustained increase in income and the standard of living of nations or regions, with a job offer wide enough to cover all possible applicants. The activity economic should not result in unsustainable external imbalances, nor in compromising the well-being of future generations.*" European Report on Competitiveness, European Commission, (2009) [31], cited by Castellanos et al. [14].
- "*The competitiveness of nations is a field of economic knowledge that analyzes the facts and policies that determine a nation's ability to create and maintain an environment that sustains the generation of greater value for its businesses and more prosperity for its people. The competitiveness of nations is related to how they create and maintain an environment that sustains the competitiveness of their companies*" [32].
- "*A sustained increase in the standard of living of the nation or region and unemployment levels as low as possible*" [31].

4. Approach that relates competitiveness to the levels of efficiency and productivity of a company's economy

- "*Development of a higher efficiency and with the capacity of an economy to increase the product of higher activities productivity, which, in turn, can generate high levels of salary in real terms*" [33].
- "*From a medium- and long-term perspective, competitiveness consists of a country's ability to sustain and expand its participation in international markets and simultaneously raise the standard of living of its population. This requires increased productivity and, therefore, the incorporation of technical progress*" [34].
- "*An economy is competitive in the production of a given good when it can at least match the current efficiency standards in the rest of the world in terms of the use of resources and the quality of the good*" [35].
- "*Competitiveness involves elements of productivity, efficiency, and profitability, but it does not constitute an end or a goal in itself. It is a powerful means to achieve better standards of living and greater social well-being - a tool for achieving goals. By increasing productivity and efficiency in the context of international specialization, competitiveness provides the global basis for increasing people's incomes without generating inflation. Competitiveness should be seen as a basic medium to improve the standard of living, create jobs for the unemployed, and eradicate poverty*" [36].
- "*Ability of companies, industries, regions and nations, and supranational regions, to generate, while exposed to international competition, relatively high factors of income and factors of employment at sustainable base levels*" [29].

B) Industrial Level

- "*The ability of an industry to produce goods with patterns of specific quality, required by specific markets, using resources at levels equal to or lower than those that prevail in similar industries in the rest of the world, for a period of time*" [37].
- "*An industry is internationally competitive if it produces goods interchangeable and is profitable. A reduction in competitiveness is, then, a reduction in the profitability of some or all tradable product industries*" [38].
- "*The ability to win and execute shipbuilding orders in open competition and stay in the business*" [39].

C) Microeconomics Level

- "*A firm will be competitive if it is victorious (or in a good position) in the confrontation with its competitors in the market*" [40].
- "*A company is competitive when it can produce products and services of higher quality and at lower costs than its domestic and international competitors. Competitiveness is synonymous with a company's long-term profitability performance and its ability to remunerate its employees and generate a higher return for its owners"* [41].
- "*Ability of companies in a given country to design, develop, produce, and sell their products in competition with companies based in other countries*" [42].
- "*Competitiveness is the ability to sell what is produced*" [43].
- "*The sustained ability to gain and maintain market share*" [44].

• "*The firm's ability to deliver goods and services at the time, place, and manner preferred by its customers, at prices as good or better than those offered by the other bidders, obtaining at least the opportunity cost of the resources used*" [45].

• "*Derives the concept of competition competitiveness, a word with the meaning of "possibility of equaling one thing to another in perfection or properties"* or *"the degree of economic rivalry existing in a market or the way of acting between the competitors in the said market". Thus, competitiveness is understood, for this author, as the ability of an economic agent to compete*" [46].

• "*Set of skills and conditions required for the use of competence*" [47].

• "*Competitiveness is what makes a consumer prefer a company's products and buy them. The essence of competitiveness is value creation*" [48].

• "*Ability to successfully enter the market, to obtain a share and sustain it or increase it over time*" [49].

• "*Competitiveness is an attribute or quality of firms, not of countries. The competitiveness of a firm or group of firms is determined by four fundamental attributes of its local base: factor conditions, demand conditions, related and supporting industries, and firms' strategy, structure, and rivalry. Such attributes and their interaction explain why they innovate and sustain competitive companies located in certain regions*" [50].

• "*Capacity that an organization has to increase, consolidate, and maintain its presence in the market*" [51].

• "*Business competitiveness is the ability to maintain a position in the market, in particular, by offering quality products in a timely manner and at competitive prices, with flexibility to respond quickly to changes in demand and properly managing the differentiation of the products by the creation of innovative capacity and an effective marketing system*" [52].

• "*It is defined as the ability of an organization, public or private, with or without profit, to achieve and maintain advantages that allow it to consolidate and improve its position in the socioeconomic environment in which it develops*" [53].

• "*A company is competitive if it can develop and implement strategies that lead it to a sustained or expanded market position in the industry segment where it operates*" [54].

• "*Ability to maintain and expand the participation of companies in local and international markets in a profitable way that allows their growth*" [55].

• "*An industry is competitive if:*

a) *total factor productivity is equal to or greater than that of its competitors.*

b) *the average unit costs are the same or lower than those of its competitors*" [56].

Table 1. *Main authors who have defined competitiveness previously*

Macroeconomic level	Industrial level	Microeconomics level
[15,16,57,58] ...	[14,39,59,60]...	[40-42,61,63]...

Then, considering our object of analysis, the definition of competitiveness for companies is defined as follows: "*Competitiveness for a shipyard in the global era, is the capacity to produce goods, equipment, and services, remaining in the profits in the middle and long term when selling them in the market*".

Therefore, competitiveness has one dimension: obtaining benefits in the medium and long term.

2.2. Grouping of Competitive Factors

most authors make a grouping of the competitiveness factors considering their relation to resources (material resources, labor, capital, etc.) and to the environment (legal framework, monetary change, etc.).

The present paper will group the competitiveness factors in a manner similar to that of the members of the ECORYS SCS group [62], but contemplating the legislative framework and analyzing a series of factors that have been detected by the authors that were not contemplated in the study of that group.

The factors that will be studied within each of the above groups are shown in Table 2.

In addition to the factors listed above, two additional factors should be mentioned because they have been highlighted by several authors:

1. Price [63-67].

2. Time [63,65,67-69].

This paper aims to go a little further than the three-term price-time-quality to enrich the debate on the factors of competitiveness in a way that is useful for shipyards. Therefore, time and price will not be studied as factors in themselves, as they are derived from many of the factors that will be studied. For example, time could be considered as a consequence of the shipyard's production capacity [CGT(Compensated gross tonnage)/year], the number of people working in the company, and the productivity of its human resources (CGT/person-year). The company could play with capacity (even through cooperation with other shipyards or the complementary industry), productivity, and the number of human resources to adjust deadlines. The example for prices is more obvious because it is a consequence of any production process carried out in the shipyard,

Table 2. *Proposed competitiveness factors for a shipyard*

1. Industry structure	2. Competitive environment
A. Value chain and production processes	**A. Competitors development (supply)**
I. Product technology	I. Competitors development (supply)
II. Quality	**B. Market development (demand): Buyers**
III. Attractiveness of the product	**C. Bargaining power of suppliers**
IV. Added value	I. Bargaining power of suppliers
V. Marketing	**D. Other exogenous factors**
VI. Selling	I. Political framework
VII. Product range	II. Currency and Exchange Rates
VIII. Customer service. After-sales service	III. Economic stability
IX. Cost control	IV. Political and legislative instability
X. Purchasing management	V. Government support - Political support
XI. Risk management	
XII. Productivity	
XIII. Production organization	
XIV. Co-operation between shipyards	
XV. Co-operation between shipyards and complementary industries	
XVI. Co-operation between shipyards and scientific institutions	
XVII. Cluster	
XVIII. Location	
XIX. Competitor Intelligence System	
B. Access to resources	
I. Manpower	
II. Capital and financing	
III. Raw materials and basic resources (e.g. energy)	
IV. Knowledge	
V. Technology and facilities	

organizational decisions, purchase and sale of materials and services, expenses and investments in different concepts, access to resources, risk management, etc. Thus, as time and price are derived factors, they will not be considered independent variables of competitiveness.

1. Industry Structure

A. Production Processes and Value Chain

I. Product technology

It is the technological level that a product incorporates (both for its design and for its engineering).

II. Quality

These are the normative standards that the shipyard can achieve in its manufacture and in the finishing of the products and services it sells (quality of the materials used, tolerances, useful life of the products, behavior throughout the life cycle, etc.).

III. Attractiveness of the product

It is the value that the market gives to a given product.

IV. Added value

It is the economic value that the company can inject into the product during manufacturing.

V. Marketing

The management process is responsible for identifying customer needs, as well as anticipating and satisfying them.

VI. Selling

Capacity to sell the company's products or services through its sales department.

VII. Product range

They are the different types of ships and structures, as well as the variants and degree of customization of the design of these, that are offered by the company.

VIII. Customer service. After-sales service

Customer service is the total sum of what an organization does to achieve customer expectations and leave them satisfied. After-sales service is the sum of everything that an organization does to achieve customer expectations and leave them satisfied after the sale of the product or service offered.

IX. Cost control

It is the control that is carried out from the management system or cost control of the company to assess the cost of production, to analyze costs and profitability, and to make management decisions related to the products or services offered.

X. Purchasing management

It is the process of planning, implementation, evaluation, and control of operational and strategic purchases, through

which all the company's purchasing activities are directed to achieve its objectives.

XI. Risk management

It is a global and integrative approach followed by a company to manage its risks and opportunities and maximize its value.

XII. Productivity

Productivity is the number of products that can be manufactured from a given number of resources. In the case of this company and for the manufacture of ships, the gross compensated tonnage produced by one person in a year (CGT/person-year) will be considered.

XIII. Production organization

They are the systems of organization and management of the company that take care of: the manpower and the organization of the work, the systems of planning and methodologies, the programing of the works of structures, the programing of the works of assembly, the control of the production, the control of warehouses, efficiency and profitability calculations, quality control, and production management information systems.

XIV. Co-operation between shipyards

Cooperation between different shipyards (from the same company or from different companies) in areas such as building blocks, equipment installation, hull and steel work, design, joint purchasing, marketing, or R&D.

XV. Co-operation shipyards: auxiliary enterprises

They are cooperative relations between the main company and complementary (auxiliary) companies. It also refers to the type of relationships that can range from simply contractual and short-term practitioners to a cooperation of long-term partnership.

XVI. Co-operation between shipyards and scientific institutions

These are the relationships between the parent company and institutions dedicated to education and training, research, development, and innovation.

XVII. Cluster

It is a group of interconnected companies and associated institutions within the same sector of work that are geographically close and linked by similarities and complementarities. The geographical area of effect of the cluster is that in which the informative, transactional, and incentive effects derived from the existence of the cluster can be observed.

XVIII. Location

It is the geographical location of the company, and it is studied in relation to the conditions of the competitive environment of that geographical location.

XIX. Competitor Intelligence System

It is an open system through which the company takes a global approach to competitive strategy. It is a system that analyzes the activities of the main company, the complementary companies, the market, and the production processes of others to make the best decision regarding the activities to be carried out. This system aims to put the company in the best possible position to implement strategic planning and to be able to defend itself and influence the competitive forces of the industry.

B. Access to Resources

I. Manpower and skills

This factor refers to the relevance that access to the workforce and the skills of the workforce may have. It considers union unity, labor costs, working conditions, and staff motivation.

II. Capital and financing

This factor refers to the relevance of access to the capital needed to develop the company's activities and the costs of financing.

III. Raw materials and basis resources (e.g. energy)

This factor refers to the relevance of accessing raw materials and equipment that the company needs to conduct its activities. It also considers the availability of companies supplying raw materials and equipment in the geographical environment of the company.

IV. Knowledge

This factor refers to the relevance that accurate knowledge may have for present and future company activities and focuses on the study of the following areas: know-how, company-owned knowledge, knowledge management, access to information, and R&D.

V. Technology and facilities

This factor refers to the relevance of accessing technology and the necessary facilities for the company's activities. Technology refers to the equipment and facilities used to build ships and other marine products: equipment and facilities necessary for steel work, production and assembly of systems and equipment, other pre-assembly systems, shipbuilding and equipment installation, shipyard and surroundings plant design, services, design, delineation, engineering of production and elaboration, means of loading and transport, and computerization.

2. Competitive Environment

A. Competitor Development (Supply)

I. Competitor's development (supply)

It is the construction capacity of shipyards globally. It will be more relevant for companies that do not operate in a niche market. It is determined by existing and future facilities, the productivity of companies, and the manpower available.

B. Market Development (Demand)

I. Market development (demand): Buyers

The development of the markets and the consequent demand reflect the construction requests of merchant companies. The relevance of demand on the competitiveness of the company can be altered depending on the ability of the company to influence the factors of demand, as well as depending on the business lines of the company and its situation or not in a niche market that offers protection against variations in demand.

C. Bargaining Power of Suppliers

I. Bargaining power of suppliers

This factor refers to the relevance that may have on the competitiveness of the company the strength of the bargaining power of companies that provide services and equipment to the parent company. Supplying companies are those that produce steel, motors, other types of equipment, components, and subcontracted services. However, labor is also considered when it is unionized and united and has bargaining power as if it were a supply company.

D. Other Exogenous Factors

I. Political framework

It is the set of rules and laws that establish the legal framework of the shipbuilding sector. These rules operate at the national level, regionally (such as in the European Union) and internationally and deal with different topics: public aid schemes, barriers to entry and exit to the market, technical standards, safety standards, environmental protection standards and intellectual property rights.

II. Currency and exchange rates

The value of the local currency or the value of the local currency at the exchange rate is the value that one currency has with respect to another in the world market. The evolution of exchange rates and the strength of the currency in which purchases are paid and sales are collected may be relevant because they are made in different currencies and because the value of the currency changes over time.

III. Economic stability

This is the economic situation resulting from a system with the absence of large variations in macroeconomic variables, along with low inflation and sustained growth in trade and employment.

IV. Political and legislative instability

It is the propensity for change in the executive of a government (either by constitutional or unconstitutional means), increasing instability when changes in government are significant.

V. Government support: Political support

Government support or political support is the help that a government provides to an industry through its actions, legislation, and institutions to enhance its competitiveness or to help it sustain itself in times of special difficulty.

2.3. Way of Observing the Information

2.3.1. Methodology

In case studies, it is necessary to use triangulation to obtain information from various perspectives. Thus, by using multiple sources of information, the result will be more accurate, reliable, and valid [70].

The instruments that will be used will be as follows (see Table 3):

1. Interviews.
2. Document analysis.
3. Questionnaires.

Table 3. *Sources of the different instruments considered. Source: Own elaboration considering González [73]*

Instrument	Source
Interviews	Multiple agents related to the company
Document analysis	Institutional, business, and academic documentation
Questionnaires	Multiple agents related to the company

2.3.2. Interviews

The interviews focused on three groups of people who had a relationship with Navantia:

1. Intermediate positions of Navantia in the Ferrol sea loch.
2. Union representatives of Navantia in the sea loch of Ferrol.
3. Management supervises the most relevant auxiliary and complementary companies for Navantia in the estuary of Ferrol.

Selecting people for the intermediate positions of Navantia, the people selected covered all areas of work of the Navantia company in the estuary of Ferrol, from the quality areas to the work carried out abroad (for instance: Australia), as well

as the specialties of repairs, technical office, production, organization, and management of the different guilds and turbines.

Regarding the group of union representatives, the unions represented in the production center of Ferrol or in the production center of Fene have been interviewed.

To select the most relevant auxiliary and complementary companies for Navantia in the Ferrol estuary, a brief questionnaire was administered to several union representatives, intermediate positions in the company, and qualified staff of the Higher Polytechnic School of the University of A Coruña. Through this brief questionnaire, these individuals help to determine the most relevant auxiliary and complementary companies to Navantia in past and present times, and from which their management staff could have a better overview of how Navantia operates. Thus, of the 44 initial companies identified as companies working with Navantia, this group of people determined that 28 were the most relevant to Navantia in the manufacturing core of the Ferrol estuary. Of the 28 companies initially identified, 10 were dependent and organically linked or run from others who were also on that list of 28. Therefore, interviews were only conducted with the management staff of the parent company. Thus, there was a group of 18 companies that were considered relevant for the purpose of this study.

The intention was that the interviews would be individualized and with a semi-structured script. That is, to meet individually with each person and follow a semistructured script of questions: with key questions but being flexible in questions and answers and encouraging the interviewees to delve into those areas of greatest interest or that provided with interesting information.

The identity of the interviewees will be coded to distinguish people from auxiliary and complementary companies, from the unions, and from the intermediate positions of the company, without knowing the comments of a particular person. Thus, there is no way to identify to whom the appointments correspond.

2.3.3. Document analysis

The document analysis is based on studying documents directly from social and institutional agents, from the company's website, from the website of the group that owns the company [Sociedad Española de Participaciones Industriales-Spanish Society of Industrial Participations (SEPI)] from various websites of magazines, associations, and individuals, from the unions, from libraries and virtual libraries, from virtual databases, from requests made to organizations and associations organizing congresses and conferences, and from applications made through "*Law 19/2013, of 9 December, on transparency, access to public information, and good governance*" [71].

2.3.4. Questionnaires

The questionnaire developed consists of a group of questions that attempt to obtain relevant information to achieve the objectives of the research. The questions are focused on obtaining information to determine what the most competitive factors are relevant to the competitiveness of Navantia.

The respondents were asked to what degree they considered each of the 32 competitiveness factors relevant to the competitiveness of the manufacturing core of Navantia Ferrol. There are four possible grades of importance: "not important" (NI), "little important" (LI), "important" (I), and "very important" (VI). However, in some questionnaires, an intermediate degree between important and crucial or between little important and important was considered, at the request of the person questioned.

2.3.5. Criteria for determining the most important competitiveness factors

Given the definition we have given of the different factors of competitiveness and considering the theoretical proposal formulated, to define the most important factors of competitiveness of the manufacturing core of the company Navantia, SA in Ferrol, a criteria to assess the most important factors of competitiveness should be defined. It is important to determine, depending on the information collected and in a descriptive way, the factors of competitiveness that the multiple agents related to the company consider of greater importance for the industrial core.

Therefore, the social and institutional agents related to the company will decide the most significant elements of competitiveness for the company based on its privileged position. Thus, the criteria for interpreting the information are as follows:

1. To each assessment made by each of the people questioned on the relevance of each of the factors of competitiveness, a numerical value will be given: "0" for "not important", "1" for "little important", "2" for "important" and "3" for "very important".

Thus, the degree of relevance that the interviewees and respondents consider will be averaged. For the calculation of this average degree of relevance, we assume:

- 0<=x <=0.5: the factor is unimportant.
- 0.5<x<=1.5: the factor is little important.
- 1.5<x<=2.5: the factor is important.
- x>2.5: the factor is critical.

2. There are significant discrepancies regarding the importance of the factors between the different agents when

there are at least two degrees of relevance of difference between one of the agents consulted and the average of relevance achieved for all agents. For example, when the relevance given by a questioned agent is of no importance and the average relevance is important or very important, or when the relevance given by a questioned person is of little importance and the average relevance is very important.

3. Case Study

3.1. Units of Analysis

As Martínez [72] explains, once the theoretical propositions have been made, it is necessary to define the units of analysis. The same author, citing Yin [73], explains that there are four basic types of units of analysis that consider the number of cases to be studied (single case or multiple cases), as well as the level of analysis (simple: main unit or multiple unit).

According to the typology described in the previous paragraph, this paper analyzes a unique and simple case: the industrial core of Navantia, S.A. in Ferrol.

The reasons why this case was selected were:

• They are the largest shipbuilding facilities in Galicia.

• Socioeconomic importance of the company in the region of location.

3.2. Description and Contextualization of Navantia, S.A.

Navantia, S.A. (simplifying Navantia), is a Spanish state-owned company in the form of a public enterprise wholly owned by the SEPI [4].

According to the SEPI website and SEPI corporate brochure [74], Navantia's lines of activity areshipbuilding, especially in the military sector, but not exclusively, control and combat systems, life cycle support, repairs and transformations, diesel engines, turbines, and naval and power generation equipment.

Navantia is a company dedicated to the design, construction, and integration of ships, mainly dedicated to military shipbuilding, despite maintaining a complementary activity in the civilian market. It has more than 250 years of experience in the construction, maintenance, and transformation of Spanish military ships [74].

3.3. Navantia Production Units and Their Locations

The company Navantia has three industrial centers: estuary of Ferrol, bay of Cádiz, and Cartagena, whose address is centralized in the social headquarters of the company in Madrid [4]. In addition to its industrial centers and headquarters, the company has subsidiaries in Spain (SAES, Submarine Electronics Joint Stock Company; and SAINSEL, SAU Naval Systems) and abroad (Australia, Chile, etc.) [4]. The company maintains its presence outside Spain with the aim of being closer to its customers and having a presence in strategic markets.

The industrial cores are made up of different production units, with centralized management in the central offices in Madrid, as follows [74]:

• Bay of Cádiz: shipyard of Cádiz, shipyard of San Fernando, and shipyard of Puerto Real.

• Cartagena: Cartagena shipyard.

• Estuary of Ferrol: Fene shipyard and Ferrol shipyard.

The present paper focuses on the Estuary of Ferrol, whose production units are divided between Fene and Ferrol (see Figure 1).

Figure 1. *Location of Navantia in Galicia. Source: elaboration by Google Earth [75]*

3.4. Present of the Navantia Industrial Center in the Ría de Ferrol: Importance of Offshore Wind

The manufacturing core of Navantia in the estuary of Ferrol is located in the municipalities of Ferrol and Fene, in the estuary of Ferrol, in Galicia, in the northwest of Spain.

The Navantia industrial core in the Ferrol estuary is made up of two production units (see Figure 2): Fene, whose facilities come from the company ASTANO, and Ferrol, whose facilities come from the company Bazán.

These production units build military ships (aircraft carriers, frigates with the AEGIS26 combat system, amphibious ships, fleet tankers and corvettes, etc.), steam turbines, wind turbines, gear reducers, shaft lines, torpedo tubes and other ship equipment [4].

Figure 2. *Location of the facilities of Navantia in the Ferrol estuary. Source: own elaboration using Google Earth [75]*

In addition to the production highlighted in the preceding paragraph, these production units have an important technical office and an after-sales service.

However, the company also dedicates these facilities to ship repair and conversion, technology transfer and technical advice, as well as life-cycle support.

Finally, the enterprise develops designs for offshore wind: jacket structures for fixed offshore wind, spar floating offshore wind structures, semisubmersible floating offshore wind structures, weather towers, installation vessels, and support vessels for deep-sea offshore wind farm. Therefore, shipbuilding can be a great pillar in the development of future new uses of the ocean.

4. Results

The interviews were focused on three groups of people who had a relationship with the company studied:

- Intermediate positions.
- Union representatives.
- Management staff of the most relevant auxiliary and complementary companies.

In the interviews with intermediate positions, all the areas of work of the enterprise Navantia in the estuary of Ferrol were considered: area of quality, works in Norway and Australia, area of repairs, area of systems, area of technical office, area of production, customer service of the life cycle, different guilds and turbines. However, not in all cases was it possible to get an interview. In this context, seven people with a very outstanding global perspective of the company were interviewed.

In the group of union representatives, the interviewees showed full collaboration and interest in the research. They were 15 people from five different unions and two production units.

The management staff of 12 auxiliary and complementary companies were interviewed of the 18 auxiliary or complementary companies or groups of companies that were considered relevant. Fifteen people were interviewed of these 12 companies, representing 67% of the companies identified as most relevant for the company Navantia in the location selected. These auxiliary and complementary companies cover various Navantia services and supplies, such as:

- Mechanized.
- Boiler making.
- Factory maintenance.
- Ship repairs.
- Detailed engineering and project development.
- Wind energy.
- Supply of parts, equipment, and industrial machinery.
- Pipe and plate welding.
- Manufacture and assembly of pipes.
- Sheet metal cutting and repair
- Surface preparation and painting.
- Habilitation work, insulation, ventilation, fine boilermaking, metal carpentry, wood carpentry.
- Construction and assembly.
- Design and execution of all types of electrical installations, elaboration of electrical panels, control consoles, and repair of electromechanical equipment, products, or services.
- Pre-assembly, piping, assembly, prefabrication of complete blocks, and joining of blocks in bleachers.

The questionnaires were given to the same people who were interviewed. Therefore, 37 people answered the questionnaire.

Figure 3 shows the assessments of these 37 people regarding the relevance of each of the competitiveness factors for the competitiveness of the Navantia industrial center in the selected location.

The following codes and valuation methods were used:

- When a cell is empty, it is because the person questioned considered that the factor was not assessable, he/she did not have the information necessary to make an assessment, or he/she did not want to do so.
- 0: Unimportant (NI).
- 1: Little important (LI).
- 2: Important (I).
- 3. Critical (VI).

On the other hand, some of the most relevant documents obtained during the observation, which were relevant, are as follows:

- Strategic reflection workshop. Navantia Strategic Plan 2014-2018 [76].
- Working document on the future of Navantia 2015–2019 (DTFN 2015) [77].

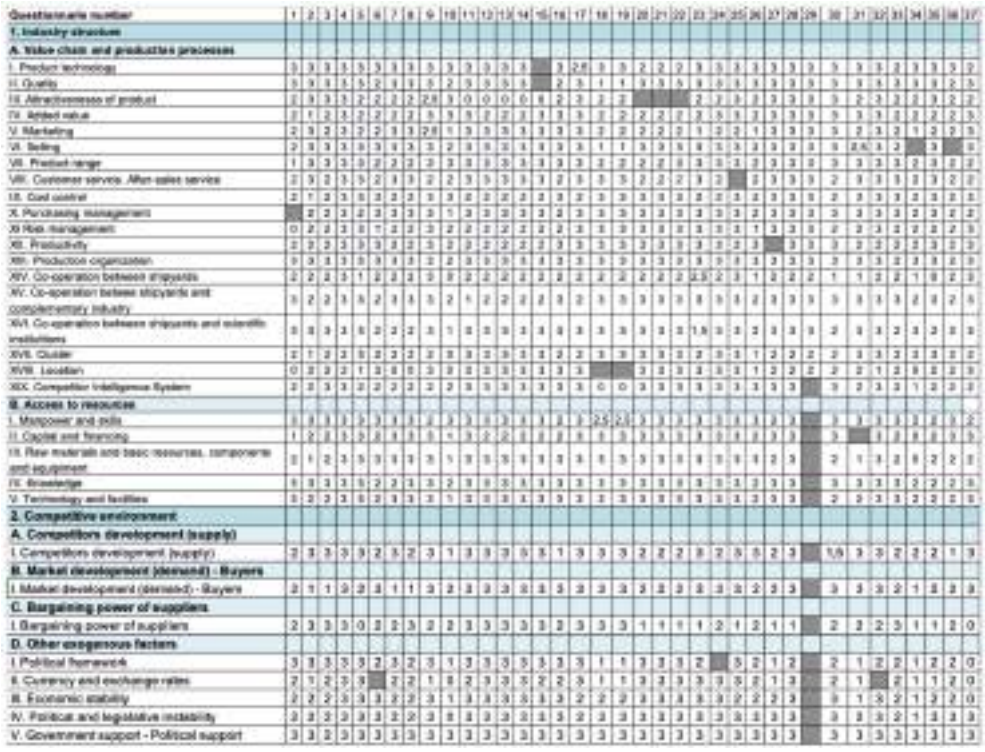

Figure 3. *Assessments of the questioned people regarding the relevance of each competitiveness factor*

• Accounts of Navantia, SA, disaggregated by industrial and joint nuclei from 2005 to 2012 [78].

• Accounts of Navantia, SA, disaggregated by industrial and joint nuclei from 2008 to 2013 [79].

• Evolution of the staff of Bazán, ASTANO, and Navantia from 1970 to 2015 [80].

5. Discussion

The greatest relevant competitive factors for the company Navantia, SA in the location selected, among the 32 initial factors taken into account by the researchers referenced, are shown in Figure 4.

Therefore, the five most important competitive factors of the Navantia production units in the Ferrol estuary are the government and political support, the production organization, the product technology, manpower, and skills and knowledge.

Thus, these five competitive factors are critical to analyze the competitiveness of a shipyard with the characteristics of the one studied for the new uses of the ocean such as offshore wind, wave energy, or aquaculture.

6. Conclusion

This study has identified the most relevant competitiveness factors of a shipyard. The method conducted interviews and questionnaires with multiple agents related to the company (intermediate positions, union representatives and management staff of the most relevant auxiliary and complementary companies) and analyzed several institutional, business and academic documentation.

The competitiveness factors were grouped into factors associated with the structure of the industry (considering the value chain & production and its access to resources)

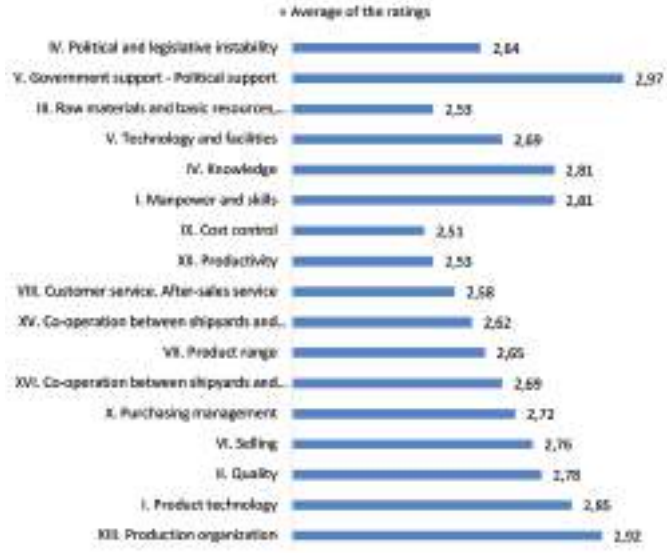

Figure 4. *The greatest competitiveness factors for Navantia's manufacturing units in the selected location. Source: Own elaboration*

and those associated with the competitive context (related to the development of competitors, the market progress (demand), bargaining power of suppliers, and other external elements).

The case of study considered was the manufacturing center of Navantia, S.A. at the Ferrol estuary (A Coruña, North-West of Spain).

After analyzing the interviews, questionnaires, and documents, the most significant competitive factors of the Navantia manufacturing units in the selected location were established. They are: the government and political support, the production organization, the product technology, manpower, and skills and knowledge.

Regarding government and political support, it can add value to the shipyard considering interest rates fewer than the competence, for instance. Considering the production organization and considering that some shipyards in the future will be focused on building offshore renewable energies, they can be re-organized considering "mass production" for building offshore substructures, such as monopiles, jackets, spar, or semisubmersible offshore wind platforms. Regarding product technology, the shipyard can design its own technology (their own designs in terms of offshore wind substructures or special vessels for offshore maintenance, for instance), not only building the technology developed by others. In terms of manpower, it is important that people have a career during their life at the enterprise, considering their qualifications and the quality of their salaries. Finally, regarding skills and knowledge, it is important that old people provide young people with all their acquired knowledge and experience before they are retired, in order to try to maintain the permanence of this knowledge at the enterprise during years.

The complete list of competitiveness factors is useful for the people who manage a shipyard, allowing them to identify where they could improve the competitiveness of a shipyard in the era of new uses of the oceans. In fact, these new uses of the ocean, such as offshore wind, wave energy, and aquaculture, can improve the competitiveness of shipyards in future years.

Future studies can investigate the difference between traditional shipyards, which are building and repairing vessels, and new production shipyards focused on offshore renewable energies (for example: offshore wind or wave energy), which should be reconverted to increase their productivity and adapt to the new uses of the sea.

Authorship Contributions

Concept design: B. Preto-Fernández, Data Collection or Processing: B. Preto-Fernández, and N. Paleo-Mosquera, Analysis or Interpretation: B. Preto-Fernández, A. Filgueira-Vizoso, R. Yáñez-Brage, and L. Castro-Santos, Literature Review: B. Preto-Fernández, N. Paleo-Mosquera, A. Filgueira-Vizoso, R. Yáñez-Brage, and L. Castro-Santos, Writing, Reviewing and Editing: B. Preto-Fernández, N. Paleo-Mosquera, A. Filgueira-Vizoso, R. Yáñez-Brage, and L. Castro-Santos.

Funding: The authors declare that no funds, grants, or other support was received during the preparation of this manuscript.

References

[1] D. Fornahl, "From the old path of shipbuilding onto the new path of offshore wind energy? the case of Northern Germany," in *Innovation, Strategy And Structure - Organizations, Institutions, Systems and Regions*, vol. 20, pp. 835-855, May 2011.

[2] C. K. Lin, and H. J. Shaw, "Feature-based estimation of preliminary costs in shipbuilding," *Ocean Engineering,* vol. 144, pp. 305-319, Nov 2017.

[3] L. Castro-Santos, V. Diaz-Casas, and R. Yáñez Brage, "The importance of the activity costs in a shipyard: a case study for floating offshore wind platforms," *Ships and Offshore Structures,* vol. 15, pp. 1-9, May 2016.

[4] Navantia, "Navantia Web Page" [Available online: www.navantia.es (accessed on 8 February 2021)].

[5] P. J. Stavroulakis, S. Papadimitriou, and F. Tsirikou, "Perceptions of competitiveness for maritime clusters," *Ocean & Coastal Management,* vol. 205, pp. 105546, May 2021.

[6] L. Jiang, E. Bastiansen, and S. P. Strandenes, "The international competitiveness of China's shipbuilding industry," *Transportation Research Part E: Logistics and Transportation Review,* vol. 60, pp. 39-48, Dec 2013.

[7] Y.-J. Song, J.-H. Woo, and J.-G. Shin, "Research on systematization and advancement of shipbuilding production management for flexible and agile response for high value offshore platform," *International Journal of Naval Architecture and Ocean Engineering,* vol. 3, pp. 181-192, Sep 2011.

[8] C. S. Tang, and L. P. Veelenturf, "The strategic role of logistics in the industry 4.0 era," *Transportation Research Part E: Logistics and Transportation Review,* vol. 129, pp. 1-11, Sep 2019.

[9] L. Castro-Santos, A. Filgueira-Vizoso, C. Álvarez-Feal, and L. Carral, "Influence of size on the economic feasibility of floating offshore wind farms," *Sustainability,* vol. 10, pp. 1-13, Nov 2018.

[10] M. Kafalı, and M. Özkök, "Evaluation of shipyard selection criteria for shipowners using a fuzzy technique," *Journal of Marine Engineering & Technology,* vol. 14, pp. 146-158, Aug 2015.

[11] A. Resa Nurlaela, F. Danny, Q. Melani, S. Hermin, and S. Rini, "Competitive advantage analysis of shipyard companies in Indonesia," *International Journal of Marine Engineering Innovation and Research,* vol. 5, pp. 111-116, Jun 2020.

[12] P. Rojas, and S. Sepúlveda, *Cuaderno Técnico Nº 09. ¿Que es la competitividad?* San José, Costa Rica: Instituto Inter-American Institute for Cooperation on Agriculture (IICA), 1999. [Online]. Available: https://www.google.com.tr/books/edition/Qu%C3%A9_es_la_competitividad_No_9/e0bC_zcWBfUC?hl=en&gbpv=0

[13] J. A. Bejarano, *Coleccion Documentos IICA. Serie Competitividad 2. Elementos para un Enfoque de la Competitividad en el Sector Agropecuario*. Ministerio de Agricultura y Desarrollo Rural de Colombia y Instituto Inter-American Institute for Cooperation on Agriculture (IICA), 1998.

[14] C. A. Castellanos Machado, Z. M. Vila Alonso, J. R. Castellanos Castillo, N. Machado Noa, and G. Barbosa Iglesias, "Contribution of clusters to the competitiveness of enterprises," *Técnica Administrativa,* Accessed: March 12, 2021. [Online]. Available: http://www.cyta.com.ar/ta/art_ficha.php?id=110202

[15] F. Chesnais, "The notion of internacional competitiveness," *Mimeo, OCDE, Paris*, 1981.

[16] B. R. Scott, G. C. Lodge, and J. L. Bower, "*US competitiveness in world economy,"* Boston: Harvard Business School Press, 1985.

[17] R. Tamanes, *Diccionario de Economía*. Madrid: Alianza Editorial, 1988.

[18] R. Feenstra, "*Trade policies for international competitiveness*," Chicago: University of Chicago Press, 1989.

[19] A. Di Filippo, "La competitividad internacional en economías abiertas de América Latina" in *Seminario-taller coordinación de políticas de fomento de la competitividad y nuevos desafíos para la integración regional*, 1991.

[20] J. I. Pérez, "Costes laborales y competitividad de la economía española," *Revista de Economía Y Sociología Del Trabajo*, 1994.

[21] T. Economist, "The economics of meaning," *Econ.*, pp. 17-18, 1994.

[22] A. Ten Kate, "La competitividad y factores que lo determinan," México, 1995.

[23] President's commission on industrial competitiveness, "Global competition: a new reality." Washington DC., 1985.

[24] P. Jones and D. Teece, "The research agenda on competitiveness. A program of research for the Nation's business schools," in *Cooperation and competition in the global economy: Issues and strategies*, A. Furino, Ed. 1988.

[25] J. Fagerberg, "International competitiveness," *The Economic Journal,* vol. 98, pp. 355-374, Jun 1988.

[26] R. Landau, *Technology, Capital Formation and U.S. competitiveness,* Oxford University Press, 1992. Accessed: March 12, 2021. [Online] Available: https://www.econbiz.de/Record/technology-capital-formation-and-us-competitiveness-landau-ralph/10001283573

[27] M. E. Porter, "The competitive advantage of nations," *Harvard Business Review*, vol. 68, pp. 73-93, Mar 1990.

[28] J. Ivancevich, *Gestión, Calidad y Competitividad*, 1° Edición. Madrid: IRWIN, 1996.

[29] T. Hatzichronoglou, "Globalisation and Competitiveness: Relevant Indicators," 1996.

[30] B. Coriat, *Los desafíos de la competitividad*. EUDEBA. Argentina, Apr 1997.

[31] European Commission, "European Competitiveness Report 2008," Brussels, 2009.

[32] IMD 2003, *Anuario de competitividad mundial*. IMD 2003, 2003.

[33] L. Cohen, S. Teece, D. Tyson, and L. Zysman, "Competitiveness in global competition. The new reality, vol. II," *Work. Pap. Pres. Com. Ind. Compet.*, 1984.

[34] F. Fajnzylber, "Competitividad internacional: evolución y lecciones," *Revista de la CEPAL,* pp. 7-24, 1988, Accessed: Mar. 12, 2021. [Online] Available: https://repositorio.cepal.org//handle/11362/11714

[35] J. T. Araújo, *Proteçao, competitividade e desempenho exportador da economia brasileira nos anos 80. IEI/UFRJ*. Mimeo, 1989.

[36] Grupo consultivo sobre la competitividad (GRUPO CIAMPI), "*La mejora de la competitividad europea. Primer informe al Presidente de la Comisión Europea, los Primeros Ministros y los Jefes de Estado. Junio 1995*" 1995.

[37] L. Haguenauer, "Competitividade, conceitos e medidas. Uma resenha da bibliografia recente com êmfase no caso brasileiro. Texto para discussão No 208." IEI/UFRJ, Rio de Janeiro, 1989.

[38] J. Lucángeli, "La Competitividad Del Mercosur Frente Al Alca".

[39] KPMG Peat Marwick, "Report of a study into the competitiveness of European Community shipyards," 1992. Accessed: March 12, 2021. [Online]. Available: https://core.ac.uk/download/pdf/10593069.pdf

[40] C. A. Michalet, "*Competitiveness and internationalization*" París, 1981.

[41] H. of Lords, "*Informe da Comisión Especial da Cámara dos Lores sobre Comercio Internacional*" London, 1985.

[42] J. A. Alic, "Evaluating industrial competitiveness at the office of technology assessment" *Technology in Society,* vol. 9, pp. 1-17, Jan 1987.

[43] J. Mathis, J. Mazier, and D. Rivaud-Danset, "*La compétitivité industrielle*" Paris 1988.

[44] E. Van Duren, L. Martin, and R. Westgren, "Assessing the competitiveness of Canada's agrifood industry," *Canadian Journal of Agricultural Economics,* vol. 39, pp. 727-738, Dec 1991.

[45] M. L. Cook, and M. E. Bredahl, "Agri-business competitiveness in the 1990s: Discussion," *American Journal of Agricultural Economics,* vol. 73, pp. 1456-1464, Dec 1991.

[46] E. Bueno, "La competitividad en la empresa: un enfoque de organización y una referencia a España," *Dirección y Organización: Revista de Dirección, Organización y Administración de Empresas,* vol. 13, pp. 5-15, 1995.

[47] G. Muller, "El caleidoscopio de la competitividad," *Revista de la CEPAL*, vol. 56, pp. 137-148, Aug 1995.

[48] J. P. Sallenave, *La gerencia integral*. Grupo Editorial Norma. Colombia, 1995.

[49] C. Pérez, "La modernización industrial en América Latina y la herencia de la sustitución de importaciones," *Comercio Exterior,* vol. 46, pp. 347-363, 1996.

[50] M. E. Porter, "*Construyendo las Ventajas Competitivas del Perú*" Lima, 1996.

[51] M. G. Álvarez, *Manual de competitividad*. México, D. F.: Ed. Panorama, 1998.

[52] J. Altenburg, Tilman ; Hillebrand, Wolfgang ; Meyer-Stamer, "Building systemic competitiveness Concept and case studies from Mexico, Brazil, Paraguay, Korea and Thailand - OpenGrey," 1998. Accessed: Mar. 12, 2021. [Online]. Available: http://www.opengrey.eu/item/display/10068/133852

[53] J. C. Mathews, *El significado de la competitividad y oportunidades de internacionalización para las mypes*, Primera. Nathan Associates Inc., 2009.

[54] J. Ferraz, D. Kupjer, and M. Looty, "Competitividad Industrial en Brasil. 10 años después de la liberalización," *Revista de la CEPAL*, vol. 82, pp. 91-119, 2004.

[55] A. Cebreros, "La competitividad agropecuaria en condiciones de apertura comercial," *Comercio Exterior*, vol. 43, pp. 946-953, 1993.

[56] J. Markusen, *Productivity, Competitiveness, Trade Performance and Real Income: The Nexus Among Four Components*. Ottawa: Supply and Services Canada, 1992.

[57] S. Tamames, R., & Gallego, *Diccionario de economia y finanzas - Libros Deschargar*. 1994. Accessed: Mar. 12, 2021. [Online]. Available: http://319110.bvw-rollgitter.de/descargar/319110/Diccionario%2Bde%2Beconomia%2By%2Bfinanzas.pdf

[58] A. Di Filippo, "La competitividad internacional en economías abiertas de América Latina," in *Seminario-taller coordinación de políticas de fomento de la competitividad y nuevos desafíos para la integración regional*, 1991.

[59] A. Pego, M. Marques, R. Salvador, C. Guedes Soares, and A. Monteiro, "The potential offshore energy cluster in Portugal," in *Proceedings of Renew 2016, 2nd International Conference on Renewable Energies Offshore.* 2016.

[60] L. Haguenauer, "Competitividade: conceitos e medidas: uma resenha da bibliografia recente com ênfase no caso brasileiro," *Revista de Economia Contemporânea,* vol. 16, pp. 146-176, Apr 2012.

[61] G. Müller, "*El caleidoscopio de la competitividad*" 1995, Accessed: Mar. 12, 2021. [Online]. Available: https://repositorio.cepal.org/handle/11362/11993#.YEuda8fzJ-U.mendeley

[62] ECORYS SCS Group, "Study on Competitiveness of the European Shipbuilding Industry." Rotterdam, 2009.

[63] V. Bertram, "Strategic control of productivity and other competitiveness parameters," in *Proceedings of the Institution of Mechanical Engineers Part M Journal of Engineering for the Maritime Environment,* vol. 217, pp. 61-70, Jun 2003.

[64] C.-C. Chou, and P.-L. Chang, "Core competence and competitive strategy of the Taiwan shipbuilding industry: a resource-based approach," *Maritime Policy & Management,* vol. 31, pp. 125-137, Apr 2004.

[65] M. Guisado Tato, Mercedes, V. Alonso, Carlos, and F. Soto, "Estado de la cuestión de la construcción naval gallega: los nuevos factores de competitividad," *Revista Galega de Economía,* vol. 11, 2002.

[66] F. C. M. Pires, and T. Lamb, "Establishing performance targets for shipbuilding policies," *Maritime Policy & Management,* vol. 35, pp. 491-502, Oct 2008.

[67] A. Rashwan, and A. Naguib, "Toward improving the cost competitive position for shipbuilding yards- Part I: Impact of technology changes," *Alexandria Engineering Journal,* vol. 45, pp. 537-543, 2006.

[68] R. Gutiérrez, "Soluciones técnicas y soluciones políticas," *Ing. Nav.*, vol. LXXIV, pp. 877-878, 2005.

[69] R. Mickeviciene, "Global competition in shipbuilding: trends and challenges for Europe," *The Economic Geography of Globalization,* pp. 201-222, 2011.

[70] M. E. González, "Intervención de la universidad en la promoción de la salud de sus estudiantes". *Innovación Educativa*, 2008.

[71] Boletín Oficial del Estado (B.O.E.), *Ley 19/2013, de 9 de diciembre, de transparencia, acceso a la información pública y buen gobierno*. Spain, 2013.

[72] P. C. Martínez, "El método de estudio de caso: estrategia metodológica de la investigación científica," *Revista científica Pensamiento y Gestión,* vol. 20, pp. 165-193, Jul 2006.

[73] R. K. Yin, *Case Study Research: Design and Methods, Applied social research, Methods Series*. Newbury Park CA: Sage, 1989.

[74] Sociedad Española de Participaciones Industriales, "SEPI webpage," 2021.

[75] Google Earth, "Web Google Earth," 2021.

[76] Navantia, "Workshop de reflexión estratéxica. Plan estratéxico de Navantia 2014-2018. Working paper, Los peñascales. Torrelodones: CIG Navantia- Ferrol.," Torrelodones, Madrid, 2013.

[77] Navantia, "Documento de traballo sobre o futuro de Navantia 2015-2019 (DTFN 2015). Working paper, Los peñascales. Torrelodones: CIG Navantia- Ferrol.," Torrelodones, Madrid, 2014.

[78] CIG Navantia - Ferrol, "Contas de Navantia desagregadas por núcleos industriais e conxuntas no período 2005-1012," Ferrol, 2013.

[79] CIG Navantia - Ferrol, "Contas de Navantia desagregadas por núcleos industriais e conxuntas no período 2008-1013," Ferrol, 2014.

[80] CIG Navantia - Ferrol, "Evolución dos cadros de persoal de Bazán, ASTANO e Navantia dende o 1970 até o 2015," Ferrol, 2016.

Journal of ETA Maritime Science 2024;12(1):50-63

A Threat to Maritime Trade: Analysis of Piracy Attacks Between 2015 and 2022 and the Period of COVID-19

Nur Jale Ece

Mersin University Faculty of Maritime, Department of Maritime Business Administration, Mersin, Türkiye

Abstract

More than 80 percent of world trade is transported by sea. Maritime piracy negatively affects international maritime transport and trade. The aim of the study is to analyze maritime piracy attacks between 2015-2022 and during the coronavirus disease-2019 (COVID-19) period. In the study, a literature review, main reasons and statistics for piracy and armed robbery attacks, international efforts to combat maritime piracy were examined and maritime piracy attacks were analyzed in 2015-2022 and the COVID-19 period. The results of the main findings are as follows; the most piracy attacks occurred in 2015, the most attacks were occurred in March-April-May majority of attacks occurred between the hours 24:00-04:00, the most attacks occurred in South East Asia, the most types of attacks against to ships was boarded. Marshall Islands-flagged ships were the most attacked. There is a weak statistical relationship between the piracy attacks by months and regions and between the piracy attacks by years and type of attacks. There is no statistical relationship between other variables.

Keywords: Maritime security, Maritime piracy, Maritime trade, Chi-square test

1. Introduction

International maritime trade amounted to 10.7 billion tons in 2021. More than 80% of the international trade of goods is transported by sea. The annual growth of international maritime trade will be estimated at 2.4% in 2023, 2.3% in 2024 and 2025, and 2.2 in 2026 [1]. The negative effects of coronavirus disease-2019 (COVID-19) on shipping and ports lead to continued disruption in supply chains, increasing production costs. Maritime piracy negatively affects ship owners, importers, exporters, carriers, crews, the environment international trade, and increases costs [2]. The International Maritime Bureau's (IMB) Piracy Reporting Center (PRC) reported that a total of 116 attacks occured in 2022. Most of these attacks occurred in Singapore Straits (48), Peru (12), Indonesia (10), Bangladesh, and Ghana (7) [3]. The highest risk region is South-East Asia with 58 attacks and respectively America (24), Africa (21), Indian subcontinent (10) and East Asia (2) [3]. Maritime piracy and armed robbery on ships increased in 2020 during the COVID-19 period. Maritime piracy increased during the pandemic period [3].

Chalk [4] analyze maritime piracy in the Southeast Asian region. The main reasons for maritime piracy can be listed as follows: economic crisis in Southeast Asia, low wages, high unemployment rates, poverty and inadequate education, inadequate coastal and port control, local law enforcement, loopholes in legal instruments demand ransom, illegal fishing activities of foreigners, and dumping nuclear and toxic wastes into the sea by foreign ships [4].

International Maritime Organization (IMO), European Union, and other relevant organizations have made legal and some regulations concerning maritime security such as the Convention for the Suppression of Unlawful Acts against the Safety of Maritime Navigation 1988, the United Nations (UN) Convention Against Illicit Traffic in Narcotic Drugs and Psychotropic Substances, 1988 (Article 17), the UN Security Council Resolutions, IMO conventions, guidances, resolutions circules and best management practices. The Djibouti Code, the Regional Cooperation Agreement on Combating Piracy and Armed Robbery against ships in Asia.

Address for Correspondence: Nur Jale Ece, Mersin University Faculty of Maritime, Department of Maritime Business Administration, Mersin, Türkiye
E-mail: jalenur@mersin.edu.tr
ORCID ID: orcid.org/0000-0003-2048-5458

Received: 07.04.2023
Last Revision Received: 13.11.2023
Accepted: 29.12.2023

To cite this article: N. J. Ece. "A Threat to Maritime Trade: Analysis of Piracy Attacks Between 2015 and 2022 and the Period of COVID-19." *Journal of ETA Maritime Science*, vol. 12(1), pp. 50-63, 2024.

The UN Convention on the Law of the Sea 1982 includes the number of provisions related to maritime piracy (Articles 100-107 and 110) [5].

Some of technical arrangements are those; maritime technologies such as AIS and LRIT System; security plans for ships and port facilities, technical collaboration between states. Military and naval antipiracy patrols such as NATO Combined Task Forces, and other States' naval forces combat piracy. The International Recommended Transit Corridor through the Gulf of Aden is patrolled against pirates by international naval forces. The coastguards, marine police, etc. in South East Asia countries have taken precautions to combat maritime piracy. Indonesia, Malaysia, Singapore have conducted joint naval patrols [5].

The PRC of the IMB reported that there were 1,422 attacks against ships between 2015 and 2022. The most attacks were in South East Asia (580) and respectively Africa (458), the Americas (207), Indian subcontinent (100), and East Asia (70) between 2015 and 2022 (IMB, ICC 2022). A total of 1,145 ships were boarded, 158 attempted attacks, 44 ships hijacked, and 75 fired upon between 2015-2022. All types of attacks except hijack decreased in 2022 according to the previous year [3]. Bulk carriers were the most attacked ships (429) and respectively product tanker (287), container ships (163), tanker (111), general cargo (71), LPG tanker (49), chemical tanker (62) and tug (54) between 2015-2022. The attacks on bulk carriers and all types of tankers increased in 2022 compared to 2021 [3].

IMB PRC reported 115 attacks against ships in 2022. The piracy attacks in the Singapore Straits increased in 2022 (38) compared to the previous year (35). The attacks dropped in Malacca Straits due to the measures taken by the littoral states [3].

The aim of the study is to analyze of maritime piracy attacks in 2015-2022 and the COVID-19 period using quantative methods such as the frequency distribution, the chi-square test (χ^2), which is a statistical hypothesis test, the Spearman's Rank correlation, the Phi coefficient coefficient and non-parametric correlation. In the study a literature review has been done, and main reasons and statistics of piracy attacks, international legal framework and arrangements on maritime piracy and international efforts to combat maritime piracy were examined. A statistical hypothesis test such as χ^2 was used to determines whether there is an relationship between categorical variables and null (H_0) and alternative (H_1) hypotheses are established.

2. Literature Review

There have been many studies on piracy. Pristrom et al. [6] conducted the statistical analysis of maritime piracy incidents. According to the some results of the analysis the ships which have speed of less than 15 knots and a low freeboard are vulnerable [6]. Soğancılar [2] reviews the previous studies concerning piracy and the effects of maritime pirate incidents on international trade. Anti-piracy measures and operations have been very effective in reducing pirate attacks [7]. Mejia et al. [8] inquire whether acts of piracy are a truly random occurrence and conduct the econometric analysis. The results of the study show that both and type of vessel and flag of registry are main factors in explaining maritime piracy [8].

Nincic [9] research on maritime piracy and statistics of pirate attacks. As a result of the study is that social and economic difficulties in Africa are among the causes of piracy and negatively affect trade and the economy. Mohn [10] examines the dangers of maritime piracy to international trade and transport, and human society. The result of the study show that the regional cooperation of Southeast Asian countries has been very effective in the fight against piracy in the region. Flückiger and Ludwig [11] conduct 2SLS instrumental variable approach, regression analysis, data and descripive analysis. It has been estimated that plankton shock caused a 10% decrease in fish production. Shepard and Pratson [12] conduct two-stage least squares regression analysis Some findings of the study show that soft restrictions on piracy on energy exports by most Persian Gulf countries have little effect in the long run.

Daxecker and Prins [13] conduct two-stage estimation approach, two-part model, empirical Analyses, Ordinary Least Squares regression, Heckman selection model. The results show that piracy in weak states and both land area and coastline length increase capital to piracy. Okoronkwo et al. [14] research sociological discourse on maritime piracy in Nigeria. Özdemir and Güneroğlu [15] conduct quantitative analysis of maritime piracy. The results of the study show piracy attacks significantly increase costs in maritime trade between Asia and Europe. The most effective reason for piracy is economic insufficiency on the region to combat the piracy. Fu et al. [16] examined the effects of maritime piracy on global economic development in 2003 and 2008 in the Far East-Europe container liner shipping service. The findings of the study show that the international community must do more to fight against maritime piracy.

Bensasi and Martinez-Zarsorro [17] estimate the impact of maritime piracy on international trade between the main European and Asian countries in 1999-2008. The results of the analysis estimated that the cost of piracy to international trade is 24.5 billion dollars. Li and Yang [18] analyzed maritime piracy events. According to some of the research's findings, the most commonly attacked are bulk

carriers, followed by container ships. Jiang and Lu [19] analyze the maritime piracy occurred in Southeast Asia. The results of the research show that if the precautions on the ship are at the highest level and other anti-piracy measures are taken, the probability of the success of the pirate attack will decrease considerably.

Yang et al. [20] review the challenges of maritime safety analysis. Yang et al. [20] reviewed studies measuring maritime safety and risks in maritime transport and A Formal Safety Assessment. Findings from the study show that adequate risk analysis and measurement are used to support regulatory measures applicable to different areas of international shipping. Tsioufis et al. [21] used analytic hierarchy process and spatio-temporal methods to identify maritime piracy hotspots. Some findings of the analysis show that pirates attack more in areas of political instability outside the Arabian Sea and closer to the coastlines of countries facing extreme poverty.

Nwokedi et al. [22] determined the empirical probability coefficients of pirate attacks on ships, ship types and threats to crews affected by hostage-taking, injury, death, loss and pirate attacks using empirical probability statistical method. According to the results of the study; taking ship crew hostage has the highest probability of trauma relative to other trauma factors. Chemical and product tankers are most often attacked. Vespe et al. [23] analyzed diminishing impact on sea routes and ship behavior. The findings of the study show that anti-piracy efforts are effective in the Western Indian Ocean. Akan et al. [24] analyze maritime piracy attacks. The results of the analysis show that maritime piracy attacks decreased by 12.2% in 2022 compared to the previous year, with the most attacks against tankers (31.9%), followed by dry cargo ships (25.4%). The most attacks occur in the South China Sea, respectively, in the Strait of Malacca and in Africa. Nnadi et al. [25] analyzed maritime piracy in the Gulf of Guinea region between 2002 and 2015. One of the findings of the study shows that the most attacks occurred in Nigeria.

Aydın et al. [26] examine the effects of pirate attacks at the Gulf of Aden on international maritime trade and performed correlation analysis and Spearman's rho analysis. According to the results of the study, the piracy costs resulting from their actions are related to the type of attack and the experience of the ships.

Nwokedi et al. [27] analyzed the economic cost of piracy attacks to Nigeria's the global shipping industry and ocean trawler fishery sector and using the empirical probability measure. According to the findings, Nigeria's loss in the industrial trawling sector due to piracy attacks is approximately $1,275,258. This figure shows that the attacks caused significant losses to the Nigerian economy.

3. Materials and Methods

The piracy and armed robbery attacks data were obtained from IMB PRC "Piracy and Armed Robbery Against Ships" Annual Reports for in the period 2015 and 2022. The piracy attacks statistics contain 11.496 non-parametric data.

In the study, frequency distribution, the χ^2 and Cramer's value (Cramer's V) tests, Spearman's Rank correlation coefficient (Spearman's Rho), Phi coefficient and non-parametric correlation were used using statistical analysis performed with Statistical Package Programme (SPSS). The non-parametric variables include attacks years, attack months, attack hours, attack regions, type of ships attacked and ship's flag attacked The non-parametric variables have divided sub groups using the classification scale. The frequency distribution tables were presented to show the number of observations for each possible non-parametric value.

The χ^2 measures whether there is a relationship between non-parametric variables. In order to the χ^2 to be used safely, the following conditions must be met; all individual expected numbers must be 1, the minimum expected number must be at least equal to 1, and the p-value must be less than 0.05 significance level; more than 20% of the expected counts should not be less than 5 [28-31]. In the study, the significance level (α) was considered as 5%. The formula for the χ^2 test statistic is given as follows [32,33]:

where Oij= Observed value, E= Expected Value, Cal= Calculated value, Tab= Table value

$$X^2_{cal} = \sum_{j=1}^{c}\sum_{i=1}^{r}\frac{(O_{ij}-E_{ij})^2}{E_{ij}} \quad (1)$$

If the differences between expected values and observed values are small, the χ^2 value to be calculated will be small and H_0 will not be rejected. If the differences are large, H_0, which indicates independence between the criteria, will be rejected. When applied with the χ^2 test, the observed frequencies in each response category are compared with the frequencies expected if the null hypothesis is true. If;

$$X^2_{cal} \geq X^2_{tab} \quad (2)$$

H_0 will be rejected. Otherwise, H_0 will be accepted [32,33].

Cramer's V and Phi coefficient values dispread between 0 and 1 and Spearman's Rank correlation coefficient (Spearman's Rho) value dispread between -1 and 1 [20].

The formulas for the Cramer's V test statistic, Spearman's Rho test as equation, and the Phi coefficient (φ) are given below [28,31,32,34,35].

Cramer's V test was used to determine whether an relationship exists between two categorical variables [28]. The Cramer's V test statistic is determined as:

$$V=\sqrt{\frac{x^2}{n*(k-1)}} \quad (3)$$

Spearman's Rho was used to measure the strength between two variables [34,36]. The formula of Spearman's Rho test is determined as:

$$rs=1-\frac{6\sum di^2}{n(n2-1)} \quad (4)$$

The Phi coefficient (φ) is used to measure the association between the two variables. The Phi coefficient (φ) is determined as:

$$\varphi=\sqrt{\frac{x^2}{n}} \quad (5)$$

In the study, the non-parametric correlation was also used to measure the association between the two non-parametric variables. The correlation matrix was created to summarize the data for more advanced analysis.

3.1. Data Presentation

Frequency distributions of maritime piracy attacks by years, regions, types of attacks, months and type of ships attacked are given in the tables below (Tables 1-5).

Table 1. *Frequency distribution of piracy attacks by years*

Attacks by years	Frequency	Percent (%)	Total cumulative percent (%)
2015	250	17.4	17.4
2016	195	13.6	31.0
2017	185	12.9	43.8
2018	202	14.1	57.9
2019	161	11.2	69.1
2020	196	13.6	82.7
2021	132	9.2	91.9
2022	116	8.1	100.0
Total	1.437	100.0	
Source: IMB ICC 2015-2022 Annual Reports			

Table 2. *Frequency distribution of piracy attacks by regions*

		2015	2022	2020	2022	Frequency	
Attacks by regions	Frequency	Percent (%)	Total cumulative (%)	2020	2021	2022	Total
Africa	436	30.3	30.3	86	37	3	126
South East Asia	632	44.0	74.3	64	58	61	183
Indian subcontinent	103	7.2	30.3	11	2	10	23
America	224	15.6	97.1	30	35	42	107
Far East	35	2.4	99.5	4	0	0	4
Others	7	0.5	100.0	1	0	0	1
Total	1.437	100.0		196	132	116	444
Source: IMB ICC 2015-2022 Annual Reports							

Table 3. *Frequency distribution by types of piracy attacks*

		2015	2022	2020	2022	Frequency	
Types of piracy attacks	Frequency	Percent (%)	Total cumulative (%)	2020	2021	2022	Total
Attempted	158	11.0	11.0	19	13	4	36
Fired upon	73	5.1	16.1	11	4	1	16
Hijack	41	2.9	18.9	3	1	0	4
Boarded	1.165	81.0	99.9	163	114	111	388
Total	1.437	100.0		196	132	116	444
Source: IMB ICC 2015-2022 Annual Reports							

Table 4. *Frequency distribution of piracy attacks by months*

		2015	2022	2020	2022	Frequency	
Attacks by months	**Frequency**	**Percent (%)**	**Total cumulative (%)**	**2020**	**2021**	**2022**	**Total**
December-January-February	373	26.0	26.0	52	39	40	131
March-April-May	425	29.6	55.5	61	33	29	123
June-July-August	290	20.2	75.7	31	30	20	81
September-October-November	349	24.3	100.0	52	30	27	109
Total	1.437	100.0		196	132	116	444
Source: IMB ICC 2015-2022 Annual Reports							

Table 5. *Frequency distribution of type of ships attacked*

		2015	2022	2020	2022	Frequency	
Type of ships attacked	**Frequency**	**Percent (%)**	**Total cumulative (%)**	**2020**	**2021**	**2022**	**Total**
NA	1	0.1	0.1	-	-		-
Fishing ships	21	1.5	1.5	6	3	0	9
General cargo	74	5.1	6.7	12	4	5	21
Bulk carrier	431	30.0	36.7	52	47	49	148
Container	160	11.1	47.8	26	30	10	66
Tanker	113	7.9	55.7	10	5	9	24
Chemical tanker	63	4.4	60.1	9	3	6	18
Product tanker	281	19.6	79.6	41	20	14	75
LPG tanker	56	3.9	83.5	5	4	2	11
Refrigerated vessel	18	1.3	84.8	4	1	0	5
Vehicle carrier	16	1.1	85.9	0	2	7	9
Tug	64	4.5	90.4	4	3	8	15
Others	138	9.6	100.0	27	10	6	43
Total	1.437	100.0		196	132	116	444
Source: IMB ICC 2015-2022 Annual Reports							

The most attacks occurred in Indonesia and respectively Nigeria as shown in Table 1S.

The most attacks occurred between the hours 24:00-04: and respectively 04:00-08:00 between the period of 2015 and 2020 as given in Table 2S.

Marshall Islands-flagged ships are most commonly attacked and respectively Panama-flagged ships between the period of 2015 and 2022 as given in Table 3S.

3.2. Chi-square Test

χ^2 concerning piracy attacks for the period in 2015-2022 are given in the following:

3.2.1. The Chi-square test piracy attacks by years and regions

Most attacks occurred in Africa in 2018 (87), and respectively South East Asia in 2015 (181), Indian subcontinent in 2015 and 2017 (20), the Americas in 2022 (42), in the Far East (16) in 2016 as shown in Table 6 [3]. Piracy attacks decreased in all regions except the Americas during the COVID-19 period.

As seen in Table 6 the differences between the observed frequencies and the expected frequencies are quite large.

Null (H_0) and alternative (H_1) hypotheses are given as follows;

H_0: There is no statistical relationship between piracy attacks by years and regions.

H_1: There is a statistical relationship between piracy attacks by years and regions.

The Pearson χ^2 value=285.925 and 31.3% of expected counts <5 as given in Table 7. P-value (0.00) < the significance level (α=0.05), but the minimum expected count <1 (0.57). Therefore, the χ^2 test can not be used safely.

3.2.2. The chi-square test between month of attack and region of attack

The most of the attacks occurred in Africa (134), South Asia (193), and the Americas (64) occurred between March and

Table 6. *Crosstabulation for piracy attacks by years and regions (2015-2022)*

Attacks by years/ regions	Count % within attack year/Expected count	Africa	South East Asia	Indian subcontinent	Americas	Far East	Others	Total
2015	Count	35	181	20	8	5	1	250
	Expected count	75.9	110.0	17.9	39.0	6.1	1.2	250.0
	% attack year	14.0%	72.4%	8.0%	3.2%	2.0%	0.4%	100.0%
2016	Count	62	72	17	27	16	1	195
	Expected count	59.2	85.8	14.0	30.4	4.7	0.9	195.0
	% attack year	31.8%	36.9%	8.7%	13.8%	8.2%	0.5%	100.0%
2017	Count	56	79	20	24	2	4	185
	Expected count	56.1	81.4	13.3	28.8	4.5	0.9	185.0
	% attack year	30.3%	42.7%	10.8%	13.0%	1.1%	2.2%	100.0%
2018	Count	87	64	19	29	3	0	202
	Expected count	61.3	88.8	14.5	31.5	4.9	1.0	202.0
	% attack year	43.1%	31.7%	9.4%	14.4%	1.5%	0.0%	100.0%
2019	Count	70	53	4	29	5	0	161
	Expected count	48.8	70.8	11.5	25.1	3.9	0.8	161.0
	% attack year	43.5%	32.9%	2.5%	18.0%	3.1%	0.0%	100.0%
2020	Count	86	64	11	30	4	1	196
	Expected count	59.5	86.2	14.0	30.6	4.8	1.0	196.0
	% attack year	43.9%	32.7%	5.6%	15.3%	2.0%	0.5%	100.0%
2021	Count	37	58	2	35	0	0	132
	Expected count	40.1	58.1	9.5	20.6	3.2	0.6	132.0
	% attack year	28.0%	43.9%	1.5%	26.5%	0.0%	0.0%	100.0%
2022	Count	3	61	10	42	0	0	116
	Expected count	35.2	51.0	8.3	18.1	2.8	0.6	116.0
	% attack year	2.6%	52.6%	8.6%	36.2%	0.0%	0.0%	100.0%
Total	Count	436	632	103	224	35	7	1437
	Expected count	436.0	632.0	103.0	224.0	35.0	7.0	1437.0
	% attack year	30.3%	44.0%	7.2%	15.6%	2.4%	0.5%	100.0%

Table 7. *The chi-square test for the piracy attacks by years and regions (2015-2022)*

	Value	df	Asymp. sig. (2-sided)
Pearson chi-square	285.925[a]	35	0.000
Likelihood ratio	301.818	35	0.000
Linear-by-Linear relationship	6.680	1	0.010
Phi (Approx. sig.)	0.446		0.000
Cramer's V (Approx. sig.)	0.199		0.000[b]
Spearman correlation	0.031		0.237[c]
Number of valid cases	1.437		

[a]15 cells (31.3%) have expected count less than 5. The minimum expected count is 0.57.

[b]Approx. sig.

[c]Based on normal approximation

May. The most of the attacks occurred Indian subcontinent (47) and Far East (15) between December and February in the period of 2015 to 2022 as shown in Table 4S [3]. As seen in Table 4S, the differences between the observed frequencies and the expected frequencies are small.

H_0: There is no statistical relationship between the piracy attacks by months and region.

H_1: There is statistical relationship between the piracy attacks by months and regions.

The Pearson χ^2 value=52,318, 16.7% of expected counts <5 as given in Table 5S. The test result shows that the p-value (0.00) <α=0.05, the minimum expected count >1 (1.41). Therefore, H_0 is rejected, H_1 is accepted. There is statistical relationship between the month of attack and the region of attack. Cramer's V value (0.110) and Phi value (0.191) confirm that there is a weak statistical relationship between month of attack and region of attack. The Spearman correlation coefficient value of -0.013 confirms that there is a negative association between month of attack and region of attack.

3.2.3. The chi-square test piracy attacks between hours and regions

The piracy attacks in Africa, Indian subcontinent, Americas and Far East were occurred between the hours 24:00-04:00. The most attacks in South Asia were occurred between the hours 16:00-20:00 during the COVID-19 period between 2020 and 2022, and the differences between the observed frequencies and the expected frequencies are small as seen in Table 6S. According to the results of χ^2 for the piracy attacks by hours and regions; χ^2=252.044, p=0.000, Likelihood ratio=261.331, p=0.000, Phi=0.419, p=0.000 (Approx. Sig.-2-sided), Cramer's V=0.187, p=0.000 (Approx. Sig.-2-sided), Spearman's correlation: 0.021, p=0.000 (Asymp. Sig.-2-sided). 28.6% of expected counts <5 and the minimum expected count =0.11.

H_0: There is no statistical relationship between the piracy attacks by hours and regions, H_1: There is statistical relationship between the piracy attacks by hours and regions.

The test result shows that the p-value (0.00) <α=0.05, but the minimum expected count <1 (0.11). Therefore, the χ^2 can not be used safely.

3.2.4. The chi-square test between attack years and attack types

The most ships attempted (16.3%) and respectively fired upon (8.9%) in 2018. The most ships hijacked and boarded in 2015 as shown in Table 8. The attacks have dropped significantly due to preventive measures, anti-piracy operations and armed guards on board ships [3]. All type of attacks decreased in the COVID-19 period (2020-2022) as shown in Table 8. Most ships were boarded between 2015 and 2022.

χ^2=62.412, p=0.000, Likelihood ratio=73.942, p=0.000, Phi=0.208, p=0.000 (Approx. Sig.-2-sided), Cramer's V=0.120, p=0.000 (Approx. Sig.-2-sided), Spearman's correlation=0.072, p=0.006 (Asymp. Sig.-2-sided).

3 cells (9.4%) have expected count less than 5. The minimum expected count is 3.31.

As seen in Table 8, the differences between the observed frequencies and the expected frequencies are small. H_0: There is no statistical relationship between the piracy attacks by years and type of attacks; H_1: There is a statistical relationship between the piracy attacks by years and type of attacks. 9.4% of expected counts <5 as given below Table 8. P-value (0.00) <α=0.05, but the minimum expected count >1 (3.31). Therefore, H_0 is rejected, H_1 is accepted. There is a statistical relationship between the year of attack and the region of attack. Cramer's V value (0.120) and Phi value (0.208) confirm that there is a weak statistical relationship between the year of attack and the region of attack. The Spearman correlation coefficient value of 0.072 confirms that there is a very weak association between year of attack and region of attack.

3.2.5. Chi-square test between attack types and attack regions

The most attacks occurred were boarded in Africa (290), in South East Asia (549), in Indian subcontinent (95), in the Americas (197) and in the Far East (31) between 2015 and 2022 as given in Table 9.

χ^2=207.936, p=0.000, Likelihood ratio=178.652, p=0.000, Phi=0.380, p=0.000 (Approx. Sig.-2-sided), Cramer's V=0.220, p=0.000 (Approx. Sig.-2-sided), Spearman's correlation: 0.195, p=0.006 (Asymp. Sig.-2-sided).

7 cells (29.2%) have expected count less than 5. The minimum expected count is 0.20.

29.2% of expected counts <5 as given below Table 9. P-value (0.00) <α=0.05, but the minimum expected count is less than 1 (0.20). Therefore, the χ^2 can not be used safely.

3.2.6. Non-parametric correlation

Non-parametric correlation measure the association between the two variables [34,35]. The correlation matrix was created to summarize the data for more advanced analysis. The correlation matrix shows a global view of the more or less strong relationship between the variables [36-38].

The correlation between some variables indicate little or no association. These are the correlation between type of ship attacked and flag of ships attacked (0.140); between flag of ships attackted and month of attack (0.043); between year of attack and hour of attack (0.178); between type of attack and year of attack (0.072); between year of attack and type of attack (0.064); between year of attack and region of attack (0.068); between region of attack and type of attack (0.122) as given in Table 10.

The correlation between some variables indicates strong negative association such as between flag of ships attacked

and year of attack (-0.082); between flag of ships attacked and type of attack (-0.020); between flag of ships attacked and region of attack (-0.065); between type of ship attacked and type of attack (-0.013), between type of ships attacked and region of attack (-0.078) as given in Table 10.

4. Results and Discussion of Findings

The purpose of the study is to help stakeholders take effective anti-piracy measures against pirate attacks by revealing the attacks by years, months, and hours, regions, type of ships attacked and ship's flag attacked, or whether there is a relationship between these parameters between 2015 and 2022 and the COVID-19 Period. The results of the frequency distributions are as follows;

There were 1,437 piracy and armed robbery attacks between 2015 and 2022. The most piracy attacks occurred in 2015 (17.4%) between 2015 and 2022. Maritime piracy attacks decreased by 32.7% in 2020 and by 12.2% in 2022 according to the previous year [35]. The annual report of IMB PRC shows 13% decrease in overall attacks in 2022 compared to 2021 [21]. The attacks decreased respectively between 2021 and 2022 during the COVID-19 period as given in Table 1. According to the study conducted by Akan et al. [24] most piracy attacks occurred in 2015 (13.3%) between 2010 and 2020 These results confirm the analysis results.

The region with the most attacks is South East Asia (44.0%) and respectively Africa (30.3%), America (15.6%), Indian subcontinent (7.2%) and Far East (2.4%) between the period of 2015 and 2022. The region with the most attacks is South East Asia (183) and respectively in Africa (126) and America (107) between 2020 and 2022 during the COVID-19 period as given in Table 2. The attacks in Africa drastically decreased in 2020-2022. The almost attacks increased in

Table 8. *Crosstabulation for the piracy attacks by years and type of attacks (2015-2020)*

Years	Count/Expected count/% within attack year	Attempted	Fired upon	Hijack	Boarded	Total
2015	Count	28	1	15	206	250
	Expected count	27.5	12.7	7.1	202.7	250.0
	% wit. attack year	11.2%	0.4%	6.0%	82.4%	100.0%
2016	Count	23	11	8	153	195
	Expected count	21.4	9.9	5.6	158.1	195.0
	% wit. attack year	11.8%	5.6%	4.1%	78.5%	100.0%
2017	Count	22	16	5	142	185
	Expected count	20.3	9.4	5.3	150.0	185.0
	% wit. attack year	11.9%	8.6%	2.7%	76.8%	100.0%
2018	Count	33	18	5	146	202
	Expected count	22.2	10.3	5.8	163.8	202.0
	% wit. attack year	16.3%	8.9%	2.5%	72.3%	100.0%
2019	Count	16	11	4	130	161
	Expected count	17.7	8.2	4.6	130.5	161.0
	% wit. attack year	9.9%	6.8%	2.5%	80.7%	100.0%
2020	Count	19	11	3	163	196
	Expected count	21.6	10.0	5.6	158.9	196.0
	% wit.attack year	9.7%	5.6%	1.5%	83.2%	100.0%
2021	Count	13	4	1	114	132
	Expected count	14.5	6.7	3.8	107.0	132.0
	% wit. attack year	9.8%	3.0%	8%	86.4%	100.0%
2022	Count	4	1	0	111	116
	Expected count	12.8	5.9	3.3	94.0	116.0
	% wit. attack year	3.4%	0.9%	0.0%	95.7%	100.0%
Total	Count	158	73	41	1165	1437
	Expected count	158.0	73.0	41.0	1165.0	1437.0
	% wit. attack year	11.0%	5.1%	2.9%	81.1%	100.0%

Table 9. *Crosstabulation for attack types and attack regions (2015-2022)*

Attack types/ Attack regions	Count/Expected count/% within attack hour	Africa	South East Asia	Indian subcontinent	Americas	Far East	Others	Total
Attempted	Count	66	57	8	23	4	0	158
	Expected count	47.9	69.5	11.3	24.6	3.8	0.8	158.0
	% att. typ.	41.8%	36.1%	5.1%	14.6%	2.5%	0.0%	100.0%
Fired Upon	Count	60	4	0	4	0	5	73
	Expected count	22.1	32.1	5,.2	11.4	1.8	0.4	73.0
	% att. typ.	82.2%	5.5%	0.0%	5.5%	0.0%	6.8%	100.0%
Hijack	Count	20	21	0	0	0	0	41
	Expected count	12.4	18.0	2.9	6.4	1.0	0.2	41.0
	% att. typ.	48.8%	51.2%	0.0%	0.0%	0.0%	0.0%	100.0%
Boarded	Count	290	549	95	197	31	2	1164
	Expected count	353.5	512.4	83.5	181.6	28.4	5.7	1165.0
	% att. typ.	24.9%	47.2%	8.2%	16.9%	2.7%	0.2%	100.0%
Total	Count	436	632	103	224	35	7	1437
	Expected count	436.0	632.0	103.0	224.0	35.0	7.0	1437.0
	% att. typ.	30.3%	44.0%	7.2%	15.6%	2.4%	0.5%	100.0%

Table 10. *The correlation matrix*

		A	B	C	D	E	F	G
Type of ship attacked (A)	Correlation coefficent	1	0.140**	-0.029	-0.046	-0.038	-0.013*	-0.078**
Flag of ships attacked (B)	Correlation coefficent	0.140**	1	-0.082**	0.043	0.044	-0.020	-0.065*
Year of attack (C)	Correlation coefficent	-0.029	-0.082**	1	-0.046	0.178**	0.064**	0.068**
Month of attack (D)	Correlation coefficent	-0.046	0.043	-0.046	1	0.013	0.023	-0.033
Hour of attack (E)	Correlation coefficent	-0.038	0.044	0.178**	0.013	1	-0.004	0.021
Type of attack (F)	Correlation coefficent	-0.061*	-0.054*	0.072**	0.036	-0.027	1	0.122**
Region of attack (G)	Correlation coefficent	-0.078**	-0.065*	0.068**	-0.033	0.051	0.122**	1

*Correlation is significant at the 0.01 level (2-tailed).

**Correlation is significant at the 0.05 level (2-tailed)

South East Asia by 5.2% in 2022 compared to the previous year. According to the analysis results performed by Jiang and Lu [19], the number of pirates in Southeast Asia has increased rapidly. This result is consistent with the results of this study. The main reasons for the most piracy incidents in Southeast Asia are low wages, unemployment, inadequate coastal-port surveillance, political instability and gaps in the legal system.

Frequency distribution of piracy attacks by locations is given in Table 1S. The most attacks occurred in Indonesia (21.4%) and respectively Nigeria (13.5%), the Straits of Malacca and Singapore (9.5%) and Malaysia (4.5%) between the period of 2015 and 2022 as given in Table 1S. The most attacks occurred in the Straits of Malacca and Singapore (98) and respectively, Indonesia (43) and Nigeria [33] during the COVID-19 period. The number of pirack attacks in the Singapore Strait increased in 2022 [34].

Most attacks were boarded (81%) and respectively attempted (11%), fired upon (5.1%) and hijack (2.9%) in the period 2020 and 2022. Most attacks were boarded (388) and respectively attempted (36) and fired upon (16) during the COVID-19 period as given in Table 3. The number of attacks in Vietnamese and Malaysian ports dropped between 2020 and 2021. The region with the most attacks is Southeast Asia, followed by Africa between the years 2015-2022 and in the 2020-2022 COVID-19 period.

Majority of attacks occurred in March-April-May (29.6%) and respectively December-January-February (26.0%), September-October-November (24.3%), and June-July-August (20.2%) between the period of 2015 and 2022 as given in Table 4. The most attacks occurred in December-January-February (131) and respectively March-April-May (123) during the COVID-19 period. All attacks decreased between 2020 and 2022 except in December-

January-February in 2022. According to the results of the analysis conducted by Li and Yang [18], in Southeast Asia, Most maritime pirate attacks occurred in April and May, the dry seasons when there is no wind. These results are consistent with the findings of this study. The most attacks occurred between the hours 24:00-04:00 (27.8%) and respectively 04:00-08:00 (19.5%), 16:00-20:00 (18.4%), 20:00-24:00 (15.8%), 12:00-16:00 (9.2%) and 08:00-12:00 (7.9%) between the period of 2015 and 2022 as given in Table 2S. According to the analysis results performed by Ece [39], most of the attacks occurred the hours between 24:01-04:00 and respectively between 04:01-08:00. This result is consistent with the results of this study.

According to the study conducted by Akan et al. [24] most attacks also occurred between the hours 24:00-04:00 (36.6%) and respectively 04:00-08:00 (25.4%). The results of the study are consistent with the results of this study The most attacks occurred between 24:00-04:00 (110) and then 16:00-20:00 (109) during the COVID-19 period.

Bulk carrier ships were the most attacked (30.0%), and respectively product tankers (19.6%), container ships (11.1%) between the period of 2015 and 2022 as given in Table 5. Bulk carrier ships were the most attacked (148) and respectively product tankers (75) during the COVID-19 period. Attacks against almost all types of ships except bulk carrier decreased during the pandemic. The attacks against bulk carriers increased 4.3% in 2022 compared to the previous year. The results of the study conducted by Akan et al. [24] show that tankers were the most attacked (31.9%) tanker (7.9%), chemical tanker (4.4%), product tanker (19.6%) between 2010 and 2020. These results regarding attack hours, and type of ships attacked are consistent with the results of this study. Marshall Islands-flagged ships are most commonly attacked (16.4%) and respectively Panama-flagged ships (14.4%), Singapore-flagged ships (15.0%), and Liberia-flagged ships (11.3%) in 2015-2022 as given in Table 3S. According to the statistical analysis conducted Jiang and Lu [19], the most attacked type of ship between 2010 and 2019 was bulk carriers (24.1%), followed by general cargo ships (14.9%), container ships (14.7%), and tankers (12.5%) and slowing the speed of big ships below 15 knots provides an opportunity for pirates. Singapore-flagged ships were also the most attacked (75) and respectively Marshall Islands-flagged ships (68), Liberia-flagged ships (59), and Panama-flagged ships (55) during the COVID-19 period.

The findings of χ^2 are as follows; There is a weak statistical relationship between the piracy attacks by regions and months; and there is also a weak statistical relationship between piracy attacks by years and type of attacks. There is no statistical relationship between other variables. According to findings of Cramer's V value and Phi value, there is a weak statistical relationship between the month of attack and the region of attack. The Spearman's Rho confirms that there is a very weak association between the year of attack and the region of attack. According to the non-parametric correlation results, there is little or no association between the region of attack and the month of atack. The correlation between is -0.109 which indicates There is a strong negative association between the type of ships and region of attack. According to the non-parametric correlation results; the correlation between some variables indicates little or no association.

5. Conclusion

In the study, quantitative analysis of maritime piracy attacks between 2015 and 2022 and during the 2020-2022 COVID-19 period were performed. The results of the frequency distributions are as follows; Most piracy attacks occurred in 2015. Maritime piracy attacks decreased by 12.2% in 2022 compared to the previous year. Majority of attacks occurred in South East Asia between 2015 and 2022 and the COVID-19 period. Most attacks occurred in March-April-May between 2015-2022. Most attacks occurred between the hours 24:00-04:00 in 2015-2022 and the COVID-19 period. Tankers were the most attacked in the same period. Most types of attacks against to ships were boarded between 2015 and 2022 and the COVID-19 period. The Marshall Islands-flagged ships were the most attacked in 2015-2022.

In the COVID-19 period most attacks occurred in Singapore and the Straits of Malacca. Most attacks occurred between December and February. The bulk carrier ships were the most attacked and respectively product tankers. The Singapore-flagged ships were also the most attacked.

There is a weak statistical relationship between the piracy attacks by months and regions; and there is also a weak statistical relationship between piracy attacks by years and type of attacks. According to the non-parametric correlation results; the correlation between some variables indicates little or no association.

It is thought that researching further studies on the coordinates of piracy incidents and the legal infrastructure for prosecution and criminal prosecution in case of catching pirates will contribute to the literature and anti-piracy measures.

Funding: The author received no financial support for the research, authorship, and/or publication of this article.

References

[1] The United Nations Conference on Trade and Development (UNCTAD), (2022). Review of maritime transport 2022. Available: https://unctad.org/rmt2022

[2] N. Soğancılar, "Maritime piracy and its impacts on international trade." *Journal of Politics, Economy and Management,* vol. 4, pp. 38-48, Jun 2021.

[3] The ICC International Maritime Bureau (IMB).,"Piracy and Armed Robbery Against Ships Annual Report for the Period 1 January-31 December", 2015-2022.

[4] P. Chalk, "Contemporary maritime piracy in southeast asia", *Studies in Conflict & Terrorism*, 1998, pp. 87-112, Jun 1998. https://core.ac.uk/download/pdf/48638874.pdf

[5] N. J. Ece, and H. Kurt, "Analysis of maritime piracy by using qualitative methods", *Mersin University Journal of Maritime Faculty*, vol. 3, pp. 37-50, Dec 2021.

[6] S. Pristrom, Kevin, X. Li, Z. Yang, and J. Wang, "A study of maritime security and piracy," *Maritime Policy & Management*, vol. 40, pp. 675-693, Nov 2013.

[7] M. Ahmad, "Maritime piracy operations: some legal issues," *Journal of International Maritime Safety, Environmental Affairs and Shipping*, vol. 4, pp. 62-69, Jul 2020.

[8] M. Q. Mejia, P. Cariou, and F. C. Wolff, "Is maritime piracy random*?," Applied Economics Letters*, vol. 16, pp. 891-895, May 2009.

[9] D. Nincic, "Maritime piracy in africa: the humanitarian dimension," *African Security Studies*, vol. 18, pp. 1-16, Jul 2010.

[10] J. Mohn, "Options to combat maritime piracy in southeast asia," *Ocean Development & International Law*, vol. 33, pp. 343-358, Nov 2010.

[11] M. Flückiger, and M. Ludwig, "Economic shocks in the fisheries sector and maritime piracy," *Journal of Development Economics*, vol. 114, pp. 107-125, Dec 2014.

[12] J. U. Shepard, and L.F. Pratson, "Maritime piracy in the strait of hormuz and implications of energy export security," *Energy Policy*, vol. 140, pp. 1-9, May 2020.

[13] U. E. Daxecker, and B. C. Prins, "Searching for sanctuary: government power and the location of maritime piracy," *International Interactions*, vol. 41, pp. 699-717, Sep 2015.

[14] U. L, Okoronkwo, E. N. Okpara, and C. E. Onyinyechi, "National security and maritime piracy in Nigeria: a sociological discourse," *Humanities and Social Sciences Letters*, vol. 2, pp. 60-71, Sep 2014.

[15] Ü. Özdemir, and A. Güneroğlu, "Quantitative analysıs of the world sea piracy by fuzzy ahp and fuzzy topsis methodologies," *International Journal of Transport Economics*, vol. 44, pp. 427-448, 2017.

[16] X. Fu, A. K. Y. Ng, and Y.-Y. Lau, "The impacts of maritime piracy on global economic development: the case of Somalia," *The Flagship Journal of International Shipping and Port Research*, vol. 37, pp. 677-697, Nov 2010.

[17] S. Bensasi, and I. Martinez-Zarsorro, "How costly is modern maritime piracy to the international community?," *Review of International Economics*, vol. 20, pp. 869-883, Nov 2012.

[18] H. Li, and Z. Yang, "Towards safe navigation environment: the imminent role of spatio-temporal pattern mining in maritime piracy incidents analysis*," Reliability Engineering and System Safety*, vol. 238, pp. 1-22, Oct 2023.

[19] M. Jiang, and J. Lu, "The analysis of maritime piracy occurred in southeast asia by using bayesian network the analysis of maritime piracy occurred in southeast asia by using Bayesian network", *Transportation Research Part E*, vol. 139, pp. 1-14, Jul 2020.

[20] Z. L. Yang, J. Wang, and K. X. Li, "Maritime safety analysis in retrospect," *Maritime Policy & Management*, vol. 40, pp. 261-277, May 2013.

[21] M. Tsioufis, A. Fytopoulos, D. Kalaitzi, and T. A. Alexopoulos, "Discovering maritime-piracy hotspots: a study based on AHP and spatio-temporal analysis," *Annals of Operations Research*, Apr 2023.

[22] T. C. Nwokedi, J. Anyanwu, M. Eko-Rapheaels, C. Obasi, I. D. Akpufu, and D. B. Ogola, "Probability theory analysis of maritime piracy and the implications for maritime security governance," *Journal of ETA Maritime Science*, vol. 10, pp. 133-143, Jun 2022.

[23] M. Vespe, H. Greidanus, and M. Alvarez Alvarez, "The declining impact of piracy on maritime transport in the indian ocean: statistical analysis of 5-year vessel tracking data," *Marine Policy,* vol. 59, pp. 9-15, May 2015.

[24] E. Akan, T. Gültekin, and S. Bayar, "Statistical analysis of maritime piracy cases in world territorial waters," *Journal of Transportation Security*, vol. 15, pp. 263-280, Aug 2022.

[25] K. U. Nnadi, T. C. Nwokedi, I. A. Nwokoro, O. C. Ndikom, G. C. Emeghara, and C. Onyemechi, "Analysis of maritime piracy and armed robbery in the gulf of guinea maritime domain," *Journal of ETA Maritime Science*, vol. 4, pp. 271-287, Oct 2016.

[26] M. Aydin, N. Gedik, Ö. Uğurlu, and U. Yıldırım, "The Impacts of maritime piracy incidents in the gulf of aden on Turkish and world maritime trade," *Journal of ETA Maritime Science*, vol. 4, pp. 61-71, Jan 2016.

[27] T. Nwokedi, C. U. Odumodu, J. Anyanwu, and D. Dike, "Frustration-aggression-theory approach assessment of sea piracy and armed robbery in nigerian industrial trawler fishery sub-sector of the blue economy," *Journal of ETA Maritime Science*, vol. 8, pp. 114-132, Apr 2020.

[28] M, W. Kearney, "Cramér's V," 2010. Available: https://www.researchgate.net/profile/Michael-Kearney-5/publication/307963787_Cramer's_V/links/57d3b4ee08ae601b39a45691/Cramers-V.pdf, [Accessed: 15 Jan 2022].

[29] W. G. Cochran, "Some methods for strengthening the common χ2 Tests," *Biometrics,* vol. 10, pp. 417-451, Dec 1954.

[30] D. J. Sheskin, "Handbook of parametric and nonparametric statistical procedures," *Boca Raton: Chapman & Hall/CRC*, New York, pp. 494-495 2004.

[31] L. M. McHugh, "The chi-square test of independence" Lessons in biostatistics, Available: https://www.science.gov/topicpages/a/analysis+chi-square+test [Accessed: 22 Jan 2022].

[32] L. Sullivan, *Hypothesis testing - chi squared test*, Available: https://sphweb.bumc.bu.edu/otlt/mph-modules/bs/bs704_hypothesistesting-chisquare/bs704_hypothesistesting-chisquare_print.html [Accessed: 22 Oct 2023].

[33] M. Güngör, and Y. Bulut, "On the chi-square test (Ki-kare testi üzerine)" *Doğu Anadolu Bölgesi Araştırmaları,* vol. 7, pp. 84-89, 2008.

[34] Royal Geographical Society (RGS), Spearman's rank correlation coefficient - excel guide, Available: https://www.rgs.org/CMSPages/GetFile.aspx?nodeguid=f6c9f42a-ac87-43d2-89ae-fa2e2788c690&lang=en-GB, Spearman's Rank Correlation Coefficient, Available: https://www.rgs.org/NR/rdonlyres/...B36D.../OASpearmansRankExcelGuidePDF.pdf [Accessed: 15 Jan 2022].

[35] Gard, *Piracy trends and high risk areas,* Available: https://www.gard.no/web/articles?documentId=34977995 [Accessed: 15 Mar 2022].

[36] C. Defaux, *Phi Coefficient A.K.A Matthews Correlation Coefficient (Binary Classification),* 2020, Available: https://medium.com/@cdefaux/phi-coefficient-a-k-a-matthews-correlation-coefficient-binary-classification-11e2c29db91e [Accessed: 22 February 2022].

[37] J. P. Verma, "*Non-parametric Correlations*", Statistics and Research Methods in Psychology with Excel, 2019, Available: https://link.springer.com/chapter/10.1007/978-981-13-3429-0_13 [Accessed: 21 Mar 2022].

[38] Feeder, *Correlation matrix: what is it and how does it work?,* https://feedier.com/blog/correlation-matrix/ [Accessed: 22 Aug 2022].

[39] N. Ece, "Analysis of maritime piracy and armed robbery attacks against ships", *Dokuz Eylul University Maritime Faculty Journal,* vol. 7, pp. 75-111, Nov 2015.

Table 1S*. Frequency distribution of piracy attacks by locations*

		2015	2022	2020	2022	Frequency	
Attacks by location	**Frequency**	**Percent (%)**	**Total cumulative (%)**	**2020**	**2021**	**2022**	**Total**
Bangladesh	49	3.4	3.4	4	0	7	11
The Gulf of Aden/Somalia	31	2.2	5.6	1	1	0	2
Indonesia	308	21.4	27.0	26	8	9	43
Malaysia	64	4.5	31.5	5	2	3	10
Nigeria	194	13.5	45.0	34	0	0	34
Vietnam	52	3.6	48.6	4	1	2	7
The Straits of Malacca and Singapore	136	9.5	58.0	24	36	38	98
Indian	53	3.7	61.7	7	1	3	11
Benin	19	1.3	63.0	11	3	4	18
Others	531	37.0	100.0	80	80	50	210
Total	1.437	100.0		196	132	116	444
Source: International Chamber of Commerce (ICC) IMB 2015-2022 Annual Reports							

Table 2S*. Frequency distribution of piracy attacks by hours*

		2015	2022	2020	2022	Frequency	
Attacks by hours	**Frequency**	**Percent (%)**	**Total cumulative (%)**	**2020**	**2021**	**2022**	**Total**
NA	22	1.5	1.5	0	2	0	2
24:00-04:00	399	27.8	29.3	59	32	19	110
04:01-08:00	280	19.5	48.8	31	19	16	66
08:01-12:00	113	7.9	56.6	17	10	8	35
12:01-16:00	132	9.2	65.8	23	19	11	53
16:01-20:00	264	18.4	84.2	31	35	43	109
20:01-24:00	227	15.8	100.0	35	15	19	69
Total	1.437	100.0		196	132	116	444
Source: International Chamber of Commerce (ICC) IMB 2015-2022 Annual Reports							

***Table 3S**. Actual and attempted piracy attacks by ship's flag attacked*

		2015	2022	2020	2022	Frequency	
Ship's flag attaccked	**Frequency**	**Percent (%)**	**Total cumulative (%)**	**2020**	**2021**	**2022**	**Total**
NA	10	0.7	0.7	2	0	1	3
Europe (Exc. Malta)	42	2.9	3.6	2	28	7	37
Malta	53	3.7	7.3	7	4	7	18
USA/Cont America	4	0.3	7.6	0	0	1	1
Russia	2	0.1	7.7	0	0	2	2
Hong Kong	70	4.9	12.6	9	0	2	11
Marshall Islands	236	16.4	29.0	33	15	20	68
Antigua & Barbuda	17	1.2	30.2	1	3	0	4
Singapore	215	15.0	45.2	29	25	21	75
Panama	207	14.4	59.6	26	6	23	55
Liberia	162	11.3	70.8	31	17	11	59
Malaysia	45	3.1	74.0	1	3	3	7
Indonesia	25	1.7	74.8	4	1	0	5
Others	349	24.3	100.0	51	30	18	99
Total	1.437	100.0		196	132	116	444
Source: International Chamber of Commerce (ICC) IMB 2015-2022 Annual Reports							

***Table 4S**. Crosstabulation for piracy attacks by months and regions (2015-2022)*

Attacks by months	**Count/Expected count/% within attack months**	**Africa**	**South East Asia**	**Indian subcontinent**	**Americas**	**Far East**	**Others**	**Total**
December-February	Count	128	120	47	62	15	1	373
	Expected count	113.2	164.0	26.7	58.1	9.1	1.8	373.0
	% w. attac. mon.	34.3%	32.2%	12.6%	16.6%	4.0%	0.3%	100.0%
March-May	Count	134	193	21	64	10	3	425
	Expected count	128.9	186.9	30.5	66.2	10.4	2.1	425.0
	% w. attac. mon.	31.5%	45.4%	4.9%	15.1%	2.4%	0.7%	100.0%
June-August	Count	70	150	16	49	4	1	290
	Expected count	88.0	127.5	20.8	45.2	7.1	1.4	290.0
	% w. attac. mon.	24.1%	51.7%	5.5%	16.9%	1.4%	0.3%	100.0%
September-November	Count	104	169	19	49	6	2	349
	Expected count	105.9	153.5	25.0	54.4	8.5	1.7	349.0
	% w.attac. mon.	29.8%	48.4%	5.4%	14.0%	1.7%	0.6%	100.0%
Total	Count	436	632	103	224	35	7	1437
	Expected count	436.0	632.0	103.0	224.0	35.0	7.0	1437.0
	% w. attac. mon.	30.3%	44.0%	7.2%	15.6%	2.4%	0.5%	100.0%
Source: International Chamber of Commerce (ICC) IMB 2015-2022 Annual Reports								

***Table 5S**. The chi-square test for the piracy attacks by months and regions (2015-2022)*

	Value	df	Asymp. Sig. (2-sided)
Pearson's chi-square	52.318[a]	15	0.000
Likelihood ratio	50.945	15	0.000
Linear-by-Linear relationship	1.590	1	0.207
Phi (Approx. Sig.)	0.191		0.000
Cramer's V (Approx. Sig.)	0.110		0.000[b]
Spearman correlation	-0.013		0.613[c]
Number of valid cases	1.437		

[a]4 cells (16.7%) have expected count less than 5. The minimum expected count is 1.41.

[b]Approx. Sig.

[c]Based on normal approximation

***Table 6S**. Crosstabulation for piracy attacks by hours and regions (2015-2022)*

Attacks by hours	Count/% within attac. hour	Africa	South East Asia	Indian subcontinent	Americas	Far East	Others	Total
NA	Count	5	12	2	2	1	0	22
	Expected count	6.7	9.7	1.6	3.4	0.5	0.1	22.0
	% attac. hour	22.7%	54.5%	9.1%	9.1%	4.5%	0.0%	100.0%
24:00-04:00	Count	169	116	27	74	13	0	399
	Expected count	121.1	175.5	28.6	62.2	9.7	1.9	399.0
	% attac. hour	42.4%	29.1%	6.8%	18.5%	3.3%	0.0%	100.0%
04:01-08:00	Count	84	86	13	91	3	3	280
	Expected count	85.0	123.1	20.1	43.6	6.8	1.4	280.0
	% attac. hour	30.0%	30.7%	4.6%	32.5%	1.1%	1.1%	100.0%
08:01-12:00	Count	47	37	4	24	1	0	113
	Expected count	34.3	49.7	8.1	17.6	2.8	0.6	113.0
	% attac. hour	41.6%	32.7%	3.5%	21.2%	0.9%	0.0%	100.0%
12:01-16:00	Count	28	77	14	8	5	0	132
	Expected count	40.1	58.1	9.5	20.6	3.2	0.6	132.0
	% attac. hour	21.2%	58.3%	10.6%	6.1%	3.8%	0.0%	100.0%
16:01-20:00	Count	42	179	24	8	9	2	264
	Expected count	80.1	116.1	18.9	41.2	6.4	1.3	264.0
	% attac. hour	15.9%	67.8%	9.1%	3.0%	3.4%	0.8%	100.0%
20:00-24:00	Count	61	125	19	17	3	2	227
	Expected count	68.9	99.8	16.3	35.4	5.5	1.1	227.0
	% attac. hour	26.9%	55.1%	8.4%	7.5%	1.3%	0.9%	100.0%
Total	Count	436	632	103	224	35	7	1437
	Expected count	436.0	632.0	103.0	224.0	35.0	7.0	1437.0
	% attac. hour	30.3%	44.0%	7.2%	15.6%	2.4%	0.5%	100.0%

Source: International Chamber of Commerce (ICC) IMB 2015-2022 Annual Reports

ORIGINAL RESEARCH (AR) DOI: 10.4274/jems.2024.46514

Journal of ETA Maritime Science 2024;12(1):64-73

Modelling Using Neural Networks and Dynamic Position Control for Unmanned Underwater Vehicles

Melek Ertogan[1], Philip A. Wilson[2]

[1]İstanbul Technical University Faculty of Maritime, Department of Maritime Transportation and Management, İstanbul, Türkiye
[2]The University of Southampton, Ship Dynamics within Engineering and Physical Sciences, Southampton, United Kingdom

Abstract

Underwater construction, maintenance, and mapping use autonomous underwater vehicles (AUVs) for path planning, path following, and target tracking operations. However, dynamic position management and localization of AUVs are critical issues. Correct localization and dynamic position management to prevent drifts can be used to acquire information on energy efficiency, another crucial topic. In this paper, AUV dynamic modeling using experimental data and position control is studied. The experiments were implemented on a Delphin2 scaled AUV model belonging to the Engineering and Environment Faculty, University of Southampton, UK. Hover and flight style motions according to the different speeds of Delphin2 were implemented in the test tank. Nonlinear coupled mathematical models were studied using shallow neural networks. The models are formed into depth-pitch and heading motion black-box models using the shallow neural network (SNN) algorithm. Proportional integral derivative control of heading motions and depth-pitch motion simulation studies were applied to the SNN model.

Keywords: Autonomous underwater vehicle, Shallow neural networks, Black box modelling, Dynamic position control

1. Introduction

Autonomous underwater vehicles' (AUVs) research and application topics include localization, path following, target tracking, underwater mapping, and dynamic position management. Energy efficiency is a key issue that can be resolved by combining precise localization with dynamic position control to halt drifts.

The goal of this study is to create and test an algorithm for dynamic position controllers for AUVs. The scaled Delphin2 AUV model from the Engineering and Environment Faculty at the University of Southampton in the UK was used for the experiments [1-6]. To provide dynamic position control during hover and flight-style operations underwater, the local position definition of AUVs is a crucial challenge.

Delphin2 has an inertial measurement unit (IMU), a depth pressure sensor, a sounding altimeter, a mechanical scanning sonar, and a global positioning system (GPS). GPS does not work underwater or in closed areas such as tank tests. The IMU includes a 3D accelerometer, gyroscope, and magnetometer. The heading-pitch-depth motions of Delphin2 can be measured in tank tests and underwater applications.

Surge and sway motions of an AUV cannot be measured during underwater operations for this research study because an ultra-short baseline (USBL) positioning system cannot be used for tank tests because of the wall effect.

An over-actuated design enables the Delphin2 AUV model to perform various missions, from hover-style operation at zero or slow speeds to flight-style operation at forward speeds up to approximately 1 m/s.

Hover and flight style motions according to the different speeds of Delphin2 were implemented in the tank. Nonlinear coupled mathematical models were studied using experimental data. Proportional integral derivative (PID) control of heading and depth-pitch motions simulation studies were performed on the nonlinear mathematical model. Previous control studies on Delphin2, such as model predictive control (MPC) depth-pitch motion control [3]

Address for Correspondence: Melek Ertogan, İstanbul Technical University Faculty of Maritime, Department of Maritime Transportation and Management, İstanbul, Türkiye
E-mail: ertogan@itu.edu.tr
ORCID ID: orcid.org/0000-0002-9968-6254

Received: 14.08.2023
Last Revision Received: 28.11.2023
Accepted: 03.01.2024

To cite this article: M. Ertogan, and P. A. Wilson. "Modelling Using Neural Networks and Dynamic Position Control for Unmanned Underwater Vehicles." *Journal of ETA Maritime Science*, vol. 12(1), pp. 64-73, 2024.

and sliding mode control heading motion control [6], were implemented.

The feedback signals were collected in the tank tests from the sensors, a sounding altimeter, a pressure depth sensor, and an IMU, according to set values on the actuator, including the vertical and horizontal tunnel thrusters, the vertical and horizontal control surfaces as the tails, and the propeller. The input-output test data were used to form nonlinear coupled mathematical models. The models were formed in two groups: altitude-pitch and heading motion black-box models using a shallow neural network (SNN) algorithm [7]. This nonlinear coupled mathematical model was used to develop a dynamic position control design. The five actuator control signals must be calculated online by a controller system using 3D depth-pitch-heading motions for the over-actuated Delphin2.

2. Literature Review

Sensor data fusion for navigation AUVs has received much attention in the literature because their localization remains a challenge. Underwater navigation techniques most commonly employed include long baseline (LBL) with IMU, USBL, and Doppler velocity log (DVL) sensors.

Because of wall effects, USBL-based echo-sounding communication cannot be used in a tank or on a shallow coast. Therefore, rangefinder sensors, such as a laser-based vision feedback sensor, and sonar systems were used to calculate AUV's localization in a tank in the literature. With the aid of an IMU and a laser-based vision system, online localization of AUVs via Kalman filtering was established [8,9]. These tests were performed in a tank. However, the laser-based vision feedback measurement range was only approximately 30 cm, and the computer vision feedback was seldom performed. After the localization study, online identification and visual control were studied [10]. Another laser-based rangefinder study was applied in a tank, and the range was approximately 5 m [11].

The position of the AUV in artificially structured environments, such as tanks, harbors, marinas, and maritime platforms, was determined using a mechanical scanning sonar with an IMU [12]. The experimental results of the simultaneous localization and mapping measurement method are presented in this thesis. To address motion-induced distortion caused by high measurement error or lengthy scan periods, a different localization of AUV based on mechanically scanned imaging sonar was investigated [13].

For open-water applications, acoustic-based USBL and LBL communication systems are used to determine the location of AUVs. According to Plueddemann et al. [14], a comparative discussion of USBL- and LBL-based AUV navigation systems is presented, along with recommendations for the limitations of USBL regarding ice area docking and shallow coast applications. The drift in the location estimation that results from DVL-based navigation makes long-range AUV navigation over 300 m considerably more challenging. To navigate underwater, a DVL is rarely used alone; instead, it is integrated with other sound sensors [15]. According to Chen et al. [16] and Paull et al. [17], survey research was conducted to investigate the mapping, navigation, and localization of AUVs.

The accuracy of AUV localization during tank tests, for example, to verify control algorithms, is compromised by wall effects when using the USBL/LBL measurement system. Additionally, the AUV's localization range, when using eye feedback, is extremely small, as is its frequency. AUV motion drifts could be caused by dead reckoning techniques. The combination of DVL and IMU for underwater vehicles was investigated using multisensor Kalman filtering [18].

There are fewer dynamic position control studies than navigation studies on AUVs. However, there have been few experimental studies on dynamic position control. Dynamic positioning systems of remotely operated vehicles and AUVs are explained comparatively [19]. Simulation studies on dynamic position control algorithms have been conducted [20,21]. In addition, experimental data were designed and verified for the 4-DOF and 6-DOF advanced controllers of AUVs [22]. The system identification (SI) method was used with experimental data for the surge and yaw modeling of AUVs [23]. Using the USBL measurement system, we demonstrated a novel optimization-based method with simulation results for dynamically placing a fully actuated AUV [24]. The neural network model reference adaptive control serves as the dynamic loop in the proposed dynamic position approach, whereas the nonlinear MPC serves as the kinematic loop.

3. Materials and Methods

3.1. AUV Characteristics

The Delphin series for AUVs was initiated in 2007 as a collaboration between the University of Southampton and the National Oceanography Centre [1]. Delphin2 was developed as a scaled model of Autosub6000 [25]. With control surfaces and a propeller, its body is designed like a torpedo. Because of the inefficiency of these types of rear control surfaces, a typical design flaw is that the AUV is unable to maintain sufficient control at zero or slow speeds. Thus, the design is expanded to include two horizontal and two vertical thrusters. Delphin2 serves as a research platform for control system development and for studying the performance of over-actuated AUVs.

A Delphin2 AUV with actuators is shown in Figure 1. This AUV has been successfully demonstrated during hover-style motions [3,4].

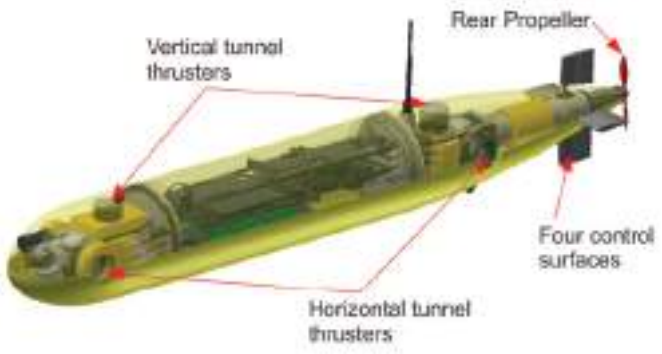

Figure 1. *Delphin2 AUV [3]*

AUV: Autonomous Underwater Vehicles

AUV Delphin2 has a mid-body diameter of 0.26 m and a length of 1.96 m, giving it a torpedo-like shape. The over-actuated Delphin2 has 7 actuators to be fully controlled. These are the propeller, the vertical and horizontal tails acting as control surfaces, the front and back vertical thrusters, and the front and rear horizontal thrusters. 3D depth-pitch-heading motion coupled control using five actuators was the focus of the research study. Consequently, it may effectively perform a range of tasks, such as survey flights at a surge speed of approximately 0-1 m/s and zero-speed hovering. In the event of a system failure, an AUV can autonomously return to the water's surface because of its small positive buoyancy. Delphin2 is typically ballasted to be buoyant at 6 N. A surge-sway motion measurement system is not present on the AUV [2].

The Delphin2 AUV has a pressure transducer rated from 0 to 5 bar to measure its depth below the free surface. For surface operation, the GPS offers a current position at a sample rate of one hertz (Hz). There is no underwater positioning option for the Delphin2 AUV. The direction and turning rate are provided at a sample rate of 20 Hz via the Xsens 4th generation MTi-30 IMU. The dynamics model is used to estimate the forward and sway velocities used in the control systems at 20 Hz to comply with the IMU. Using acoustic backscatter techniques, the altimeter and scanning-sonar track the distance between the AUV and the seabed. Delphin2 is equipped with two analog color charge-coupled device cameras, one facing ahead and the other below [2,6].

During the testing, propeller demands of uprop = {0, 10, 16, 22} were employed. These values, which roughly translate to 2.4, 4.5, and 6.15 rev/s, agree with prop. The motor control board needs these set points to operate the motor. For fully submerged operation, they roughly correspond to forward speeds of u = {0, 0.26, 0.6, 1.0} m/s or u = {0, 0.42, 0.82, 1.03} m/s for operating on the water surface. However, these speeds were calculated according to the operation time and measured distance regardless of the drifts of the Delphin2 AUV.

Accordingly, they are referred to as zero, low, mid, and high-speed cases. The thrusters function well at low and zero speeds. However, the tails work effectively at high speeds. In addition, both thrusters and tails cannot work fully effectively at mid-speeds. The effectiveness of the actuators at mid-speeds is determined with weighting functions, and the illustration is shown in Figure 2. ω_{th}, a tunnel thruster weight, and ω_{s}, a control surface tail weight.

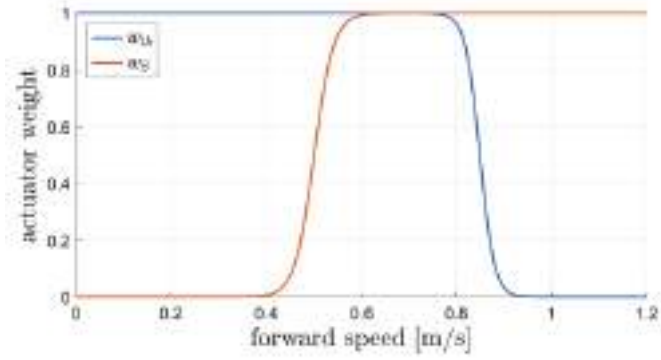

Figure 2. *Actuator weighting functions [6]*

3.2. Nonlinear Dynamic Modeling

Before control applications on the Delphin2 AUV model, dynamic modeling of the model was investigated; hence, a modeling strategywas chosen: a) nonlinear modeling is somewhat complex but might better capture actual dynamics. The coefficients can be determined using data from scaled-model testing or full-scale sea trials when the model's structure is readily accessible for the specific type of sample AUV. b) Linearized models such as state-space models or transfer functions may be adequate for the initial control design. The simplicity of these linear models is one of their advantages. However, the simulation results and actual system reactions could vary significantly.

AUV dynamics can be modeled using three different approaches: white box modeling, which employs the Navier-Stokes equations to characterize fluid structure interactions; gray box modeling, which combines experimental data with partial theoretical structures; and black box modeling, which uses only experimental data. White box modeling promises accurate predictions of AUV motions, but due to its time-consuming nature, it is not useful for control design. The term "System Identification-SI" approach refers to studies including gray and black box modeling in transdisciplinary disciplines. The SI method has proven to be very accurate

when compared with both empirical and theoretical methodologies [26]. There are few studies on AUV motion modeling using the SI technique for controller design.

The feedback signals were collected with the sensors of Delphin2, while the actuators were sending various signals in the tank experiments. These input-output data were used for nonlinear modeling of the AUV. Nonlinear coupled mathematical modeling based on the black-box model method was studied. Nonlinear depth-pitch motions and heading motions were modeled using SNNs to develop a nonlinear coupled control algorithm.

SNNs typically have fewer hidden layers, whereas deep neural networks can have dozens or even hundreds of layers. There are several layers in the network structure, including an input layer, hidden layers, and an output layer. While the hidden layer routes inputs to the output layer, the input layer handles intermediate calculations. When input values are applied, the primary goal of the network is to generate the desired output. For neural network training, the well-liked supervised learning method back propagation (BP) is propesed [27]. Due to the typical BP algorithm's slower convergence and longer training times, BP with adaptive learning rate and momentum term (BPALM) is advocated [28]. Because of the shorter training time, the BPALM, which is based on the standard BP, adjusts its learning rate and momentum rate at each iteration. Traingdx in Matlab is used to implement the BPALM method [29]. An output layer of linear neurons follows one or more hidden layers of sigmoid neurons in feedforward networks. Many layers of neurons with nonlinear transfer functions within the network enable the learning of both nonlinear and linear interactions between input and output vectors. The linear output layer indicates that the network may produce values outside the 1 to +1 range. The feedforward network models were trained using the BPALM technique [7].

In Figure 1, the actuators used as input data for modeling heading dynamics SNNs and depth-pitch dynamics SNNs are displayed. Figures 3 and 4, respectively, show the input-output data for heading dynamics and depth-pitch dynamics.

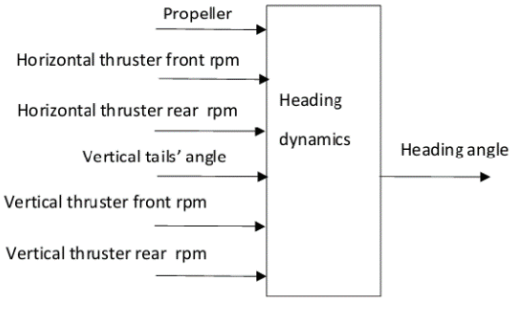

Figure 3. *Input-output data for heading dynamics*

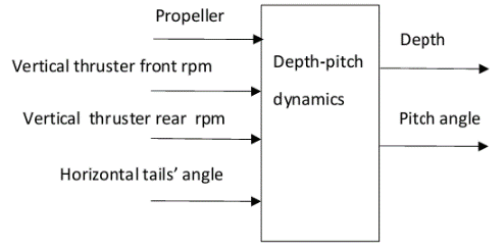

Figure 4. *Input-output data for depth-pitch dynamics*

Two datasets-training and test data-are prepared and used in SNN modeling. Test data are used to gage the model's performance after it has been developed using training data. Several acronyms of input and output data are employed in the following figures. The AUV's propulsion data are displayed as "uprop". During the testing, propeller demands of uprop = {0, 10, 16, 22} were employed. These values, which roughly translate to 2.4, 4.5, and 6.15 rev/s, agree with prop. The horizontal control surfaces as tail are abbreviated as "tailH", their unit is degree. The vertical control surfaces as tail are indicated as "tailV". The altimeter measures the vertical distance of the AUV from the tank bottom, and this distance is called the "altitude". In addition, the vertical thrusters located at the rear and front are abbreviated as "thrVrear" and "thrVfront", respectively. The horizontal thrusters located at the rear and front are shown as "thrHrear" and "thrHfront", respectively. All thrusters' units are rpm.

The experimental data used in the SNN modeling includes the depth, pitch, and heading motions of the AUV in hover- and flight-style conditions at various speeds. In addition, data on the actuators of the AUV, such as the horizontal-vertical thrusters and control surfaces (tails), were obtained. Depth-pitch motion and heading motion were modeled as decoupled. The depth-pitch and heading motion training data of the AUV given in Figures 5-11 are data of the same mission motions. In addition, the depth-pitch and heading motion validation/test data of the AUV given in Figures 6-12 are data of the same mission motions.

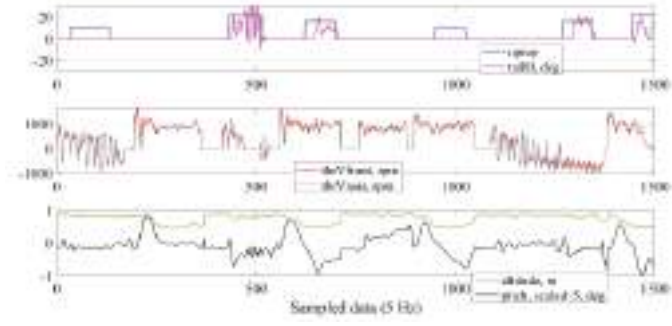

Figure 5. *SNN model training data for depth-pitch motion*

SNN: Shallow neural network

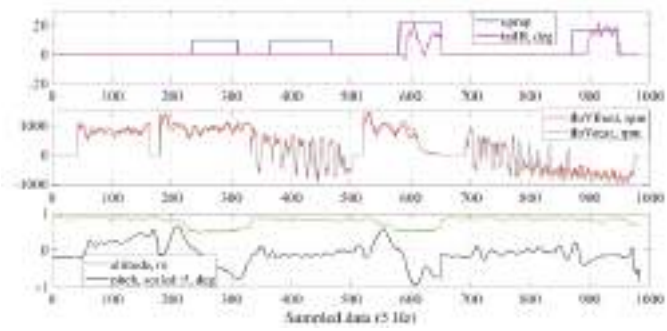

Figure 6. *SNN model test data for depth-pitch motion*

SNN: Shallow neural network

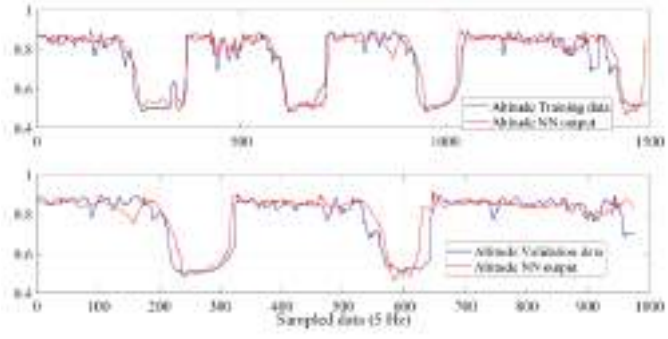

Figure 7. *Comparison between SNN output and experimental altitude data for training and validation*

SNN: Shallow neural network

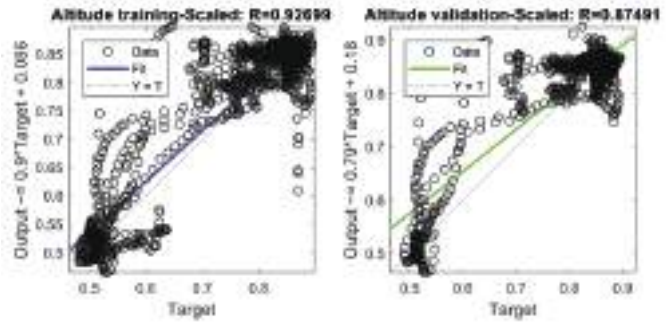

Figure 8. *Correlation coefficients, R, of NNM for training and validation altitude data*

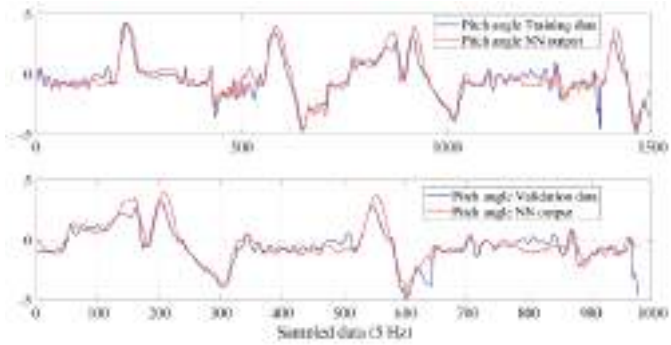

Figure 9. *Comparison between SNN output and experimental pitch data for training and validation*

SNN: Shallow neural network

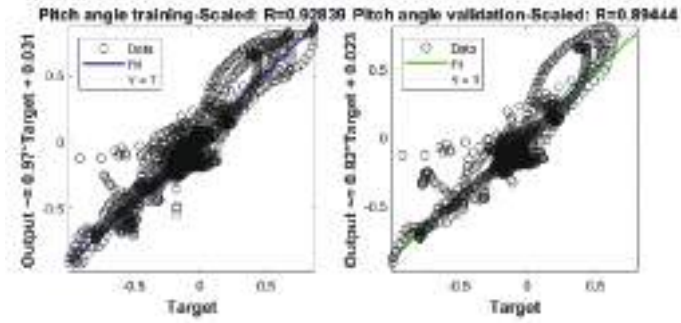

Figure 10. *Correlation coefficients, R, of the SNN model for training and validation pitch angle data*

SNN: Shallow neural network

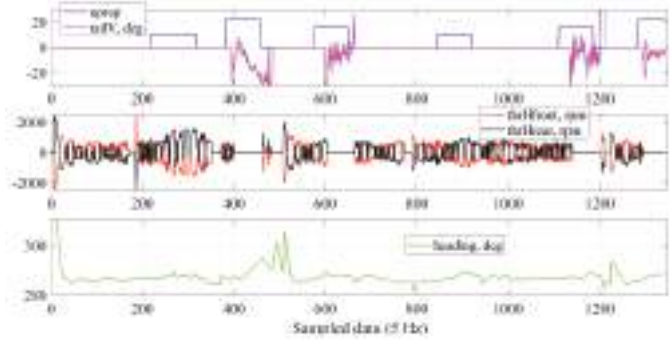

Figure 11*. SNN model training data for heading motion*

SNN: Shallow neural network

Figures 5 and 6 show the depth-pitch motion modeling training and validation/test data, respectively. If the horizontal control surface, tailH, is sent saturated limit signals, it causes large amplitudes, as seen in Figure 5, with approximately 500 sampled data.

The correlation coefficient (R-value) is used to assess the outcomes of SNN model applications created with the aid of Matlab software. The linear link between two continuous variables is measured by the R-value, which also indicates the direction of the association. The values fall between -1 and +1. This coefficient range can be interpreted as negligible if it falls between 0 and 0.09, weak if it falls between 0.1 and 0.39, moderate if it falls between 0.4 and 0.69, strong if it falls between 0.7 and 0.89, and very strong if it falls between 0.9 and 1.00 [30,31]. In the application results, the R-value is expressed as a proportional percentage.

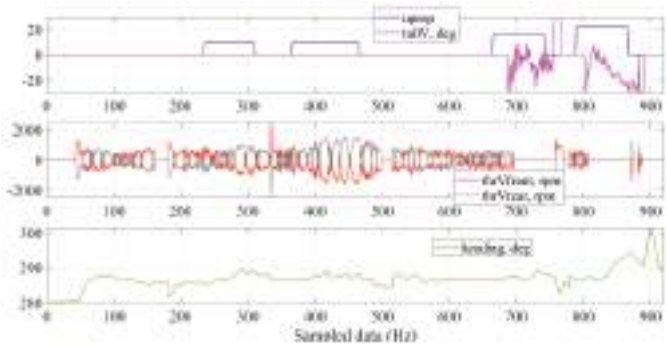

Figure 12*. SNN model validation data for heading motion*

SNN: Shallow neural network

Altitude and pitch motions of SNN depth-pitch model outputs have high R-values, approximately 90%. These comparisons between the SNN output and experimental test data and the R-values are shown in Figures 7-10.

Training and validation data for SNN heading motion modeling are given in Figures 10-12. A comparison between the SNN output and experimental heading data for training and validation is given in Figure 13. R-values, of SNN heading modeling training and validation outputs are 78% and 87%, respectively.

4. Dynamic Position Control

The PID controller is the most common type of closed-loop control system. These controllers continually monitor and modify a system's output to maintain a specified set point. The comparator loops back to the system output, y(t), and compares it to the set point, r(t), to produce the error signal, e(t)=r(t)-y(t). The closed-loop control reduces this error signal as much as possible before using it to produce the control signal u(t). The most general mathematical representation of the entire control function, Equations 1-4, can be represented as the sum of the three individual contributions [26].

$$u(t) = u_P(t) + u_I(t) + u_D(t) \quad (1)$$

$$u_P(t) = K_P * e(t) \quad (2)$$

$$u_I(t) = K_I * \int_0^t e(\tau) d\tau \quad (3)$$

$$u_D(t) = K_D * \frac{de(t)}{dt} \quad (4)$$

It is possible to find many methods in the literature regarding the adjustment of K_P, K_I, and K_D coefficients. The main adjustment method is the Ziegler-Nichols rule [32]. In practically adjusting these control coefficients, the proportional K_P coefficient should first be adjusted according to the gain rate of the system. The K_P coefficient should be increased until the response of the system reaches the reference signal. In the second step, if there is a steady-state error in the system response, the integrative K_I coefficient should be increased/decreased until this steady-state error is eliminated. However, the disadvantage of increasing the integration coefficient is that delays and oscillations in the system response increase. In the third step, the derivative K_D coefficient may need to be adjusted to optimally adjust the system response time and oscillation.

There are two operating conditions in which depth-pitch control is used. The first involves modifying the type equation using a hover-style control method (at zero speed). Using vertical thrusters, the AUV depth and pitch may be changed. The second is a flight-style control approach that uses vertical thrusters for depth control and horizontal control surfaces (tails) for pitch motion reduction control. When operating across a wide range of speeds, the horizontal aft surfaces, ω_s, and the vertical tunnel thrusters, ω_{th}, offer a transition between the two control techniques. The integration (I) coefficient was the most effective in depth control based on simulation studies. When dealing with a significant shift in depth demand, an integrator for the generalized thrust control law may grow unreasonably large while the AUV is diving. The impact of the integral windup phenomenon is minimized using a conditional integration technique. The pitch for depth for hover-style and flight-style operations, proportional (P), integral (I)-derivative (D), and PI-D controls are used. It implemented a PI-D strategy instead of a PID to avoid a spike in the derivative term when changing the demand [2,6]. The Enhanced Differentiator (ED) approach was used to differentiate between variables and error variables [33]. If the ED algorithm is used for derivation, PID control can be used.

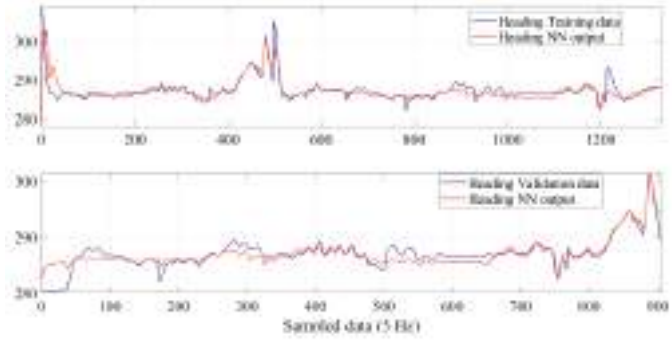

Figure 13*. Comparison between SNN output and experimental heading data for training and validation*

SNN: Shallow neural network

Due to their effectiveness and energy efficiency, the rudders (the vertical control surfaces for the Delphin2 AUV) are frequently used for heading control during high-speed operation. However, when operating in a low-speed regime where the control surfaces lose their effectiveness or when coping with significant heading mistakes, additional pressures from the horizontal tunnel thrusters are necessary. The AUV model can be maintained at the desired equilibrium with the help of the proportional (P)-derivative (D) (PD) function. Two cascade modules make up the heading control; the first module establishes a generalized moment for following heading demand, and the second module divides the generalized moment between the thrusters and rudders [34]. The horizontal thrusters and vertical control surfaces of the Delphin2 AUV model are responsible for distributing the generalized yaw moment [6]. The control signal can be applied in two ways for depth control, as Equations 5 and 6. The definitions of symbols are as follows; u_{c_total}, total control signal, u_{c_prev}, total control signal calculated one step earlier, Δu, calculated according to PD control. Conversely, u_c control signal can be calculated according to PID control.

$$u_{c\_total} = u_{c\_prev} + \Delta u \quad (5)$$

$$u_c = u_{PID} \quad (6)$$

The controller includes a two-layer PID controller so that the AUV vehicle can descend to the given reference depth while diving at zero speed, i.e., in a hover-style state. In the first layer, the total PD control signal, which calculates the total force required for the vehicle to dive to the reference depth, is calculated depending on the depth error. In the second layer, the dynamic change in the vehicle's longitudinal rotation center relative to the initial rotation center due to pitch error is calculated with PID control. Force allocation of the vertical thrusters is achieved with the PID control calculated in the second layer [6].

The control signal, according to Equation 5 and 6, was applied separately in the depth control of the AUV, while the altitude referenced 0.5 m, hover-style operation. A comparison of the two simulation results is shown in Figure 14. The result showed that the total PD control signal should be applied for depth control because when the vehicle reference altitude comes, the signal to the thrusters is not reset. The PID control signal method was applied in pitch motion control, as shown in Figure 15.

It is not possible to use the hover-style control approach at fast forward speeds. This is because as forward speed increases, thruster performance diminishes. As the AUV's speed increases, the thruster weight, w_{th}, decreases from 1 to 0. In this case, the total force calculated in the first layer required for the vehicle to dove in the hover-style condition multiplied by the thruster weight coefficient can be met by vertical thrusters in the flight-style condition. In addition, as the AUV's speed increases, the control surface, w_s, increases from 0 to 1. To calculate the horizontal control surface deflection for compensating pitch motion, the PID control equations are calculated in two layers. In the first layer calculation, the pitch bias, i.e., the reference value, is obtained by PID calculation, depending on the depth error of the vehicle. In the second layer, the deflection of the horizontal control surfaces is calculated using the PID calculation depending on the pitch error and multiplied by w_s according to the speed of the vehicle. The heading control problem includes two cascade modules. In the first module, the PID controller determines the total moment depending on the heading error. In the second module, the controller allocates the total moment between the horizontal thrusters and the vertical control surfaces based on the AUV speed. In addition, the moment sharing between front and rear horizontal thrusters should be calculated based on the changing center of rotation of the vehicle [6].

In addition, the control was applied for altitude referenced 0.5 m, flight-style operation. The control signal, according to Equation 5 and 6, was applied separately in the depth

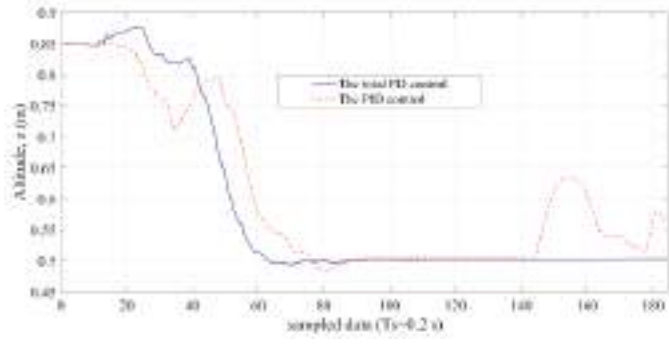

Figure 14*. Altitude outputs of the control result data during altitude referenced 0.5 m, hover-style operation*

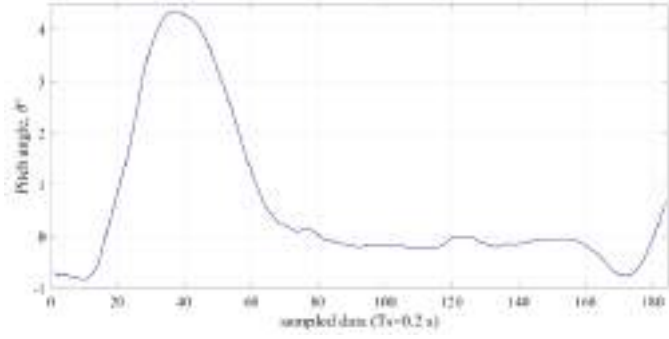

Figure 15*. Pitch angle outputs of PID control result data during altitude referenced 0.5 m, hover-style operation*

PID: Proportional integral derivative

control of the AUV, while the altitude referenced 0.5 m, flight-style operation. A comparison of the two simulation results is shown in Figure 16. The outcome demonstrated that the total PD control signal should be used for depth control because the signal to the thrusters is not reset when the vehicle reference altitude arrives, as shown in Figure 17. The PID control signal method was applied to pitch and heading motion control. The other simulation results are shown in Figures 18-20.

5. Conclusions and Proposed Methods

5.1. Conclusions

An over-actuated design enabled the AUV model to perform various missions, spanning from hover-style operation at zero or slow speeds to flight-style operation at forward speeds up to approximately 1 m/s. The current heading and turning rates were obtained from the IMU at a sample rate of 20 Hz. Surge and sway motions used in the control systems were estimated as dead reckoning using the dynamics model at 20 Hz to comply with the IMU, whereas the control systems were implemented at 5 Hz so that they could synchronize to the sensor and actuator interfacing nodes. However, the localization calculation based only on the dynamic model, without DVL measuring the speed of the AUV, caused drifts, and this case negatively affects the running control algorithms.

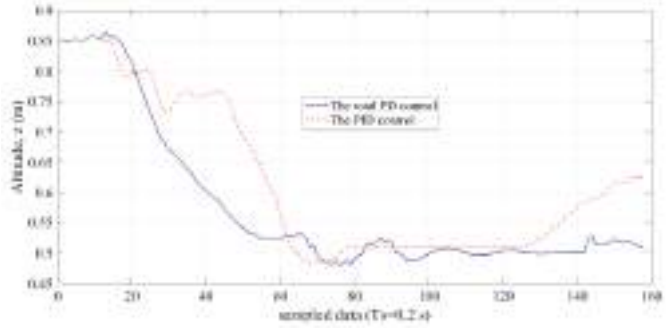

***Figure 16**. Altitude outputs of the control result data during altitude referenced 0.5 m, flight-style operation*

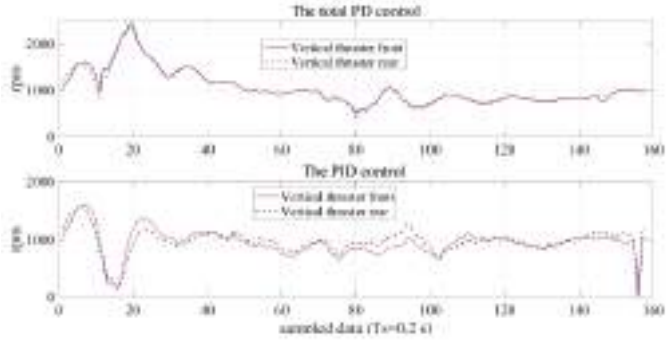

***Figure 17**. Vertical thruster front outputs of the control result data during altitude referenced 0.5 m, flight-style operation*

The depth of the AUV was measured using both an echo-sounding altimeter and a pressure sensor. The depth pressure sensor was negatively affected by the vertical tunnel thrusters, and its signal was very unstable and noisy. The altimeter output signal was more stable than the pressure depth sensor output; therefore, the altimeter output signal data were used for depth-pitch control.

The depth-pitch and PD heading motion operations were performed for each mission operation in the tank tests. Feedback signals were collected in the tank tests from

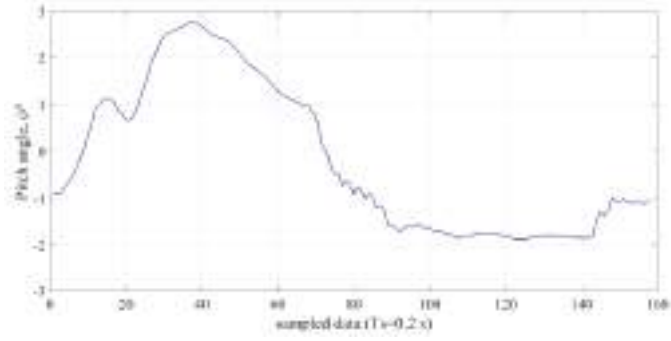

***Figure 18**. Pitch angle outputs of PID control result data during altitude referenced 0.5 m, flight-style operation*

PID: Proportional integral derivative

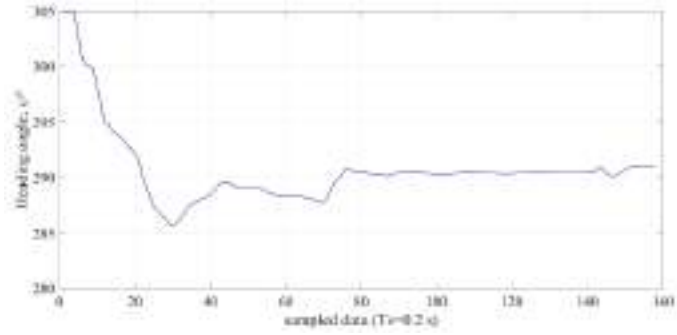

***Figure 19**. Heading angle outputs of PID control result data during altitude referenced 0.5 m, flight-style operation*

PID: Proportional integral derivative

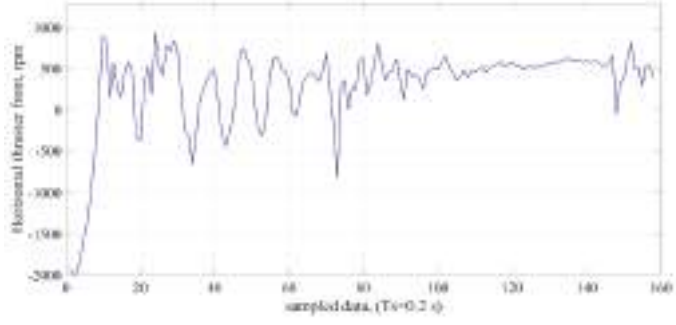

***Figure 20**. Horizontal thruster front outputs of PID control result data during altitude referenced 0.5 m, flight-style operation*

PID: Proportional integral derivative

the sensors, altimeter, pressure depth sensor, and IMU, according to set values on the actuator, including the vertical and horizontal tunnel thrusters, the vertical and horizontal control surfaces as the tails, and the propeller. The input-output test data were used to form nonlinear coupled mathematical models. The models were formed in two groups as depth-pitch motion and heading motion black-box models using the SNN algorithm. The SNN R-value, of the depth-pitch motion SNN model and the SNN R-value, of the heading motion SNN model were approximately 0.90 and 0.80, respectively. This nonlinear coupled mathematical model was used to develop the control design.

The control process was applied for altitude-referenced 0.5 m, hover-style, and flight-style operations. The control signal, according to the total PD and PID control, was applied separately in the depth control of the AUV. The outcome demonstrated that the total PD control signal should be used for depth control because the signal to the thrusters is not reset when the vehicle reference altitude arrives. The PID control signal method was applied to pitch and heading motion control. Good performance was obtained in the simulation studies. To achieve better results in every mission, there is a need to study an advanced control algorithm in the future.

5.2. Proposed Methods

The Delphin2 software's dead reckoning technique results in AUV motion drifts. The DVL/IMU measuring system can be employed because of less drift. Because of wall effects, USBL and LBL measurement equipment do not function properly in tanks. In addition, the AUV's localization range (about 30 cm) when using vision feedback from a laser and camera is relatively small.

To locate the AUV during tank testing, it has been recommended to integrate two or three echo-sounding altimeters with the IMU and a pressure depth sensor on the AUV. An AUV can measure the x- and y- axes positions when two echo-sounding altimeters are added. The frequency range of the altimeter is 1-4 Hz. If a magnetometer displays large drifts during tank tests, three-echo-sounding altimeters can also identify the yaw angle. Furthermore, DVL is more expensive than an altimeter that emits an echo [35].

In addition, an echo-sounding altimeter would be used to maintain distance control on AUVs in real-world circumstances, such as during the flight of AUVs in shallow coastal and under-ice areas, as well as during AUV docking, because the USBL measurement system might not work properly close to shore. Both stationary and moving targets might aid in avoiding AUV collisions.

Acknowledgments

The authors would like to thank Sophia SCHILLAI for her help in providing the AUV model test data.

Authorship Contributions

Concept design: M. Ertogan, Data Collection or Processing: M. Ertogan, and P. A. Wilson, Analysis or Interpretation: M. Ertogan, and P. A. Wilson, Literature Review: M. Ertogan, and P. A. Wilson, Writing, Reviewing and Editing: M. Ertogan, and P. A. Wilson.

Funding: This study was supported by The Department of Science Fellowships and Grant Programs (TÜBİTAK)-2219 International Program. Application no. 1059B191501331, ID: 841558.

References

[1] J. Liu, et al. *Design and Control of a Flight-Style AUV with Hovering Capability*: In Proceedings of the International Symposium on Unmanned Unethered Submersible Technology (UUST 2009), pages 1-9, Durham NH, USA. Autonomous Undersea Systems Institute (AUSI), 2009.

[2] A. B. Phillips, et al. "Delphin2: an over actuated autonomous underwater vehicle for manoeuvring research." *Transactions of The Royal Institution of Naval Architects Part A. International Journal of Maritime Engineering*, vol. 155, pp. 171-180, 2013.

[3] L. V. Steenson, *Experimentally Verified Model Predictive Control of a Hover-Capable AUV*. PhD thesis, University of Southampton, UK, 2013.

[4] L. V. Steenson, et al. "Model predictive control of a hybrid autonomous underwater vehicle with experimental verification," *Proceedings of the Institution of Mechanical Engineers, Part M: Journal of Engineering for the Maritime Environment*, vol. 228, pp. 166-179, Feb 2014.

[5] S. M. Schillai, S. R. Turnock, E. Rogers, and A. B. Phillips, "Evaluation of terrain collision risks for flight style autonomous underwater vehicles," *Published in: 2016 IEEE/OES Autonomous Underwater Vehicles (AUV),* Tokyo, Japan, 2016, pp. 311-318.

[6] K. Tanakitkorn, *Guidance, Control and Path Planning for Autonomous Underwater vehicles*. Ph.D. thesis, University of Southampton, UK, 2017.

[7] M. Ertogan, P. A. Wilson, G. T. Tayyar, and S. Ertugrul, "Optimal trim control of a high-speed craft by trim tabs/interceptors Part I: Pitch and surge coupled dynamic modelling using sea trial data," *Ocean Engineering*, vol. 130, pp. 300-309, Jan 2017.

[8] C. G. Karras, D. J. Panagou, and K. J. Kyriakopoulos, "Target-referenced localization of an underwater vehicle using a laser-based vision system," in *IEEE, OCEANS, Boston, MA, USA, 2006*.

[9] G. C. Karras, and K. J. Kyriakopoulos, "Localization of an underwater vehicle using an IMU and a laser-based vision system," in *IEEE, Mediterranean Conference on Control and Automation, Athens-Greece, 2007*.

[10] G. C. Karras, S. G. Loizou, and K. J. Kyriakopoulos, "Towards semi-autonomous operation of under-actuated underwater vehicles: sensor fusion, on-line identification and visual servo control." *Autonomous Robots*, vol. 31, pp. 67-86, May 2011.

[11] C. Cain, and A. Leonessa, "Laser based rangefinder for underwater applications." in *Proceedings of the American Control Conference American Control Conference, (ACC), 2012 Canada*, pp. 6190-6191, 2012.

[12] D. R. Romagos, *Underwater SLAM for structured environments using an imaging sonar*. Ph.D. thesis, Department of computer Engineering, University of Girona, Spain, 2008.

[13] A. Burguera, Y. Gonzalez, and G. Oliver, "The UspIC: performing scan matching localization using an imaging sonar," *Sensors*, vol. 12, pp. 7855-7885, Jun 2012.

[14] A. J. Plueddemann, A. L. Kukulya, R. Stokey, and L. Freitag, "Autonomous underwater vehicle operations beneath coastal sea ice," *IEEE/ASME Transactions on Mechatronics*, vol. 17, pp. 54-64, Feb 2012.

[15] D. Bandara, Z. Leong, H. Nguyen, S. Jayasinghe, and A. L. Forrest, "Technologies for underwater-ice AUV navigation." *2016 IEEE/OES, Autonomous Underwater Vehicles (AUV),* Tokyo, Japan, 2016.

[16] L. Chen, S. Wang, K. McDonald-Maier, and H. Huosheng, "Towards autonomous localization and mapping ofAUVs: a survey," *International Journal of Intelligent Unmanned Systems*, vol. 1, pp. 97-120, May 2013.

[17] L. Paull, S. Saeedi, M. Seto, and L. Howard Li, "AUV navigation and localization: a review," *IEEE Journal of Oceanic Engineering*, vol. 39, pp. 131-149, Jan 2014.

[18] C.-M. Lee, P.-M. Lee, S.-W. Hong, and S.-M. Kim, "Underwater navigation system based on inertial sensor and doppler velocity log using indirect feedback Kalman Filter," *International Journal of Offshore and Polar Engineering*, vol. 15, pp. 8895, Jun 2005.

[19] J. Davis, I. Tena, "Dynamic positioning of underwater vehicles (tethered or not)," *Dynamic Positioning Conference, Dynamic Positioning Committee, Marine Technology Society*, pp. 1-15, 2008.

[20] S. Liu, D. Wang, E. K. Poh, and Y. Wang, "Dynamic positioning of AUVs in shallow water environment: obeserver and controller design," in *Proceedings of the IEEE/ASME, International Conference on Advanced Intelligent Mechatronics, Monterey, California,* pp. 705-710, 2005.

[21] A. P. Aguiar, and A. M. Pascoal, "Dynamic positioning and way-point tracking of underactuated AUVs in the precence of ocean currents," in *Proceedings of the 41st IEEE, Conference on Decision and Control Las Vegas, Nevada USA*, pp. 2105-2110, 2002.

[22] S. Zhao, *Advanced control of autonomous underwater vehicles*, PhD thesis, The University of Hawai, USA, 2004.

[23] N. Miskovic, Z. Vukic, I. Petrovic, and M. Barisic, *Distance keeping for underwater vehicles – tuning Kalman Filters using self-oscillations,* IEEE, OCEANS 2009-EUROPE*,* 11-14 May 2009.

[24] J. Gao, C. Liu, and A. Proctor, "Nonlinear model predictive dynamic positioning control of an underwater vehicle with an onboard USBL system." *Journal of Marine Science and Technology,* vol. 21, pp. 57-69, Aug 2015.

[25] S. D. McPhail, "Autosub6000: A Deep Diving Long Range AUV," *Journal of Bionic Engineering*, vol. 6, pp. 55-62, Mar 2009.

[26] L. Ljung, *System identification: theory for the user*, Prentice Hall, Second Edition, 1999.

[27] D. E. Rumelhart, C. E. Hinton, and R. J. Williams, "Learning Internal Representations by Error Propagation," in *Parallel Distributed Processing: Explorations in the Microstructures of Cognition*, vol. 1, Cambridge, MA: MIT Press, 1986.

[28] C. C., Yu, and B. D. Liu, "A backpropagation algorithm with adaptive learning rate and momentum coefficient." in *Proceedings of the 2002 International Joint Conference on Neural Networks. IJCNN'02 (Cat. No. 02CH37290), IEEE, 2002.* vol. 2, pp. 1218-1223, 2002.

[29] H. Demuth, and M. Beale, *Neural Network Toolbox for use with Matlab*. User's Guide Version 4, 2004.

[30] M. G. Kendall, *The Advanced Theory of Statistics,* 4th Ed., Macmillan, 1979.

[31] J. Frost, *Introduction to statistics: an intuitive guide for analyzing data and unlocking discoveries*, Statistics by Jim Publishing, 2020.

[32] K. Ogata, *Modern Control Engineering*, Fifth Edition. Pearson Education, Inc., publishing as Prentice Hall, New Jersey, 2010.

[33] Y. X. Su, C. H. Zheng, P. C. Mueller, and B. Y. Duan, "A simple improved velocity estimation for low-speed regions based on position measurement only," *IEEEE Transactions on Control Systems Technology*, vol. 14, pp. 937-942, Sep 2006.

[34] T. I. Fossen, T. Johansen, "A survey of control allocation methods for ships and underwater vehicles," in *2006 14th Mediterranean Conference on Control and Automation*, IEEE, 2006, pp. 1-6.

[35] M. Ertogan, G. T. Tayyar, P. A. Wilson, and S. Ertugrul, "Marine measurement and real-time control systems with case studies," *Ocean Engineering*, vol. 159, pp. 457-469, 2018.

ORIGINAL RESEARCH (AR) DOI: 10.4274/jems.2024.97769

Journal of ETA Maritime Science 2024;12(1):74-82

Analysis of the Structure of Marine Propeller Blades for Ice Navigation

Aydın Bozkurt[1], Melek Ertogan[2]

[1]Istanbul Technical University, Graduate School of Science Engineering and Technology, Maritime Transportation Engineering Program, İstanbul, Türkiye
[2]Istanbul Technical University Faculty of Maritime, Department of Maritime Transportation and Management, İstanbul, Türkiye

Abstract

This study's analysis of the maritime propeller blade structure in ice navigation was motivated by an incident that caused the tip of a propeller blade to bend. The aim of this study was to demonstrate how the ice layer's confined space effect causes propeller blade tips to bend. Using computer-based software, a three-dimensional model of the propeller was created. The geometry of the three-dimensional propeller model was imported using the finite element approach into another piece of software. The propeller model and the environment were constructed after designing the ice environment. Using the computational fluid dynamics method, flux was calculated, and the composed pressure was derived. Following the specification of the alloy material for the propeller, the static structural module applied pressure values acquired to the propeller to measure the total deformation and stress. The data comparing the results of the simulation study are based on full-scale measurements. The maximum deformation in Ansys was 2.7-3.5 cm, whereas in the incident, it was 12 cm, which can be explained by persistent pressure or repeated initial movement steps. Considering these findings, the reason for blade tip bend, preventive measures, and recommendations have been proposed.

Keywords: Marine propeller, Ice navigation, Structure analysis, Computational fluid dynamics

1. Introduction

Shipping is a crucial component of global trade. Compared with other transportation modalities, large quantities of cargo can be transported over long distances for less money. As a result, ships travel on a variety of voyages, depending on cargo trade transactions, to practically every region of the world.

Diverse environments and locations expose ships to rare occurrences such as propeller blade deformation brought on by ice navigation. Analyses and evaluations of these unique occurrences must be disseminated throughout the maritime sector to prevent the recurrence of unfavorable effects. Propeller blade deformations, which can occur in both ducted and open-type propellers, are a significant issue for ice navigation. The cause of the blade deformations was found to be ice loads.

Hydrodynamic loads were studied on a high-density polyethylene propeller stopped by simulated ice in a cavitation tunnel. As they approached an obstacle larger than the propeller, they saw how erratic the thrust of a single blade might be, which led designers to account for impact and milling loads for strength and wear [1].

Experimental studies were conducted in a 200-mm cavitation tunnel with two open and two ducted propeller models. They studied the non-contact interaction between the propeller and ice that results in cavitation and obstruction. The ice block and propeller were subjected to a maximum pressure of 110 kPa, although this pressure was inadequate to cause the blade to deform. They claimed that cavitation was caused by decreased hydrodynamic loads, which were also ice milling loads for open-type propellers [2].

Address for Correspondence: Melek Ertogan, Istanbul Technical University Faculty of Maritime Department of Maritime Transportation and Management, İstanbul, Türkiye
E-mail: ertogan@itu.edu.tr
ORCID ID: orcid.org/0000-0002-9968-6254

Received: 13.08.2023
Last Revision Received: 05.11.2023
Accepted: 04.01.2024

To cite this article: A. Bozkurt., and M. Ertogan. "Analysis of the Structure of Marine Propeller Blades for Ice Navigation." *Journal of ETA Maritime Science*, vol. 12(1), pp. 74-82, 2024.

A process model was developed based on quasistatic contact and ignoring non-contact forces to penetrate an ice block by a propeller blade. Experimental study of leading edge machining of a large ice block. At full scale, it was claimed that sharp angles of attack caused the blades to bend backward, but the subject model did not fully consider these pressures [3].

The accumulation of total ice loads was studied, which includes separate hydrodynamic loads (cavitation-related proximity and blockage effects) and inseparable hydrodynamic loads (cavitation-related proximity and blockage effects). They used a 0.3-m diameter propeller and a "puller mode" podded propeller to analyze blade loads and cut depth. They calculated shaft thrust values for ice-related stresses using mounted dynamometers at varying cut depths [4].

Ice loads have been categorized into non-contact hydrodynamic and contact loads, focusing on open-water propulsion and ice blocks, highlighting their distinct differences [5].

The IACS Polar Class Rules (URI3) were used to optimize the strength and integrity of the polar class propellers. The study found that the out-of-plane bending moment is crucial for strength, considering spindle torque and the in-plane bending moment. The IACS found that Polar Classes 1 and 7 have equal strength requirements, and R Class propeller blades can save 1400 kg of material [6].

To simulate the propeller-ice contact at various advance coefficients, an ice block and a 2.8 m diameter, 120 rpm propeller were used. Using the ice class rule formula or the simulated model, they computed the blade ice load. The finite element method calculates propeller blade deformation based on the ice load. Advance coefficient increased blade distortion. A 6-m diameter, 0.7 EAR propeller was used to create a finite element method model for ice contact issues [7].

The transient propeller-ice block interaction in an ice milling scenario was modeled using peridynamics techniques. Their findings that the maximum force equals 9216.99 kN and the maximum moment equals 6007.40 kN m indicate that applied forces in the x-axis are the source of blade bending stress. For accurate numerical modeling, further investigation is advised [8].

The overlapping grids approach and CFD were used to predict the flow parameters and hydrodynamic performance of an ice-class propeller in the event of ice blockage. They used an ice block with dimensions of length: 200 mm, width: 200 mm, and height: 40 mm to test an ice-class 1 propeller with four blades and a diameter of 20 cm. The experimental test revealed a five percent difference in pressure, coefficients of thrust, and torque when the blade and ice block distance was less than 10% R. However, because of the rudder frame, keel, stern tube, and bottom of the aft hull body, finding an ice block smaller than 10% R is challenging [9].

CFD was utilized, and an overlap grid approach was used to analyze the exciting force generated by the propeller during ice block cutting. They found pressure variations in the P1 and P4 regions of a four-blade propeller and emphasized the three-stage decline caused by the interval between blade entry and ice block entry [10].

Five load scenarios were applied to the tip and furthest edges of a PC3 ice-class propeller, adhering to the IACS URI3 norm. They obtained stress and deformation values, developed a minimum safety factor of 1.5, and advised ice-class propellers to use this strength assessment approach during the design phase [11].

The hydrodynamic performance of a propeller was studied in a ship-model towing tank by adjusting the amount, size, and axial placement of synthetic ice. They used particle image velocimetry (PIV) to analyze the obstructed flow field of the propeller. This study discovered that thrust and efficiency are highly dependent on the model ice thickness. The torque and progress coefficients are negatively correlated with ice thickness. With constant advance coefficients, wider ice models have a greater impact on thrust and torque. Propeller efficiency is unaffected when the ice model width is greater than the propeller diamete. The PIV approach showed that the inflow velocity was lower than that in open water [12].

In ice-covered waters, the accelerating effect of the spinning propeller on brash ice is critical for a polar ship to break free of the ice. A new coupling model that uses computational fluid dynamics (CFD) and the discrete element method (DEM) is proposed to investigate brash ice loads and pressure fluctuations. The simulation results show that multiple peaks are caused by a low reversing speed, which accelerates and reduces ice loads. For optimal acceleration and pumping effects during moderate-speed reversals, fortifying the stern structure is advised [13].

Predicting self-propulsion performance is an important matter, and the brash ice channel is a crucial topic for polar ships. Using the CFD-DEM coupling approach, the propeller's hydrodynamic performance was simulated and the ice load was calculated. The simulation results accurately replicate the ship-ice and propeller-ice interaction processes, offering a technical tool for hull line building and navigation guidance in brash ice channels [14].

The Canadian Coast Guard investigated the connection between sea ice conditions and ice-induced propeller loads

in a study on ship operations in ice-covered seas. Using the Henry Larsen icebreaker as a case study, numerical analysis and experimental data were used to predict ice-induced impact loads on the propeller. The results showed considerable torque response values even in thin ice [15].

The safe and efficient operation of the Baltic Sea's winter navigation system is the aim of the Finnish-Swedish Ice Class Rules. In brash ice channels, vessel resistance is predicted using model-scale experiments. However, there are restrictions on the current norms. This study uses both full-scale and model-scale measurements to investigate the relationship between vessel resistance and brash ice qualities. For all hull forms, accurate modeling of the interaction between ice fragments enhances prediction quality [16].

The Baltic Sea is an area where ship performance is critical because different ice thicknesses have an impact on maneuverability and speed. Proposals have been made for numerical simulation techniques to improve accuracy and analyze complex operations. This research focuses on ship– ice interaction and proposed a framework for creating effective models. A prototype model is created, and its validity as a prototype is shown by contrasting simulation results with full-scale measurements [17].

This work analyzes numerical simulation approaches for ice tanks, dividing them into cohesive elements, discrete elements, lattice Boltzmann, smoothed particle hydrodynamics peridynamics and smoothed particle hydrodynamics. It assesses their effectiveness, precision, and usefulness in scenarios involving ship-ice contact. This study underlines the difficulties with current numerical techniques and stresses the significance of multidisciplinary applications in fluid-structure interactions [18].

Nearly all research concentrated on the contact load of ice, which was characterized as ice milling, impact, or contact of ice masses, and attempted to explain propeller blade deformation using various techniques, including ice tanks and cavitation tunnels. This study aims to demonstrate that the limited space impact of the ice layer causes propeller blade tips to bend in addition to the contact stresses of ice assumptions. If the ice layer is sufficiently thick and the suction side is not broken during the first part of the power-driven motion of the vessel, the tips of the propeller blades are bent until the ice layer breaks. It creates the illusion of an impermeable wall.

1.1. Investigate Investigating Propeller Blade Bent Incident in Iced North China Sea

Ice milling and ice block impact create contact stresses on the blades, causing permanent bends. The incident lacks indications of an ice milling groove, and the thinnest areas of blade tips and edges should also be deformed or have an ice milling groove. The blades should show impact indicators while assessing the impact of ice chunks. However, the bulb of a ship penetrates the ice as it moves forward, causing the bow to chisel out a split-like channel. Because the ship is 230 m long, it is above the ice layer and ice blocks aft of the ship, and big chunks of ice float instead of being dragged below. It is impossible to conclude that ice block contact or ice milling recess are the main causes of blade deformations in ice navigation because ducted propellers can also fail because of blade deformation.

Ice loads are non-contact loads that are too close to ice blocks, causing obstruction and ice milling. Ice block collisions or milling are likely to happen when traveling quickly and there is less than ten percent of the propeller's radius between it and the ice block. The rudder frame and stern tube, keel, and rear bottom hull shape prevent approaches to ice blocks with a diameter equal to that of the propeller.

The goal of this study is to demonstrate how the restricted space effect of the ice layer causes propeller blade tips to bend. If the ice layer is sufficiently thick and the suction side is not broken during the first part of the power-driven motion of the vessel, the tips of the propeller blades are bent until the ice layer breaks. It creates the illusion of an impermeable wall. Examine the propeller blade tip bend based on an incidence and use the inductive method to make generalizations. Full-scale measurements served as the basis for the data used to compare the outcomes of the simulation study. By the time this study is complete, a new word for the thick ice layer's enclosed space effect has been added to the literature.

This study investigates a propeller blade tip bend on a 230 m long bulk carrier in Liaodong Bay, North China Sea, and Bayuquan Port in January 2013. The enclosed space effect of the thick ice layer can cause of blade deformations.

The inductive technique was used to investigate the incident-based propeller blade tip bend in a range of propeller designs, including fixed-pitch, right-handed, four-bladed, low-skewed copper alloy (Cu 3) propellers. Despite the possibility of modeling a large variety of habitats, the study only supported astern propeller motion in a limited subset of environments.

2. Technical Details and a Description of the Incident

2.1. Description of the Incident

In January 2013, a Panamax ship encountered ice cover in Liaodong Bay, North China, as shown in Figures 1 and 2. The master advised dropping the anchor and reporting the

suspension to the Bayuquan Port Authority. The ice covering was 20-25 cm deep. The port authority instructed the ship to move forward to the pilot station, but the sea surface remained covered in ice, as shown in Figure 3. Despite pulling four tugs, the vessel could not reach the wharf for four hours due to ice masses re-accumulating.

Figure 1. *Bayuquan Port, Liaodong Bay, North China*

Figure 2. *The roads around Bayuquan Port are covered in ice*

Figure 3. *Aft view of the Panamax ship at Bayuquan Port*

The ship, with a single main engine and fixed-pitch propeller, was moving around 25-30 m to the rear. With the help of a pilot and tugs, the ship was propelled backward. During the growth and freezing of the ice cover, the ship departed the quay with 2 pilots and 2 tugs. The master issued stern engine directives to leave the basin because of depth restrictions, but the engine's rpm did not rise quickly.

The ship's main engine is a four-bladed, right-handed engine with a fixed-pitch propeller. She was driven backward after loading the cargo. The ice covering broke, and the ship departed the wharf with 2 tugs and a pilot. The ship had a draft of 11.2 meters and approached from the basin's starboard side. Due to a basin depth restriction, the master left the berth using the astern engine directives. The ship was issued a dead slow forward command, but the engine's rpm did not rise quickly.

The ship's engine's rpm increased slowly and did not reach the desired level during its voyage. Initially, propeller fouling was suspected, but the outcome was negative. The ship was headed to Quanzhou, China, to load cargo. A diver survey of the propellers was conducted, but no irregularities were found. Singapore was the next stop for bunkering, and the shipyard service engineer was scheduled to visit. Upon landing, underwater inspection of the hull, propeller, and rudder was conducted, but no abnormal findings were found. The ship dropped anchor in Singapore to allow for more inspections. The diver requested a new survey of the propeller once more. Decided to measure the horizontal distance from the rudder frame to the propeller blades. Measurements showed that the tips of the propeller blades were bent. There were no signs of a likely significant impact.

2.2. Propeller Technical Information

The horizontal distances between each blade and rudder frame were measured by the divers in the Singapore AEBB anchoring area from four different locations, as shown in Figure 4. The horizontal distances between the rudder frame and the reference locations B, C, and D on each blade are the same. The horizontal length varies only at points A, 30 cm within the tip ends [19].

The horizontal distances of blades "1", "2", "3", and "4" from point A to the rudder frame were 272, 264, 265, and 260 cm, respectively.

According to the final diver report, all blade tips-aside from "1"-were bent between 7 and 12 cm toward the pressure side or the stern side of the ship.

Bulk Carrier, Panamax, 80,370 DWT, has one main engine and a fixed four-blade propeller. The main engine's maximum continuous output is 11,060 kW, and the maximum

revolution per minute is 127 rpm. The propeller's diameter, pitch at 0.7R, expanded area, skew are D:6.2 m, $P_{0.7}$:4.1362, A_e:15.548 m^2, and SK:23.856 deg, respectively. The other specifications are given in Table 1 [20].

3. Methodology of the Research

The ice propellers can be impacted by both non-contact (hydrodynamic) and contact (ice) loads. In this instance, the hydrodynamic tension on the blade serves as the non-contact load for propulsion in open water. The primary source of contact load is the ice load generated by the impact and ice milling processes. These non-contact and contact loads are very different from each other.

The literature employed a variety of methods to explain the deformation of propeller blades, including discrete, finite, and cohesive element methods, smoothed particle hydrodynamics, peridynamics lattice Boltzmann, and coupled models. The majority of these studies concentrated on the contact load of ice, which was defined as ice milling, impact, or contact of ice masses. Nevertheless, there was no indication of a likely significant impact on the propeller in the event involving the Panamax vessel, which lacks an ice-class propeller. Measurements showed that the tips of the propeller blades were bent. For comparison with the actual data, the widely used CFD method was chosen because the experienced scenario is not typical.

Three-dimensional propeller models were created using Solidworks and Rhinocerossoftware. A commercial tool called Rhinoceros is used for 3D graphics and computer-aided design (CAD). Software for CA engineering and CAD that models solids is called SolidWorks.

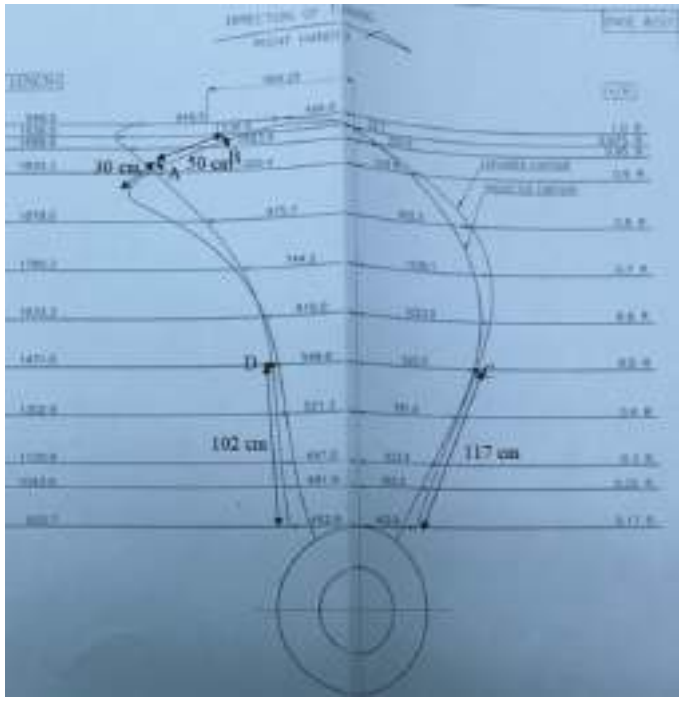

Figure 4. *Propeller blade measurement [20]*

Engineers simulate interactions in every branch of physics, including vibration, fluid dynamics, and structural analysis, using the general-purpose software Ansys. The unstable Navier-Stokes equations in their conservation form are the set of equations that ANSYS CFX has solved. A chart of the computation operation steps is shown in Figure 5.

A stationary frame can be used to depict the instantaneous equations for mass, momentum, and energy conservation (ANSYS CFX-Solver Theory Guide, November 2009, s.18). The symbols are shown in Table 2. The continuity equation is given by equation (1). The momentum equations are obtained from Equations (2) and (3). If there is a connection between the strain rate and the stress tensor, τ.

Table 1. *Propeller specifications*

Technical Specifications of the Propeller	
Diameter	D=6.200 m
Pitch at 0.7 R	$P_{0.7}$=4.1362 m
Pitch ratio at 0.7 R	$P_{0.7}$/D= 0.6671
Mean pitch	P_{MEAN}=3.9370 m
Number of blades	Z=4 EA
Expanded area	A_e=15.548 m^2
Expanded area ratio	A_e/A_o= 0.515
Boss ratio	D_{hub}/D=15.548 m^2
Rake	RK=0.0 Deg
Skew	SK=23.856 Deg
Turning direction	Right Handed (Looking from stern)
Material	Ni-Al-Br (CU3)
Section	KH 40
Propeller weight	abt. 17.590 kg
M.O.I in water	abt. 394.340 kg cm s^2
St/Point	454.9 KN
Push up 0 °C	11.98 mm
Push up 35 °C	10.10 mm
Type of ship	Bulk Carrier, Panamax, 80370 dwt
Produced by	Silla Metal Co., Ltd. Drawing No: 09-P-22
Production date	14.05.2010
Approved by	Lloyd's Register (LR BUS1002132)

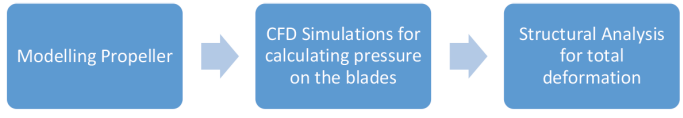

Figure 5. *Operation steps of the computations*

$$\frac{\partial \rho}{\partial t} + \nabla \cdot (\rho U) = 0 \quad (1)$$

$$\frac{\partial (\rho U)}{\partial t} + \nabla \cdot (\rho U \otimes U) = -\nabla p + \nabla \cdot \tau + S_M \quad (2)$$

$$\tau = \mu \left(\nabla U + (\nabla U)^T - \frac{2}{3} \delta \nabla \cdot U \right) \quad (3)$$

The total energy equation is written as Equations (4) and (5). where the static enthalpy, h (T,p), is related to the total enthalpy, h_{tot}. The term $\nabla \cdot (U \cdot \tau)$ stands for work caused by viscous strains and is referred to as the viscous work term. The term $U \cdot S_M$, which is currently underutilized, denotes work resulting from external momentum sources.

$$\frac{\partial (\rho h_{tot})}{\partial t} - \frac{\partial p}{\partial t} + \nabla \cdot \left(\rho U h_{tot} \right) = \nabla \cdot (\lambda \nabla T) + \nabla \cdot (U \cdot \tau) + U \cdot S_M + S_E \quad (4)$$

$$h_{tot} = h + \frac{1}{2} U^2 \quad (5)$$

4. Propeller Modeling and Simulation Studies

Three-dimensional modeling of the propeller was performed in accordance with the data from the offset table and propeller sketch [19]. A 3D model of a propeller covered with a frozen shroud was imported into Ansys. The seawater had a depth of 12 m at the time of the incident. As a result, the surrounding environment is defined as a limited zone with a depth of 12 m and a length of 10 m, and the shroud is placed close to the boundary. The geometry of the propeller and shroud and the confined space scenario are shown in Figures 6a and 6b, respectively.

The frozen shroud and propeller were meshed using the following parameters (Physics Reference: CFD, Solver Preference: CFX, Element Order: Linear, Element Size: 9,8,7 cm). With a maximum of 5 layers and a growth rate of 1.2, the mesh's inflation parameters were changed to produce a smooth transition.

Table 2. *The Symbols*

Symbols	
ρ	Density
U	Vector of velocity
p	Pressure
τ	Shear stress, subgrid scale stress, molecular stress tensor
S_M	Momentum source
μ	Molecular (dynamic) viscosity
T	Temperature
δ	Identity matrix or the Kronecker Delta function
h_{tot}	Specific total enthalpy
λ	Thermal conductivity
S_ε	Energy source
h	Specific enthalpy

The settings for a constrained environment were merged (Physics Reference: CFD, Solver Preference: CFX, Element Order: Linear, Element Size: 50, 40, 30 cm). The limited space/shroud boundary size settings were changed to match the size of the shroud element. The following three meshing combinations were tried in order: 9, 8, 7 cm for the shroud element and 50, 40, 30 cm for the restricted space element. Figure 7 displays the mesh modeling of the propeller and shroud. In addition, Figure 8 shows the meshed constrained environment.

Impermeable walls are those found in limited environments, such as the seabed at the bottom and the ice layer at the top. Since it is believed that a revolving propeller cannot initially shatter the ice layer, the ice layer is a wall. The propeller's far parallel plane is known as the inlet, while its opposite plane is known as the outlet. The remaining planes fall within the category of openings. The CFD model of the propeller is shown in Figure 9. The propeller speed is adjustable to three distinct values: 55, 65, and 75 rpm. Seawater having a density of 1 t/m^3 is defined as a flowing substance. The root mean square (RMS), 0.0001, is used as the convergence criterion for the residual target value. Iterations are limited to 800.

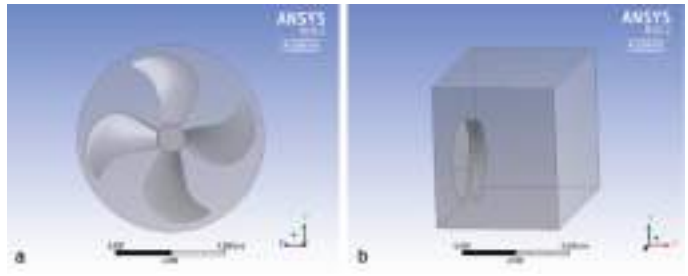

Figure 6. *a) Geometry of the propeller and shroud. b) The confined space scenario*

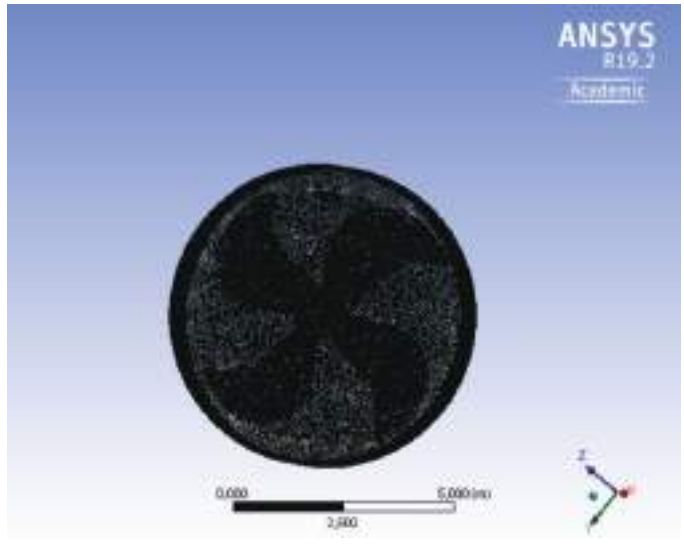

Figure 7. *Meshed modeling of the propeller and shroud*

The CFD solver finished in an auto period of 0.0146912 s, or approximately 9.08 s, at the 618th iteration. ANSYS (2019) claims that while CFX-Solver iteratively approaches the solution, it under-reaches the equations for steady-state scenarios. Using shorter timeframes and under-relaxing limits the amount that the variables vary between iterations. Pressure values were obtained using the CFX Solver (suction side view) at 65 rpm and a 9 cm mesh element size, as shown in Figure 10. Pressure values were obtained using the CFX Solver and a mesh element size of 9 cm for the pressure side view, as shown in Figure 11. Specifications for the propeller alloy material (Cu 3) according to the load register material requirements.

Then, to observe the deformations, the propeller was meshed with elements that were 1 cm smaller than the fixed propeller. Propeller blades that are bent beyond the point of permanent deformation will lose their flexibility due to Push Up, which is 11.98 mm at 0 °C. The pressure values from the CFX Solver were then applied to the propeller in the static structural module. The results of pressure applications of 200,000, 250,000, 300,000, and 350,000 Pascal to normal propeller surfaces were calculated as 1.8207, 2.2758, 2.7310, and 3.1862 cm total deformation, respectively.

Figure 12 illustrates the resulting static structural deformation at 8 cm mesh element size. The blade tip exhibited a maximum deformation of approximately 2.7 cm, as shown in Figure 12.

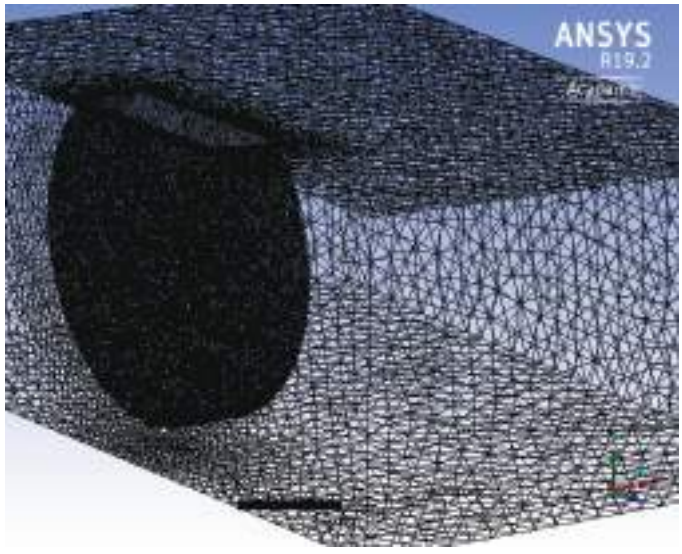

Figure 8. *Meshed confined environment*

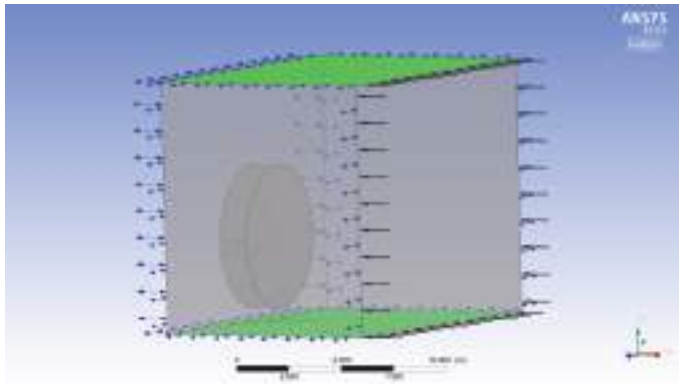

Figure 9. *Walls (green) and openings (gray) in a confined space*

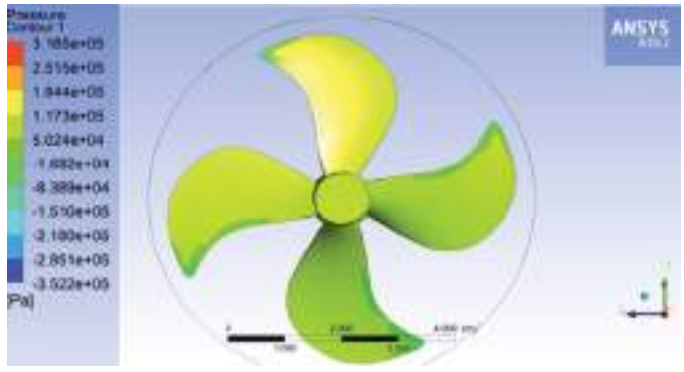

Figure 10. *Pressure values were obtained using the CFX Solver (suction side view) at 65 rpm and a 9 cm mesh element size*

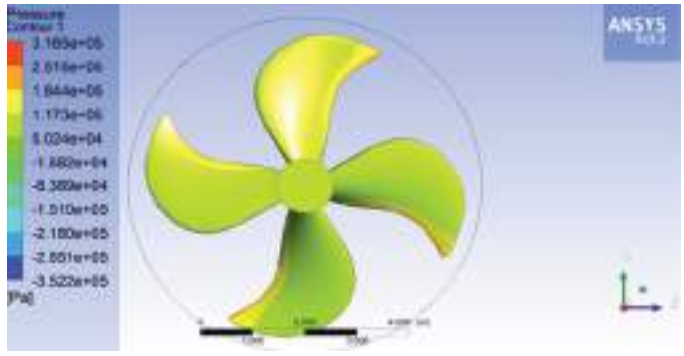

Figure 11*. Pressure values were obtained using the CFX Solver with a mesh element size of 9 cm for the pressure side view*

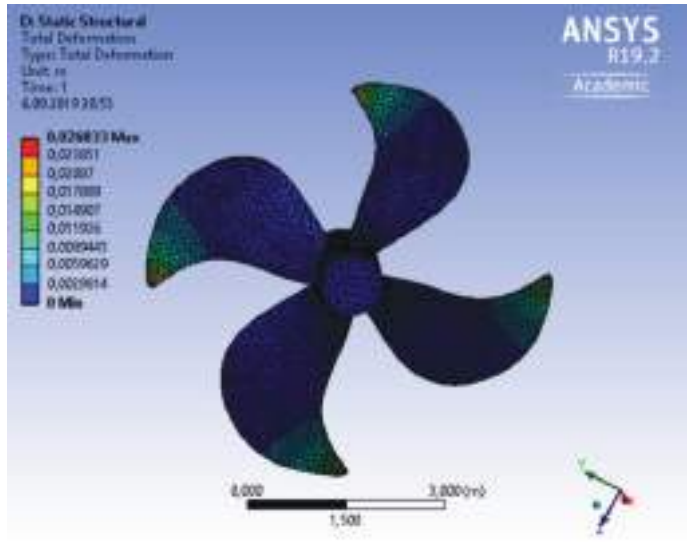

Figure 12*. At 8 cm mesh element size, there is a resultant static structural deformation*

The highest deformation, however, in a static structural module with a 1 cm mesh element size was 2.4704 cm; nonetheless, the black mesh in Figure 12 made it difficult to distinguish the colors of the deformation. Consequently, 8 cm mesh elements were chosen. The difference in mesh element size between 1 cm and 8 cm in the static structural module was only 2.13 mm. The diver's final report stated that the highest measured distortion was around 12 cm. Variations may be attributed to longer exposure periods or different exposure phases to the ice load. It takes less force to bend the blade tip farther once it has been permanently bent.

At various revolutions, the CFX pressure and deformation are produced, as given in Table 3. The study was undertaken to determine the CFX pressure in open water under towage conditions with a propeller turning astern at 65 rpm and the ship's speed at 0 knot. Near the tip, there was just one spot point with a pressure range of 152600 to 218300 Pa. 86920 to 152600 Pa was the pressure range between the nearest line and the trailing edge's tip (the leading edge in astern motion) was 86920 to 152600 Pa. The remaining propeller blades experienced pressures lower than 86920. It can be shown that propellers are typically designed for forward motion when equivalent forward and astern speeds are considered at the same rotation. Therefore, the towage pressure result from the CFX Solver was considered to be normal.

5. Conclusions and Recommendations

This study investigated a marine incident that resulted in a bent propeller blade tip. A vessel vibrated when its tips bent, directing pressurized propeller water toward the aft of the hull. Furthermore, rising exhaust temperatures and increased fuel consumption of the main engine were observed, and the engine's revolution could not be adjusted to match the ship's entire rotation. For normal maintenance of the main engine, 2% of the propeller tips were removed. The tips of the propeller blades were then correctly fixed by welding at the right time and place for propeller condition alignment, which required significant financial and labor investment.

This study aimed to demonstrate that, in addition to the ice contact load assumptions, the subject incident's propeller blade tips bent due to the ice layer's restricted space impact. This study only examined fixed-pitch, right-handed, four-bladed, low-skewed copper alloy (Cu3) propellers, despite the wide variety of propeller types. The primary emphasis of this study was the propeller's astern motion in a constrained environment.

A 12-m-deep enclosed enclosure for the surrounding environment was created by Ansyssliding mesh inserted in a 3D propeller model with a surrounding frozen shroud. The LR material requirements were followed in defining the propeller alloy material (Cu3) parameters.

The following three meshing combinations were conducted in order: 9, 8, and 7 cm for the propeller and frozen shroud element, and 50, 40, and 30 cm for the element in the constrained environment.

The top plane (the ice layer) and bottom plane (the seafloor) of the confined environment are defined by the impermeable wall. The ice coating is believed to function as a wall because the propeller revolves and cannot initially break through it while moving. The opposite plane is designated as the outlet, and the plane far parallel to the propeller is the inlet. The remaining planes are designated as openings. Three distinct propeller rotation values were set: 55, 65, and 75 rpm.

For the residual target value, the convergence criterion was set at 0.0001 RMS. Maximum iteration set to 800. Pressure values from the CFX Solver were then applied to the propeller in the static structural module.

According to the propeller manufacturer's statement, the push-up measures 11.98 mm at 0 °C. This claimed that the propeller blade will become less flexible and undergo irreversible deformation if it is bent by more than 11.98 mm at 0 °C.

The location of the bent at the tip and the blade tip bent area percentage ratio 2% are consistent with the Ansys results. The propeller's rotation can be used to explain the deformation of the three blades. While rotating, the propeller is subjected to high pressure; however, with the Ansys program, the propeller only experiences pressure when it is fixed. The maximum deformation in Ansys was 2.7-3.5 cm, whereas in the incident, it was 12 cm. Longer exposure times or sequential phases in the exposure of the ice load can account for this difference. More deformation can be achieved with less force once the blade tip is permanently bent.

Table 3. *At various revolutions, the CFX pressure and deformation are calculated*

Revolution (rpm)	55			65			75		
Mesh element size (cm)	7	8	9	7	8	9	7	8	9
Maximum pressure (Pascal)	2.603e+05	2.650e+05	2.578e+05	3.234e+05	3.300e+05	3.185e+05	3.980e+05	4.067e+05	3.906e+05
Total deformation (cm)	1.8660	1.8262	1.7842	2.6069	2.5517	2.4704	3.4703	3.3922	3.2825

If the ice layer is sufficiently thick and its suction side is not broken at the start of the vessel's power-driven motion, this leads to an impermeable wall effect that generates pressure and bends the propeller blade until the ice layer is broken.

It must be ensured that a tug or icebreaker breaks the propeller suction side of the ice layer to prevent bent blades. Even a small trail will be sufficient to release the pressure. When the ship accelerates, its displacement (mass) will be sufficient to break the ice.

In addition, placing high-pressure sensors near the propeller at the bottom of the hull can be advised. These sensors will turn off the main engine when the high-pressure level is set. The Polar Code can analyze ice-class propellers using this form of enclosed space modeling if it receives approval from IACS. Nonetheless, further materials science research can be conducted to investigate the use of stronger, more resilient materials because the tips and edges of a blade are by nature their thinnest parts.

Acknowledgments

The authors would like to thank Dr. Metin Aytekin Demir who supported them with his kind assistance in this study.

Authorship Contributions

Concept design: M. Ertogan, Data Collection or Processing: A. Bozkurt, Analysis or Interpretation: M. Ertogan, and A. Bozkurt, Literature Review: A. Bozkurt, Writing, Reviewing and Editing: M. Ertogan, and A. Bozkurt.

Funding: The authors received no financial support for the research, authorship, and/or publication of this article.

References

[1] D. Walker, N. Bose, H. Yamaguchi, and S. J. Jones, "Hydrodynamic loads on ice-class propellers during propeller-ice interaction." *Journal of Marine Science and Technology,* vol. 2, pp. 12-20, Mar 1997.

[2] D. L. N. Walker, *The influence of blockage and cavitation on the hydrodynamic performance of ice class propellers in blocked flow*. Memorial University of Newfoundland, 1996.

[3] H. Soininen, *A propeller-ice contact model.* VTT Technical Research Centre of Finland, VTT Publications 343, 1998.

[4] J. Wang, et al. "Ice loads acting on a model podded propeller blade." *Journal of Offshore Mechanics and Arctic Engineering,* vol. 129, pp. 236-244, Aug 2007.

[5] S. K. Lee, "Engineering practice on ice propeller strength assessment based on IACS polar ice rule-URI3." *ABS Technical Papers,* 2007.

[6] P. Liu, N. Bose, and B. Veith, "Evaluation, design and optimization for strength and integrity of polar class propellers" *Elsevier Cold Regions Science and Technology,* vol. 113, pp. 31-39, May 2015.

[7] A. Kinnunen, V. Lamsa, P. Koskinen, M. Jussila, and T. Turunen, "Marine propeller-ice interaction simulation and blade flexibility effect on contact load" in *Proceedings of the 23rd International Conference on Port and Ocean Engineering under Arctic Conditions, Trondheim, Norway,* June 14-18, 2015.

[8] L. Y. Ye, and C. Wang, "Propeller-ice contact modeling with peridynamics." *Ocean Engineering,* vol. 139, pp. 54-64, Jul 2017.

[9] W. Chao, S. Sheng-Xia, C. Xin, and Y. Li-yu, "Numerical simulation of hydrodynamic performance of ice class propeller in blocked flow–using overlapping grids method." *Ocean Engineering,* vol. 141 pp. 418-426, Sep 2017.

[10] C. Wang, X. Li, X. Chang, and W. P. Xiong, "Numerical simulation of propeller exciting force induced by milling-shape ice." *International Journal of Naval Architecture and Ocean Engineering,* vol. 11, pp. 294-306, Jan 2019.

[11] L. Y. Ye, C. Y. Guo, C. Wang, C. H. Wang, and X. Chang, "Strength assessment method of ice-class propeller under the design ice load condition." *International Journal of Naval Architecture and Ocean Engineering* vol. 11, pp. 542-552, Jan 2019.

[12] C. Y. Guo, P. Xu, C. Wang, and W. P. Xiong, "Experimental investigation of the effect of ice blockage on propeller hydrodynamic performance." *Hindawi Mathematical Problems in Engineering,* vol. 2019, pp. 1-19.

[13] L. Zhou, S. Zheng, S. Ding, C. Xie, and R. Liu, "Influence of propeller on brah ice loads and pressure fluctuation for a reversing polar ship" *Ocean Engineering*, vol. 280, pp. 114624, 2023.

[14] C. Xie, L. Zhou, S. Ding, R. Liu, and S. Zheng, "Experimental and numerical investigation on self-propulsion performance of polar merchant ship in brash ice channel" *Ocean Engineering*, vol. 269, pp. 113424, Feb 2023.

[15] A. Zambon, L. Moro, A. Kennedy, and D. Oldford, "Torsional vibrations of Polar-Class shaftlines: Correlating ice–propeller interaction torque to sea ice thickness*" Ocean Engineering*, vol. 267, pp. 113250, Jan 2023.

[16] R. Matala, and M. Suominen, "Investigation of vessel resistance in model scale brash ice channels and comparison to full scale tests" *Cold Regions Science and Technology*, vol. 201, pp. 103617, Sep 2022.

[17] F. Li, F. Goerlandt, and P. Kujala, "Numerical simulation of ship performance in level ice: A framework and a model" *Applied Ocean Research*, vol. 102, pp. 102288, Sep 2020.

[18] Y. Xue, R. Liu, Z. Li, and D. Han, "A review for numerical simulation methods of ship–ice interaction" *Ocean Engineering*, vol. 215, pp 107853, Nov 2020.

[19] A. Bozkurt, *Marine Propeller Blade Structure Analysis in Ice Navigation*. ITU Graduate School of Science Engineering and Technology, Maritime Transportation Engineering Program, September 2019.

[20] J. Y. Lee, Sil La Metal Co., Ltd. Propeller drawing, (Drawing No: 09-P-22), September 2010.

Journal of ETA Maritime Science 2024;12(1):83-91

Model Validation and Hydrodynamic Performance of an Oscillating Buoy Wave Energy Converter

Giri Ram[1], Mohd Rashdan Saad[1], Noh Zainal Abidin[2], Mohd Rosdzimin Abdul Rahman[1]

[1]Universiti Pertahanan Nasional Malaysia, Faculty of Engineering, Department of Mechanical Engineering, Kuala Lumpur, Malaysia
[2]Universiti Pertahanan Nasional Malaysia, Faculty of Defence Science and Technology, Department of Science and Maritime Technology, Kuala Lumpur, Malaysia

Abstract

An oscillating buoy (OB) could function simultaneously as a wave energy converter and a breakwater. In this work, a numerical study is conducted to assess the ability of the buoy to perform both aforementioned tasks by quantitatively and qualitatively assessing its hydrodynamic performance. The computational fluid dynamics solver used for the numerical study is ANSYS Fluent, which uses Reynolds-averaged Navier-Stokes equations and Volume of Fluid method for the design and simulation of the numerical model, which consists of a rectangular OB that floats on the surface of a numerical wave tank. First, a total of six independent studies, namely the time, meshing, damping, overset geometry, flow viscosity, and spatial studies, were conducted for validation purposes. Second, calculation and analysis of the heave and transmission coefficients and vorticity magnitude were conducted to assess the hydrodynamic performance. Results of independent studies show cases with a high degree of accuracy to the experimental model, whereas results for hydrodynamic performance show a generally increasing heave movement of OB and transmission coefficient across the range of wave periods studied. Meanwhile, the vorticity magnitude flow fields show at least two vortices for all wave periods studied, except for the shortest two wave periods.

Keywords: Computational fluid dynamics, Wave energy converter, Oscillating buoy, Breakwater, Hydrodynamic performance

1. Introduction

Considering the urgent need to address the issue of climate change, most countries have pledged to go net-zero carbon in terms of emissions by 2050. One way to do so is to replace non-renewables with renewable energy sources, and wave energy is a key component in the mix of renewable energies. It is seen to be the preferred source of energy for remote and island regions that are difficult to access through the national grid system [1] but have abundant ocean wave energy potential from the nearby ocean.

Wave energy converters (WEC), which convert wave energy to electrical energy, come in various types, such as oscillating bodies, overtopping devices, and oscillating water columns. An oscillating buoy (OB) is a type of oscillating body that either floats or is submerged in the ocean and works based on translational (heave) or rotational movement [2]. The system bypasses the secondary conversion process that uses a power take-off unit, typically found in other types of WECs, by direct drive to a linear electrical generator [3]. Aside from its electrical energy-generating properties, the OB could also act as a breakwater, which is a protective barrier between ocean waves and coastal infrastructure, which could experience frequent wear and tear due to the constant barrage of ocean waves. This hybrid use of the device makes it more space-efficient and cost-effective than single-use ocean devices.

The validation study serves the purpose of creating a numerical model that can accurately replicate real-life conditions either in a controlled experimental setup or in an open environment. In the case of a numerical model consisting of a floating body that is subjected to wave oscillations, the level of accuracy could vary depending on

Address for Correspondence: Giri Ram, Universiti Pertahanan Nasional Malaysia, Faculty of Engineering, Department of Mechanical Engineering, Kuala Lumpur, Malaysia
E-mail: ramamethyst@gmail.com
ORCID ID: orcid.org/0000-0002-9970-861X

Received: 23.08.2023
Last Revision Received: 14.12.2023
Accepted: 19.01.2024

To cite this article: G. Ram, M. R. Saad, N. Z. Abidin, and M. R. A. Rahman. "Model Validation and Hydrodynamic Performance of an Oscillating Buoy Wave Energy Converter." *Journal of ETA Maritime Science*, vol. 12(1), pp. 83-91, 2024.

the technique used. One technique is smoothed-particle hydrodynamics, which is a mesh-free approach that uses an array of particles to form a simulation domain [4]. In addition, a layering technique was used by Luo et al. [5], where dynamic layering to add or remove meshes next to a moving boundary was used. Gomes et al. [6] also used layering, wherein the inlet acted as a moving wall. Other techniques include smoothing and remeshing. Ringe [7] used both techniques to model a one-directional wave tank.

A relatively newer technique for modeling moving bodies is the overset mesh technique, which works based on the principle that two separate mesh regions move relative to each other while having a static internal condition with fixed mesh connectivity [8]. Zhang et al. [9] used the overset mesh technique because of its better accuracy for large-scale deformations compared with the dynamic mesh. Lakshmynarayana [10] also used overset grids, which are attached to a floating body and move with it freely according to the motion response.

The hydrodynamic performance of WEC has been studied extensively and is typically assessed using several coefficients that are calculated based on measurements of various waves, pressure, velocity, and other gages installed in the wave tank. In the case of an OB, the coefficient related to heave movement provides an understanding of the level of wave energy that is converted to electrical energy. Cheng et al. [11] experimentally and numerically studied a hybrid WEC-breakwater system, where the breakwater, in the form of an OB, is subjected to a heave-only motion and the heaving displacement and velocity of the OB are analyzed.

In addition to the quantitative analysis of heave movement, qualitative analysis in the form of velocity flow fields allows for the detection of energy loss in the system in the form of vortices, as studied by Zhang et al. [12]. On the other hand, the calculation of the transmission coefficient determines the ability of the OB to act as a breakwater, as shown by Ji et al. [13], who studied the effects of variations in draft, wave frequency, and curtain height of a heaving WEC-breakwater device on the transmission coefficient.

This study can be divided into two parts. The first part involves a validation study whereby a total of six independent studies, concerning the time, spatial, mesh, numerical beach, overset mesh design, and viscosity model, are conducted on a rectangular buoy. In the second part, the hydrodynamic performance of the OB, concerning its ability to generate wave power and act as a breakwater, is studied.

A novelty of this study is that six independent studies were conducted to develop an accurate numerical model. Besides that, to the best knowledge of the authors, a comprehensive study on the vorticity magnitude flow fields, because of the interaction of waves at the surface of water body and OB, for different wave periods and cycles, has not been published before.

2. Numerical Model

2.1. Governing Equations

Numerical modeling and simulations were carried out using ANSYS 2023 R2: Fluent, a computational fluid dynamics solver that works according to the finite volume method, wherein regions of interest are segmented into sub-regions and governing equations are discretised and solved iteratively over every sub-region [6]. The simulation was performed using an Intel(R) Xeon(R) Platinum 8260 CPU @ 2.40 GHz and 2.39 GHz (two processors) with 128 GB of RAM. A total of 45 parallel processors were used during the simulation.

Reynolds-averaged Navier-Stokes equations were used in the system along with some additional variables. Equations 1-3 show the mass continuity and Navier-Stokes equations [14].

$$\frac{\partial(\rho u)}{\partial x}+\frac{\partial(\rho v)}{\partial y}=0 \tag{1}$$

$$\rho\left(\frac{\partial u}{\partial t}+u\frac{\partial u}{\partial x}+v\frac{\partial u}{\partial y}\right)=-\frac{\partial p}{\partial x}+2\mu\frac{\partial^2 v}{\partial y^2} +\frac{\partial}{\partial y}\left(\mu\left(\frac{\partial u}{\partial y}+\frac{\partial v}{\partial x}\right)\right)+F_x \tag{2}$$

$$\rho\left(\frac{\partial v}{\partial t}+u\frac{\partial v}{\partial x}+v\frac{\partial v}{\partial y}\right)=-\frac{\partial p}{\partial x}+2\mu\frac{\partial^2 u}{\partial y^2} +\frac{\partial}{\partial x}\left(\mu\left(\frac{\partial u}{\partial y}+\frac{\partial v}{\partial x}\right)\right)-\rho g+F_y \tag{3}$$

Volume of fluid method was used to simulate an immiscible, multiphase mixture. The scale of the model is considered to be small, where air and water compressibility are assumed to be negligible.

To evaluate the results of independent studies, heave movement, wave elevation, and flow time calculations are plotted as per Equations 4-6. The relative error of the present cases relative to the experimental data is calculated as per Equation (7) [15].

$$\textit{normalized heave movement}=\frac{Z}{d} \tag{4}$$

$$\textit{normalized wave elevation}=\frac{\eta}{d} \tag{5}$$

$$normalized\ flow\ time = \frac{t}{T} \quad (6)$$

$$error = \frac{\epsilon_{Numerical} - \epsilon_{Experimental}}{\epsilon_{Experimental}} \text{ x } 100 \quad (7)$$

To calculate the performance of the OB, the heave coefficient and transmission coefficient are calculated as per Equations 8 and 9 respectively.

$$Ch = \frac{A_{Heave}}{A_{Incident}} \quad (8)$$

$$Ct = \frac{A_{Transmission}}{A_{Incident}} \quad (9)$$

2.2. Numerical Wave Tank (NWT)

The layout of the model along with dimensions and applied labels during boundary conditions is shown in Figure 1. The dimensions of the two-dimensional NWT were set to 18 m x 0.8 m, where the point of origin is at the centroid of the domain. Therefore, the water depth is 0.4 m, which is similar to the experimental setup used by He et al. [16] and the numerical model used by Lyu et al. [17].

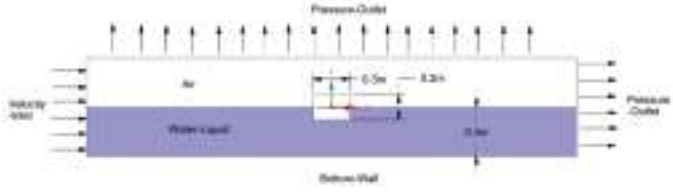

Figure 1. *Two-dimensional schematic of NWT with added rectangular buoy and details of dimensions, phases, and boundary types*

NWT: Numerical wave tank

The OB was partially immersed in still water, has dimensions of 0.3 m x 0.3 m x 0.2 m, and is located at the center of the background (Figure 1). Two phases, namely air and water-liquid phase, were selected as shown in Table 1. The boundary and initial conditions are shown in Table 2. The wave theory is selected in accordance with the graph for limits of validity for wave theories [18].

2.3. Validation

The six independent studies conducted for validation are time, mesh, numerical beach, overset geometry, viscosity model, and spatial studies. For heave movement, an NWT with a rectangular buoy was used for simulation, whereas for wave elevation, an empty NWT was used, where the result of WG0 was compared with experimental data, except for spatial study.

Table 1. *Properties of the phases*

Material name	Density (kg/m^3)	Viscosity (kg/ms)
Air	1.225	1.789x10-3
Water-Liquid	1000	1003x10-3

Table 2. *Setting the boundary condition*

Description	Value
Free surface level (m)	0
Depth (m)	-0.4
Wave boundary condition option	Shallow/Intermediate waves
Wave theory	Third-order stokes
Wave height (m)	0.1
Wavelength (m)	1.9897
Operating pressure (Pa)	101325
Operating density (kg/m^3)	1.225
Wave period (rad/s)	1.2

A time study was conducted to assess the flow time at which wave elevation attains stability. The simulation was allowed to run until 126 s and results of 6 s range, between 30 s intervals was collected. Second, the mesh study involves coarse mesh with bias and fine mesh with bias, as shown in Figure 2a and b, respectively. To reduce computational time for coarse mesh, a biased mesh was used whereby Δx =0.015 m with a bias factor of 1.2, while Δy =0.015 m with a bias factor of 5 was set. Face meshing was used to attain a more uniform, hexahedron-shaped mesh.

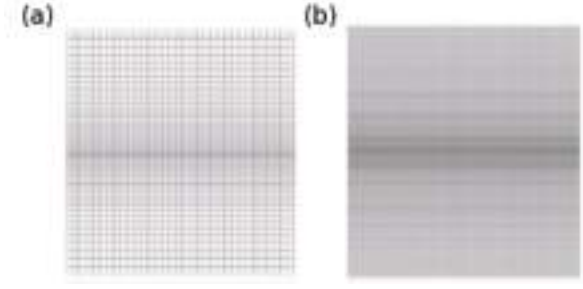

Figure 2. *Schematic of (a) coarse mesh with bias and (b) fine mesh with bias*

Lyu et al. [17] found that a mesh of Δx =0.02 m and below and Δz =0.01 m and below improved the reading on the maximum crest compared to mesh Δx =0.06 m and Δz =0.02 m. The coarse mesh case has a mesh structure that is comparable to the meshes improved by Lyu et al. [17]. As for the fine mesh, the element size is three times smaller at Δx and Δy of 0.005 m (Table 3).

Table 3. *Details of the mesh study*

Mesh type	Mesh Size (m)	Number of cells
Coarse	0.015	64800
Fine	0.005	576000

Third, the beaching effect in a wave tank prevents wave reflection from the outlet, thereby not distorting the measurements. Typically, a slope produces the beaching effect in experimental studies; however, in numerical studies, a numerical beach could also perform a similar task. Three numerical beach lengths from the outlet were tested.

The OB is subjected to heave movement using the overset mesh technique. It works based on the principle that two separate mesh regions move relative to each other while having a static internal condition with fixed mesh connectivity [8]. For the overset design study, circular and rectangular overset meshes were compared for their accuracy with experimental data.

In the flow viscosity study, laminar, standard k-epsilon, and Shear Stress Transport (SST) k-omega turbulence models were studied. These are commonly used viscosity models, based on the Windt et al. [8] study, where 41% of studies did not disclose model type, 18% used standard k-epsilon model, 13% SST k-omega, 10% laminar, 7% re-normalization group k-epsilon, 4% inviscid, and 5% others.

Finally, a spatial study looks into wave elevation at different locations from the inlet to the OB. A total of nine wave gages (shown in Figure 3), based on their distance to the point of origin, were used to measure wave elevation. Through this study, the characteristics of wave propagation can be observed.

2.4. Hydrodynamic Performance

To assess the ability of the OB to convert wave energy into useful electrical energy, the heave coefficient is calculated and compared for various wave periods. Second, the ability of the OB to function as a breakwater and reduce the amount of wave energy transmitted downstream of the OB is assessed using the calculated transmission coefficient. Finally, vorticity magnitude, which refers to the magnitude of spinning motion, is visualized in a velocity flow field diagram to detect vortices in the water phase and the magnitude of vorticity.

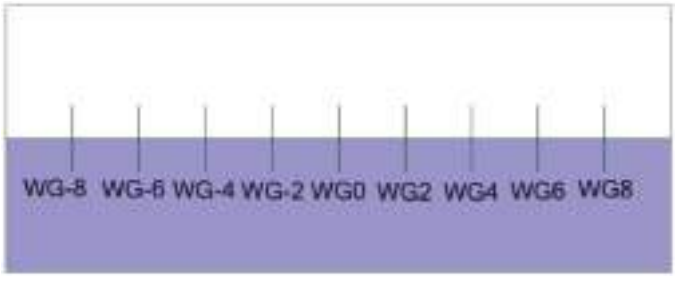

Figure 3. *Schematic of the wave gage location in NWT*

NWT: Numerical wave tank

3. Results and Discussion

3.1. Validation

The result for heave movement is shown in Figure 4, wave elevation in Figure 5, and the percentage of error relative to the experimental data is shown in Figure 6. For the time study, shown in Figures 4a, 5a, and 6a, the lowest error is seen to be for time ranges of 40-46 s and 50-56 s for both heave movement and wave elevation, respectively. Beyond the flow time of 56 s, the computing time was deemed too long and taxing for the computer. The results of relative error show that heave movement more accurately replicates experimental data compared to wave elevation, and that the optimal accuracy was found for the flow time range 50-56 s. This result is similar to the findings of Jiang et al. [19], where a steady state is observed between flow times of 40 s and 60 s.

For the results of the mesh study, shown in Figures 4b, 5b, and 6b, all cases show good accuracy to the experimental data, at a maximum error of 6% for the heave movement of the coarse mesh. This means that the coarse mesh case is favorable compared to the fine mesh case because of the reduced computing time. For the results of the spatial study, WG-2 shows a predictably shorter amplitude compared to WG-8, WG-6, and WG-4 because of its distance from the inlet and interference from wave reflection from the OB. Findings by Ji et al. [13] show that coarser meshes agree well with finer meshes for heave motion, but show little difference in peak and trough for wave elevations. This study shows the opposite result, where a higher similarity and accuracy to the experimental data is found for wave elevation compared to heave motion.

The results of the numerical beach study are shown in Figures 4c, 5c, and 6c. A higher irregularity in wave propagation could be observed for the no beach case compared with the beach cases, despite the lower error for heave movement. The optimal value for both heave and wave elevation was observed to be the beach 7-9 m case. Besides the numerical beach, a common method for wave absorption is to design a slope at the outlet. Ringe [7] studied the wave absorption of slopes with different steepness levels, perforated screens, and step-up absorbers and observed that the steepest slope with a 1:3 ratio showed the best result.

Both circular and rectangular overset designs show a low percentage of error (as shown in Figures 4d, 5d, and 6d). However, the rectangular overset case shows almost half the % of errors and is therefore considered to be more accurate in replicating the experimental results.

The viscosity model study (shown in Figures 4e, 5e, and 6e) shows a high accuracy for the laminar model compared to the SST k-omega and standard k-epsilon turbulence models.

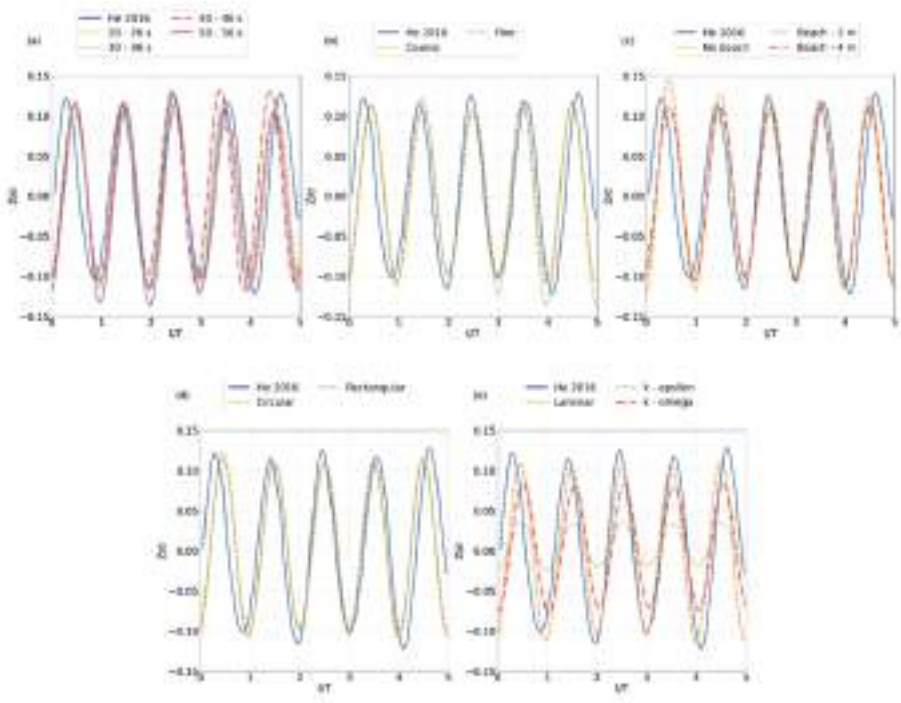

Figure 4. *Comparison of normalized heave movement versus normalized time between experimental data [16] and various cases of a) time study, b) mesh study, c) numerical beach study, d) overset geometry study, and e) viscosity study*

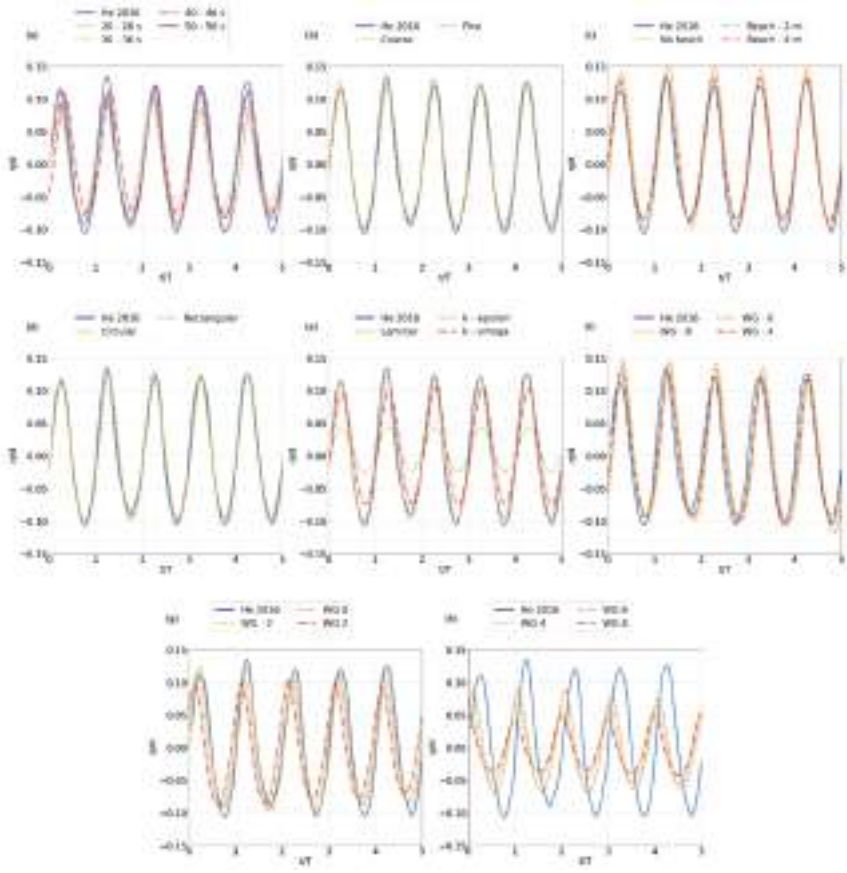

Figure 5. *Comparison of normalized wave elevation versus normalized time between experimental data [16] and various cases of a) time study, b) mesh study, c) numerical beach study, d) overset geometry study, e) viscosity study, f) spatial study for wave gauges WG-8, WG-6, and WG-4, g) spatial study for wave gages WG-2, WG0, and WG2, and h) spatial study for wave gauges WG4, WG6, and WG8*

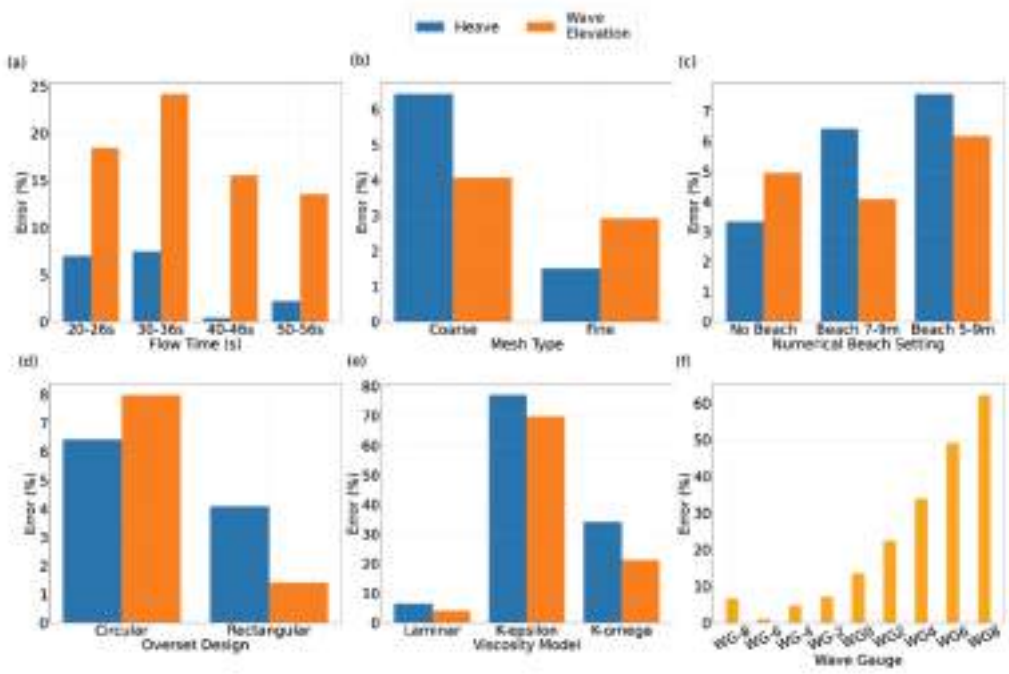

Figure 6. *Comparison of relative error between experimental data [16] and various types of cases for a) time study, b) mesh study, c) numerical beach study, d) overset geometry study, e) viscosity study, and f) spatial study*

This indicates that the experimental conditions produced a flow type that is closer to laminar flow in the wave tank, rather than turbulence. The results also indicate that the SST k-omega model, which is known to be more accurate in modeling near-wall turbulent flow, does a better job than the standard k-epsilon model at replicating flow in the experimental study.

Several previous studies have also demonstrated an accurate replication of experimental results using a laminar model. Zhang et al. [20] used the laminar model and concluded that it was able to predict various phenomena accurately under certain conditions. Zhang et al. [9] used the laminar model to simulate wave propagation on a dual-floater system and found trends similar to those of the experimental data.

Finally, the spatial study, shown in Figures 5f, 5g, 5h, and 6f, shows a high wave elevation before WG0 and continued damping until WG8, because of the beaching effect from the numerical beach. In addition, the offset of wave elevation at downstream locations compared to upstream location intensifies further downstream.

When compared with experimental data, WG-6 shows the most accurate reading, where at WG-8, the amplitude is higher and after WG-6, all values show a lower amplitude than that of experimental data. Downstream of WG0, the amplitude was found to damp more than that upstream of WG0. Location WG0, which shows an error of 13.5%, is considered to be of reasonable accuracy considering the much higher error because of damping for locations WG2-WG8.

3.2. Hydrodynamic Performance

For further study of the numerical model, the most accurate models of independent studies were used, with the same aspects of fixed boundary conditions and NWT dimensions. When a quantitative analysis was conducted using cases of varying wave angular frequencies, the results of heave movement and transmission coefficient, as shown in Figure 7, demonstrated a non-uniform decreasing trend across the ranges of frequencies studied. A valley is observed at wave periods 1.5 s and 1.8 s for heave movement and transmission coefficient, respectively.

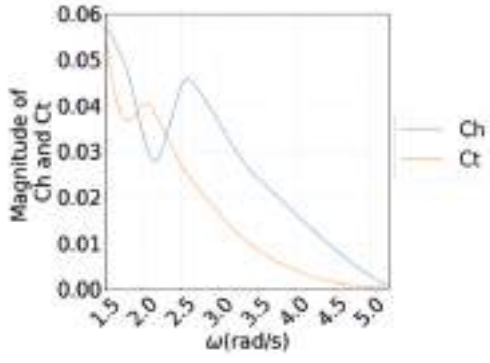

Figure 7. *Comparison of the heave coefficient (Ch) of OB-B and transmission coefficient (Ct) versus wave frequency*

The result of a general decreasing trend in the heave movement of OB across the frequency indicates that more energy can be generated through direct drive when the wave period is longer. This indicates that a location with a higher wavelength and wave period profile is beneficial for wave power generation using OB. Zhang et al. [9], who studied the heave motion of a single WEC with a square bottom, observed a similar trend. A general downward trend across similar frequency ranges, plus the presence of a small valley, is consistent with the result of the heave coefficient of the present study.

Meanwhile, the amount of wave energy transmitted downstream is also generally higher with a longer wave period, which indicates that a lower wavelength and wave period profile is more beneficial for the OB to perform its function as a breakwater.

When the transmission coefficient result is compared to the transmission coefficient at WG2 when OB is absent, the result shows that for a frequency of 2.62 rad/s and a wave period of 1.2 s, models with and without OB have transmission coefficient values of 0.024 and 1.085, respectively. This shows that the OB reduced 97.8% of transmitted wave energy, which makes it an effective floating breakwater that can be used to protect coastal infrastructure. In comparison, only 2% of the incident-wave energy was transmitted in an experimental study of a Berkeley Wedge-shaped floating breakwater by Madhi et al. [21]. This indicates that further improvement to lower the transmitted energy is possible through a geometric optimization approach.

These results are in agreement with the findings of Zhang et al. [9], who studied a dual-floater system where the upstream and downstream buoys are WEC and breakwater, respectively. A general decrease in heave motion and transmission across the wave angular frequency was observed for a single WEC with a square bottom. Another dual-floater system studied by Chen et al. [22] also shows a general decreasing trend across the frequency for all draft ratios.

The results for the vorticity magnitude flow fields are shown in Figures 8 and 9, where the presence of at least one vortex near the front and back edges of the OB is observed for all wave periods except period 0.6 s. The vortex does not increase in size across the wave period and cycle, nor does it increase in intensity. Vortices are phenomena that contribute to energy loss, which then reduces the magnitude of the heave coefficient of the OB. Therefore, solutions such as shape optimization could be implemented for a possible future study.

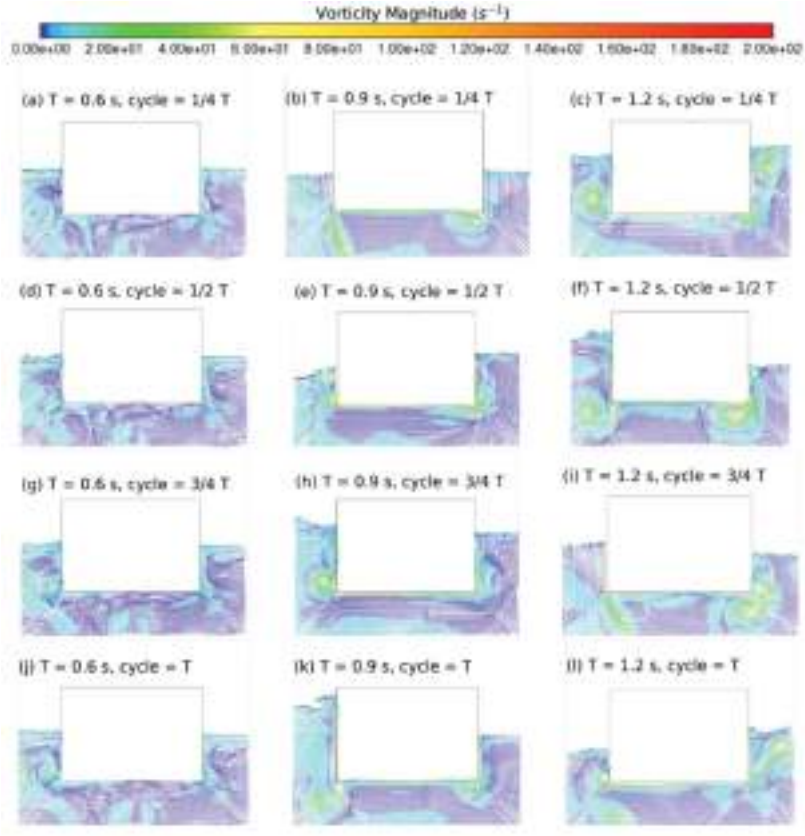

Figure 8. *Flow fields of vorticity magnitude for wave periods 0.6, 0.9, and 1.2 s, for cycles 1/4 T [(a), (e), (i)], 1/2 T [(b), (f), (j)], 3/4 T [(c), (g), (k)], and T [(d), (h), (l)], respectively*

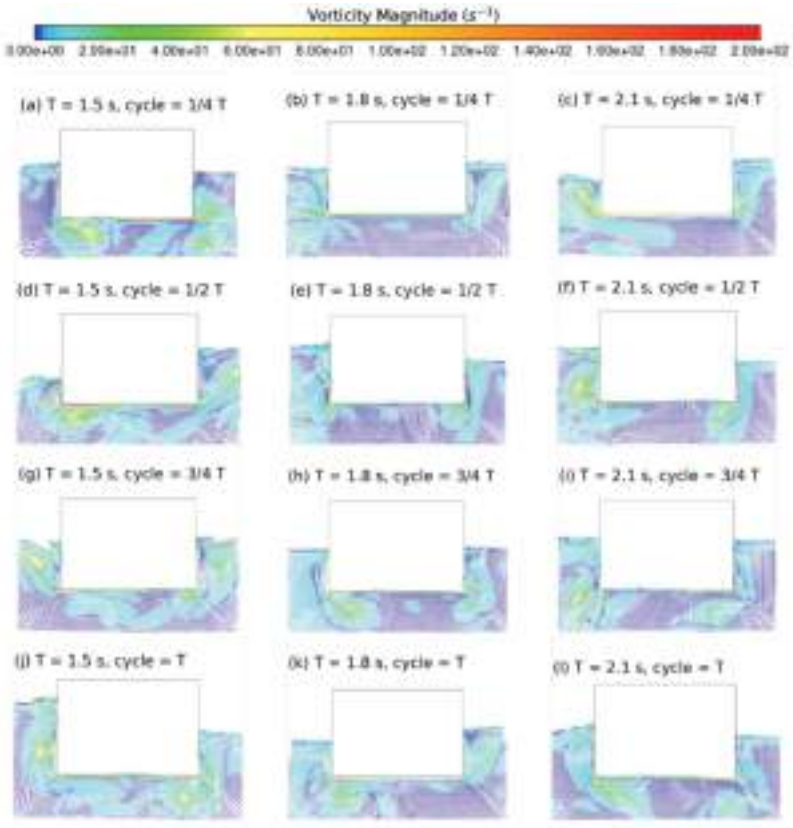

Figure 9. *Flow fields of vorticity magnitude for wave periods 1.5 s, 1.8 s, and 2.1 s for cycles 1/4 T [(a), (e), (i)], 1/2 T [(b), (f), (j)], 3/4 T [(c), (g), (k)], and T [(d), (h), (l)], respectively*

This result is similar to the findings of Zhang et al. [12], who found vortices in the front and back of the studied buoy. In addition, a proposal of a streamlined design of the buoy bottom was made to reduce the flow separations and improve energy conversion, similar to the findings of the present study. When Chen et al. [22] displayed the result of the vorticity magnitude contour of dual-floaters of varied draft ratios, the result showed a higher presence of vortices for models with smaller draft ratios.

4. Conclusion

A study was conducted to create an accurate numerical model and assess the wave conversion and breakwater abilities of an OB. Six independent studies were conducted for the first objective, and three hydrodynamic coefficients were calculated for the second objective.

Some of the limitations of this study are the two-dimensional design of the numerical model, the motion of the OB that is confined to only heave movement, and the assumption of negligible compressibility of air due to the small-scale study.

The findings of this study can be summarized as follows:

Six independent studies were used as validation to derive the ideal numerical setup that replicates the experimental condition at a flow time of 40-46 s for fine mesh setup, 7-9 m numerical beach setting, rectangular overset mesh design, laminar flow viscosity, and location WG0.

Quantitative analysis results for the heave and transmission coefficients show a generally decreasing trend across the wave angular frequency, with a notable presence of a valley at different locations. For the transmission coefficient, the OB was found to eliminate 97.7% of the transmitted wave energy compared to the model without an OB.

Qualitative analysis results of the vorticity magnitude flow field show vortices for all wave periods except the lowest 0.6 s. The vortices appear close to the front and back edges of the OB.

For further studies, geometric optimization of the OB to improve its hydrodynamic performance can be conducted. In addition, the slamming effect on the structural integrity of the OB needs further study to reduce the occurrence of structural failure that increases the cost of maintenance.

Authorship Contributions

Concept design: M. R. A. Rahman, Data Collection or Processing: G. Ram, Analysis or Interpretation: G. Ram, Literature Review: G. Ram, and M. R. A. Rahman, Writing,

Reviewing and Editing: G. Ram, M. R. Saad, N. Z. Abidin, and M. R. A. Rahman.

Funding: The authors declare that no funds, grants, or other support was received during the preparation of this manuscript.

References

[1] N. H. Samrat, N. B. Ahmad, I. A. Choudhury, and Z. Taha, "Prospect of wave energy in Malaysia." In *2014 IEEE 8th International Power Engineering and Optimization Conference (PEOCO2014)*, IEEE, pp. 127-132. Mar 2014.

[2] A. Falcao, "Wave energy utilization: a review of the technologies." *Renewable and Sustainable Energy Reviews,* vol. 14, pp. 899-918, Apr 2010.

[3] W. Sheng, "Wave energy conversion and hydrodynamics modelling technologies: a review." *Renewable and Sustainable Energy Reviews,* vol. 109, pp. 482-498, Jul 2019.

[4] M. Sasson, S. Chai, G. Beck, Y. Jin, and J. Rafieshahraki. "A comparison between smoothed-particle hydrodynamics and rans volume of fluid method in modelling slamming." *Journal of Ocean Engineering and Science,* vol. 1, pp. 119-128, Apr 2016.

[5] Y. Luo, et al. "Numerical simulation of a heave-only floating OWC (oscillating water column) device." *Energy,* vol. 76. 799-806, Nov 2014.

[6] M. N. Gomes, L. A. Isoldi, C. R. Olinto, L. A. O. Rocha, and J. A. Souza. "Computational modeling of a regular wave tank." In *2009 3rd Southern Conference on Computational Modeling*, IEEE, pp. 60-65, Nov 2009.

[7] S. Ringe. *Designing of One Directional Wave Tank*, 2020.

[8] C. Windt, J. Davidson, and J. V. Ringwood. "High-fidelity numerical modelling of ocean wave energy systems: a review of computational fluid dynamics-based numerical wave tanks." *Renewable and Sustainable Energy Reviews,* vol. 93, pp. 610-630, 2018.

[9] H. Zhang, B. Zhou, C. Vogel, R. Willden, J. Zang, and J. Geng. "Hydrodynamic performance of a dual-floater hybrid system combining a floating breakwater and an oscillating-buoy type wave energy converter." *Applied Energy,* vol. 259, pp. 114212, Feb 2020.

[10] P. A. Lakshmynarayanana, *Application of 3D-CFD modelling for dynamic behaviour of ship in waves*., University of Southampton, Apr 2017.

[11] Y. Cheng, et al. "Experimental and numerical analysis of a hybrid wec-breakwater system combining an oscillating water column and an oscillating buoy." *Renewable and Sustainable Energy Reviews,* vol. 169, pp. 112909, Nov 2022.

[12] X. Zhang, Q. Zeng, and Z. Liu. "Hydrodynamic performance of rectangular heaving buoys for an integrated floating breakwater." *Journal of Marine Science and Engineering,* 7, vol. 8, pp. 239, Jul 2019.

[13] Q. Ji, C. Xu, and C. Jiao. "Numerical investigation on the hydrodynamic performance of a vertical pile-restrained reversed l type floating breakwater integrated with wec." *Ocean Engineering,* vol. 238, pp. 109635, Oct 2021.

[14] H. I. Yamac, and A. Koca. "Shore type effect on onshore wave energy converter performance." *Ocean Engineering,* vol. 190, p. 106494, Oct 2019.

[15] K. O. Connell, and A. Cashman. "Development of a numerical wave tank with reduced discretization error." In *2016 International Conference on Electrical, Electronics, and Optimization Techniques (ICEEOT),* IEEE, pp. 3008-3012, Mar 2016.

[16] M. He, B. Ren, and D. Qiu. "Experimental study of nonlinear behaviors of a free-floating body in waves." *China Ocean Engineering,* vol. 30, pp. 421-430, Apr 2016.

[17] S. Lyu, H. Luofeng, and T. Giles. "Motions of a floating body induced by rogue waves." OpenCFD Limited, Jul 2019.

[18] B. LeMéhauté. *An introduction to hydrodynamics and water waves*. *Environmental Science Servies Administration*, vol. 52, pp. 205, 1969.

[19] S.-C. Jiang, W. Bai, and G.-Q. Teng. "Numerical simulation of wave resonance in the narrow gap between two non-identical boxes." *Ocean Engineering,* vol. 156, pp. 38-60, May 2018.

[20] H. Zhang, S. Liu, M. C. Ong, and R. Zhu. "CFD Simulations of the propagation of free-surface waves past two side-by-side fixed squares with a narrow gap." *Energies*, vol. 12, pp. 2669, Jul 2019.

[21] F. Madhi, M. E. Sinclair, and R. W. Yeung. "The "berkeley wedge": an asymmetrical energy-capturing floating breakwater of high performance." *Marine Systems & Ocean Technology*, vol. 9, pp. 5-16, Jun 2014.

[22] L. Chen, X. Cao, S. Sun, and J. Cui. "The effect of draft ratio of side-by-side barges on fluid oscillation in narrow gap." *Journal of Marine Science and Engineering,* vol. 8, pp. 694, Jul 2020.

Journal of ETA Maritime Science 2024;12(1):92-105

A TAM-Based Study on the Adoption of Digital Transformation in the Maritime Transportation Logistics Sector

Orçun Gündoğan, Tuba Keçeci

İstanbul Technical University Faculty of Maritime, Department of Maritime Transportation Management Engineering, İstanbul, Türkiye

Abstract

Digital transformation is a significant global trend of the 21st-century that has substantial ramifications for various companies and sectors. It is inconceivable to envision that the maritime transport logistics industry will remain unaffected by these advancements. Digital transformation has the capacity to fundamentally revolutionize the business processes, services, and strategies of organizations working within this industry. This study examines the process of digital transformation within the maritime sector and identifies the key factors that influence its adoption. The research used structural equation modeling methodology to examine the variables and specific components indicated in the technology acceptance model. The data used in the analysis were collected via a questionnaire administered to individuals engaged in the maritime transport industry. The findings of the study indicate that the degree to which employees in the industry embraced digital transformation technologies was influenced by various factors, including their perception of how easy these technologies were to use and the perceived benefits they offered. The study's findings offer strategic suggestions for improving the successful implementation of digital transformation in the maritime logistics sector.

Keywords: Maritime transport logistics, Digitalization, Structural equation modeling (SEM), Technology acceptance model (TAM)

1. Introduction

Digital transformation refers to the use of technological innovations to revolutionize the commercial processes, organizational structures, and value propositions of various industries. Digital transformation is currently exerting a significant impact on various sectors, resulting in notable breakthroughs and advantages. The aforementioned transformation process yields significant advantages, including enhanced operational effectiveness, financial savings, and the identification of novel avenues for business growth [1]. This shift also impacts the maritime transport logistics sector. Utilization of digital technologies within the realm of maritime transportation procedure yields enhanced efficiency and reduced operational expenditures. Furthermore, the presentation of novel digital technologies within the maritime transport logistics industry offers environmental sustainability benefits through the reduction of carbon emissions, thus promoting a greener and more ecologically friendly sector [2,3].

The digital transformation process in the maritime logistics industry enabled the use of many cutting-edge technologies and applications The field of technology has witnessed notable developments in the form of the Internet of Things (IoT), artificial intelligence, big data analytics backchain autonomous ships, and drone technologies. The implementation of these technologies enhances the sustainability, safety, and efficiency of the maritime transportation sector by streamlining its logistical procedures. The implementation of IoT technology can facilitate the optimization of ship and port operations, enabling the real-time collection and analysis of data. Route optimization, energy conservation, and enhanced maintenance process management are just a few notable benefits of using big data analytics. These advantages

Address for Correspondence: Orçun Gündoğan, İstanbul Technical University Faculty of Maritime, Department of Maritime Transportation Management Engineering, İstanbul, Türkiye
E-mail: orcun.gd@gmail.com
ORCID ID: orcid.org/0000-0001-6013-2441

Received: 03.11.2023
Last Revision Received: 25.01.2024
Accepted: 29.01.2024

To cite this article: O. Gündoğan, and T. Keçeci, "A TAM-Based Study on the Adoption of Digital Transformation in the Maritime Transportation Logistics Sector." *Journal of ETA Maritime Science*, vol. 12(1), pp. 92-105, 2024.

are achieved through the processing and analysis of substantial volumes of data [4]. The implementation of AI in business operations, namely aboard operations and port operations, enhances efficiency through the use of automated decision-making and process optimization [5]. In the realm of shipping logistics procedures, the use of backchain technology yields expedited transaction speeds and reduced expenses. This is primarily attributed to the inherent characteristics of blockchain, which facilitate safe and transparent data sharing [6]. The use of autonomous ships and drone technologies has facilitated the advancement of safer procedures that require reduced human involvement in maritime transportation and port operations [7,8]. The digital transformation process poses considerable challenges and obstacles for the maritime transport logistics sector. The problems encompass various factors, such as the financial implications associated with investing in digital technology, the lack of interoperability between current infrastructure and digital systems, concerns over cybersecurity, the need for staff training, and the scarcity of a skilled workforce. Overcoming these hurdles and expediting the process of digital transformation will enhance the industry's capacity to respond to global competitive conditions and foster growth [9-11].

The integration of cutting-edge digital technology and processes within the sector is expected to yield improvements in efficiency, sustainability, and customer-centricity. The use of innovation is anticipated to significantly contribute to the facilitation of efficient international commerce operations. Collaboration and concerted efforts among enterprises, policymakers, and regulatory agencies within the sector are of utmost importance for facilitating and expediting the digital transformation process. It is vital for all stakeholders to prioritize the adaptation of the maritime transportation logistics sector during the digital transformation period. This study employed the technology acceptance model (TAM) to examine the adaptability of the maritime industry to digital transformation. This articlerepresents one of the initial studies in the maritime field and provides useful data for integrating technology into the maritime industry.

2. Literature Review

The concept of digitization emerged as a notable and consequential phenomenon in the 21st-century, driven by rapid advancements in technology. This ongoing evolution is not just confined to institutions but also profoundly influences societal structures. The effects of these advancements extend across various industries and disciplines, reflecting the comprehensive impact of digital transformation. Scholarly literature provides an extensive investigation into the application of digital transformation in several domains, meticulously outlining the inherent advantages and associated challenges.

In contemporary technology adoption research, the integration of structural equation modeling (SEM) with TAM has proven to be highly effective. This combination allows for a detailed examination of the interplay between perceived ease of use (PEOU) and perceived usefulness (PU), along with other latent variables, thereby offering a more comprehensive understanding of the factors influencing technology acceptance. The synergy between SEM's complex variable analysis and TAM's user-centric focus has been instrumental in enhancing the robustness and applicability of research across diverse technological domains [12-15].

The evaluation of digital transformation within the maritime industry demonstrates notable progress in enhancing operational efficiency, fortifying cybersecurity measures, promoting environmental sustainability, and optimizing supply chain management. The incorporation of big data, AI technology, and machine learning significantly enhances operational practices in the domains of route optimization, fuel efficiency, and preventive maintenance. Within the domain of cybersecurity, digital technologies play an essential role in protecting critical infrastructure from cyber threats while also fulfilling environmental responsibilities and reducing carbon emissions. The adoption of backchain technology enables greater transparency in supply chain transactions and improves the entire customer experience. Therefore, this transition is expected to guide the maritime sector toward a future that is both competitive and sustainable, but it will require ongoing innovation and adaptation [16-20].

TAM is a theoretical structure that aims to provide insight into the various aspects that influence individuals' adoption of technology, as well as the underlying motivations for their acceptance. Davis [21] created the model in 1986 with the intention of analyzing computer usage patterns within an organizational context. The primary objective of this study was to determine the fundamental elements that influence the adoption of a particular technology [21].

The examination of the digital transition within the maritime industry might be conducted using TAM. Davis [21] proposed a model in which the adoption of novel technologies is contingent on individuals' perceptions of their utility and simplicity. The successful use of technologies in maritime operations necessitates the recognition of their benefits in improving operational efficiency, strengthening cybersecurity protocols, addressing environmental impacts, and optimizing supply chain management. In addition, the acceptance of technologies is more likely when they are designed to be user-friendly [22].

In conclusion, the application of TAM in evaluating digital transformation initiatives in the maritime industry offers a full understanding of the factors that impact the acceptance and successful integration of new technology.

TAM is widely used as the primary conceptual structure in academic studies concerning the adoption of information technology. Venkatesh [23] asserts that it facilitates the interpretation of individuals' dispositions toward information systems, their conduct in using these systems, and the prospective ramifications of information systems on society in forthcoming times. TAM has been subjected to comprehensive empirical examination in numerous research investigations and is widely acknowledged as a robust theoretical framework for understanding consumers' propensity to embrace technology [24,25]. Mathieson [25] found that the Theory of Planned Behavior and the TAM were equally effective at predicting user intentions. Nevertheless, TAM was seen as a more parsimonious model because of its ability to attain the same outcomes with a reduced number of components. The model is widely recognized and highly regarded in the field of information systems adoption, making it one of the most prominent and well-supported theories in the current academic literature [26].

Numerous studies have employed TAM in various technical domains and user populations. Notably, the field of e-learning has emerged as a significant area of investigation concerning the use of TAM. Al-Gahtani [27] examined the degree to which university students adopt e-learning technologies. The study's results demonstrated that TAM served as a beneficial theoretical framework for understanding the various elements that impact students' acceptance and use of e-learning systems.

The application of TAM has also been observed in the domain of electronic health (e-health) research. Kijsanayotin et al. [28] examined the connection between TAM and adoption of digital health records in healthcare services. The study found that TAM offers a useful theoretical structure for understanding the acceptability of technology within the healthcare industry.

TAM is also used in the domain of electronic commerce in relation to the literature. Gefen et al. [29] performed an analysis with the objective of investigating the application of TAM in understanding the various aspects that impact the adoption of online shopping. The study posits that TAM provides a beneficial theoretical framework for understanding the numerous elements that influence the acceptance of online purchases.

TAM is widely regarded as a prominent model used in several industries to gain comprehensive insights into the processes of technological adoption. These studies provide insights into the applicability and efficacy of TAM in understanding the factors influencing users' acceptance of technology across different technological domains. Despite the considerable amount of research conducted, the inquiry into the mechanisms and motivations underlying users' adoption of novel technologies remains unresolved in its entirety. However, empirical research has shown that the degree of user acceptance plays a key role in determining the rate at which a particular technology is adopted [23,26,30,31].

TAM has garnered extensive recognition in research on the use of information technologies, offering valuable insights into the acceptance and adoption of technology. Nevertheless, the complete extent of the model's capabilities has not been fully realized. Further investigation is warranted to explore the potential applications of TAM in diverse technological environments and among varied user demographics [32].

3. Empirical Study Design and Data Analysis

The current research focuses on the subject of digital transformation and TAMs, both of which are a noteworthy and contemporary concern within the maritime sector. In the present-day setting, which is marked by the swift displacement of traditional practices and the increasing significance of technology, the maritime sector is not immune to these global changes. Nevertheless, it is worth noting that there is an important dearth of comprehensive academic research and modeling endeavors focused on this particular form of transformation within the sector.

The primary aim of this study is to produce empirical evidence and provide practical recommendations for improving the implementation of technology within the maritime industry. TAM is a significant theoretical framework that aids in understanding the various aspects that impact the adoption of new technologies by both organizations and individuals. The application of this model to the maritime sector will provide valuable insights into the optimal integration of technology within the industry.

Following the identification of gaps and demands in the existing literature, a comprehensive plan has been devised to effectively conduct the study (Figure 1). The data of the industry that is relevant to the study have been gathered. Following the initial compilation, the dataset was thoroughly examined, where missing data, careless responses, and outlier variables were detected and then eliminated from the dataset. Normality was examined using the Statistical Package for the Social Sciences (SPSS), where the skewness and kurtosis values were assessed. Subsequently, factor analysis was conducted on the statements used in the study.

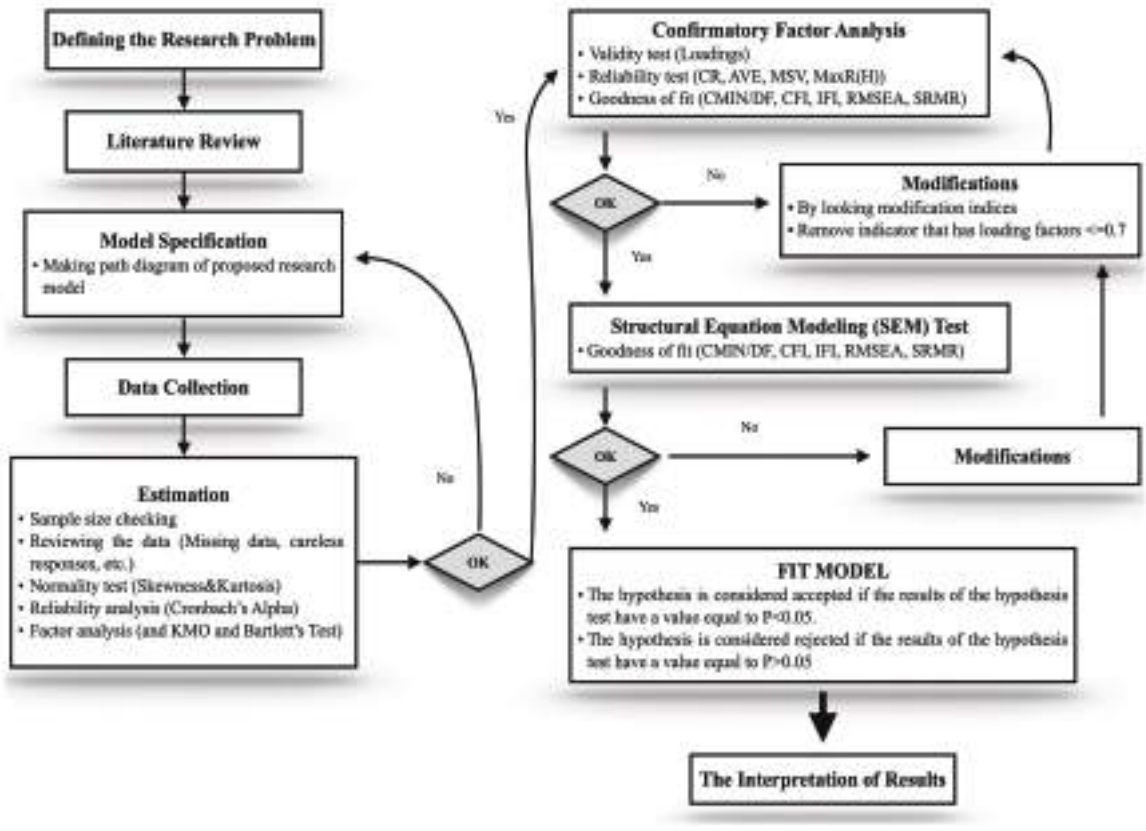

Figure 1. *Steps of the analysis*

3.1. Model Specification and Hypothesis Development

This study aims to enhance the current model by integrating insights derived from pertinent literature and concepts, with a particular focus on the maritime sector. The factors being studied in this study involve PEOU, behavioral intention (BI), PU, and use behavior (UB) as dependent variables. The independent variables in this study include subjective norms (SN), output quality (OQ), result demonstrability (RD), job relevance (JR), computer anxiety (CA), and perceptions of external control (POEC). The succeeding sections provide a detailed elaboration on the links among the variables and the hypotheses offered. The improvement of the model was based on a comprehensive evaluation of existing research. A comprehensive examination and documentation of numerous research domains' detailed analyses of studies related to TAM were conducted, with the findings being recorded in an Excel spreadsheet. The collection of data served as the fundamental basis for constructing our model in a careful and deliberate manner.

SN

SN refer to the societal influences that shape an individual's attitudes and beliefs regarding their engagement or non-engagement in a particular action [33,34]. The significance of SN is crucial within the specific environment being examined because they have a pivotal impact on the acceptance and use of new technology. Additional research on this variable is vital in both scholarly and practical contexts to enhance the implementation of TAMs and digital transformation initiatives. Hypotheses 1a and 1b have been developed for the following reasons:

Hypothesis 1a. SN exerts a substantial influence on PU.

Hypothesis 1b. SN exerts a substantial influence on PEOU.

JR

The concept of JR pertains to an individual's personal assessment of the extent to which a system or technology aligns with their job requirements and objectives [22]. The variable of JR holds significant importance in the realm of study concerning the acceptance and adoption of technology. A thorough analysis of this characteristic will aid companies and individuals in enhancing their technology selection and usage strategies with greater effectiveness. Hypotheses 2a and 2b have been developed on the basis of the aforementioned grounds.

Hypothesis 2a. JR exerts a substantial influence on PU.

Hypothesis 2b. JR exerts a substantial influence on PEOU.

OQ

The variable of OQ pertains to subjective evaluations conducted by individuals regarding the extent to which

a specific technology or system enhances their work performance capabilities [18]. The variable OQ should be regarded as a crucial element in comprehending and operationalizing TAMs and strategies for digital transformation. By engaging in comprehensive studies on the quality of output, organizations and individuals can enhance their ability to effectively manage their technology choices and adaptation processes. Hypotheses 3a and 3b have been developed on the basis of the aforementioned grounds.

Hypothesis 3a. OQ exerts a substantial influence on PU.

Hypothesis 3b. OQ exerts a substantial influence on PEOU.

RD

Variable RD measures individuals' beliefs that employing a new technology will provide tangible and measurable outcomes [31]. In the present setting, it is important to conduct a thorough examination of the variable known as RD to enhance the effect of technology adoption and adaptation processes. This variable can also play a crucial role in efficient and expeditiously assessing the return on investment of a technology expenditure. Hypotheses 4a and 4b have been developed on the basis of the following rationales:

Hypothesis 4a. RD exerts a substantial influence on PU.

Hypothesis 4b. RD exerts a substantial influence on PEOU.

CA

CA is a psychological phenomenon characterized by the presence of anxiety or fear in people during their interactions with technology or computers [23,31]. It is imperative to acknowledge CA as a noteworthy factor within technology adoption models, necessitating the formulation of solutions aimed at mitigating this anxiety. The reduction of anxiety levels is associated with an increased likelihood of swift and efficient adoption of technology within the workplace, thus potentially enhancing job performance in a positive manner. Hypotheses 5a and 5b have been developed for the following reasons:

Hypothesis 5a. CA exerts a substantial influence on PU.

Hypothesis 5b. CA exerts a substantial influence on PEOU.

POEC

Individuals' perceptions of the adequacy of institutional and technological resources for the acceptance and effective utilization of new technologies constitute POEC [23,31]. It is widely recognized as a crucial factor within models of technological acceptance. Organizations must prioritize the allocation of strategies and resources to enhance their perception, as this is crucial for quickening processes of digital transformation and technology adaptation. Hypotheses 6a and 6b have been developed for the following reasons:

Hypothesis 6a. POEC exerts a substantial influence on PU.

Hypothesis 6b. POEC exerts a substantial influence on PEOU.

PEOU

The term "perceived ease of use" describes the perceived amount of work that a person thinks is necessary to use a certain system or technology, as well as their subjective evaluation of this exertion [23,24]. The notion of PEOU plays a considerable role in the acceptance and assimilation of technology within businesses. Organizations can enhance the efficiency and expediency of technology adaptation procedures by considering this factor and implementing user-friendly interfaces, effective training programs, and continuous support mechanisms. Consequently, the subsequent hypotheses, hypothesis 7 and Hypothesis 9, are posited in the following manner:

Hypothesis 7. PEOU exerts a substantial influence on PU.

Hypothesis 9. PEOU exerts a substantial influence on BI.

PU

The concept of PU is a considerable factor that influences consumers' decision-making processes regarding the acceptance and use of specific technologies or systems [21,22]. PU occupies a pivotal role within technology adoption models and tactics of digital transformation. A significant degree of this characteristic can accelerate the process of technology acceptance and have a beneficial influence on the overall work performance of an organization. To promote a perception of high usefulness, firms can execute a range of training programs, initiatives aimed at maximizing user experience, and activities designed to develop staff's technological competencies. Based on the preceding information, we propose the following proposition:

Hypothesis 8. PU exerts a substantial influence on BI.

BI

The construct of BI is a reliable indicator of the likelihood that people will engage in a particular behavior. This idea pertains to an individual's inclination to exhibit a specific behavior and incorporates the various motivational factors that impact the likelihood of the behavior being displayed [33,35,36]. With further examination, it can be shown that there is typically a positive association between BI and UB, namely the tangible use of technology [25]. A thorough understanding of these components is essential for the successful integration and implementation of an innovation in technology. Considering the factors described above, we contend that:

Hypothesis 10. BI has a significant impact on UB.

UB

Within conventional iterations of TAM, considerable attention is frequently allocated to the construct of "intention to use", which functions as a reliable indicator of an individual's inclination to interact with a specific technological innovation. Nevertheless, it is imperative to acknowledge that intentions may not always translate into tangible acts. The concept of "use behavior" becomes pertinent in this context. This dimension explores the empirical component of technology consumption, encompassing the examination of both the actual usage of technology by individuals and the specific manner in which it is employed [21,22,36]. A thorough understanding of the factors that impress "use behavior" is crucial for developing efficient training programs, enhancing system design, and ensuring ongoing support systems. These elements collectively contribute to the successful implementation of the technology under consideration.

In summary, TAM, initially introduced by Davis et al. [30], offers a significant foundational framework for comprehending the psychological and behavioral aspects that could influence an individual's decision to embrace a particular technology. However, a more detailed analysis of "use behavior" provides a more nuanced understanding of the elements that translate BIs into actual actions [37]. Figure 2 depicts the visual representation of the offered theories.

3.2. Data Collection

Prior to the initiation of the data collection process, approval was obtained from the İstanbul Technical University Social and Human Sciences Human Research Ethics Committee (approval no: 315, date: 23.02.2023), ensuring that our study adhered to the ethical standards required for research within the realm of social and human sciences.

During this study, an extensive survey was administered to professionals involved in maritime and port operations. The scientific literature that was already available served as a guide for selecting the sample size. After conducting a comprehensive investigation of the existing scholarly works, it becomes clear that determining the optimal sample size for factor analysis is a multifaceted task, dependent upon numerous variables. Consequently, it is difficult to establish a definitive number. However, the academic literature provides numerous rules and criteria of this subject matter.

A frequently accepted practice in empirical research is to use a sample size ranging from 100 to 200 when the components under investigation are robust and distinguishable and the number of variables being studied is not unduly high. According to existing literature, it is often advised that the sample size should exceed the number of observed variables by a factor of at least five, which is typically regarded as a general heuristic. In situations characterized by robust and dependable associations as

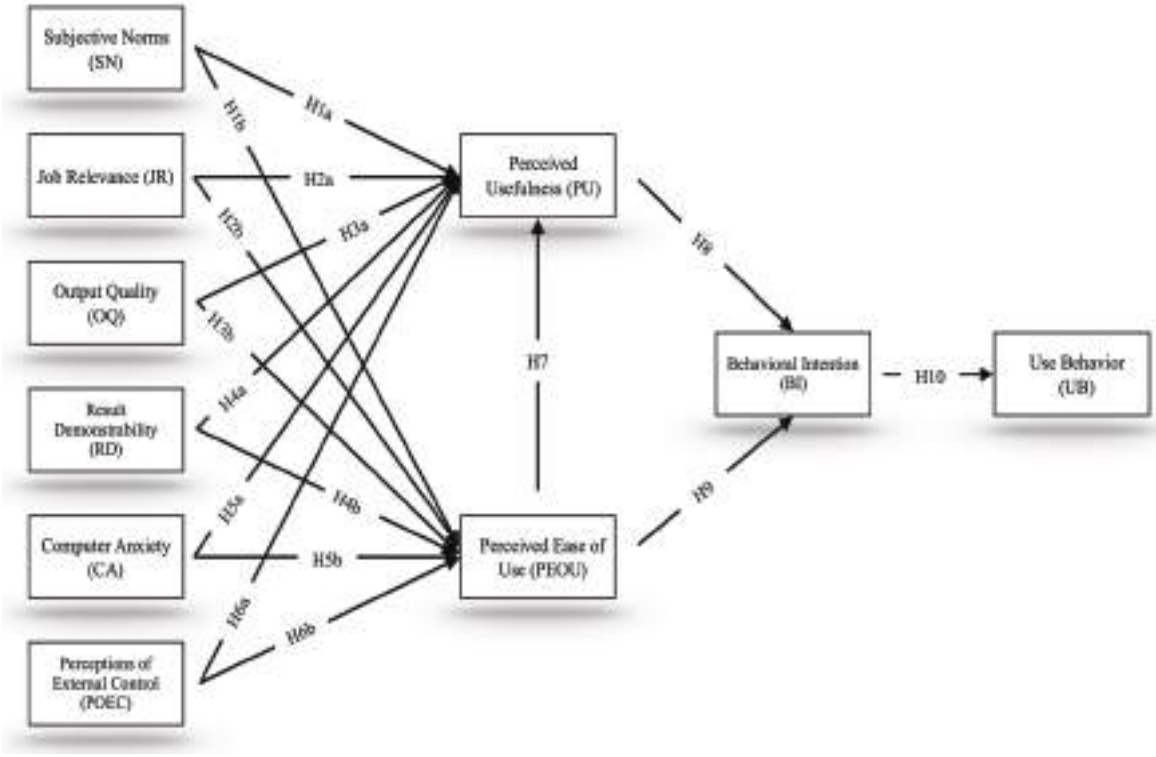

Figure 2. *Representation of the proposed hypotheses*

well as a well-defined factor structure, a sample size as small as 50 may be deemed sufficient, as long as it surpasses the number of variables [38].

These guidelines provide researchers with a framework for many scenarios and contingencies. However, it is important to always consider the particulars of the research environment and aims when establishing a suitable sample size.

The current study involved the collection of data from a sample of 570 people who were actively involved in the maritime logistics industry. Given the wide array of vocational fields within the sector and the inherent difficulties in obtaining sufficient data from each, this study primarily concentrates on two domains: maritime logistics (ship-based), which pertains to activities conducted on ships, and terrestrial logistics (port-based), which encompasses operations carried out in ports.

After the preliminary analysis, 31 questionnaires with careless or inconsistent responses were removed from the dataset. As a result, the final sample size for further analyses consisted of 539 responses. Throughout the data collection process, a comprehensive set of statistical controls was implemented, which encompassed various procedures such as assessing normal distribution, conducting reliability assessments, and performing factor analyses. The subsequent portions of the study will offer a comprehensive analysis and understanding of the results obtained by employing these specific methodological approaches.

After eliminating outliers from our dataset, we analyzed demographic characteristics. Data were classified based on gender, age, professional experience, educational attainment, and occupational field. The findings of the analyses are shown in Table 1.

4. Results

Before conducting the study, the dataset was subjected to a normality examination, which involved examining the kurtosis and skewness of individual variables. The thresholds for these measures were determined to be ±1, in accordance with accepted statistical recommendations [39]. The results obtained indicate that both the kurtosis and skewness values were within the range of ±1, suggesting that there was no substantial departure from normalcy [40]. On the basis of the aforementioned observations, it may be inferred that the dataset conforms to the normal distribution, exhibiting no discernible abnormalities associated with normality.

4.1. Evaluation of the Model's Discriminant and Convergent Validity

The evaluation of the suitability of the dataset employed in this study involved an examination of the Kaiser-Meyer-Olkin (KMO) measure of sampling adequacy. The KMO statistic in SPSS is used as a metric to evaluate the adequacy of the sample size for factor analysis, as stated by Field [41]. This statistical analysis was derived from the examination of correlations and partial correlations among all variables. In essence, it quantifies the extent to which a certain variable may be elucidated isolated from all other variables. According to Hair [42], a KMO value equal to or greater than 0.60 is typically deemed satisfactory for factor analysis. The KMO value obtained for this investigation was determined to be 0.942, indicating a substantial degree of adequacy in the sampling process.

This study seeks to analyze the intricate mechanisms that influence technology adoption in this particular business by employing confirmatory factor analysis (CFA) as a fundamental analytical method. The purpose of the CFA model is to assess the validity and reliability of the theoretical framework that elucidates the adoption of technology. This analysis offers valuable insights into the structural integrity and internal coherence of the scale.

To validate the proposed model, various fit indices were employed to assess how well the model matches observed data. These encompass measures that gage the model's overall fit, the relationship between observed and expected covariance, and other fit statistics. In addition, the study integrates several reliability and validity metrics to thoroughly evaluate the consistency of the measurements and the distinction between the constructs.

Table 1. *Demographic information (n=539)*

Categories		Number of participants	Rate (%)
Gender	Women	149	27.6
	Men	390	72.4
Age	21-30	73	13.5
	31-40	303	56.2
	41-50	110	20.4
	51-60	44	8.2
	61 and over	9	1.7
Education	Associate degree	12	2.3
	Bachelor's degree	390	72.3
	Graduate degree	137	25.4
Professional experience	1-5 years	122	22.6
	6-10 years	117	21.7
	11-15 years	146	27.1
	16-25 years	141	26.2
	26 years and over	13	2.4
Field of occupation	Ship-based	156	28.9
	Port-based	383	71.1

Given these factors, the outcomes of the assessments of validity and reliability are displayed in Table 2. After careful examination, it can be noticed that all values fall within acceptable ranges.

In the realm of evaluating the validity and reliability of the models, a thorough examination of multiple criteria was conducted with considerable attention to detail. The convergence dependability of the study was supported by the average variance extracted (AVE) values, which surpassed the established threshold of 0.5 for all latent constructs. The presence of internal consistency was demonstrated by the consistent surpassing of the 0.7 benchmark by the composite reliability (CR) values. Furthermore, the dependability of the indicators was confirmed by all measures, which showed Cronbach's alpha values exceeding 0.7. The affirmation of discriminant validity was achieved

Table 2. *Validity and reliability tests*

Latent variable	Items	Loadings	α	CR	AVE	MSV	MaxR (H)
Perceived usefulness	PU1	0.77	0.912	0.903	0.571	0.561	0.906
	PU2	0.79					
	PU3	0.799					
	PU4	0.768					
	PU6	0.699					
	PU7	0.676					
	PU8	0.78					
Perceived ease of use	PEOU1	0.755	0.912	0.902	0.536	0.468	0.904
	PEOU2	0.746					
	PEOU3	0.73					
	PEOU6	0.682					
	PEOU7	0.724					
	PEOU8	0.681					
	PEOU9	0.738					
	PEOU10	0.794					
Subjective norms	SN1	0.781	0.824	0.827	0.614	0.468	0.828
	SN2	0.763					
	SN3	0.806					
Job relevance	JR1	0.771	0.800	0.802	0.670	0.464	0.815
	JR2	0.864					
Output quality	OQ1	0.822	0.801	0.802	0.670	0.381	0.802
	OQ2	0.815					
Perceptions of external control	POEC2	0.885	0.782	0.797	0.664	0.110	0.828
	POEC3	0.738					
Computer anxiety	CA1	0.854	0.894	0.895	0.741	0.487	0.900
	CA2	0.895					
	CA3	0.832					
Result demonstrability	RD1	0.838	0.825	0.829	0.708	0.342	0.829
	RD2	0.845					
Behavioral intention	BI1	0.781	0.817	0.852	0.659	0.561	0.857
	BI2	0.851					
	BI3	0.801					
Use behavior	UB1	0.897	0.845	0.852	0.659	0.411	0.877
	UB2	0.818					
	UB3	0.709					
CMIN/DF: 2.812, SRMR: 0.0432, CFI: 0.920, RMSEA: 0.058, IFI: 0.921							

by observing that the maximum shared variance values continually exhibited lower values than their corresponding AVE measures. In addition, the MaxR (H) values were used to assess the explanatory capacity of individual factors. Higher values were seen as evidence of greater contributions of the factors to the overall variance in the dataset.

The researchers employed a measurement model to systematically investigate the factor loadings of observable variables on their respective latent components. The model's structural validity was rigorously evaluated using CFA. The model was subjected to thorough validation procedures that included assessments of both discriminant and convergent validities, as well as reliability metrics, in accordance with the criteria established by Hair [39]. The data shown in Table 2 demonstrate that all constructs in the model achieved a CR score that exceeded the stated threshold of 0.7, thereby confirming the model's dependability. Furthermore, it is worth noting that the factor loadings and AVE values in this study exceeded the minimum standards of 0.7 and 0.5, respectively, as established by Hair et al. [43]. This finding provides additional support for the strong validity of the model. The discriminant and convergent validity were assessed by examining the variance-covariance matrix between the measurement items and their corresponding latent variables. Concurrently, Table 3 provides an illustration of the values that meet the criteria for establishing discriminant validity. The comprehensive statistical analysis supports the sufficiency of the model in accurately capturing the facts. Similarly, the reliability of the questionnaire was validated by employing a cut-off score of 0.7 [44].

4.2. Structural Model (SM) Evaluation

The primary objective of this study was to investigate the relationships between relevant variables and evaluate the effectiveness of a specified theoretical framework. The researchers opted for structural equation modeling (SEM) as the methodological framework to evaluate the adequacy of the proposed model. SEM was selected because of its capability to model intricate connections among various variables and specifically for its capacity to manage latent variables and measurement errors [43].

To conduct SEM analysis on the collected data, a two-step methodology was employed. The measurement model involved performing CFA using AMOS software to establish the connections between observable and latent variables. Following this, the researchers conducted an empirical examination of SEM to assess the hypothesized correlations between the dependent and independent variables. The adequacy of the SEM model was assessed by examining the coefficient parameters and goodness-of-fit indices in accordance with the criteria established in previous scholarly works [43,45].

The SEM results for the causal links of the hypothesized model, and the R^2 results, are depicted in Figure 3. The significance values for all paths were assessed at a p-value of 0.05. In SEM, the coefficient of determination (R^2) gages how well independent variables account for the variability in the dependent variable. To enhance the goodness-of-fit of the SM, covariances were introduced between the error terms. The incorporation of these covariances led to a noticeable improvement in the fit indices of the model.

Accurate representation of data using the suggested model is highly significant, requiring assessment using several fit indices. The indices encompass various fit measures, namely χ^2, RMSEA, CFI, IFI, and SRMR. These indices are frequently used in both CFA and SEM assessments. Based on the data provided in Table 4, fit indices such as CMIN/df, CFI, IFI, RMSEA, and SRMR indicate satisfactory compliance with the accepted criteria.

Table 3. *Discriminant validity*

	PU	PEOU	SN	JR	OQ	POEC	CA	RD	BI	UB
PU	**0.756**									
PEOU	0.674	**0.732**								
SN	0.660	0.684	**0.784**							
JR	0.550	0.574	0.595	**0.819**						
OQ	0.591	0.570	0.617	0.532	**0.819**					
POEC	0.294	0.332	0.118	0.159	0.282	**0.815**				
CA	0.578	0.524	0.501	0.559	0.428	0.264	**0.861**			
RD	0.575	0.542	0.585	0.519	0.564	0.206	0.489	**0.842**		
BI	0.749	0.609	0.599	0.681	0.522	0.153	0.698	0.562	**0.812**	
UB	0.641	0.506	0.376	0.442	0.348	0.314	0.429	0.420	0.531	**0.812**

PU: Perceived usefulness, PEOU: Perceived ease of use, SN: Subjective norms, JR: Job relevance, OQ: Output quality, POEC: Perceptions of external control, CA: Computer anxiety, RD: Result demonstrability, BI: Behavioral intention, UB: Use behavior

Table 4. *Summary of fit indices*

Fit Indices	CMIN/DF	CFI	IFI	RMSEA	SRMR
Acceptable fit	<5	>0.90	>0.90	<0.08	<0.08
Obtained fit CFA	2.812	0.920	0.921	0.058	0.043
Obtained fit SEM	3.080	0.906	0.907	0.062	0.054

Table 5 presents an overview, encapsulating the outcomes of the hypothesis testing conducted in this study. This table is prepared to provide a clear and concise summary of the hypotheses that were supported and those that were not, based on the empirical data analyzed. The acceptance or rejection of these hypotheses is grounded in statistical significance and adheres to the standards of the adopted methodology.

5. Discussion of the Findings

The results from the AMOS analysis clearly support the significant influence of all variables examined in this study. SN had a significant impact on both PU (H1a: β=0.293, p<0.05) and PEOU (H1b: β=0.413, p<0.05). The magnitude of these β-coefficients emphasizes the considerable role of SN in affecting both PU and PEOU. The findings underscore the critical impact of SN on shaping individuals' acceptance and approaches towards adopting new technologies, reinforcing the necessity to consider subjective norms in understanding technology adoption dynamics.

Based on the SEM analysis, it is evident that JR significantly influences PEOU (H2b: β=0.172, p<0.05), indicating a favorable relationship. However, no statistically significant relationship was observed between JR and PU (H2a: p>0.05). While JR's effect on PEOU is significant, its impact on PU remains undetermined. Notably, similar studies have yielded mixed results regarding JR's impact on PU, with some findings indicating a negligible influence [46], while others report a significant effect [47,48]. This highlights the complexity of JR's relationship with PU and the need for further investigation, especially in the context of technology adoption.

The analysis of SEM reveals a significant relationship between OQ and PU (H3a: β=0.151, p<0.05), indicating that as OQ increases, PU also improves. However, no significant relationship was found between OQ and PEOU (H3b: p>0.05). These findings suggest that while OQ impacts PU, it does not significantly influence PEOU. Hart and Porter [49], in their research on on-line analytical processing, discovered a positive correlation between OQ and PU, thereby affirming OQ's influence on PU. Similarly, Davis et al. [50] observed a positive impact of OQ on PU in their examination of computer technology.

The findings of the study indicate that RD had a significant effect on PU (H4a: β=0.147, p<0.05) but did not have a significant impact on PEOU (H4b: p>0.05). SEM analysis confirmed a notable association between RD and PU, with a β value of 0.147, reflecting a moderate effect size. Despite its significance for PU, the p-value for the RD-PEOU relationship surpassed the 0.05 threshold, indicating its lack of significance within this dataset. This aligns with various studies in the literature, where RD is frequently observed to positively influence PU in different contexts [22,49]. In essence, RD emerges as a key factor in shaping user opinions on technology's utility but does not appear to affect their views on its usability.

The presence of CA had a statistically significant impact on both PU (H5a: β=0.237, p<0.05) and PEOU (H5b: β=0.100, p<0.05). The SEM study indicates a significant relationship between CA and both PU and PEOU, with the standardized beta coefficients being 0.237 for PU and 0.100 for PEOU, both significant at the 0.05 level. As CA increases, there is a corresponding decrease in the perception of the usefulness and ease of use of computer applications. These findings underscore the ramifications of CA on technology usage and are supported by other studies in the literature, highlighting the influence of CA on technology adoption and user experience [51-54].

The study found that POEC had a statistically significant effect on PEOU (H6b: β=0.172, p<0.05). However, it did not have a significant influence on PU (H6a: p>0.05). SEM results underscored POEC's influence on PEOU, with a β of 0.172, significant at the 5% level. This suggests that individuals perceiving higher external control are more likely to find the system user-friendly. However, POEC's impact on PU was found to be insignificant, suggesting that PU and PEOU are influenced differently by external control factors. These findings align with various studies in the field. Fisher [55] highlighted the importance of external factors in shaping technology perceptions. Venkatesh [23] integrated external factors into the TAM, emphasizing their role. Additionally, research by Abbad et al. [56] in Jordan's banking sector supports the idea that external variables significantly influence PEOU, corroborating the impact of external control on technology acceptance. These studies affirm that external factors such as POEC significantly influence PEOU, as observed in this study, but their impact on PU may differ.

The study revealed that PEOU had a significant impact on both PU (H7: β=0.203, p<0.05) and BI (H9: β=0.331, p<0.05). SEM analysis supports these associations, with both p-values indicating statistical significance at the 5% alpha level. The positive β coefficients suggest that as perceptions of a system's ease of use rise, there is a corresponding increase in its PU and BI. In summary, user friendliness

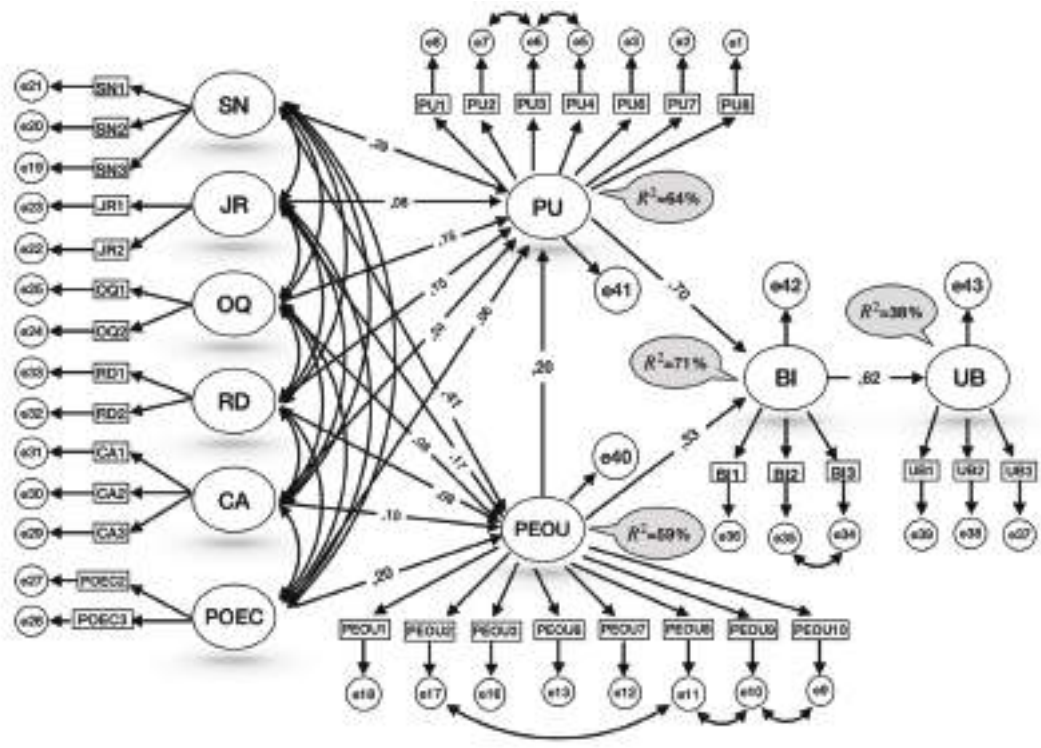

Figure 3. *Output produced by the structural model (SM)*

Table 5. *Hypotheses testing results*

Hypotheses	Impact	β value	P	Status
H1a	SN→PU	0.293	0.001	Acceptance
H1b	SN→PEOU	0.413	***	Acceptance
H2a	JR→PU	0.08	0.115	Rejection
H2b	JR→PEOU	0.172	0.002	Acceptance
H3a	OQ→PU	0.15	0.019	Acceptance
H3b	OQ→PEOU	0.08	0.161	Rejection
H4a	RD→PU	0.15	0.010	Acceptance
H4b	RD→PEOU	0.08	0.126	Rejection
H5a	CA→PU	0.24	***	Acceptance
H5b	CA→PEOU	0.10	0.042	Acceptance
H6a	POEC→PU	0.06	0.165	Rejection
H6b	POEC→PEOU	0.20	***	Acceptance
H7	PEOU→PU	0.20	***	Acceptance
H8	PU→BI	0.70	***	Acceptance
H9	PEOU→BI	0.33	***	Acceptance
H10	BI→UB	0.62	***	Acceptance

PU: Perceived usefulness, PEOU: Perceived ease of use, SN: Subjective norms, JR: Job relevance, OQ: Output quality, POEC: Perceptions of external control, CA: Computer anxiety, RD: Result demonstrability, BI: Behavioral intention, UB: Use behavior

is pivotal in shaping users' views on a system's value and their inclination to engage with it. This finding aligns with numerous studies in the literature that consistently demonstrate the significant influence of PEOU on both PU and BI in various technological contexts [21,22,30].

PU was found to have a statistically significant positive effect on BI (H8: β=0.703, p<0.05). The SEM analysis showed a robust association between PU and BI, with a substantial β of 0.703, significant at the 5% alpha level. This indicates that users are more likely to use a system they perceive as useful. In conclusion, these results reinforce the pivotal role of PU in determining users' bis, aligning with the core principles of TAM. This is supported by extensive research in the literature, validating the positive impact of PU on BI as a fundamental assertion of TAM [21,22,48].

The variable of BI had a significant impact on UB (H10: β=0.618, p<0.05). SEM analysis confirmed this association with a standardized beta coefficient of 0.618, which was statistically significant at the 5% alpha level. This suggests that an increase in BI correlates with a rise in UB. These findings indicate that BI is a key predictor of UB, thereby reaffirming the core tenets of TAM. Numerous studies in the literature also find BI to be a crucial factor influencing actual system use, validating the importance of BI and UB in TAM for predicting technology adoption [21,22,30].

6. Conclusion

This research has elucidated the intricate dynamics between various independent variables and their collective impact on the dependent variable, offering valuable insights that

can inform the development of more nuanced and effective strategies. This study has crafted a detailed analytical tool, shedding light on the multifaceted interactions and relationships within the theoretical model applied to the digital transformation of the maritime transportation logistics sector.

The results corroborate the significance of classical factors such as PU and PEOU in the TAM, especially in the context of the maritime transportation logistics industry's digital transformation. Furthermore, specific determinants such as industry characteristics and digital capabilities were also found to be instrumental. Notably, investment in digital technologies and the enhancement of digital capabilities have emerged as decisive factors for swift and effective adaptation to digital transformation within the maritime logistics sector. This underscores the imperative for organizations to foster and expand their digital capabilities to take the lead in adopting and implementing digital technologies, thereby securing a competitive edge.

The outputs also acknowledge the separate impact of different aspects, including CA, SN, OQ, JR, POEC, and RD. Each of the aforementioned variables exhibits varied degrees of interaction with PU and PEOU, consequently influencing the dynamics of digital adoption within the maritime logistics sector. Furthermore, beliefs concerning external control, particularly institutional support and infrastructural readiness, emerge as significant, emphasizing the essential role of organizations in adeptly spearheading digital initiatives and fostering a conducive environment for digital transformation.

The aforementioned insights play a crucial role in comprehending the present condition of digital integration in maritime transportation logistics. However, they also emphasize the necessity for continuous study to completely unravel the intricate nature of digital transformation. The ongoing investigation is essential for determining the most effective approaches to effectively include and assimilate digital technologies in this field.

The proposed research has a limitation that needs to be addressed. A single country was the source for selecting 539 participants. Conducting a study that involves participants from different countries can improve this study. Additionally, the research methodology was confined to the use of SEM and TAM. Moreover, enhancing geographical representation and refining data gathering methodologies will contribute to enhancing the comprehensiveness of the study. It might be advisable for future studies to conduct a study in which maritime sector employees assess the factors that influence the digital transformation process using multi-criteria decision-making methods to improve the results of this study.

Acknowledgments

This article is based on a doctoral thesis entitled "An Analysis of the Adaptation of Maritime Transportation Logistics to the Digital Transformation Process through the Technology Acceptance Model". The research was carried out within the Maritime Transportation Engineering Department of the Graduate School at İstanbul Technical University.

Authorship Contributions

Concept design: O. Gündoğan, and T. Keçeci, Data Collection or Processing: O. Gündoğan, and T. Keçeci, Analysis or Interpretation: O. Gündoğan, Literature Review: O. Gündoğan, Writing, Reviewing and Editing: O. Gündoğan, and T. Keçeci.

Funding: The authors declare that no funds, grants, or other support was received during the preparation of this manuscript.

References

[1] E. Tijan, M. Jović, S. Aksentijević, and A. Pucihar, "Digital transformation in the maritime transport sector." *Technological Forecasting and Social Change*, vol. 170, 120879, Sep 2021.

[2] M. Jović, E. Tijan, D. Vidmar, and A. Pucihar. "Factors of digital transformation in the maritime transport sector." *Sustainability,* vol. 14, pp. 9776, Aug 2022

[3] J. Kern, The digital transformation of logistics: a review about technologies and their implementation status. In book: The Digital Transformation of Logistics, pp. 361-403, Apr 2021.

[4] C. Dong, A. Akram, D. Andersson, P. O. Arnäs, and G. Stefansson, "The impact of emerging and disruptive technologies on freight transportation in the digital era: current state and future trends." *The International Journal of Logistics Management*, vol. 32, pp. 386-412, Apr 2021.

[5] T. Song, et al. "A review of artificial intelligence in marine science." *Frontiers in Earth Science*, vol. 11, 1090185, Feb 2023.

[6] K. Czachorowski, M. Solesvik, and Y. Kondratenko, "The application of blockchain technology in the maritime industry." *Green IT Engineering: Social, Business and Industrial Applications*, vol. 171, 2019;561-567.

[7] A. Devaraju, L. Chen, and R. R. Negenborn, "Autonomous surface vessels in ports: applications, technologies and port infrastructures." *Computational Logistics*, vol. 11184, pp. 86-105 Sep 2018.

[8] W. Wasilewski, K. Wolak, and M. Zaraś, "Autonomous shipping. The future of the maritime industry?" *Zeszyty Naukowe Małopolskiej Wyższej Szkoły Ekonomicznej w Tarnowie*, vol. 51, pp. 155-163, Sep 2021.

[9] W. A. Ahmed, and A. Rios, "Digitalization of the international shipping and maritime logistics industry: a case study of TradeLens." *The Digital Supply Chain,* pp. 309-323, 2022.

[10] V. Babica, D. Sceulovs, and E. Rustenova, "Digitalization in maritime industry: prospects and pitfalls." *ICTE in Transportation and Logistics,* pp. 20-27, 2020.

[11] A. M. Gomez-Trujillo, and M. A. Gonzalez-Perez, "Digital transformation as a strategy to reach sustainability." *Smart and Sustainable Built Environment*, vol. 11, pp. 1137-1162, Dec 2022.

[12] R. S. Al-Maroof, S. A. Salloum, A. Q. M. AlHamadand, and K. Shaalan, *"A unified model for the use and acceptance of stickers in social media messaging."* AISI 2019: Proceedings of the International Conference on Advanced Intelligent Systems and Informatics 2019, pp. 370-381, Oct 2019.

[13] M. Hubert, M. Blut, C. Brock, R. W. Zhang, V. Koch, and R. Riedl, "The influence of acceptance and adoption drivers on smart home usage." *European Journal of Marketing*, vol. 53, pp. 1073-1098, Sep 2018.

[14] Na S, Heo S, Han S, Shin Y, Roh Y. Acceptance Model of Artificial Intelligence (AI)-Based Technologies in Construction Firms: Applying the Technology Acceptance Model (TAM) in Combination with the Technology–Organisation–Environment (TOE) Framework. *Buildings*, vol. 12, pp. 90, Jan 2022.

[15] S. Schubring, I. Lorscheid, M. Meyer, C. M. Ringle, "The PLS agent: Predictive modeling with PLS-SEM and agent-based simulation." *Journal of Business Research*, vol. 69, pp. 4604-4612, Oct 2016.

[16] M. Del Giudice, A. Di Vaio, R. Hassan, and R. Palladino, "Digitalization and new technologies for sustainable business models at the ship–port interface: a bibliometric analysis." *Maritime Policy & Management*, vol. 49, pp. 410-446, 2022.

[17] Z. H. Munim, M. Dushenko, V. J. Jimenez, M. H. Shakil, and M. Imset, "Big data and artificial intelligence in the maritime industry: a bibliometric review and future research directions." *Maritime Policy & Management,* vol. 47, pp. 577-597, Jun 2020.

[18] M. A. Ben Farah, et al. "Cyber security in the maritime industry: a systematic survey of recent advances and future trends." *Information,* vol. 13, pp. 1-33, 2022.

[19] S. Singh, and B. Sengupta, "Sustainable maritime transport and maritime informatics." *Maritime Informatics*, In: Lind, M., Michaelides, M., Ward, R., T. Watson, R. (eds) Maritime Informatics. Progress in IS. Springer, Cham. pp. 81-95, 2021.

[20] D. Yang, L. Wu, S. Wang, H. Jia, and K. X. Li, "How big data enriches maritime research - a critical review of Automatic Identification System (AIS) data applications." *Transport Reviews*, vol. 39, pp. 755-773, Jul 2019.

[21] F. D. Davis. "Perceived usefulness, perceived ease of use, and user acceptance of information technology." *MIS Quarterly*, vol. 13, pp. 319-340, Sep 1989.

[22] V. Venkatesh, and F. D. Davis, "A theoretical extension of the technology acceptance model: Four longitudinal field studies." *Management Science*, vol. 46, pp. 186-204, Feb 2000.

[23] V. Venkatesh, "Determinants of perceived ease of use: Integrating control, intrinsic motivation, and emotion into the technology acceptance model." *Information Systems Research*, vol. 11, pp. 342-365, Dec 2000.

[24] D. A. Adams, R. R. Nelson, and P. A. Todd, "Perceived usefulness, ease of use, and usage of information technology: a replication." *MIS Quarterly*, vol. 16, pp. 227-247, Jun 1992.

[25] K. Mathieson, "Predicting user intentions: comparing the technology acceptance model with the theory of planned behavior." *Information Systems Research*, vol. 2, pp. 173-191, Sep 1991.

[26] F. D. Davis, and V. Venkatesh, "A critical assessment of potential measurement biases in the technology acceptance model: three experiments." *International Journal of Human-Computer Studies*, vol. 45, pp. 19-45, Jul 1996.

[27] S. S. Al-Gahtani, "Empirical investigation of e-learning acceptance and assimilation: A structural equation model." *Applied Computing and Informatics*, vol. 19, pp. 27-50, Jan 2016.

[28] B. Kijsanayotin, S. Pannarunothai, S. M. Speedie, "Factors influencing health information technology adoption in Thailand's community health centers: applying the UTAUT model." *International Journal of Medical Informatics,* vol. 78, pp. 404-416, Jun 2009.

[29] D. Gefen, E. Karahanna, and D. W. Straub, "Trust and TAM in online shopping: an integrated model." *MIS Quarterly*, vol. 27, pp. 51-90, Mar 2003.

[30] F. D. Davis, R. P. Bagozzi, and P. R. Warshaw, "User acceptance of computer technology: a comparison of two theoretical models." *Management Science*, vol. 35, pp. 982-1003, Aug 1989.

[31] V. Venkatesh, and H. Bala, "Technology acceptance model 3 and a research agenda on interventions." *Decision Sciences*, vol. 39, pp. 273-315, May 2008.

[32] A. H. Turan, and F. B. Özgen, "Adoption of e-declaration system in Turkey: an empirical assessment with the extended technology acceptance model. *Dogus University Journal,* vol. 10, pp. 134-147, Jan 2009.

[33] M. Fishbein, and I. Ajzen, "Belief, attitude, intention, and behavior: An introduction to theory and research." Reading, MA: Addison-Wesley, May 1975.

[34] I. Ajzen, "Understanding attitudes and predictiing social behavior." *Englewood Cliffs*, J: Prentice-Hall, 1980.

[35] G. C. Moore, and I. Benbasat, "Development of an instrument to measure the perceptions of adopting an information technology innovation." *Information Systems Research*, vol. 2, pp. 192-222, Sep 1991.

[36] I. Ajzen, "The theory of planned behavior." *Organizational Behavior and Human Decision Processes*, vol. 50, pp. 179-211, Dec 1991.

[37] W. R. King, and J. He, "A meta-analysis of the technology acceptance model." *Information & Management*, vol. 43, pp. 740-755, Sep 2006.

[38] B. G. Tabachnick, and L. S. Fidell*, "Using multivariate statistics*." 6th ed. 2001.

[39] B. G. Tabachnick, L. S. Fidell, and J. B. Ullman, "*Using multivariate statistics*." 6th ed. Boston, MA: Pearson, 2013.

[40] D. George, and P. Mallery, "*IBM SPSS statistics 26 step by step."* 16th ed. Routledge, 2019.

[41] A, Field, "*Discovering statistics using IBM SPSS statistics.*" 5th ed. UK, 2009.

[42] J. F. Hair, "*Multivariate data analysis.*" 2009.

[43] J. F. Hair, W. C. Black, B. J. Babin, and R. E. Anderson, "Advanced diagnostics for multiple regression: a supplement to multivariate data analysis: multivariate data analysis." P. Prentice, Hall Publishing, 2010.

[44] J. C. Nunnally, and I. H. Bernstein. Psychometric theory. *McGraw-Hill*. 1967.

[45] B. M. Byrne, "Structural equation modeling with AMOS." *Basic Concepts, Applications, And Programming (Multivariate Applications Series). Taylor & Francis Group,* 2010; 7384.

[46] F. Purwantoro, B. Purwandari, and M. R. Shihab, "*E-audit system acceptance in the public sector: An Indonesian perspective*." In ICACSIS 2015 - 2015 International Conference on Advanced Computer Science and Information Systems, Proceedings, pp. 189-194, 2015.

[47] M. G. Ogundeji, E. Oluwakayode, and O. M. Tijani, "Critical factors of XBRL adoption in Nigeria: A case for semantic model-based digital financial reporting." *Computer Science and Information Technology,* vol. 2, pp. 45-54, 2015.

[48] S. Okcu, G. Hancerliogullari Koksalmis, E. Basak, and F. Calisir, "Factors affecting intention to use big data tools: an extended technology acceptance model." In: Calisir, F., Cevikcan, E., Camgoz Akdag, H. (eds) Industrial Engineering in the Big Data Era. Lecture Notes in Management and Industrial Engineering. Springer, Cham. pp. 401-416, Jan 2019.

[49] M. Hart, and G. Porter, "The impact of cognitive and other factors on the perceived usefulness of OLAP." *Journal of Computer Information System,* vol. 45, pp. 47-56, Jan 2016.

[50] F. D. Davis, R. P. Bagozzi, and P. R. Warshaw, "Extrinsic and intrinsic motivation to use computers in the workplace 1." *Journal of Applied Social Psychology,* vol. 22, pp. 1111-1132, 2006

[51] R. L. Divine, J. H. Wilson, and H. G. Daubek, "Antecedents of student attitudes toward computers." *Journal of Marketing Education,* vol. 19, pp. 54-65, 1997.

[52] B. Hasan, "Effectiveness of computer training: the role of multilevel computer self-efficacy." *Journal of Organizational and End User Computing (JOEUC),* vol. 18, pp. 50-68, Jan-Mar 2006.

[53] B. Hasan, and M. U. Ahmed, "A path analysis of the impact of application-specific perceptions of computer self-efficacy and anxiety on technology acceptance." *Journal of Organizational and End User Computing,* vol. 22, pp. 82-95, Jul 2010.

[54] M. Igbaria, S. J. Schiffman, and T. J. Wieckowski, "The respective roles of perceived usefulness and perceived fun in the acceptance of microcomputer technology." *Behaviour & Information Technology,* vol. 13, pp. 349-361, 1994.

[55] C. Fisher, "The impact of perceived environmental uncertainty and individual differences on management information requirements: A research note." *Accounting, Organizations and Society,* vol. 21, pp. 361-369, May 1996.

[56] M. Abbad, G. Alkhatib, K. A. Qeisi, and F. Jaber, "Jordan banks' perceptions of customer relationship management: a TAM-based investigation." *Journal for Global Business Advancement,* vol. 12, pp. 820-838, 2019.

Journal of ETA Maritime Science 2024;12(1):106-114

LNG Shipping as a Diversification Tool for Energy Security: The Impact of the Ukraine-Russia War on LNG Ship Orders

Abdullah Açık

Dokuz Eylül University, Faculty of Maritime, Department of Maritime Business Administration, İzmir, Türkiye

Abstract

Natural gas is one of the most important energy sources used in many fields since ancient times. Because it is monopolized by some countries due to its random distribution throughout the world, it can be difficult to supply this energy source in times of crisis with its suppliers. The most recent example of this is the war between Russia and Ukraine. Especially since European countries are mostly dependent on Russia and have problems in gas supply, they have turned to LNG transportation for resource diversification and increased demand. On the other hand, increasing demand caused a backlog in LNG ship orders. In this study, we aimed to determine whether there is a structural break in the order amounts of LNG ships, especially due to the recent war. As a result of the structural break analysis applied to monthly data, it was determined that an increase in orders started months before the war and that the highest orders of all time were placed during the war period. This situation can be explained by the fact that European countries accelerate their LNG infrastructure investments in order not to experience the problems brought by high dependency again, and this situation increases the high demand expectations in the sector and increases ship orders. Thus, the LNG market will continue to be an important sector in ensuring energy supply security in the near future.

Keywords: Shipbuilding, Energy security, Liquefied natural gas

1. Introduction

Natural gas is one of the most important fuel types known and used since ancient times. While resources near the surface could have been used economically in the past, nowadays its accessibility and global trade volume have increased thanks to the development of drilling techniques, pipeline projects, and widespread liquid natural gas (LNG) technologies [1]. In 2021, approximately 24.4% of the total energy consumption in the world was provided by natural gas [2]. It is generally used as an energy source for heating in homes, as a fuel in power plants, as an input in the production of products in industry, as a diversification tool in the energy security of countries, and as a transition fuel in projects that reduce environmental pollution.

However, the fact that natural gas resources are concentrated in certain countries may in some cases threaten the energy security of countries. As of 2020, Russia has 19.9% of the world's proved reserves and ranks first in the world in this regard. It is followed by Iran with 17.1% and Qatar with 13.1%. Russia alone accounts for 23.6% of the world's natural gas exports and ranks first in the world in this regard. This dominant role causes many countries to depend on Russia for natural gas energy resources. European countries' dependence on Russia for natural gas is very high and is at a level that can cause political disapproval [3]. As of 2021, European countries supply 71.7% of their total natural gas imports from Russia through the pipeline. They also supply 16% of their total LNG imports from Russia. The natural gas that Europe supplies from Russia via pipelines and LNG ships constitutes 54% of its total imports [2]. However, because of the sabotage that occurred in the Nord Stream in September 2022, there were problems in the gas flow from Russia to Europe [4]. In December 2022, natural gas flow from Russia to Europe decreased by 79% compared with the same month

Address for Correspondence: Abdullah Açık, Dokuz Eylül University Faculty of Maritime, Department of Maritime Business Administration, İzmir, Türkiye
E-mail: abdullah.acik@deu.edu.tr
ORCID ID: orcid.org/0000-0003-4542-9831

Received: 09.06.2023
Last Revision Received: 24.01.2024
Accepted: 31.01.2024

To cite this article: A. Açık, "LNG Shipping as a Diversification Tool for Energy Security: The Impact of the Ukraine-Russia War on LNG Ship Orders." *Journal of ETA Maritime Science*, vol. 12(1), pp. 106-114, 2024.

in 2021 [5]. European countries are attempting to solve this gap in their energy needs by primarily turning to coal [6] and extending the life of existing nuclear power plants [7].

On the other hand, the US, as one of the main LNG providers in the world, has turned the energy crisis between Europe and Russia into an opportunity and has become one of the main energy providers in the European market [8]. While the European market accounted for 34% of the total US LNG exports in 2021, this rate increased to 68% in 2022. In addition, LNG exported to Europe increased by 119% in 2022 compared to 2021 [9]. Moreover, there are even those who argue that the Nord Stream incident could have been a sabotage of the US state [10]. As a result of this event, while obtaining a large market for its LNG industry, the US also had the opportunity to increase its influence in Europe with a factor other than military power.

With the restriction of gas flow from Russia to Europe, especially with the Nord Stream event, and the increase in Europe's global demand, LNG supply increased by 5.5% in 2022 compared to 2021. Due to the increasing demand for LNG in Europe and the insufficient infrastructure, congestion has occurred at LNG terminals around Europe, and thus the amount of LNG on floating platforms broke a record in the last quarter of 2022. For this reason, especially Germany has started the construction of LNG import structures in numerous capacities. Thus, it plans to increase its energy security by increasing its gas supply and storage capacity via LNG [11]. Due to all these factors, the awareness of other countries to ensure energy security by diversifying their energy supply, especially by LNG ships, has increased. Thus, the demand for LNG ships will increase, and naturally, as there will be a shortage in the market, freight rates will also increase. In this case, shipowners may want to order new ships to meet demand sustainably and to obtain more returns from high freight levels in the market. It was basically the war between Russia and Ukraine that destroyed the perspective of countries on energy security and encouraged them to generate a new paradigm. Therefore, the period when gas flow problems started due to the war may have generated a structural break in the order trends of LNG ships.

In this study, considering the use of LNG imports to increase energy diversification of countries due to the war, we aimed to econometrically analyze whether there was a positive break in order quantities of LNG ships. Accordingly, monthly LNG ship orders as cubic meters (CBMs) by date was used in the analysis. Since delivery times for ships can take several years considering shipyard density and complexity of ship construction, changes in the energy security paradigm may be reflected primarily in the amount of tonnage ordered. Rather than evaluations based on the current situation and policies in the literature, the supply changes of LNG ships ordered in the near future as a result of very detailed analyses and studies by companies can provide more concrete findings. Our research focuses on whether environmental policies, climatic changes, geopolitical events, and especially the Russia-Ukraine war generate a scientifically significant break in the trend in the LNG ship order book. The results showed that the demand for LNG ships experienced a positive break, especially in the period when the risk of war increased. In other words, countries attempted to prepare in advance for supply restriction situations. However, the construction period of the ships, which took a few years, prevented the fruits of these preparations from being taken in a short time. In the next section, the literature studies that form the framework of our research have been compiled. Then, the dataset and the method used in the study are introduced.

2. Literature Review

LNG is an important energy source in terms of being used in the economic activities of countries due to policies aimed at minimizing emissions and reducing dependence on natural gas supplied by pipelines. In addition, since transportation is carried out by sea, LNG supply countries can be easily changed in case of any dispute, and this provides great flexibility compared to pipelines, which have much lower transportation costs. Today's disputes between countries show that energy security is much more important than supplying cheaper energy. In addition, the use of LNG in maritime vessels is becoming widespread [12], and challenging policies are being developed for the use of LNG as a secondary alternative fuel in newly designed ships. Although we could not find any studies directly related to the demand for LNG ships within the scope of our research, we have compiled several studies that indirectly affect the demand for LNG transportation.

Studies on the diversification of LNG in terms of energy security have focused not only on the use of LNG as a means of diversifying natural gas and other types of energy but also on issues related to the diversification of LNG suppliers. In the study conducted by Shaikh et al. [13], LNG supply security was examined using the ecological network analysis method for the countries of the Asia-Pacific region. As a result of the research, they found that increasing supplier diversity increases energy security and that the country with the highest energy security is China, followed by India, Japan, South Korea, and Taiwan. In a similar context, Vivoda [14] examined LNG import diversification in its research through the 5 largest LNG-importing countries in Asia, namely, China, India, Japan, South Korea, and Taiwan. The author conducted his research using the Herfindahl-Hirschmann index, which was developed to measure market concentration. Although there were fluctuations

in some periods, the results generally showed that all the countries subject to the research developed their LNG import portfolios.

Since the natural gas dependence between the European Union (EU) and Russia is at a very high level, studies on energy diversification have also been conducted in the literature on this subject. A study examining the impact of the Russia-Ukraine war on EU's energy diversification policies was conducted by Lambert et al. [15]. The effects of the sanctions imposed by the EU on Russia and Russia's classification of the EU countries as unfriendly nations were examined within the scope of the current capacities, contract agreements, and growth strategies of the LNG exporting countries. As a result, they determined that the EU's diversification policies could produce effective results in the medium and long term, even if not in the short term. Hauser [16], who examined Europe's diversification policies in the natural gas market, stated that the natural gas pipeline coming in transit through Ukraine poses a risk, that Europe's purchasing of gas from North African countries via pipeline and investing in LNG infrastructures will increase energy security, but the cost will be high, and that the most cost-effective way for EU is establishing trusting relations with Russia. Since EU and Russian relations directly determine the system costs of the European gas market, establishing trust-based relationships will reduce the costs to the most effective level and cause diversification policies to be kept aside. In a similar framework, Devaraj et al. [17] examined the importance of diversification in terms of supply security for Ireland and Portugal using the MCDM method. As a result, it has been shown that European countries are largely dependent on Russia and Norway for natural gas supply and that to increase energy security, increasing the number of FSRU units, expanding the pipeline import network, and investing in increasing gas storage capacities are some options. As mentioned in the study by Gritsenko [18], policies aimed at making investments to increase energy security through LNG infrastructure investments in the Baltic region have been implemented for a while. The use of natural gas as a weapon in the Ukraine conflict due to Europe's dependence on Russia was reflected as a shock to Europe's energy security. In the research conducted by Gritz and Wolff [19], it was determined that this shock was a compelling factor for European countries to develop their policies regarding LNG, an alternative energy source. Also, Russian supply can be replaced by supplying sufficient gas from the LNG market, increasing energy savings, and turning to alternative renewable energy sources. Some LNG markets that Europe is turning to increase its energy security are located in North Africa and the Middle East regions. The effect of the war and the role of the countries in this region in Europe's energy security has been examined by Al-Saidi [20]. The author has determined that the problem posed by the Ukrainian war in Europe's energy security has increased the importance of African and Middle Eastern countries, and partnerships with LNG supplier countries in the region should be increased to ensure long-term energy security.

The US's desire to turn the crisis between Europe and Russia into an opportunity in terms of LNG has also found its place in the literature. The US's efforts to become a dominant actor in the natural gas market and its efforts to use this situation to strengthen its ties with Asian and European countries and weaken their dependence on Russia were evaluated in a study conducted by Medlock et al. [8]. The authors stated that the liberalization of the LNG market would support policies in line with the interests of the US.

On the other hand, focusing on LNG is used not only to increase energy security by diversification but also to reduce dependence on a single source by energy-rich countries. In the study conducted by Shabaneh and Schenckery [21], the effects of Saudi Arabia's low- and high-capacity LNG terminals on global prices and the country's energy supply cost were examined using general equilibrium modeling by two scenarios. As a result, the opportunity cost between switching to LNG fuel and using oil was not much different and supported the country to become an actor in the gas market in the long term. This will also contribute to the country's rapid transition from oil-fired generation to natural gas-fired generation.

Geographical conditions, as well as countries' demands and policies toward LNG, can have significant effects on the market. The LNG market may undergo a major change if the ice disappears or breaks along the route in an economically sustainable way on the Northeast Passage (NEP) route, which is currently not economically navigable due to ice. In a study conducted by Schach and Madlener [22], it was stated that if the ice problem in the NEP is solved, Russia's power in the LNG market may increase significantly due to its rich reserves in North-Western Siberia. This will enable the formation of a competitive shipping route with the Asian market.

When the literature is examined in general, issues such as the diversification of LNG-importing countries, the diversification of the EU region countries' energy resources with LNG, the US's effort to increase its influence in the region by turning the crisis into an opportunity, the turning of countries trying to transition to clean energy to LNG, and the possible effects of climate changes on the LNG market are examined. The findings of all these studies indicate that the demand for the LNG market will increase both in terms of infrastructure and LNG ships. The event that largely accelerated this process was the devastating shock

of the war between Russia and Ukraine on energy security. Since the construction processes of ships take time and can vary between 1 and 4 years depending on the density of the shipyards and the complex engineering of the ship, the first reflections of the paradigm shift in the perspective on energy security can be seen in LNG ship order quantities. In this direction, whether there is a significant break in the order trend makes it possible to scientifically determine the paradigm transition. In parallel with the existing literature, we tested whether there was a break in LNG ship tonnage on order at points close to the war period and aimed to offer a unique complementary perspective to the literature.

3. Data and Methodology

The data used in this study is the CBMs value of LNG ship tonnage ordered monthly [23]. CBM over deadweight tonnage was used as a variable because we decided that it was a more accurate measure for gas transportation. The reason why tonnage was used rather than the number of ships ordered is to take into account the changing trend in ship sizes. The data used shows the tonnage in the order book in the relevant month. In other words, when these ships are completed in the near future, they will enter the market and increase the supply side of the world LNG fleet. The data set consists of 337 monthly observations covering the period of May 1995 to May 2023. Descriptive statistics of our variable are presented in Table 1. Descriptive statistics contain important parameters, including the central tendency values and characteristics of the variables.

Table 1. *Descriptive statistics*

Variable	CBM
Mean	482096.5
Median	170520.0
Maximum	4868520.
Minimum	0.000000
Std. Dev.	749660.5
Skewness	2.600537
Kurtosis	11.64394
Jarque-Bera	1429.005
Probability	0.000000
Observations	337
Source: Braemar [9] CBM: Cubic meter	

However, since the orders for ships, especially LNG- type ships, were not placed very heavily and were greatly affected by market sentiment, no ships were ordered for 129 months in the period under consideration. In addition, the standard deviation value is very high and even higher than the mean. Therefore, the coefficient of variation (standard deviation/mean) emerges as 155%, indicating that ship order tonnage is highly volatile.

The course of the data used in the study between May 1995 and May 2023 is presented in Figure 1. It follows very volatile course. In some months, there was no ship order, whereas in some months, this rate was very high. In fact, no LNG ships were ordered during 2009 because of the shrinking of demand due to the global economic crisis. Because the figure is difficult to read, the trend value obtained using STL decomposition has also been added. Especially after the period when coronavirus disease-2019 started, there was a very high order trend. Since the Russia-Ukraine crisis, where tension was felt until February 2022 and then turned into a physical war, increased the demand for LNG ships, there is an increase in ship orders in 2022. Of course, in this case, the sabotage of the Nord Stream pipeline was also effective, and Europe had to supply its needs with LNG ships.

The variables in the time series show fluctuations and changes over time, as shown in Figure 1. These changes can sometimes occur on a very small scale and on a large scale. Events that significantly affect the course of the series generate structural breaks in the series. These breaks show the effect of an important event in that period on the series. Thus, inferences can be made about that event and future policies can be developed considering its effect on the trend of the variable.

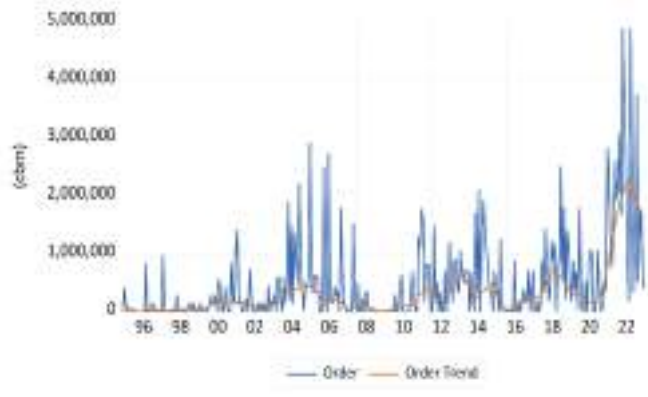

Figure 1. *Monthly orders of LNG ships and its trend*

Bai and Perron [24] test was preferred to analyze possible structural breaks in LNG ship order books. These breaks may be due to global events, policy changes, geopolitical crises, or random shocks that change the demand trend for LNG ships. The test is one of the most widely used methods for investigating structural breaks in a series. Its main purpose is to determine whether there is a structural break in the series and, if so, in which period. The test can achieve this by starting from the changes in some statistical properties

of the series, such as mean, variance, autocorrelation, and distribution. Therefore, it is important to identify structural breaks to detect incoming regime shifts, change the relationships between variables, and make more successful predictions. The most important advantage of this method is that there is no need for prior knowledge of the date of the structural break. This test makes it possible to detect multiple unknown break dates [25].

There are multiple versions of the test developed by Bai and Perron [24]. In this study, the author preferred the version of Global Information Criteria that determines the possible break dates in the series through the Schwarz (Sic) and Lagrange Multiplier-Wald-Zhao (LWZ), which is the modified version of the Schwarz [26]. In this method, it is recommended to use a consistent covariance estimator against heteroscedasticity or serial correlation. Therefore, the heteroskedasticity and autocorrelation consistent (HAC) [27] estimator can be used. In this estimator, Quadratic Spectral Kernel and Andrew's bandwidth options can be preferred. Analysis was performed using the EViews econometric software. The null hypothesis of this test is that there is no break in the series.

4. Results

In this study, it was decided to apply tests to both the raw order data and the order trend data to detect the break in LNG ship orders. This is because in some months no ships are ordered, and the value is 0 in those months. To reduce the possible negative effect of this situation on the results, the series was separated into its components using the STL decomposition method, and analyses were applied to the trend of the data as well.

For the application of the Bai and Perron [24] test, the series is first estimated by a single regressor (constant) as the series is a dependent variable, as shown in Equation 1. Then, multiple structural break tests are applied.

$$Y_t=\beta_0+u_t \quad (1)$$

Since the break in LNG ship order amount will be tested in the research, the order amount has been estimated as a dependent variable by a constant, as in Equation 2. Also, the analysis was applied to the trend of the series as shown in Equation 3. The ordinary least squares method was used to estimate the regression equations.

$$Order_t=\beta_0+u_t \quad (2)$$

$$OrderTrend_t=\beta_0+u_t \quad (3)$$

The estimated regression models for LNG order and LNG order trend variables are presented in Table 2. HAC was chosen for the covariance method because it was desired to allow serial correlation of errors while estimating the model. Quadratic-spectral and Andrew Bandwidth were selected from kernel settings in HAC. Since the frequency of data is monthly, it was decided to automatically determine the lag number in the HAC settings by minimizing the Akaike Information Criterion (Aic). Aic was selected because it is asymptotically efficient and better in larger samples [28]. The model that minimizes the information criterion value is determined to be the most effective one. As a result, constant terms are significant at the 1% and 5% levels. However, the model has no explanatory power because independent variables are not included in the equation. This does not matter because the test that will give the real result is the structural break test.

Table 2. *Regression estimation results*

	Order	Order Trend
C	482096.5 [0.00]	317416.8 [0.03]
Adjusted R-Squared	0.00	0.00
Durbin-Watson	1.16	0.006649
Aic	29.98	28.82
Sic	29.90	28.83
(1) Probabilities are shown in square brackets, (2) the HAC (Newey-West) Covariance method was applied		

After the regression model was estimated, the multiple break test was applied. While applying the test, the Global Information Criterion was chosen as the method. This method compares the information criteria for structural breaks from 0 to M. The information criteria used were Schwarz (Sic) and LWZ. While performing the analysis, the maximum number of breaks was determined as 5. In addition, the trimming rate was chosen as 5% because a high trimming rate may lead to data loss in the series.

The results obtained for the raw LNG order variable are presented in Table 3. Values that minimize the information criteria show the number of breaks in the series. According to the analysis, Sic indicates four breaks, while Lwz indicates 1 break since their values are the minimum in these break numbers. The dates of the breaks are presented in Table 4.

Table 3. *Structural break test for order*

Breaks	# of Coefs.	Log-L	Sic Criterion	Lwz Criterion
0	1	-5036.407	27.06905	27.09059
1	3	-4970.426	26.71201	26.77667[α]
2	5	-4959.314	26.68060	26.78841
3	7	-4954.362	26.68576	26.83675
4	9	-4946.169	26.67168*	26.86589
5	11	-4943.733	26.69176	26.92924
(1) The number of breaks that minimize the information criterion is shown by * for Sic and [α] for Lwz (2) Sic: Schwarz, Lwz: Lagrange Multiplier-Wald-Zhao				

Table 4. *Break dates considering the number of breaks*

1[α]	2	3	4*	5
2021M06	2003M09	2004M04	2004M04	2004M04
	2021M06	2006M07	2006M07	2006M07
		2021M06	2011M04	2011M04
			2021M06	2015M02
				2021M06
Suggested structural break dates by *Sic and [α]Lwz				

The Sic suggested 4 break dates, while Lwz suggested only 1 break date. The common date for both Sic and Lwz is June 2021. On the other hand, other break dates suggested by Sic are April 2004, July 2006, and April 2011.

The results of the structural break test applied to the trend of LNG order amount are presented in Table 5. In this case, both Sic and Lwz point to 5 structural breaks. The structural break dates are presented in Table 6.

Table 5. *Structural break test for the order trend*

Breaks	# of Coefs.	Log-L	Sic Criterion	Lwz Criterion
0	1	-4855.827	25.99736	26.01890
1	3	-4568.404	24.32613	24.39078
2	5	-4513.804	24.03663	24.14444
3	7	-4498.066	23.97777	24.12876
4	9	-4472.735	23.86198	24.05619
5	11	-4458.271	23.81068*	24.04815[α]
(1) The number of breaks that minimize the information criterion is shown by * for Sic and [α] for Lwz (2) Sic: Schwarz, Lwz: Lagrange Multiplier-Wald-Zhao				

Table 6. *Break dates considering the number of breaks*

1	2	3	4	5 *α
2021M08	2011M04	2000M01	2003M08	2003M08
	2021M09	2011M04	2006M02	2006M02
		2021M09	2011M04	2011M03
			2021M09	2018M01
				2021M09
Suggested structural break dates by *Sic and [α]Lwz				

Both information criteria suggested 5 break dates: August 2003, February 2006, March 2011, January 2018, and September 2021. Although the break dates are close to those in the previous analysis, there are some differences.

The dates determined after the structural break tests are presented in Figure 2. The dates of the 4 breaks are very close to each other. Apart from that, trend data indicates one more break at the beginning of 2018 as well. The effects of the war between Russia and Ukraine can be clearly seen in the figure. According to the raw and trend variables, after the war, order quantities reached all-time highs monthly. When the data is analyzed annually, the highest LNG ship order of all time was given in 2022 with 27.4 million cbm, and even 16% of the total orders in the sample were given in that year. In 2021, the highest ship order after 2022 was given with a total of 14.5 million cbm. In addition, while the number of ships ordered in 2022 was 163, it was 89 in 2021. Considering that the annual average ship order in the period under consideration was 36, it can be understood how unusual these order quantities are [23].

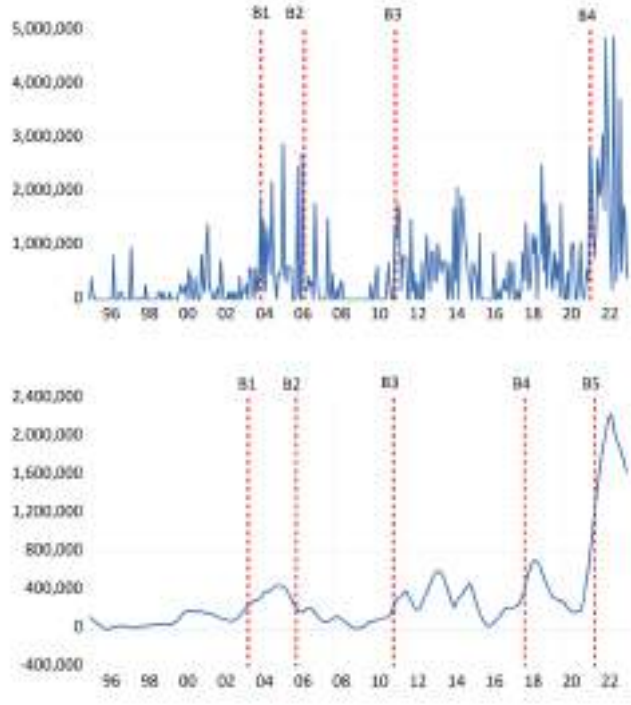

Figure 2. *Positions of break dates in the dataset*

Before February 2022, the date when the war officially started, it is seen that orders entered an upward trend and there was a break in orders in June 2021 according to raw data and in September 2021 according to trend data. This situation can be interpreted as countries and companies evaluated this war probability months before the war started actively and increased their LNG ship orders due to energy security concerns. Also, just before the war, on November 10, 2021, the US detected abnormal military activity on the Ukrainian border. On November 28, Ukraine informed the world that Russia was preparing to attack the border with 92,000 soldiers [29]. Such news has also been events that increase tension and worry countries in terms of energy security. They have probably also caused the demand for LNG ships to rise.

Apart from the war period, there are some periods in which there is an increase in LNG ship orders. For instance, the positive structural break in late 2003 and early 2004 was probably due to Chinese influence. Between 2000 and 2004, energy consumption in China increased by an average of 16% annually, and during this period, China alone accounted for more than half of global energy consumption [30]. In 2006, however, there was a negative structural break this time, and order quantities remained low for a while, probably due to a lower-than-expected demand in China, resulting in an oversupply of LNG ships.

Figure 2 shows an increase in orders after March 2014, when Russia invaded Crimea. However, this situation was not reflected in the series as a break. It is even argued that the rich natural gas reserves around Crimea played a role among the factors causing this invasion [31]. Therefore, countries may have increased their order quantities to diversify their energy security.

The increase seen in 2018 is probably due to the Kerch Strait Incident event, which increased the tension in the region [32]. There may have been an increase in LNG ship orders in response to the possibility that the problem between Ukraine and Russia could generate a problem in the flow of natural gas through Ukraine or EU countries that may impose sanctions on Russia. Because there is an annual gas flow capacity of 40 billion cbm to Europe via Ukraine, this constitutes a very significant amount of the total flow capacity [33].

5. Conclusion

The war between Russia and Ukraine greatly affected the natural gas market and forced the countries to produce new policies regarding the supply of natural gas. In particular, the European region has been the area most affected by the natural gas problems due to the war. In particular, the overall EU natural gas dependency rate is 97% in 2022 [34]. This great dependency can make the European economy fragile. In 2021, 54% of the total European natural gas imports were from Russia [2]. The disruption of natural gas flow through Ukraine, sanctions against Russia, and sabotage of the Nord Streamline due to the war made other suppliers mandatory for Europe. Since it is possible to supply natural gas by pipeline only from North Africa, it has had to supply its needs mostly with LNG ships from countries such as the US, Qatar, Algeria, and Nigeria. Therefore, the demand for LNG transportation has increased, which can be expected to cause an explosion in orders for new LNG ships. Of course, the structure of the LNG market should also be considered to make healthier inferences about this issue.

The LNG market can be defined as having an oligopoly market structure. While a certain number of companies manage the market, there are barriers to entry, such as large capital and knowledge accumulation. As LNG company owners make long-term contracts with buyers, a stable market trend occurs. In addition, because there are a limited number of players, they can easily cooperate with each other. Therefore, it can be said that the LNG market has an oligopoly structure, especially in the short term. Since LNG ships are complex in structure and require high technology, their prices are much higher than those of other ships [35]. This situation is also reflected in global fleet statistics. While LNG ships constitute only 3.7% of the world fleet in number [36], they constitute 8.3% in monetary value [37]. In addition, according to a monthly shipbuilding report, the average value of the ships ordered in January 2023, according to their types, were $34.7 million for bulkers, $57 million for tankers, $64.6 million for LPG ships, $83.1 million for container ships, $97.1 million for car carriers, $223 million for LNG ships [38]. These values are also sufficient to understand the capital barrier required to enter this market. However, there may still be a structural break in LNG orders due to the increasing demand and because the energy needs of countries are strategic and security issues.

According to the results of the analyses applied, the periods when orders increased and the dates of various structural breaks were determined in the data range discussed. If the China boom period is excluded in general, these breaks coincide with periods of military and political tension between Russia and Ukraine. As Russia is one of the most important natural gas suppliers in the world, the increase in LNG ship orders shows that countries are trying to diversify their energy supplies. Especially during the Russian-Ukrainian war, the highest LNG ship orders of all time were given. In this regard, when the studies in the literature are examined, policies and projects are being carried out to diversify energy resources with LNG both before [16-18] and after [15,19] the Russia-Ukraine crisis. This situation has increased the importance of suppliers in Africa and the Middle East, generating a need for more LNG ships [20]. In addition, environmental concerns and policies regarding emission reduction have encouraged countries such as Saudi Arabia to switch from oil-fired power plants to environmentally friendly natural gas power plants. Such countries, whose infrastructures are not yet suitable for processing their own natural gas, have turned to LNG for a rapid transition and aim to have a say in this market in the near future [21]. Finally, the possibility of the NEP route becoming more functional in the near future may also contribute to Russia's easier access to the Asian market [22]. All these diversification policies, climatic events, environmental policies, and geopolitical events increased the demand for LNG ships and caused a positive trend-break in the tonnage in the order book. Our

findings constitute scientific evidence as a concrete result of developments in this direction. Although it is a capital-intensive sector and gas supplied with LNG is expensive, countries cannot give up on this energy source in the near future. Existing infrastructure and industry are highly dependent on this gas.

Because the cost of supplying gas with LNG is higher, the cost to the European economy will likely be somewhat higher, adding to the inflationary effects in the region. Perhaps countries may consider entering this oligopoly market with the power of the state to reduce costs in the future, as it is a very important issue that affects energy security and costs. On the other hand, the increase in the number of LNG ships ordered will cause a large increase on the supply side after a few years. The effects of this situation on the LNG freight market can be examined. In addition, since which companies place orders will affect future market concentration and competition levels, a possible oligopoly structure may cause an increase in LNG supply prices and new energy security crises. Such possible situations can be analyzed using simulation and general equilibrium modeling, and proactive policies can be developed. Finally, the situation in the FSRU order book can be analyzed with a similar approach because the construction of physically fixed facilities is a process that can take a long time and requires know-how. The effect of the sudden energy shock may also have caused disruptions in the orders of such mobile vehicles that offer such quick solutions. These issues may also be important for further research.

The inability to access ship size-based order book data can be shown as a limitation of the study. Since ship sizes may vary depending on factors such as distance, value of cargo, commercial trends, and market competition structure, a distinction based on size would have made it possible to analyze the future market better.

Funding: The author declare that no funds, grants, or other support was received during the preparation of this manuscript.

References

[1] G. A. Karim. *Fuels, Energy, and the Environment*. 1st Ed. CRC Press, 2013.

[2] *BP World Energy Outlook*. [Online]. Available: https://www.bp.com/en/global/corporate/energy-economics/statistical-review-of-world-energy/downloads.html. [Accessed: May 23, 2023].

[3] J. Haselip, N. Al-Shafai, and S. Morse, "EU energy security, sustainability and globalisation: What role for Qatari LNG amid calls for greater energy diversification?" *International Journal of Global Energy Issues*, vol. 33, pp. 38-55, May 2010.

[4] Euronews, "*Explosions in September destroyed at least 50 metres of Nord Stream pipeline, investigators show,*" October 18, 2022. [Online]. Available at: https://www.euronews.com/2022/10/18/explosions-in-september-destroyed-at-least-50-metres-of-nord-stream-pipeline-investigators, [Accessed: May 23, 2023].

[5] S&P Global, "*Russian pipeline gas flows to Europe drop to new low in January.*" February 2, 2023. [Online]. Available at: https://www.spglobal.com/commodityinsights/en/market-insights/latest-news/natural-gas/020223-russian-pipeline-gas-flows-to-europe-drop-to-new-low-in-january#:~:text=Russia%20gradually%20choked%20gas%20supply,September%2C%20rendering%20the%20system%20unusable. [Accessed: May 23, 2023].

[6] Euronews, "*Avrupa'da birçok ülke Ukrayna savaşı sonrası yeniden kömüre yöneldi.*" January 12, 2023. [Online]. Available at: https://tr.euronews.com/my-europe/2023/01/12/avrupada-bircok-ulke-ukrayna-savasi-sonrasi-yeniden-komure-yoneldi. [Accessed: May 24, 2023].

[7] Enerdata, "Belgium will extend the life of two nuclear reactors (2 GW) by 10 years," January 11, 2023. [Online]. Available at: https://www.enerdata.net/publications/daily-energy-news/belgium-will-extend-life-two-nuclear-reactors-2-gw-10-years.html. [Accessed: May 24, 2023].

[8] K. B. Medlock, A. M. Jaffe, and M. O'Sullivan. "The global gas market, LNG exports and the shifting US geopolitical presence." *Energy Strategy Reviews,* vol. 5, pp. 14-25, Dec 2014.

[9] *EIA Natural Gas.* [Online]. Available at: https://www.eia.gov/dnav/ng/hist/n9133us2A.htm. [Accessed: May 23, 2023].

[10] The Brussel Times. *EU dismisses report that US blew up Nord Stream pipeline as 'speculation'.* Feb 2023. https://www.brusselstimes.com/376022/eu-dismisses-report-that-us-blew-up-nord-stream-pipeline-as-speculation

[11] *IEA Gas Market Report Q1-2023*. [Online]. Available at: https://www.iea.org/reports/gas-market-report-q1-2023. [Accessed: May 23, 2023].

[12] M. Doymus, G. D. Sakar, S. T. Yildiz, and A. Acik, "Small-scale LNG supply chain optimization for LNG bunkering in Turkey." *Computers & Chemical Engineering*, vol. 162, 107789, Jun 2022.

[13] F. Shaikh, Q. Ji, and Y. Fan, "Assessing the stability of the LNG supply in the Asia Pacific region." *Journal of Natural Gas Science and Engineering*, vol. 34, pp. 376-386, Aug 2016.

[14] V. Vivoda, "LNG import diversification and energy security in Asia." *Energy Policy*, vol. 129, pp. 967-974, Jun 2019.

[15] L. A. Lambert, et al. "The EU's natural gas Cold War and diversification challenges." *Energy Strategy Reviews*, vol. 43, 100934, Sep 2022.

[16] P. Hauser. "Does 'more'equal 'better'? - Analyzing the impact of diversification strategies on infrastructure in the European gas market." *Energy Policy,* vol. 153, 112232, Jun 2021.

[17] D. Devaraj, E. Syron, and P. Donnellan. "Diversification of gas sources to improve security of supply using an integrated multiple criteria decision making approach." *Cleaner and Responsible Consumption*, vol. 3, 100042, Dec 2021.

[18] D. Gritsenko, "Explaining choices in energy infrastructure development as a network of adjacent action situations: The case of LNG in the Baltic Sea region." *Energy Policy*, vol. 112, pp. 74-83, Jan 2018.

[19] A. Gritz, and G. Wolff, "Gas and energy security in Germany and central and Eastern Europe." *Energy Policy*, vol. 184, 113885, Jan 2024.

[20] M. Al-Saidi, "White knight or partner of choice? The Ukraine war and the role of the Middle East in the energy security of Europe." *Energy Strategy Reviews*, vol. 49, 101116, Sep 2023.

[21] R. Shabaneh, and M. Schenckery, "Assessing energy policy instruments: LNG imports into Saudi Arabia." *Energy Policy*, vol. 137, 111101, Feb 2020.

[22] M. Schach, and R. Madlener, "Impacts of an ice-free Northeast Passage on LNG markets and geopolitics." *Energy Policy*, vol. 122, pp. 438-448, Nov 2018.

[23] *Braemar LNG Ship Orders.* [Online]. Available at: https://braemar.com/. [Accessed: May 23, 2023].

[24] J. Bai, and P. Perron, "Computation and analysis of multiple structural change models." *Journal of Applied Econometrics*, vol. 18, pp. 1-22, Feb 2003.

[25] Y. He, "*The institutional paradigm of economic geography: A perspective from natural resource and environmental econometrics*." The Institutional Paradigm of Economic Geography A Perspective from Natural Resource and Environmental Econometrics, Springer Nature. Jul 2022.

[26] J. Bai, and P. Perron, "Multiple structural change models: a simulation analysis." *Journal of Applied Econometrics*, vol. 18, pp. 212-237, Feb 2006.

[27] W. K. Newey, and K. D. West, "Hypothesis testing with efficient method of moments estimation." *International Economic Review*, vol. 28, pp. 777-787, Oct 1987.

[28] F. Emmer-Streib, S. Moutari, and M. Dehmer, "*Elements of Data Science, Machine Learning, and Artificial Intelligence Using R*." Springer, 2023.

[29] NDTV World. "Soldiers, separatists, sanctions: a timeline of the Russia-Ukraine crisis." Feb 2022.

[30] L. M. Jensen, and T. B. Weston. "*China's transformations: The stories beyond the headlines*." Rowman & Littlefield Publishers. 2006.

[31] W. J. Broad, "In taking crimea, Putin gains a sea of fuel reserves." *The New York Times,* May 2014.

[32] The Guardian. *Kerch strait confrontation: what happened and why does it matter?* 2018.

[33] Statista. *The gas pipelines linking Russia and Europe*. 2022.

[34] *Eurostat natural gas supply statistics*. [Online]. Available at: https://ec.europa.eu/eurostat/statistics-explained/index.php?title=Natural_gas_supply_statistics. [Accessed: May 23, 2023].

[35] S. Ma, "*Economics of Maritime Business*." Routledge, 2020.

[36] Statista. "Number of ships in the world merchant fleet as of January 1, 2022, by type." Water Transport, 2022.

[37] *RMT Review of Maritime Transport.* 2022.

[38] *Golden Density Monthly Newbuilding Market Report.* 2023.

Reviewer List of Volume 12 Issue 1 (2024)

Ahmet Lütfi Tunçel	İstanbul Technical University	Türkiye
Ali Can Takinacı	İstanbul Technical University	Türkiye
Ali Doğrul	National Defense University	Türkiye
Ali Tehci	Ordu University	Türkiye
Ana Slišković	University of Zadar	Croatia
Ayfer Ergin	İstanbul University	Türkiye
Cemile Solak Fışkın	Ordu University	Türkiye
Cihad Delen	İstanbul Technical University	Türkiye
Çağatay Kandemir	Ordu University	Türkiye
Didem Yılmazer	Tekirdağ Namık Kemal University	Türkiye
Emre Akyüz	İstanbul Technical University	Türkiye
Emre Kahramanoğlu	İstanbul Technical University	Türkiye
Enes Fatih Pehlivan	Ordu University	Türkiye
Erdem Üçer	İstanbul Technical University	Türkiye
Gizem Kayişoğlu	İstanbul Technical University	Türkiye
Gökhan Budak	İzmir Katip Çelebi University	Türkiye
Hülya Karakuş Cihan	Yüksel Proje	Türkiye
Iraklis Lazakis	University of Strathclyde	Scotland
İshak Altınpınar	Karadeniz Technical University	Türkiye
K. Emrah Erginer	Dokuz Eylül University	Türkiye
Mehmet Doymuş	Dokuz Eylül University	Türkiye
Muhammet Gül	İstanbul Technical University	Türkiye
Murat Özkök	Karadeniz Technical University	Türkiye
Mustafa Kafalı	İzmir Katip Çelebi University	Türkiye
Naz Yılmaz	Bursa Technical University	Türkiye
Onur Usta	National Defense University	Türkiye
Serdar Kum	İstanbul Technical University	Türkiye
Serdar Yıldız	Karadeniz Technical University	Türkiye
Serim Paker	Dokuz Eylül University	Türkiye
Taner Çoşgun	Yıldız Technical University	Türkiye
Tanzer Satır	İstanbul Technical University	Türkiye
Theophilus Chinoyerem Nwokedi	Federal University of Technology	Nigeria
Yasemin Arıkan Özden	Yıldız Technical University	Türkiye

Volume 12 Issue 1 (2024) is indexed in

TRID

the TRIS and ITRD database

TÜBİTAK

ULAKBİM

DOAJ DIRECTORY OF OPEN ACCESS JOURNALS

Scopus

JEMS's Sponsors

INCE SHIPPING GROUP

GEMLIK PILOTS

DENIZ ÇALIŞANLARI DAYANIŞMA DERNEĞI

EGE GAZ INC.

SEFİNE SHIPYARD

GÜRDESAN SHIP MACHINERY CORP.

ER SHIPPING


UCTEA CHAMBER OF MARINE ENGINEERS
1960